PERFORMANCE OF HYDROFOIL SYSTEMS

by

Robert Hamilton Cannon, Jr.

B.S., University of Rochester
(1944)

Submitted in Partial Fulfillment of the
Requirements for the Degree of
Doctor of Science

at the

MASSACHUSETTS INSTITUTE OF TECHNOLOGY
(1950)

Signature of Author _____
Department of Mechanical Engineering

Certified by _____
Thesis Supervisor

_____
Chairman, Department Committee on Graduate Students

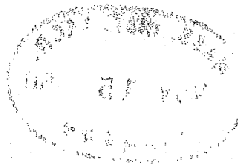

Cambridge, Massachusetts

May 12, 1950

Professor J. P. Den Hartog, Chairman
Department Committee on Graduate Students
Department of Mechanical Engineering
Massachusetts Institute of Technology

Dear Professor Den Hartog:

A thesis, "Performance of Hydrofoil Systems", is herewith submitted in partial fulfillment of the requirements for the degree of Doctor of Science.

Very truly yours,

Robert Hamilton Cannon, Jr.

PERFORMANCE OF HYDROFOIL SYSTEMS

Abstract

Results are presented of a study of the probable performance of water surface craft supported by hydrofoil systems operating in ocean waves, and of the effects of all the factors which are expected to influence the performance. Attention is centered particularly on the rising and pitching motions of the system and on the establishment of conditions for which ventilation - sudden aeration of the hydrofoil surfaces - is imminent.

Derivation of the equations of motion of a hydrofoil system is preceded by preparatory studies of the lift on a hydrofoil near a free surface, the mechanisms of cavitation and ventilation of a lifting hydrofoil, and the pertinent properties of ocean waves.

Theories are developed and correlated with analyses of existing experimental data to give relations of design and analytical value concerning the lifting properties and the ventilating characteristics of hydrofoils as affected by their orientation with respect to the free surface.

The equations governing the pitching and rising motions of hydrofoil systems are derived in general form. Two basic types are considered: rigid systems using variable area to maintain elevation, and non-rigid systems

using incidence control. When the area of submerged hydrofoils is variable these equations are found to contain non-linear terms of the same order of magnitude as the linear terms.

Several preliminary approximate analyses are made of the equations, including linearization and reduction to one degree of freedom. Finally, the method of solving the complete equations for variable-area systems by means of a recently-developed electronic differential analyzer is explained, and the results of approximately 450 solutions are presented with pertinent conclusions.

It is found that it is of paramount importance to use the deepest hydrofoils permissible whenever possible, at least as deep as the height of the largest waves to be traversed. The largest possible ratio of boat-length to chord-size and the smallest ratio of radius of gyration to boat-length should be used.

It is shown that as the speed of a hydrofoil system is increased, its stability is reduced and its susceptibility to cavitation and ventilation increased, so that careful design of the load distribution on the hydrofoils is of critical importance at high speeds.

The transient performance of a hydrofoil system entering a wave near its crest is found to be very much worse than its steady-state performance.

The combined effects of increasing speed and of changing direction of travel with respect to the waves are studied for hydrofoil systems of several configurations traveling in waves of varying size and steepness.

It is concluded that at moderately high speeds (up to 80 feet per second) a carefully designed rigid hydrofoil system traveling in waves having a height which is less than the running depth of the foils should exhibit good stability and smooth performance. In larger waves the system will probably undergo transient motions of intolerable character. At higher speeds, automatic incidence control may be necessary.

AKNOWLEDGMENTS

The author welcomes the opportunity to express his sincere appreciation to a number of people who - through guidance and through generous assistance-rendered this study possible.

First, inspiration for the study came from Mr. J. G. Baker, who envisioned the hydrofoil boat as a vehicle for pleasure, and who demonstrated clearly the two salient facts that (1) reliable hydrofoil systems can be developed, and (2) the greatest pleasure accrues from the development.

The successful operation of several passenger-carrying models - which convinced the author that further analytical study could be worth while - was due in no small measure to the careful design of Mr. D. Cadman, and to the technical skill and ingenuity of machinist George Buehler.

Professor J. P. Den Hartog, as thesis advisor for the study has lent astute and welcome guidance to ideas of frequently dubious maturity, always mixing generous quantities of friendship and wit with wisdom.

Many thanks are due to the M.I.T. Research Laboratory of Electronics for making available the newly-built differential analyzer, and for hospitality in extending the use of its laboratory facilities.

Particular gratitude is expressed to Dr. Alan B. Macnee, the machine's inventor, who carefully and patiently

taught the author its operation and appreciation, and to Mr. R. Maartmann-moe, its curator, who gave tirelessly and generously of his time and experience to maintain the new equipment in working order, and to expand and develop it in directions adaptable to the hydrofoil problem.

Very helpful suggestions on various particulars of the problem were received from Professor S. Crandall of M.I.T.; from Frederick Imlay, James M. Benson, John Parkinson, Douglas King, and Norman Land -- all currently or formerly connected with the N.A.C.A. Towing Tank Group at Langley Field, and Christopher Hook of Cowes, England.

Finally, the author expresses endless thanks to his wife and family, who have willing lived under thesis conditions for many months in the interest of science.

TABLE OF CONTENTS

Page

ACKNOWLEDGEMENTS i

TABLE OF CONTENTS ii

NOMENCLATURE vi

SUMMARY 1

CHAPTER I: INTRODUCTION 5

CHAPTER II: LIFT ON HYDROFOILS NEAR A FREE SURFACE . . .

A. Introduction 17

B. Theory 20

C. Experiment 26

D. Summary 31

CHAPTER III: CAVITATION AND VENTILATION

A. Introduction 33

B. Theory 36

C. Experimental Data 42

D. Summary 48

CHAPTER IV: OCEAN WAVES

A. Introduction 50

B. Wave Theory 51

C. Wave Experiments in Tanks 55

D. Open Water Observations of Waves 57

CHAPTER V: DERIVATION OF THE EQUATIONS OF MOTION
Introduction 58

PART I: VARIABLE AREA SYSTEMS

A. One Degree of Freedom 59

TABLE OF CONTENTS
(continued)

Page

B. Two Degrees of Freedom 67

C. Dimensional Analysis 69

D. Linearization -- Two Degrees of Freedom 75

PART II: VARIABLE ANGLE OF ATTACK SYSTEMS

A. The Problem of Incidence Control 78

B. An Automatic Control System 80

C. A Particular Case -- The Hook System . . 84

CHAPTER VI: APPROACH TO SOLVING THE EQUATIONS OF MOTION

Introduction 87

A. Linear Analysis of a Hydrofoil System Having One Degree of Freedom 88

B. Linear Analysis of a Hydrofoil System Having Two Degrees of Freedom 93

C. Method of Obtaining Non-Linear Solutions . . 104

CHAPTER VII: RESULTS OF CALCULATIONS

PART I: LINEAR SOLUTIONS 114

PART II: SOLUTIONS TO THE NON-LINEAR EQUATIONS OF A HYDROFOIL SYSTEM HAVING TWO-DEGREES OF FREEDOM -- TRANSIENT MOTIONS IN SMOOTH WATER 121

PART III: SOLUTIONS TO THE NON-LINEAR EQUATIONS OF A HYDROFOIL SYSTEM HAVING TWO-DEGREES OF FREEDOM -- PERFORMANCE IN WAVES . . . . . .

Introduction 130

A. General Discussion of Results 136

TABLE OF CONTENTS
(continued)

Page

B. The Effect of Initial Depth 146

C. The Effect of Phase 152

D. The Effect of Frequency of Wave Encounter 158

E. The Effect of Speed 169

F. The Effect of Running Depth 180

G. The Tietjens System 182

H. Summary of Results 184

CHAPTER VIII: CONCLUSIONS 188

APPENDIX A: PRIMARY RELATIONS 195

FIGURE 1: Lift on Hydrofoils Near a Free Surface; Summary of Experimental Data 196

FIGURE 2: Basic Lift-Depth Relation; 30°-Dihedral Hydrofoil 197

FIGURE 3: Cavitation Conditions for 16-Series Hydrofoils 198

EQUATIONS (2), (3), (4): Relations Between Wave Parameters 199

FIGURE 4: Frequency of Wave Encounter for a Boat Traveling Directly Up- or Downwind 200

PLATE 1: Derivation of the Equations of Motion of a Rigid Hydrofoil System Having Freedom to Pitch and Rise 201

PLATE 2: Additions to PLATE 1 for a Hydrofoil System Having Incidence Control 202

TABLE 1: The Relations Between Speed, Loading, and Angle of Attack 203

TABLE OF CONTENTS
(continued)

Page

PLATE 5, PLATE 6: Differential Analyzer Solutions to the Non-Linear Equations of Motion of a Hydrofoil System Having Two Degrees of Freedom 204

APPENDIX B: NUMERICAL RESULTS 206

FIGURES II-5, 6, 7: Study of Lift Data 207

FIGURES III-2 to 7: Study of Cavitation and Ventilation Data 210

FIGURES VII-1 to 41: Results of Differential Analyzer Calculations . . . 216

APPENDIX C: EXTRAPOLATION OF DIHEDRAL HYDROFOIL DATA 246

APPENDIX D: BIOGRAPHICAL NOTE 249

NOMENCLATURE

English Letters

A	Aspect Ratio (ratio of length to chord).
a	Constant of proportionality between lift coefficient (C_L) and angle of attack (α).
a_n	Gain factor for n^{th} adder of Differential Analyzer.
B_m	Equivalent damping constant of depth-measuring element in automatic control system.
b	Wave height, trough to crest.
C	Wave velocity.
C_L	Lift Coefficient.
C_{L_D}	Lift Coefficient for which a foil is Designed.
c	Chord.
cg	Center of Gravity.
σ	Cavitation Index, defined by: $\sigma = \frac{L/S}{p_a}$.
f	Frequency.
f_n	Natural Frequency.
g	Acceleration of Gravity, dimensional units.
g'	Acceleration of Gravity, non-dimensional units: $g' = \frac{gc}{V}$.
H	Depth below hypothetical surface (near true water surface); see page 31.
H_i	Depth of initial entry into waves (measured from wave crest.
H_w	Height of column of water supported by atmospheric pressure (34 feet).
h	Depth below real water surface.
h_{av}	Average depth of a dihedral hydrofoil.

NOMENCLATURE
(continued)

h^*	Desired Depth (in control system).
i	Distance between wave trough and mean water level.
i_n	Gain factor for n^{th} integrator of Differential Analyzer.
K_m	Equivalent spring constant of depth-measuring element in automatic control system.
K_J	Spring constant in Hook jockey system.
k_n	Constants of automatic incidence-control system. (n's from 1 to 7).
L	Lifting force on a foil.
ℓ	Length between forward and after hydrofoils (measured in chords).
$\ell\theta$	Product of length between hydrofoils and angle of pitch, and therefore the difference in height of the forward and after hydrofoils.
m	Total Mass of hydrofoil system.
m_m	Mass of depth-measuring element in automatic control system.
N	Frequency of encountering waves.
n	Number of hydrofoils. (n_1 = number forward; n_2 = number aft.)
p	Pressure.
p_a	Atmospheric pressure.
p_l	Pressure on lower foil surface.
p_o	Pressure of free stream at hydrofoil depth.
p_u	Pressure on upper foil surface.
p_v	Vapor pressure of water.
q_n	Natural frequency of damped system.

NOMENCLATURE
(continued)

R_p	Index of Pressure Distribution: ratio of maximum pressure to average pressure on entire foil
R_t	Ratio of C_L/α for experimental foils in shallow water to that for theoretical foils at infinite depth.
r	Distance from center of vortex (p. 21).
r_c	Index of Chordwise Pressure Distribution: ratio of maximum to average pressure at a given section of foil.
r_s	Index of Spanwise Pressure Distribution: ratio of maximum to average values along the span of average chordwise pressure.
r_o	Radius of orbit of water particle (p. 54).
S	Submerged, projected area of hydrofoil (measured in horizontal plane).
t	Time (dimensional units -- in seconds).
u_p	Horizontal component of velocity of water particle in surface waves.
u	Error in depth -- i.e. difference between actual depth and desired depth in control system.
V	Horizontal Velocity of hydrofoil system.
v_i	Velocity produced by image vortex in vortex theory (p. 24).
v_p	Vertical component of velocity of water particle in surface waves.
v_r	Velocity produced by real vortex in vortex theory (p. 24).
x	Horizontal position in waves (measured from a trough).
x_1	Distance from center of gravity to forward hydrofoils.
x_2	Distance from center of gravity to after hydrofoils.
y	Vertical position in waves (measured from mean water level, positive downward).

NOMENCLATURE
(continued)

y_1 or y_2	Output signal from depth-measuring device of automatic control system.
z	Vertical displacement of center of gravity of hydrofoil system from its equilibrium position (measured positive downward).
z_o	Maximum value of z.

Greek Letters

Λ	Ratio: $\frac{\partial(\frac{\alpha}{\alpha}_m)_o}{\partial(b/H_o)}$ defined on page 165.
α	Angle of Attack (measured from the angle of zero lift).
α_s	Set angle of attack.
α_t	True Angle of attack.
β	Ratio of forcing frequency to natural frequency.
Γ	Strength of Vortex.
γ	Dihedral Angle of a hydrofoil.
γ_w	Specific weight of water.
δ	Distance between hypothetical surface and real surface of water (see page 31).
ζ	Height of wave surface, measured from trough level.
θ	Angle of pitch, measured positive when bow is higher.
λ	Wave length.
ξ	Slope of σ - H curve.
ρ	Mass-density of water.
σ	The quantity: $\frac{C_L}{\alpha} S$.

NOMENCLATURE
(continued)

τ Time (non-dimensional units): $\tau = \frac{t}{V/c}$.

ϕ Potential function for wave velocity.

ψ Phase of hydrofoil system in waves--i.e., amount of wave traversed by forward hydrofoils as after hydrofoils enter same wave, and therefore the ratio of boat-length to wave-length.

ω_n Undamped Natural Frequency.

Common Subscripts

$_o$ Equilibrium value of quantity.

$_1$ Refers to forward hydrofoils.

$_2$ Refers to after hydrofoils.

$_m$ With a variable, denotes maximum value of variable.

SUMMARY

The possibility of using hydrofoils to support water surface-craft is of interest because of the theoretical promise of improved efficiency and smoother, more stable operation. Numerous hydrofoil craft of several types have been built which accomplished one or the other of these expectations, but to date, attempts to build high-speed hydrofoil boats fulfilling both have been unsuccessful. It is believed that this failure may be due in part to dynamic and hydrodynamic effects of a free surface which become increasingly important at high speeds.

It is therefore the purpose of this thesis to study the theoretical behavior of hydrofoil systems operating in surface waves over a large speed range, and to evaluate the influence of each of the parameters of the hydrofoil system and of the waves.

Before deriving the general equations of motion of a hydrofoil system, several preparatory steps are taken, the results of which are presented in sequence in Appendix A.

First, the relation between the lifting force on a hydrofoil and its orientation with respect to the free surface is investigated. A preliminary theoretical study is made and a review of existing experimental data is summarized in FIGURE 1 (Appendix A). The relation between lift and depth in the form required in the differential

equations is derived from FIGURE 1 and presented in FIGURE 2.

Next a study is made of the conditions under which cavitation and ventilation will probably occur, and the important relations are presented in design form in FIGURE 3.

The characteristics of ocean waves are reviewed, and the relations pertinent to the motions of hydrofoil systems in waves are presented in Equations 2, 3, and 4, and FIGURE 4.

The General Equations of Motion of a Hydrofoil System having Two-Degrees of Freedom -- to rise and to pitch -- are derived on PLATE 1. Several approximate preliminary analyses are made of these equations, including linearization and reduction to one degree of freedom.

Next, the method of solving the non-linear, two-degree-of-freedom equations by means of an electronic differential analyzer is described. A typical analyzer solution to the equations is pictured in PLATES 5 and 6, which show the striking difference between the transient and steady-state performance of hydrofoil systems.

Finally, the results of about 450 solutions to the non-linear equations are presented, and a number of conclusions are reached.

It is found that is is of paramount importance to use the deepest hydrofoils permissible -- at least as deep as the height of the largest waves to be traversed where-

ever possible. The largest possible ratio of boat-length to chord-size and the smallest ratio of radius of gyration to boat-length should be used.

It is shown that as the speed of a hydrofoil system is increased, its stability is reduced and its susceptability to cavitation and ventilation increased, so that careful design of the load distribution on the hydrofoils is of critical importance at high speeds.

The permissible loading per unit area of the hydrofoils depends upon speed, approximately as follows: below 30 feet per second -- less than 300 pounds per square foot; 30 to 80 fps -- between 200 and 1000 psf; over 80 fps -- between 400 and 700 psf.

It is found that the transient performance of a hydrofoil system entering a wave near its crest is very much worse than its steady-state performance (This fact is evident from PLATES 5 and 6.)

If the ratio of boat-length to wave-length is small (less than .1) the motions are more stable, but the dynamic hydrofoil loadings are worse than if the ratio is near .5.

At low frequencies of wave-encounter (near resonance for the system) the stability of the motions improves, but the dynamic loadings and accelerations become worse as frequency is increased. At very high frequencies the motions and loadings become nearly independent of the frequency of encounter. Travel directly upwind is there-

foreto be preferred at high speed.

It is concluded that at moderately high speeds (up to 80 feet per second) a rigid hydrofoil system traveling in waves having a height which is less than running depth of the system should exhibit good stability and smooth performance. In larger waves the system will probably undergo transient motions of intolerable character. At higher speeds automatic incidence control may be necessary.

CHAPTER I

INTRODUCTION

General Description and History:

A hydrofoil boat is one whose hull is supported in motion clear of the surface of the water by a system of underwater wings -- called hydrofoils -- which obtain their lifting force in the same manner as the airfoil wings of an airplane.

Some confusion frequently arises between the terms "hydrofoil" and "hydroplane". Actually the operation of these two devices is quite different. Hydroplanes skim the surface of the water and obtain a lifting force by assuming a relatively large angle of incidence with respect to the water surface, which consequently exerts a large pressure on the hull bottom (Fig. 1-1a). Hydrofoils, on the other hand, operate well below the water surface, with a very small angle of incidence (Fig. 1-1b). Like ordinary airfoils, they obtain a large percentage of their lifting force from the creation of a low pressure on their upper surface, and very little from increased pressure below.

In theory, hydrofoil boats offer two marked advantages over planing hulls: (1) they should be considerably more efficient, and (2) they should produce a much smoother ride in waves.

The idea of supporting water craft on hydrofoils has held strong appeal for a number of scientists and

inventors for many years.

The first recorded experiments were those of an Italian inventor named Forlanini, in 1905[1]. (It is recalled that the first successful flight at Kitty Hawk took place in 1903.) Forlanini used a lattice-work of hydrofoils resembling a venetian blind (see Fig. 1-2a). This boat was reported to be perfectly stable, and to give a considerably smoother ride than a planing hull. It is suspected that it was not very efficient.

Shortly after Forlanini's tests another Italian, Col. Crocco, constructed a boat using the system shown in Fig. 1-2b[1]. This system was probably more efficient, but was quite unstable.

In 1911 a remarkable step forward was taken by Guidoni, who built and flew a seaplane which took off and landed on sets of hydrofoils instead of pontoons (Fig. 1-2c)[1]. He reported that landings in waves were much smoother and steadier. Furthermore, he was able to use smaller, lighter floats of much improved aerodynamic shape, because the hydrofoils made a planing bottom unnecessary.

In 1919 Alexander Graham Bell built a hydrofoil

---

[1] Reference 1.

boat, called the HD-4, which was specifically designed for high speed and stability.[1] He used a "tricycle" arrangement of three sets of foils having slight dihedral, and stacked, ladder-wise. (See Fig. 1-2d). This boat was powered by two 320 hp Liberty aircraft engines driving air propellors, and reportedly achieved a top speed of 70 mph. It was entirely stable and extremely maneuverable under all sea conditions tried. (On one occasion it recovered gracefully from a high-speed collision with a lobster-pot.)

The HD-4 achieved its exceptional speed (for that period) by means of a preponderance of power. It is doubted that its high-speed efficiency was very great. (Calculations based on the information available indicate that the ratio of the lift to drag at top speed was about 4. This calculation includes air drag. At cruising speeds the efficiency was undoubtedly better.)

In 1932 Dr. O. Tietjens made preliminary tests at Philadelphia on a motorboat-sized model of the system shown in Fig. 1-2e.[2] This system was designed for efficiency and high speed, and was very much cleaner than its ladder type predecessors. (It is noted that it bears some resemblence to the unsuccessful Crocco system of

---

[1] Reference 2.

[2] Reference 3.

Fig. I-2b.)

The results of the tests at Philadelphia are not clear, but during the recent war hydrofoil boats of the PT-type were built in Germany in sizes 2, 11-1/2, and 80 tons[1]. The first two sizes employed the same Tietjens system shown in Figure I-2c. Unstable performance has been reported.

It is noted that in all of the hydrofoil systems so far discussed the foils are so arranged that an increase in depth is accompanied by an increase in the amount of hydrofoil area submerged. (e.g. in the Forlanini system additional foils are submerged, while in the Tietjens system an additional section of the dihedral part of the hydrofoil is submerged.) The purpose of this arrangement is of course so that a constant altitude (with respect to the water surface) can be stably maintained: if the boat becomes displaced from its equilibrium level a restoring force due to a change in area is automatically set up.

The use of area-variation has frequently been found to have two undesirable results, particularly at high speed: (1) the large wake which may be produced by a lifting hydrofoil piercing the water surface may seriously impair efficiency; and (2) a ventilation of the entire foil may

[1] Reference 4.

occur, causing unstable dipping. The latter effect is discussed in detail in Chapter III.

For the above reasons it may be necessary to use hydrofoils which are completely submerged at all times, and which are maintained at a desired depth by controlling their angle of attack, or incidence, with respect to the direction of travel.

In 1937, V. Grunberg published a paper[1] in France proposing (for the first time, to the author's knowledge) a very simple method of automatically controlling the angle of attack which is shown in Fig. 1-2f. The operating principle of the system is evident; the entire boat pivots about the forward planing surface, so that if the center of gravity is depressed the angle of attack of the hydrofoil is increased, causing a restoring force.

This system has performed very well in tests in the NACA's towing tank at Langley Field. (A commercial motorboat version of the system is currently being prepared for market in Sweden[2].) However, by using a rigid planing surface forward, the system loses some of the independence of water-surface roughness which "pure" hydrofoil systems may have. Instead, the planing surfaces may transmit a considerable buffeting to the hull in waves.

---

[1] Reference 5.

[2] Reference 6.

A more refined incidence-controlled system has been developed recently by C. Hook[1], of England. This system is shown in Fig. I-2g, and is discussed more fully in Chapter V, Part II.

The NACA Towing Tank Group at Langley Field, Va., has undertaken a number of projects to secure additional data on various phases of hydrofoil performance.[2] One of their main objectives has been to study the possibility of using hydrofoils to assist the take-off of flying boats. Several aircraft companies have also attempted to attach hydrofoils to full-size flying boats, but so far the only known successful hydrofoil-assisted take-offs have been those of Guidoni in 1911.

Activity in the field of hydrofoil development has been steadily increasing in recent years. The application of hydrofoil systems to pleasure boats - motor-powered and sail - and to military craft of several types has been proposed.

With this increase in activity, a corresponding need for more hydrofoil information has developed. It is hoped that the present thesis may help to formulate a small segment of that information.

---

[1] Information on Mr. Hook's craft may be obtained by addressing C. Hook, Cowes, Isle of Wight, British Isles.

[2] References 7, 8, 9, 10, 11. Some theoretical work done by the NACA and reported in Reference 12 will be discussed in Chapter VII.

Statement of the Problem:

Some of the major obstructions to the development of satisfactory hydrofoil craft can be deduced from the proceeding historical account.

First, it appears that the two principle advantages of using a hydrofoil system - improved stability, and improved efficiency - have been more or less incompatible. This can be seen by comparing the first two hydrofoil boats made (Figs. I-2a and b), or by comparing the largest and fastest two that have been built (The HD-4 of Dr. Bell and the German PT-types, Figs. 1-2d and e). In each case the first boat was a ladder type which was stable but inefficient, while the second was a monoplane which was efficient but unstable.

Of the two basic problems in hydrofoil development, this thesis deals with the first; the problem of obtaining stable performance. However, an important concession is made to efficiency at the outset, in that the study is confined to monoplane systems.

It might be thought curious that in nearly forty years of development there has been no successful repetition of Guidoni's hydrofoil seaplane. It is certainly to be wondered that the tremendous strides in aircraft technology have not excited even remotely comparible advances in hydrofoil development.

It is believed that the principle reason for this situation lies with some important differences between the water and air media, and in the marked decrease in

the quality of performance of hydrofoil craft at high speeds. These factors will be introduced in the next section, and will be carefully studied in the chapters that follow.

Approach to the Problem:

The analogy between hydrofoil craft and airplanes is of course valid and extremely useful. There are, however, certain important differences between the two which must be held responsible for the difference in their states of development.

The differences are first, that the hydrofoil craft travels at a free surface, and second, that it travels in a liquid medium.

To begin with, the free surface presents the hydrofoil craft with a competitor - the planing hull - which the airplane does not have. For this reason there has been much less necessity for hydrofoil development than for aircraft development. The free surface also places on the boat a much more stringent altitude requirement: changes in depth of a few feet may cause serious instabilities. Next, hydrofoils and appendages piercing the free surface are subject of the phenomenon of ventilation, which is a very serious threat to stability.

Because hydrofoils travel in a liquid medium, they are subject to the same problems of cavitation as are marine propellors, except that cavitation of a supporting

foil is generally more important than cavitation of a propelling foil.

The relations governing cavitation and ventilation will be developed on a quantitative basis in Chapter III. It will be found that they are basically high-speed phenomena. Furthermore, it will be shown in Chapter VII that the stability of the motions is also reduced at high speed.

It is the purpose of this thesis to study the theoretical motions and performance characteristics of rigid hydrofoil systems in surface waves, and particularly to study the limitations placed on hydrofoil operation at high speed.

The fundamental program consists of deriving the general equations of motion of a hydrofoil system, and then of solving the equations for the interesting ranges of all the variables involved.

The relationships between the lifting force on a hydrofoil element and location of the element with respect to the free surface are developed in Chapter II.

The limitations imposed on hydrofoil operation by cavitation and ventilation are investigated in Chapter III, while the important properties of ocean waves are presented in Chapter IV.

The general equations of motion are derived in Chapter V. Linearizations and other approximations are discussed, and a dimensional analysis is presented. Some

preliminary analyses of the equations are made in Chapter VI, and the method employed to solve the general non-linear equations is explained.

Finally, in Chapter VII, the results of about 450 solutions to the non-linear equations of motion of a hydrofoil system having two degrees of freedom are presented. A number of conclusions are drawn from these solutions in Chapter VIII.

HYDROPLANE
(a)

HYDROFOIL BOAT
(b)

FIGURE I-1

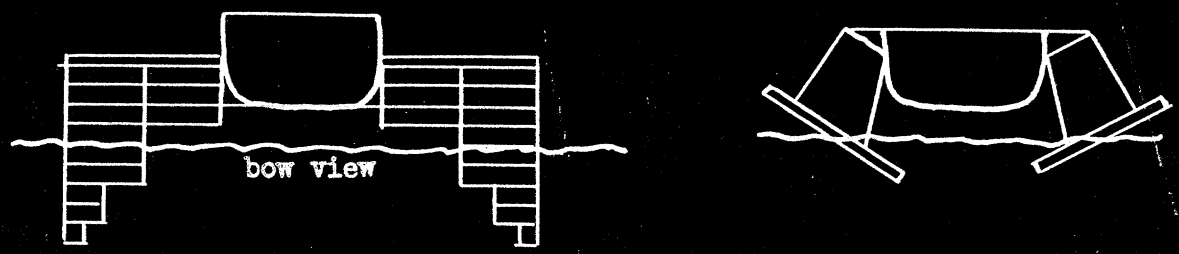

FORLANINI
(1905)

(a)

CROCCO
(1908)
(
(b)

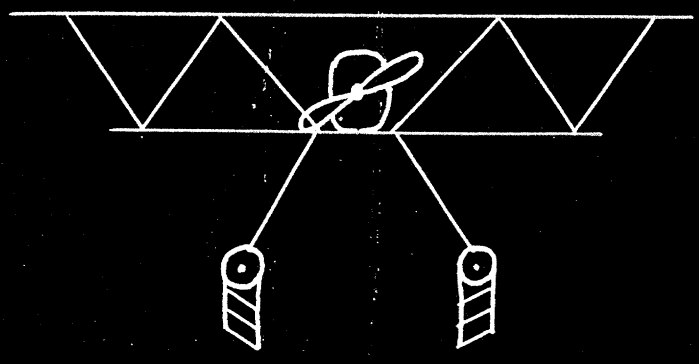

GUIDONI
(1911)
(c)

FIGURE I-2

FIGURE I*2 (continued)

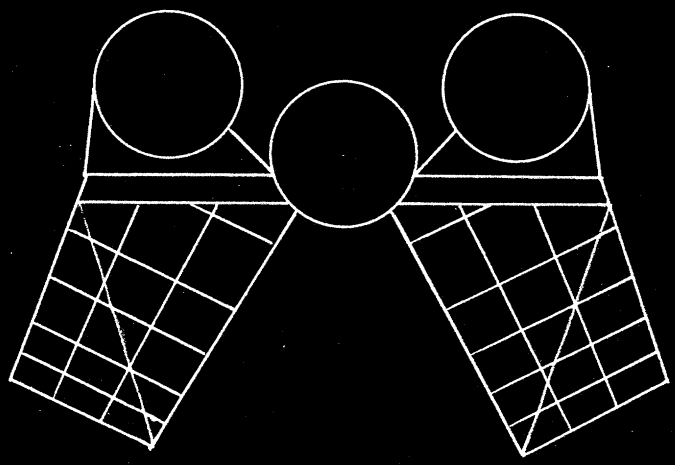

BELL
(1919)
(d)

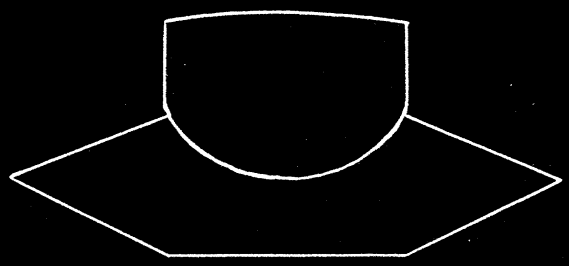

TIETJENS
(1933)

(e)

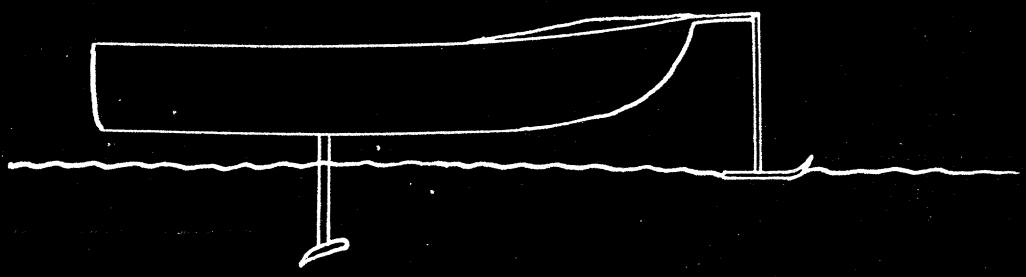

Grunberg
(1937)
(f)

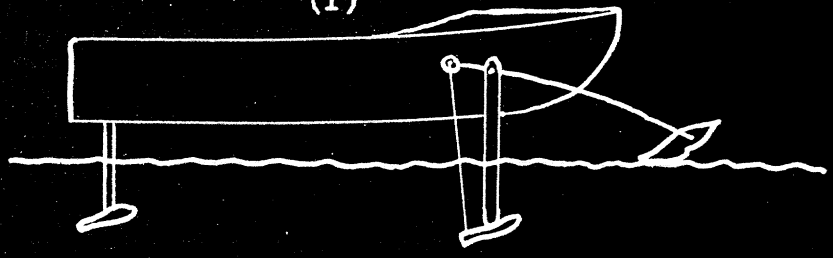

HOOK
(Current)

CHAPTER II

LIFT ON HYDROFOILS NEAR A FREE SURFACE

A. Introduction

In order to write the equations of motion of a hydrofoil system it is necessary to be able to compute the lifting force on each hydrofoil at any instant.

The lift on a hydrofoil may be expressed in the same form as that on an airfoil:

$$L = C_L S \frac{\rho}{2} V^2$$

In applying the relation, however, two important differences between airfoils and hydrofoils must be kept in mind. First, the area S may be a variable (depending on depth) for a hydrofoil. Second, the lift coefficient depends on orientation with respect to the free surface, as well as on angle of attack and the other quantities familiar in aerodynamic studies.

The quantities affecting the lift coefficient of a hydrofoil will now be discussed in turn.

Angle of Attack:

(Throughout this thesis, angle of attack is measured from the angle of zero lift, unless otherwise specified.)

It has been shown experimentally (see page 27) that the relation between lift coefficient and angle of attack for a hydrofoil (near a free surface) is similar to that of

an airfoil: the lift coefficient is exactly proportional to the angle of attack over a limited range. The constant of proportionality is denoted by a.

Profile:

The foil profile determines what the chordwise pressure distribution on the foil will be at various angles of attack. The pressure distribution in turn affects the limit of the proportional range between C_L and α. It also helps determine the point at which cavitation and/or ventilation will commence. Within the proportional range, however, the foil profile does not affect a.

Plan Shape:

As with an airfoil, a is a strong function of the ratio of foil length to chord, or aspect ratio, A. Such other plan shape characteristics as sweep-back, taper, curved edges, etc. also affect the value of a. However, in the present study only straight, rectangular foils are considered. Thus the aspect ratio, A, specifies the plan shape completely. The important relation between a and A will be developed.

Elevation Shape:

In the present study only single, symmetrical, straight (untapered and unswept) dihedral foils are considered. Thus, the dihedral angle, Γ, and the aspect ratio, A, completely define the elevation shape. (Note: A is always based on projected length, i.e. length as

seen in a plan view.) γ has some affect on a, especially near a free surface.

Free Surface:

The presence of a free surface above a hydrofoil is known to decrease the lift on the foil. If the free surface is less than two chords away, the decrease is substantial. Enough theory will be presented to help explain this decrease (page 20). Experimental measurements of the decrease will also be reviewed (page 26).

Lift coefficient, C_L, is proportional to angle of attack. Angle of attack is measured from the zero-lift angle. The constant of proportionality, a, is a function of aspect ratio, A, dihedral angle, γ, and depth of submergence, h. For a given depth and dihedral angle, the effect of A on the $C_L - \alpha$ relation is qualitatively the same as for an airfoil, as demonstrated in figure II-1.

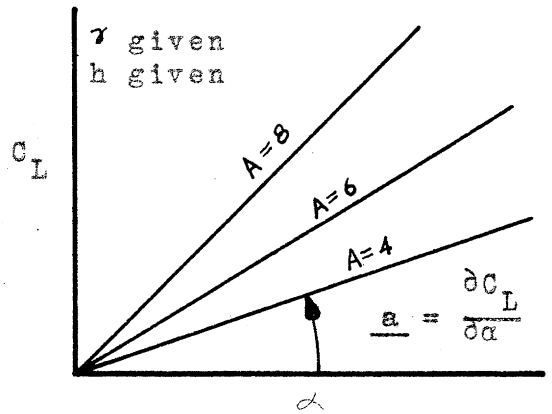

Figure II-1

In the dynamic analysis of this thesis, only two dihedral angles are considered: 0° and 30°. Further, when $\gamma = 30^\circ$, the tips are considered to emerge from the water always. Therefore, when $\gamma = 30^\circ$, A is a function of h only (figure II-2); when $\gamma = 0^\circ$, A is fixed.

A review of the equation for lift:

$$L = C_L S \frac{\rho}{2} V^2$$

now shows that the first term, C_L is a function of α, $\underline{a}$, γ and h. The second term, S, is a function of h and γ or is fixed. The analysis will be simplified if the terms are regrouped so that for fixed γ each is a function of α or h only. This can be done by noting that $\frac{C_L}{\alpha} = \frac{\partial C_L}{\partial \alpha} = \underline{a}$ is a function of h only. Therefore $\frac{C_L}{\alpha} S$ is also a function of h only. Now, with the lift equation in the form:

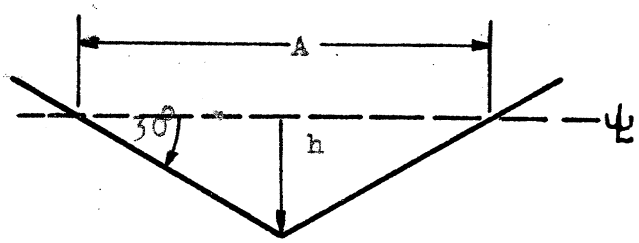

Front View

Figure II-2

$$L = \left(\frac{C_L}{\alpha} S\right)\alpha \frac{\rho}{2} V^2$$

the first term is a function of h only and the second, of α only. The group $\frac{C_L}{\alpha} S$ has been given the symbol σ.

It is the main purpose of Chapter II to evolve the important relation between σ and $\underline{h}$ for $\gamma = 0^\circ$ and $\gamma = 30^\circ$.

B. Theory

Exact Theory:

It is found that an exact theory of lift for a dihedral hydrofoil near a free surface is extremely complicated and would be laborious to formulate. It is believed that the purpose of this thesis can be accomplished

on the basis of the available experimental data. The development of an exact theory has therefore been considered unwarrented.

However, by making some convenient assumptions, an approximate theory can be developed which will be valuable in helping to explain the mechanism by which a decrease in lift occurs near the free surface. The theory will be based on the well-known vortex-image method. To this end the vortex theory will be briefly reviewed.[1]

Vortex Theory

According to the Kutta-Joukowski theory the effect of an airfoil on the surrounding fluid can be thought of as being produced by a circulation, Γ superimposed on the uniform flow of velocity V. The lifting force, L, on the foil is then related to the circulation by:

$$d_L = \rho V \Gamma \, d\ell$$

($d\ell$ is the increment of span.) The above relation leads to the following expression for the lift coefficient:

$$c_L = \frac{2\Gamma}{Vc}$$

The velocity induced at any point in the flow is perpendicular to a line from the center of Γ , and is of magnitude:

$$v = \frac{\Gamma}{2\pi r}$$

---

[1] For a complete treatment of the theory see, for example, reference 13 .

where r is the distance from the center of Γ .

In the exact theory a given foil is replaced by a system of vortices, whose total circulation is Γ . In the approximate theory, which will be used here, the foil is replaced by a single vortex at its center of pressure.

Vortex Image Method:

A method of studying the lift of a hydrofoil near a free surface is suggested by the well-known solution to the similar problem of the effects of wind-tunnel walls on airfoils being tested. The method consists of meeting the conditions at a boundary by imagining a mirror image of the airfoil vortex to exist on the other side of the boundary. The boundary conditions imposed by a free water surface will now be investigated.

Consider a hydrofoil at depth h,[1] and angle of attack α (Figure II-3). Let this α correspond to a lift coefficient of C_{L_∞} at infinite depth. The lift coefficient at depth h is to be found.

By the approximate vortex theory (above) the foil may be replaced by a vortex having circulation $\Gamma = \frac{Vc}{2} \times C_L$. "c" is the chord and C_L is the (undetermined) lift coefficient.

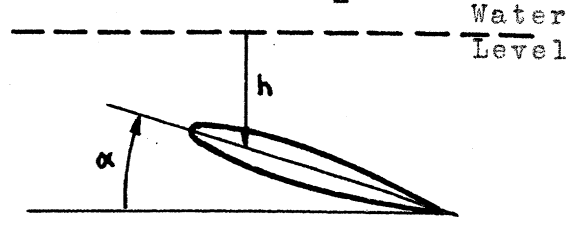

Figure II-3

[1] All lengths are measured in chords of the foil.

The pressure at all points of the free surface must be atmospheric. This places certain requirements on the free surface which may be obtained by writing the Bernoulli Equation for two points in the free surface (which is a streamline). One point is just above the foil, and the other is at an infinite distance in the approaching flow ahead of the foil. Bernoulli's Equation may be applied because the flow is steady, incompressible, and inviscid. The equation states that the sum of the pressure "head", velocity "head" and elevation must be the same for the two points. The entire surface is at atmospheric pressure and the surface elevation will change very little. Therefore, as a first approximation the surface will be considered flat so that the velocity at the surface will be constant.

Consider a point in the (flat) free surface at a distance x upstream (see figure II-4.). A velocity v_r is induced at this point by the circulation, Γ . This has a horizontal component, $v_r \sin \theta$, which increases the velocity, V, along the streamline. But according to the above analysis V must be constant. This contingency is met by assuming an image vortex of strength Γ to be located a distance h above the free surface. (The new vortex has the same direction of rotation as the original vortex.[1])

[1] In the problem of calculating wind-tunnel wall effects the velocity perpendicular to the streamline at the boundary must be zero, and the image vortex therefore rotates in the opposite direction from the original vortex.

The image vortex produces a velocity $\bar{v}_i$ at the point under observation. $\bar{v}_i$ has a horizontal component equal and opposite to that of v_r. The condition of constant (horizontal) surface velocity is thus upheld.

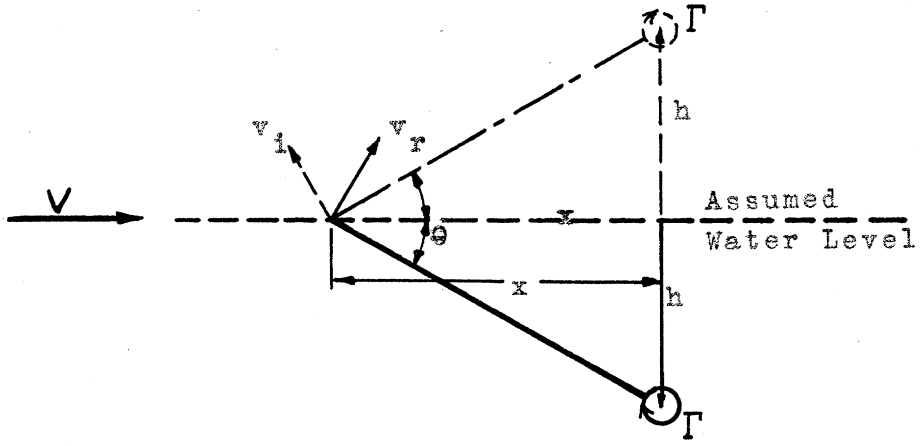

Figure II-4

It is noticed that the pair of vortices in figure II-4 represents a flow pattern analogous to that about a biplane. Because biplane theory has been considerably developed[1], this analogue is instructive in understanding the mechanism by which lift is decreased.

The presence of the image vortex (representing the free surface) has three principle effects upon the flow around the real vortex (representing the hydrofoil): (1) it causes velocities having horizontal components in a direction opposite to V; (2) these same velocities have ver-

---

[1] Reference 13 , page 171

tical components which in effect curve the streamlines (around the hydrofoil) downward; (3) the "bound" image vortex, and (in the case of finite foil length) the trailing vortex system, both cause additional downwash behind the hydrofoil. All three effects tend to decrease lift. (The effects must of course be considered simultaneously.)

The presence of free surface therefore effects a decrease in the lift on a hydrofoil by causing (1) a decrease in the velocity of flow over the hydrofoil, (2) a downward-curving of the streamlines around the foil, and (3) an increase in downwash behind the foil.

For purely instructional purposes the biplane theory was applied to a flat hydrofoil with aspect ratio 6. These calculated results are compared with experimental data in figure II-7a (Appendix B). The agreement is good over the range of available data. (The measured values of $\underline{a}$ are consistently somewhat lower than the theoretical.)

Actually the free surface could not remain flat under the action of the pair of vortices, because the vertical components of v_i and v_r add, to give the surface a net upward velocity at all points upstream of the foil (and downward at all points downstream). (The amount of surface distortion has been observed by the author and others to be of the order of one-half chord.)

For a more refined analysis based on the vortex image method a more elaborate vortex system would need to

be developed - probably in three dimensions. The deflection of the free surface should certainly be taken into account.

Closure:

The purpose of inserting the theory at this point was to provide a vehicle for explaining the loss of lift near a free surface.

Values of the lift parameters for use in the dynamic analysis will be based on the experimental data reviewed in the next section.

C. Experiment

Available Data:

Excellent data have been taken at the NACA Towing Tank on the characteristics of hydrofoils near a free surface.[1] Measurements of lift and drag were made over an angle of attack range of -6° to $+ 12^\circ$ and a speed range of twenty to eighty feet per second. These measurements were made for six foil sections, four dihedral angles (0°, 10°, 20°, 30°), and over a depth range from one-quarter chord to five chords. The author has made less precise observations on 45° - dihedral foils. A comparitive summary of these results is given in FIGURE 1, Appndx.A. The method of computing the results in FIGURE 1 will now be discussed.

---

[1] References 7 and 8.

The NACA lift data are presented in the manner shown in Figure II-5[1](Appndx.B). The point where upper surface cavitation first appeared is marked with an arrow.

In general the curves are seen to be horizontal straight lines until some point after the arrow. Then they bend downward. At high angles of attack the lift curve is erratic. Mr. James Benson, who directed the second set of tests, states that the erratic behavior at high α is due to the foil being ventilated in varying degree (see Chapter III). The highest points correspond to the least ventilation.

Development of Data for Analytical Use:

On page 20 it was explained that the relation necessary for solving the dynamic equations is $\frac{C_L}{\alpha} S$ as a function of depth, h. The first step in obtaining this form is to replot figure II-5 in the form C_L vs α. These results are shown in figure II-6, (Appndx. B.). The slope $\frac{\partial C_L}{\partial \alpha} = \frac{C_L}{\alpha}$ is desired. It is obtained by drawing the best straight line through the points. (In drawing this line a careful averaging process was used, with weight being given to the angle of zero lift as found from wind tunnel measurements on the same foil section.)

The next step is to plot $\frac{C_L}{\alpha}$ as a function of depth, h. A sample of this plot is shown in figure II-7.

---

[1] For dihedral foils the lift coefficient, C_L, is based on projected area.

In the same figure is plotted the theoretical value of $\frac{C_L}{\alpha}$ for a rectangular foil at infinite depth and having the same aspect ratio as the experimental foil.

Some special consideration must be given to the dihedral foils in comparing them with flat foils. First the angle of attack of all foils was measured by measuring the strut angle. The angle thus obtained is presented in the NACA data. This is also the angle which is applicable to the dynamic analysis. It differs, however, from the true angle of attack at which the foil profile is operating. The relation between true angle of attack, α_t and the measured angle of attack, α, is found to be $\alpha_t = \alpha \cos \gamma$. ($\gamma$ is the dihedral angle.) In making the comparison in FIGURE 1 true angle α_t was used. In all other parts of this thesis the angle of attack is measured in the vertical plane - i.e. it is synonymous with strut angle.

Another question which arises in dealing with dihedral foils is what dimension should be used as a measure of depth. In the dynamic analysis it will be found convenient to use arbitrarily the depth h to the lowest point as shown in figure II-8. In making the comparison with flat foils, however, the average depth, h_{av}, was used.

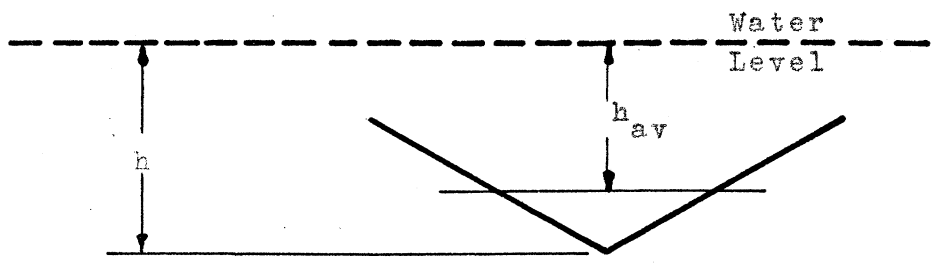

Figure II-8

There is one more step which should be taken to facilitate comparison of dihedral foils with flat foils. The nominal aspect ratio of all foils in the NACA tests was 6. But when dihedral foils approached the free surface their tips emerged, and the area and aspect ratio were decreased. To compare foils on the same area basis the NACA data has been converted so that the lift coefficient of dihedral foils is based on submerged, projected area[1]. To compare all foils on the same aspect ratio basis, the data have been replotted using the ratio of experimental $C_{L/\alpha}$ to the theoretical $C_{L/\alpha}$ for the same aspect ratio.

The ordinate in FIGURE 1 is the ratio, R_t, of $C_{L/\alpha}$ for experimental foils in shallow water to that for theoretical foils at infinite depth. The abcissa is average depth.

The curve in FIGURE 1 should, of course, approach the value 1.0 at large h_{av}. The two 23 series results are within a few percent of this at depth 5. But the 16-509 series foils all appear to be approaching a value of about .85. The reason for this discrepency will not be explored here. It is noted, however, that the conventional air foils with pressure distributed well forward approach closely the theoretical values. The experimental foils with nearly uniform pressure distribution do not.

---

[1] The conversion has been made in all calculations in this thesis.

Because of cavitation and ventilation limitations (Chapter III) it is probable that all hydrofoils developed will have approximately uniform pressure distribution. Other profile details will vary with the designer and the course of new research.

Foil profile will not be a variable in this study.

A hydrofoil profile, on which sufficiently complete data are available, is the 16-509 foil. Moreover, it is a uniform-pressure-distribution foil. The dynamic analysis will therefore be based on this data.

The data in FIGURE 1 will not be put in the form directly applicable in the dynamic analysis. This form is $\sigma = \frac{C_L}{\alpha} S$ as a function of h.

Flat Foils

For $\Upsilon = 0$, S is constant. The desired relation is thus obtained immediately from FIGURE 1 by multiplying R_t by 4.54.

Dihedral Foils

In the dihedral case the tips will always be considered to pierce the water surface. S is therefore a function of h: $S = 2h \cot \Upsilon$. A problem of extrapolation arises because the experimental data are for foils which have a constant area (S = 6 square chords) for depths greater than h = 1.73.

The method of extrapolation is explained in Appendix C . Briefly, the effects of aspect ratio, average depth, and surface piercing are evaluated,

and the value of σ at $h = 5$ for a foil whose tips pierce the surface is estimated. The estimation is based on data for a completely submerged foil of aspect ratio 6.

A plot of σ vs. h is given in FIGURE 2. This plot is based on a large amount of carefully analyzed data, for depths to 1.73 chords. It is based on extrapolated data for depths greater than 1.73 chords.

Approximation to FIGURE 2:

In the dynamic calculations of the present study it has been necessary to approximate the curved black line in FIGURE 2 (Appx. A) by the red, straight line. The error involved in this approximation is shown in figure II-9.

It is noted that replacing the black curve in FIGURE 2 by the red curve could be thought of as an assumption that the upper δ chords of water are entirely absent. (In this case, $\delta = .4$ chords.) This point of view will be found quite convenient in the dynamic analysis.

FIGURE 2 has been used as the basis for all of the dynamic analysis of variable-area hydrofoil systems in this thesis.

D. Summary

As part of the dynamic analysis of hydrofoil systems a thorough knowledge of the lifting properties of hydrofoils will be needed. In particular it will be nec-

essary to know the value of the quantity $\sigma = \frac{C_L}{\alpha} S$ under all conditions of operation.

The important factors affecting σ are dihedral (γ) and proximity to the free surface (h).

A theoretical investigation shows that the effect of the free surface is to bend the free streamlines downward near the hydrofoil, decrease the local velocity of flow past the hydrofoil, and increase the downwash at the trailing edge. All three effects contribute to a reduction in lift as the hydrofoil approaches the free surface.

The theory also shows that the degree of effect of the free surface on a hydrofoil depends upon the number of chords below the free surface at which the foil is operating.

The NACA hydrofoil test-data have been most useful. These data have been developed for use in the dynamic analysis and are presented as FIGURES 1 and 2. The accuracy of straight-line approximations to these curves is investigated and the conclusions shown in figure II-9.

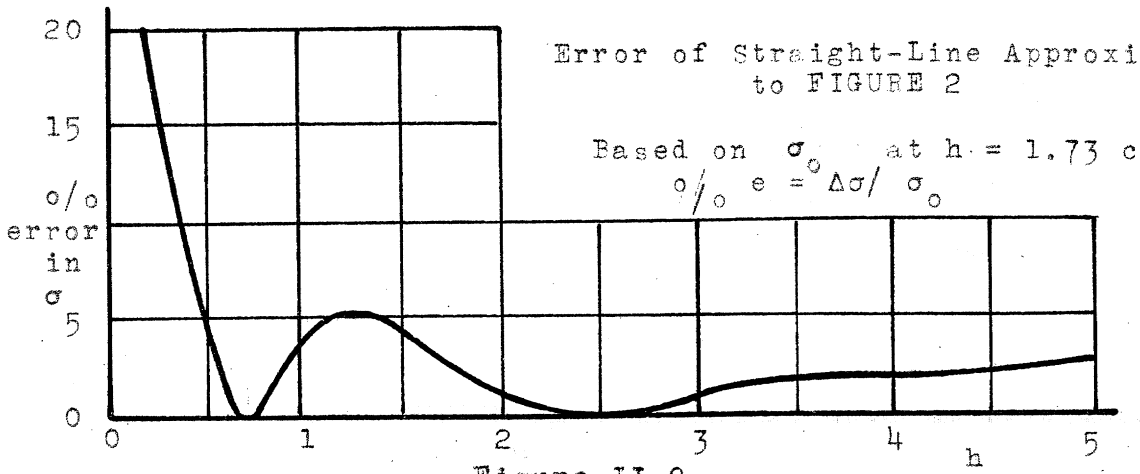

Figure II-9

CHAPTER III

CAVITATION AND VENTILATION

A. Introduction

Cavitation:

The phenomenon of cavitation on underwater lifting surfaces (particularly marine propellors) has been the subject of many theoretical and experimental investigations. Briefly, the mechanism is as follows: when the local pressure at some point on the surface of a hydrofoil becomes lower than the vapor pressure of the water at that point, water evaporates, forming small bubbles of vapor. As the bubbles grow, the pressure near them is increased, and they are caused to collapse. This process of growth and collapse recurs with very high frequency, and causes fluctuations in the lift and drag forces on the hydrofoil. Under some conditions these fluctuations may be a source of serious instability of motion. They also result in decreased efficiency and damaged foil surfaces.

Ventilation:

Of considerably greater danger to stability (in the author's opinion) is the phenomenon of ventilation. This consists of air being sucked from above the free water-surface down onto the upper surface of the hydrofoil. The air is usually observed to be sucked down in

gulps, so that the upper hydrofoil surface pressure is suddenly increased locally. The resulting reduction in total lift causes a sudden dipping of the foil. The foil may persist in its new location, or the flow may re-establish itself at the ventilated point, and the foil return to its original level. The total result is an erratic jumping from one level of operation to another (i.e. from one lift coefficient to another).

From static equilibrium conditions alone it is clear that the possibility of ventilation exists whenever the pressure at any point on a foil becomes lower than the atmospheric pressure on the water surface - i.e. practically all the time, but experience shows that well designed hydrofoils will not ventilate until a very much lower pressure is reached.

At this time the mechanism of ventilation is not well understood. A comprehensive theoretical and experimental study of the conditions under which ventilation is likely to occur would form an important contribution to hydrofoil development.

There are, however, a few experimental observations of ventilation available, which will be discussed in part C of this chapter.

The incipience of ventilation certainly depends upon the depth of the foil beneath the water surface, and upon the manner in which the foil pierces the surface.

But it also depends greatly upon the local pressure along the upper hydrofoil surface. To this extent it is a phenomenon similar to cavitation. A careful study of cavitation conditions should therefore be helpful in evaluating the probability of ventilation.

One objective of the present thesis is to study all motion characteristics which might contribute to ventilation and cavitation. The purpose of this chapter is to investigate what characteristics are important.

B. Theory

Prediction of cavitation conditions:

Cavitation is expected to occur when the local pressure (on the upper surface of the foil) becomes as low as the vapor pressure of the water:

$$(a) \quad p_u = p_v$$

It is more convenient to think of the "gage" pressures $p - p_a$, so that (a) may be written:

$$(b) \quad (p_a - p_u) = (p_a - p_v)$$

To learn what $(p_a - p_u)$ is, the average upper surface pressure will first be calculated. The chordwise and spanwise pressure distributions will then be investigated to find the maximum value of the ratio of local to average pressure, to which the symbol R_p is given:

$$(c) \quad R_p = \frac{(p_a - p_u)_{Local}}{(p_a - p_u)_{av.}}$$

The difference in upper and lower surface pressures is the loading per unit area:

$$(d) \quad (p_\ell)_{av.} - (p_u)_{av.} = L/S, \text{ or}$$

$$(p_a - p_u)_{av.} = L/S - (p_\ell - p_a)_{av.}$$

By substitution, equation (b) now becomes:

$$\left[R_p \, (p_a - p_u)_{av.}\right]_{cav} = (p_a - p_v)$$

or

$$(e) \quad [R_p] \cdot \left[(L/S)_{cav} - (p_\ell - p_a)_{av.}\right] = (p_a - p_v)$$

Equation (e) expresses the condition for cavitation to occur. The order of magnitude of the terms in (e) can be seen by dividing all terms by p_a and solving for the loading per unit area which will cause cavitation:

$$(1)\quad \left(\frac{L/S}{p_a}\right)_{cav} = \frac{1}{R_p}\left(1 - \frac{p_v}{p_a}\right) + \left(\frac{p_{\ell av}}{p_a} - 1\right)$$

For convenience of reference, the ratio L/S will be given the general symbol, $\sqsubset$, and will be called the "Cavitation Index". (It is different from the "cavitation number" used in hydraulic and marine engineering.) $\sqsubset$ has several convenient alternative forms, as follows:

$$\sqsubset = \frac{L/S}{p_a} = \frac{\frac{\rho}{2} C_L V^2}{p_a} = \frac{\frac{\rho}{2} C_{L_\alpha} V^2 \alpha}{p_a} = \frac{V^2}{2gH_w} .$$

H_w = 34 feet, the height of a water column which can be supported by atmospheric pressure.

Since the quantity $\sqsubset$ is easily calculated for a hydrofoil element, the purpose of this chapter takes the form of predicting the values of $\sqsubset_{cav}$, at which cavitation will begin.

Evaluation of $\sqsubset_{cav}$:

To avoid cavitation, R_p should be as small, and $\left(\frac{p_\ell}{p_a}\right)_{av}$ as large, as possible. Some of the terms in equation (1) can be approximated to good advantage.

The ratio $\frac{p_v}{p_a}$ is about 1/25 and may thus be

dropped (compared to 1) with small error. For a given depth, h, the last term in equation (1) may be written:

$$(f) \quad \frac{p_{\ell\,av}}{p_a} - 1 = \frac{p_{\ell\,av}}{p_o}\,\frac{p_o}{p_a} - 1 = \frac{p_{\ell\,av}}{p_o}\left(\frac{p_a + \gamma_w h}{p_a}\right) - 1 =$$

$$= \frac{p_{\ell\,av}}{p_o}\left(\gamma_w \frac{h}{p_a} + 1\right) - 1$$

$$(f) \quad \left(\frac{p_\ell}{p_a}\right)_{av} - 1 = \left(\frac{p_\ell}{p_o}\right)_{av}\left(\frac{\gamma_w h}{p_a} + 1\right) - 1,$$

where p_o is the free stream pressure.

For a hydrofoil at a depth of 3.4 feet, $\frac{\gamma_w h}{p_a} = .1$ which is also small, compared to 1. When the foil is operating near its design angle of attack, ratio $\left(\frac{p_\ell}{p_o}\right)_{av}$ varies approximately between .8 -- for nearly symmetrical foils with convex lower surfaces -- and 1.1 for foils with concave lower surfaces. Equation (1) may thus be written in the very approximate form:

$$(1') \quad \left(\frac{L/S}{p_a}\right)_{cav} \approx \frac{1}{R_p}$$

The ratio R_p may be considered (with little error) to be the product of two other ratios: r_c, representing chordwise pressure distribution, and r_s, representing spanwise pressure distribution. For a flat foil with elliptical spanwise pressure distribution, the ratio r_s is:

$$r_s = \frac{p_a - (p_u)}{p_a - (p_u)}_{min,\,av} = \left(\frac{p_a - p_u}{p_a - p_u}\right)_{max,\,av} = \frac{4}{\pi}$$

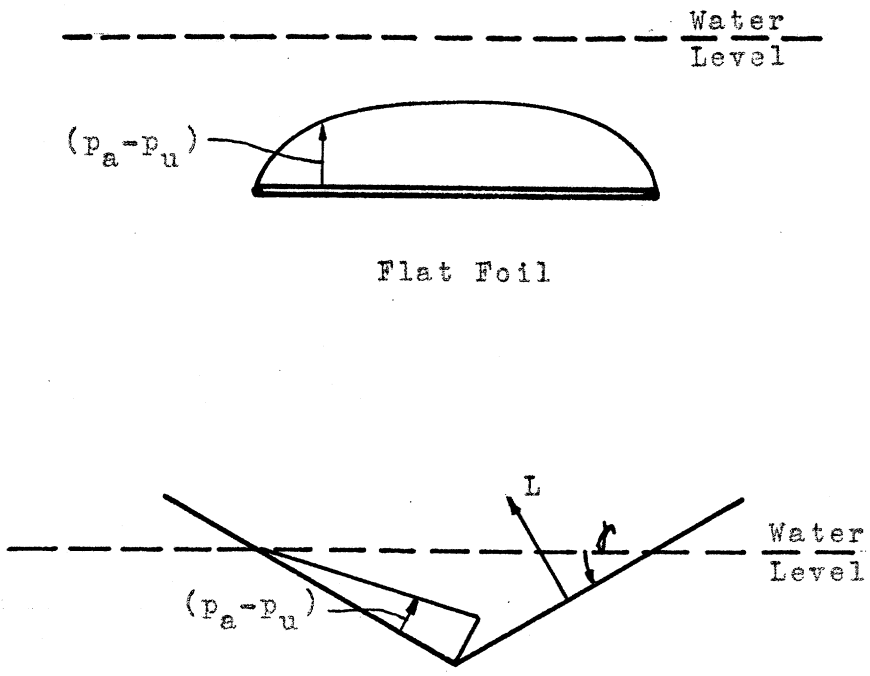

Figure III-1

For a dihedral foil the lift near the surface is greatly reduced, so that the pressure distribution may be nearly triangular (figure III-1) and $(p_a - p_u)_{max}$ may be nearly twice $(p_a - p_u)_{av}$; $r_s = 2$.

(Note: at first glance it appears that the load per unit area of a dihedral foil must be greater than that of a flat foil because the lifting forces are at angle γ with the vertical, and must be larger by sec γ . However, the foil area is also increased by sec γ , so that the ratio L/S is the same whether computed on the basis of true lift and true area or of vertical load and projected area.)

To make r_c as small as possible foil profiles giving nearly uniform pressure distributions are desired. Such foils have been quite thoroughly developed by the NACA for use at very high Mach numbers. It is possible, in fact, to attain values of r_c only slightly greater than 1.

To summarize: for flat hydrofoils operating at near their design lift coefficients $R_p = r_s r_c$ will be about 1.3. For dihedral foils R_p will be between 1.5 and 2.

By substituting into equation (1) the limiting values of each term (as discussed above) the range of values for σ_{cav} can be estimated:

$$\sigma_{cav} = \frac{L/S}{p_a}_{cav} \equiv \frac{1}{R_p}\left(1 - \frac{p_v}{p_a}\right) + \frac{p_{\ell\, av}}{p_o}\left(\frac{\gamma h}{p_a} + 1\right) - 1$$

$$\sigma_{cav\ largest} = \frac{1}{1.3}(.96) + 1.1\ (1.1) - 1 = .95$$

$$\sigma_{cav\ average} = \frac{1}{1.4}(.96) + 1.0\ (1) - 1 = .69$$

$$\sigma_{cav\ smallest} = \frac{1}{2}(.96) + .8\ (1) - 1 = .28$$

Effect of Varying Angle of Attack:

Thus far, the discussion has been limited to the case in which the foil is operating near its design angle-of-attack, so that a nearly uniform chordwise pressure

distribution becomes uneven, r_c increases, and the value of σ for which cavitation begins decreases markedly.

Application to Ventilation Conditions:

Since both cavitation and ventilation have very low pressure as their prime cause, the above discussion holds qualitatively in predicting the likelihood of ventilation. Particularly pertinent are the discussions of the importance of even pressure distribution and of the danger of operating at unfavorable angles of attack.

C. Experimental Data

Cavitation

During the NACA hydrofoil tests[1] careful observations were made of the onset of cavitation. The speed and lift coefficient were recorded each time cavitation was observed. (The method of recording is illustrated in figure II-5.) From these data the value of σ_{cav} can be calculated and a check on the foregoing theory can be obtained.

All of the cavitation data for the 16 - 509 section are shown in figure III-2 (page 210) for convenience of comparison. Some constant-speed lines are drawn in the figure. These are straight of course, because when V is constant L/S varies directly with C_L.

The general shape of all the curves coincides closely with what is expected from the theoretical discussion: near the design lift coefficient ($C_L = .5$) the value of σ_{cav} varies from .7 to .95 thus coinciding nicely with the theory. As C_L increases from the design value σ_{cav} drops rapidly to a value between .3 and .5 at $C_L \approx .7$.

The most favorable lift coefficient appears(in figure III-2) to be .4, rather than the design value, .5. It is interesting to note in this connection that when

---

[1] Reference 8. See also Fig. II - 5.

the same foil section was tested in the wind tunnel at its design angle of attack, it produced a lift coefficient of .42[1].

To show the separate effects of depth below the free surface and of dihedral the data of figure III-2 have been separated into plots for a single depth (III-3) and for varying depth with two different dihedral angles (III-4 and III-5).

No conclusions about the effect of dihedral on cavitation seem warranted by figure III-3. Similarly, in figure III-4 the data shows slight effect of depth on cavitation conditions for a flat foil. In figure III-5 the data seem to indicate that the shallow, dihedral foil (with tips breaking surface) is subject to earlier cavitation than the deep foil at high lift coefficients.

Consider again graph III-2. The performance of a 16-509 foil at a given speed can be studied conveniently by means of the constant speed lines. Suppose, for example that when the hydrofoil is operating in waves the angle of attack (and hence C_L) may vary up to a maximum of twice its normal, smooth-water value. Then the largest lift coefficient for which the hydrofoil should be set to avoid cavitation is shown by the red dotted line.

But the hydrofoil operation is efficient only when the lift coefficient is near the design value (in this

---

[1] Reference 14.

case $C_L \approx .5$) The 16-509 section is therefore useful only for slow speeds, say up to 40 ft per second. At higher speeds a lower-camber foil should be used (i.e. one having a lower design lift coefficient).

This speed limitation on the 16-509 foil is shown in another way in graph III-6. Here the cavitation-lift coefficient is plotted as a function of speed. For speeds above 75 feet per second it appears that the foil will cavitate regardless of C_L.

The NACA has developed complete families of airfoil profiles designed to give uniform chordwise pressure distribution[1]. One such family is the "16-series" of which the 16-509 is a member.

To extrapolate the data of figure III-2 for possible use in design at high speeds the average of the values of σ_{cav} in figure III-2 have been plotted in FIGURE 3, as a function of the ratio $\frac{C_L}{(C_L)_{design}}$ where $(C_L)_{design}$ is in this case .5. The lines of constant speed have been replaced by lines of constant σ_o

$$\sigma_o = (C_L)_{Design} \frac{V^2}{2gH_\omega} \quad .$$

An example of the use of FIGURE 3 will be given. Suppose that it is desired to operate a hydrofoil at a speed of 80 feet per sec. Suppose further that the true angle of attack in waves is expected to vary up to twice the angle set; (1) draw the red line representing $\frac{C_L}{C_{LD}}$ to

---

[1] Reference ibid.

be set. Decide upon the lowest value of $\frac{C_L}{C_{LD}}$ which can be used efficiently; for example, .8. The foil will then be operating along the dotted black line and will have $\sigma_o = .26$.

Then $(C_L)_D = \sigma_o \frac{2gH_w}{V^2} = .26 \frac{(64.4)(34)}{(80)^2} = .089$

and a 16-09--hydrofoil section should be used. The last two blanks will denote the thickness of the foil, which should be just as thin as strength requirements permit.

Ventilation Data:

Although it was not the purpose of any of the NACA tests to study ventilation, a small amount of information can be obtained from them. Whenever ventilation was sufficiently serious to cause double valued lift coefficients both values were noted in the data[1]. (Double-valued lift coefficients indicate that the hydrofoils were being intermittently ventilated, as explained on page 27.)

Figure III-7,Appndx B is a plot of some conditions under which double-valued lift coefficients were noted in reference 8. A plot of cavitation conditions for the same foil is also given.

The most startling feature of figureIII-7 is the preponderant effect of depth on ventilation. For completely submerged foils no ventilation was ever observed.

---

[1] The possibility of using the double-vlaued coefficients as an indication of ventilation was suggested to the author in talks with Dr. James M. Benson, who supervised the NACA tests.

Interpolation indicates that for depths greater than about 1.5 chords (with tips piercing the surface), cavitation is likely to occur sooner than ventilation. Operation of dihedral foils at depths shallower than 1/2 chord seems hardly worthwhile.

It is concluded that hydrofoils operated at depths greater than 1.5 chords and carefully designed to avoid cavitation will be reasonably safe also from ventilation. At lesserdepths good anti-cavitation design will still be the best way to prevent ventilation, but ventilation becomes increasingly likely as depth is decreased.

Ventilation of Completely Submerged Hydrofoils:

Because of serious limitations placed on hydrofoil operation by the phenomenon of ventilation a strong case can be made for the use of completely submerged foils, using automatic incidence control for stability. It might then be possible to operate the foils at a great depth with no part of any foil ever coming within ventilating range of the surface.

Effect of Struts:

For a completely submerged foil, strut design becomes important. Although it seems certain that a non-lifting strut would be much less likely to induce the entry of air onto a hydrofoil than a low-pressure lifting foil element which pierces the surface, the possibility

of strut ventilation should be given careful consideration.

An example of advanced anti-ventilation strut design is the (patented) arrangement used on the Hook "Hydrofin" (see Introduction, page 10.)

In this system the strut is well astern of the hydrofoil, the foil being fastened to the strut by its lower surface only (see figure III-8). With this arrangement it is ostensibly impossible for air to reach the upper low pressure surface of the hydrofoil by way of the strut.

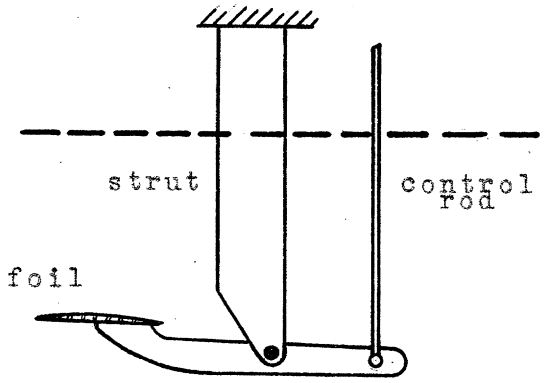

Figure III-8

D. Summary

Cavitation of hydrofoils - vaporization of water in low pressure regions - causes reduced efficiency and foil damage. It may result in serious instability of motion.

Ventilation of hydrofoils by air "sucked down" from the free surface is very dangerous to motion stability.

Since both cavitation and ventilation are primarily the result of very low-pressure regions, the two phenomena may be studied in parallel to good advantage.

The cavitation index, σ, is defined as the ratio of foil loading to atmospheric pressure:

$$\sigma = \frac{L/S}{p_a} = \frac{\left(\frac{\rho}{2}\frac{C_L}{\alpha}\right) V^2 \alpha}{p_a} = \frac{V^2}{2gH_w}$$

where:

L = total load on foil

S = foil area

p_a = atmospheric pressure

H_w = 34 feet.

For a well-designed hydrofoil operating near its design angle of attack, cavitation is expected when $\sigma = .7$. When a higher angle of attack is used, cavitation will occur for a much smaller value of σ (e.g., .3).

Many useful data are available on cavitation experiments. The results of some particularly pertinent tests on the NACA 16-509 hydrofoil are shown in figures III-2 through III-6, pages 211through 214 . These data do not

indicate conclusively the dependence of cavitation on either depth or dihedral. Foil-tip emergence appears to increase the likelihood of cavitation.

The available experimental cavitation information is summarized in FIGURE 3. These data are in concurrence with the result anticipated by the theory. It is believed that FIGURE 3 will be useful in design.

There is great need for a comprehensive set of experimental ventilation data. From the small amount of existing data it is concluded that:

(1) Ventilation is unlikely for fully submerged foils.

(2) For foils submerged to a depth of more than 1.5 chords, ventilation conditions can be safely predicted from cavitation considerations.

(3) For shallow foils ventilation is likely and unpredictable.

CHAPTER IV

OCEAN WAVES

A. Introduction

Complete theoretical treatment has been given the possible forms of water surface waves. In experimental tanks waves have been produced having -- within the accuracy of the measurements -- all the theoretically derived characteristics.

Many systematic obervations of waves on oceans and inland bodies of water have been recorded. These indicate that the waves actually occuring are made up of superpositions of endless combinations of the theoretically derived waves. One size is usually predominant, and the variation in wave shape is produced by addition and subtraction of smaller waves of varying velocities.

The problem pertinent to this thesis was that of choosing the characteristics of waves to which hydrofoil systems would be subjected in the proposed study. It was quickly decided that to used endless random wave shapes and sizes would be a cumbersome procedure at best. More important, it would have been impossible to trace the effect of the various wave parameters.

For directness and simplicity, therefore, pure waves having the theoretically derived characteristics were used, with sizes and steepness based on open water observations. The applicability of the results thus obtained will be discussed at the end of this chapter.

B. Wave Theory

Two slightly different schools of wave theory have developed. One, originated by Stokes, and developed by Rayleigh and Lamb, is based on the assumption of irrotational flow. The other, originated by Gerstner, is based on geometrical considerations, and permits rotation. The differences in wave characteristics given by the two methods are smaller than the accuracy required by the purposes of the present investigation.

However, it happens that the form in which the irrotational theory is presented by Stokes and Rayleigh is considerably easier to use mathematically. On the other hand the Gerstner rotational theory leads to a clearer physical picture, and is easier to interpret geometrically. It will therefore be convenient to review the results of both theories.

The results presented hold for deep water. It is true, of course, that in shallow water the wave characteristics become dependent on the depth. But for depths greater than one-quarter of a wave length the effect of the proximity of the bottom is less than the accuracy requirements of this study. Operation in such shallow water is expected to be much less important than deep-water operation, and has therefore been excluded from the present preliminary study.

Irrotational Theory:

Rayleigh[1] shows that, for irrotational, frictionless wave

---

1 Reference 15 , page 261

motion at a free surface of constant pressure above water of great depth, the shape of the free surface is given by:

$$\left(\frac{y}{b/2}\right)_{surf.} = \cos 2\pi \frac{x}{\lambda} - \tfrac{1}{2}\pi \frac{b}{\lambda} \cos 4\pi \frac{x}{\lambda} \quad 3/8\left(\frac{\pi b}{\lambda}\right)^2 \cos 6\pi \frac{x}{\lambda}$$

The velocity of the waves is:

$$C^2 = \frac{g\lambda}{2\pi} \left(1 + \frac{\pi^2 b^2}{\lambda^2}\right)$$

The horizontal and vertical components of the water particles in the waves (as derived from a velocity potential[1]) are:

$$\frac{u_p}{C} = \frac{\pi b}{\lambda}\left(1 - 5/8\ \frac{\pi^2 b^2}{\lambda^2}\right) e^{-\frac{2\pi y}{\lambda}} \cos 2\pi \frac{x}{\lambda}$$

$$\frac{v_p}{C} = -\frac{\pi b}{\lambda}\left(1 - 5/8\ \frac{\pi^2 b^2}{\lambda^2}\right) e^{-\frac{2\pi y}{\lambda}} \sin 2\pi \frac{x}{\lambda}$$

where: y is measured vertically downward from the mean wave height,

x is measured horizontally to the right,

u_p and v_p are "perturbation" velocities in the directions x and y,

b is the wave height, trough to crest,

C is the wave velocity.

The preceeding results are an approximation based on the assumption that $\left(\frac{\pi b}{\lambda}\right)^3$ is small enough to be neglected. If $\left(\frac{\pi b}{\lambda}\right)^3$ is taken

---

1 The potential function is: $\phi = -\frac{bC}{2}\left[1 - 5/8\left(\frac{\pi b}{\lambda}\right)^2\right] e^{-\frac{2\pi y}{\lambda}} \sin 2\pi \frac{x}{\lambda}$,

and $u = \frac{\partial \phi}{\partial x}$, $v = \frac{\partial \phi}{\partial y}$

into consideration, but $\left(\frac{\pi b}{\lambda}\right)^4$ neglected, Lamb[1] gives:

$$\left(\frac{y}{b/2}\right)_{surf.} = \cos 2\pi\frac{x}{\lambda} - \left[\frac{\pi}{2}\frac{b}{\lambda} \cdot \frac{17}{24}\left(\frac{\pi b}{\lambda}\right)^3\right]\cos 4\pi\frac{x}{\lambda}$$

$$3/8\left(\frac{\pi b}{\lambda}\right)^2 \cos 6\pi\frac{x}{\lambda} - 1/3\left(\frac{\pi b}{\lambda}\right)^3 \cos 8\pi\frac{x}{\lambda}$$

The quantities of interest in this thesis are the wave profile, the wave velocity (i.e. the velocity with which the wave as a whole moves), and the vertical component of the water-particle velocity. It will be more convenient to measure the height of a point on the wave profile positive upward from the trough. (The wave height so measured is given the symbol ζ.) Also, it will sometimes be convenient to measure x positive upwind, and sometimes positive downwind (to comply with the direction in which the hydrofoil system is traveling). The preceeding results are accordingly rearranged and presented as EQUATIONS (2), (3) and (4), in Appendix A.

Rotational Theory[2]

The mathematical formulae for wave profile as presented by the Gerstner rotational theory are more difficult to manipulate than those of Rayleigh. However, the resulting geometrical construction of the profile shape is more direct.

---

1 Reference 16 , page 418

2 Ibid, p. 421

Consider a cylinder of radius R rolling on a flat plane. (Fig. IV - 1). A concentric circle of diameter b is painted on the cylinder. The path described by a particular point p (on the circle) as the cylinder rolls will be a trochoid of total height b and wave-length $\lambda = 2\pi R$. This is the wave shape assumed by the Gerstner theory.

The paths of the water particles are next shown(on the basis of assumed rotation) to be closed circles of radius $r_o = \frac{b}{2} e^{\frac{2\pi y}{\lambda}}$ and frequency $f = C/\lambda$ cycles per second. (The particles "roll with the waves".) The magnitude of the velocity of a particle at any time is therefore given by: $|\vec{v}_p| = 2\pi r_o f$, which leads to the same expressions for horizontal and vertical components as the irrotational theory.

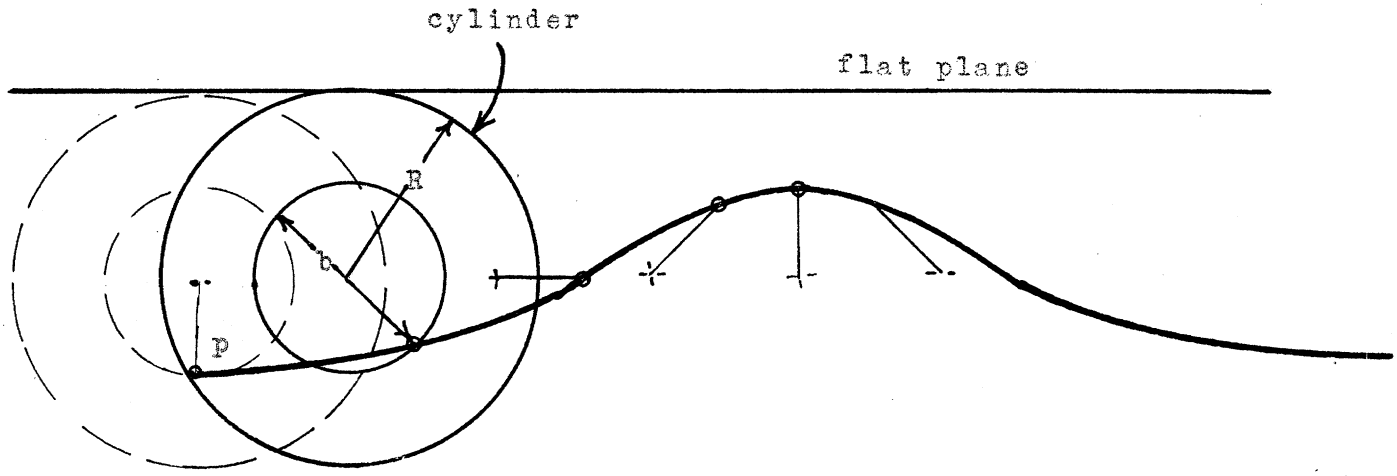

Generation of Trochoidal Wave Shape

Fig. IV - 1

C. Wave Experiments in Tanks

Reference 17 describes the results of systematic tests in an 85 foot by 14 foot tank of 4 foot depth. The purpose of the tests was to produce surface waves of permanent form, and to compare their characteristics with theoretical values. Measurements were made of wave length, height, velocity, period, profile, mass transport (net horizontal particle motion) and particle orbit radius. (The redundancy of measuring wave length, velocity, and period, permitted a check on the accuracy of the measurements.) Measurements were made for λ/b ratios of 14 to 31.

The quantities of interest in the hydrofoil study are wave profile, wave velocity, and particle velocity, for waves of various lengths and length-height ratios.

Two measured wave profiles are shown in Figs. 3, 4, and 5 of Reference 17. Deviation from the theoretical profiles is made up of (a) deviation in vertical position of the entire wave, (b) deviation in shape due to smaller, superimposed waves, and (c) deviation in mean shape. The deviation in verticle position of the entire wave is not considered in the hydrofoil study, because the transient caused when the hydrofoil starts in various vertical positions will be carefully studied separately. The effects of smaller, superimposed waves may likewise be considered as a transient condition, and have been excluded as explained in the introduction to this chapter.

A tracing of the mean profiles in Figs. 3, 4, and 5 of Reference 17 shows very good agreement (usually within 5 percent) with the theoretical paths given by the theory. This agreement seems adequate to recommend the use of theoretical profiles in the present study.

The measurements made of wave velocity, wave length, and period were found to differ on the average by less than one per cent with the theoretical values, with the maximum deviation 5 percent.

Finally, the orbital paths of the water particles were found to be nearly circular, and their radii were again within one per cent of the theoretical values, on the average. It is recalled from the Gerstner theory that the water particle velocities are proportional only to orbit radius and period. Therefore, the theoretical expressions for particle velocity are also varified.

It is concluded that the use of the theoretical expressions for all of the pertinent wave characteristics is amply justified, so long as only pure wave shapes are to be considered.

D. Open Water Observations of Waves

A number of people have made systematic observations of the characteristics of waves appearing on the oceans and inland bodies of water, and have recorded their findings in technical reports like reference 18 , or in narrative form, such as reference 19.

The observations universally made are that the waves occurring in open water are actually endless superpositions of the trochoidal waves produced in tanks and mathematics. The wave sets are of different sizes and velocities and are travelling at odd angles to one another, so that all sorts of shapes and sizes of waves result.

Usually, however, one large wave set predominates the picture. In general the theoretical relations between wave velocity, height, and length have been well borne out by the performance of the predominant waves in the groups observed.

Waves of a large range of steepnesses have been observed, with the steepest length-height ratio about 9 for short waves (under 10 feet), and 13 for waves as long as 50 feet.

CHAPTER V

DERIVATION OF THE EQUATIONS OF MOTION

Introduction:

There are two basic types of hydrofoil systems. One maintains desired depth of immersion by area variation of the airfoil. The other emoloys variation in angle-of-attack. The general equations of motion for each system will be written. The important variables will appear in the equations. The important ranges of the variables will then be selected for study.

Part 1. VARIABLE AREA SYSTEMS

A. One-Degree of Freedom

Before beginning the general analysis it will be instructive to analyze the simple single-degree-of freedom system. Consider the system in figure V-1. It consists of a single dihedral foil supporting a mass m (by means of struts). The foil is always considered to pierce the surface. The system is permitted to move freely in the vertical direction only.

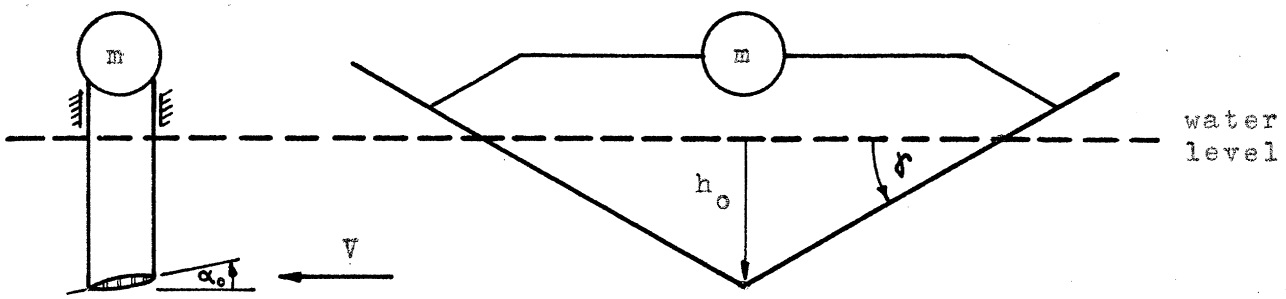

Hydrofoil System Having
One degree of Freedom

Figure V-1

Equilibrium Conditions:

It is assumed that the system is proceeding horizontally through the water with velocity V and a coordinate system is chosen which moves also with (constant)

velocity V. The system then appears stationary horizontally with the water approaching it with velocity V.

The vertical equilibrium position, h_o, of the foil is determined as follows:

The foil supports mass m, Therefore, the equilibrium lifting force on the foil, L_o, must be equal to the weight, mg:

$$L_o = \frac{\rho}{2} V^2 C_{L_o} S_o = mg,$$

$$\text{or } L_o = \frac{\rho}{2} V^2 \alpha_o \frac{C_{L_o}}{\alpha_o} S_o = mg.$$

The area of the foil is given by:

$$S_o = 2h_o \cot\gamma \qquad \text{(figure V-1)}$$

$$\therefore L_o = \frac{\rho}{2} V^2 a_o \alpha_o 2h_o \cot\gamma = mg$$

$$\text{with } a_o = \left(\frac{C_L}{\alpha}\right)_o = f(h_o, \gamma).$$

h_o can be obtained from this equation. (Values of α_o are available - from figure II-7(b), for example.)

Equation of Motion:

The equation of motion of the system in smooth water is written by applying Newton's Second Law. Let z be the downward displacement of the system from the equilibrium position. For a positive (downward) velocity, $\dot{z}$, the water velocity relative to the foil has an upward component, $\dot{z}$. The true velocity of the water relative to the foil is, therefore, the vectorial sum of $\dot{z}$ and V.

(figure V -2). The true angle of attack is thus increased by the amount $\Delta\alpha = \frac{\dot{z}}{v}$. ($\dot{z}$ is considered always to be small compared to V.)

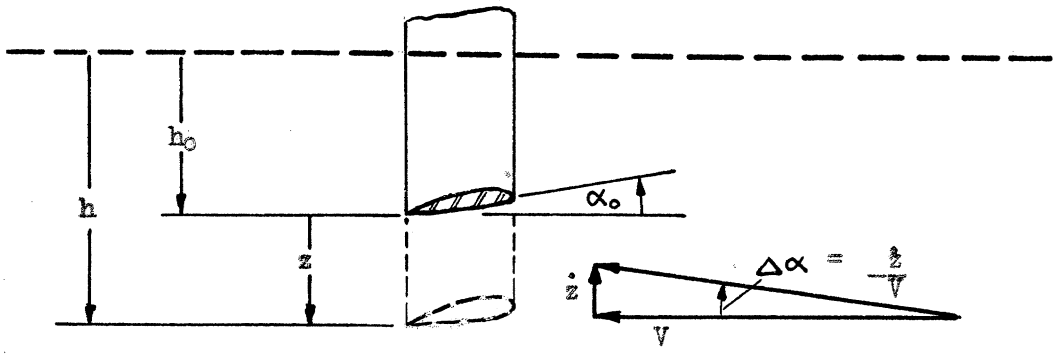

Figure V-2

The lift now becomes:

a) $$L = \frac{\rho}{2} V^2 \frac{C_L}{\alpha} S \alpha = \frac{\rho}{2} V^2 \sigma\alpha ;$$

where:

b) $$\alpha = \alpha_o + \frac{\dot{z}}{v} ,$$

and

$$\sigma = \frac{C_L}{\alpha} S .$$

σ is a function of h and γ , and is given by a curve such as figure V-3. (The relation between σ and h has been developed in chapter II. c.f. FIGURE 2.)

Newton's Second Law now states that the force $(L-L_o)$ pushing the system upward will cause an upward acceleration given by:

$$-\ddot{z} = \frac{L - L_o}{m}$$

or

$$m\ddot{z} + (L - L_o) = 0,$$

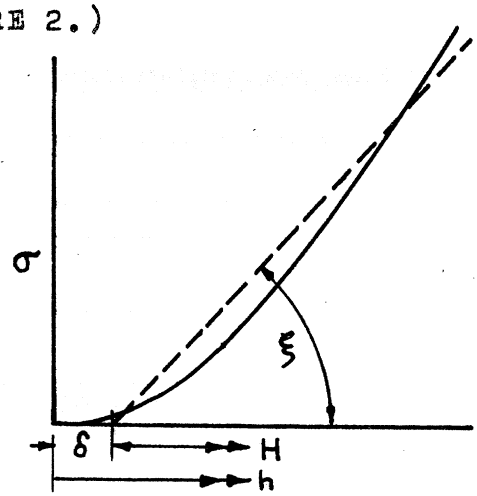

Figure V-3

$$(c) \qquad m\ddot{z} + \frac{\rho}{2} V^2 \left[\sigma(\alpha_o + \frac{\dot{z}}{V}) - \sigma_o \alpha_o\right] = 0$$

This is the general equation for the free vertical vibrations of the simple system considered.

It is noted that a tedius stepwise method of solution is required to solve it because the value of σ must be varied according to the arbitrary curve of figure V-3.

First Approximation:

To facilitate the computation it has been necessary in the current program to approximate the σ -h curve by a straight line (shown dotted in figure V-3). The error resulting from this approximation is discussed in Chapter II. The equation of motion then becomes:

$$(d) \qquad m\ddot{z} + \frac{\rho}{2} V^2 \xi \left[(h-\delta)(\alpha_o + \frac{\dot{z}}{V}) - (h_o-\delta)\alpha_o\right] = 0.$$

But:

$$(e) \qquad h = h_o + z,$$

and thus:

$$m\ddot{z} + \frac{\rho}{2} V^2 \xi \left[(z+h_o-\delta)(\alpha_o + \frac{\dot{z}}{V}) - (h_o-\delta)\alpha_o\right] = 0$$

The equation can be conveniently non-dimensionalized by dividing all terms by

$$L_o = \frac{\rho}{2} V^2 \sigma_o \alpha_o = mg:$$

(Note: $\sigma_o = \xi(h_o-\delta) = \xi H_o$, where H is defined by: $H = h-\delta$.)

$$(5) \qquad \frac{\ddot{z}}{g} + \left(\frac{z}{H_o} + 1\right)\left(1 + \frac{\dot{z}/V}{\alpha_o}\right) = 1$$

The quantity H may be though of as the depth below a mythical water surface. That is, the upper δ chords of water are considered absent. It has been shown

(FIGURE 2) that the mythical surface is about 1/2 chord below the real surface.

The equation in the form (5) lends itself readily to the solution by analogue type computers. The computer circuit is shown schematically in figure V-4:

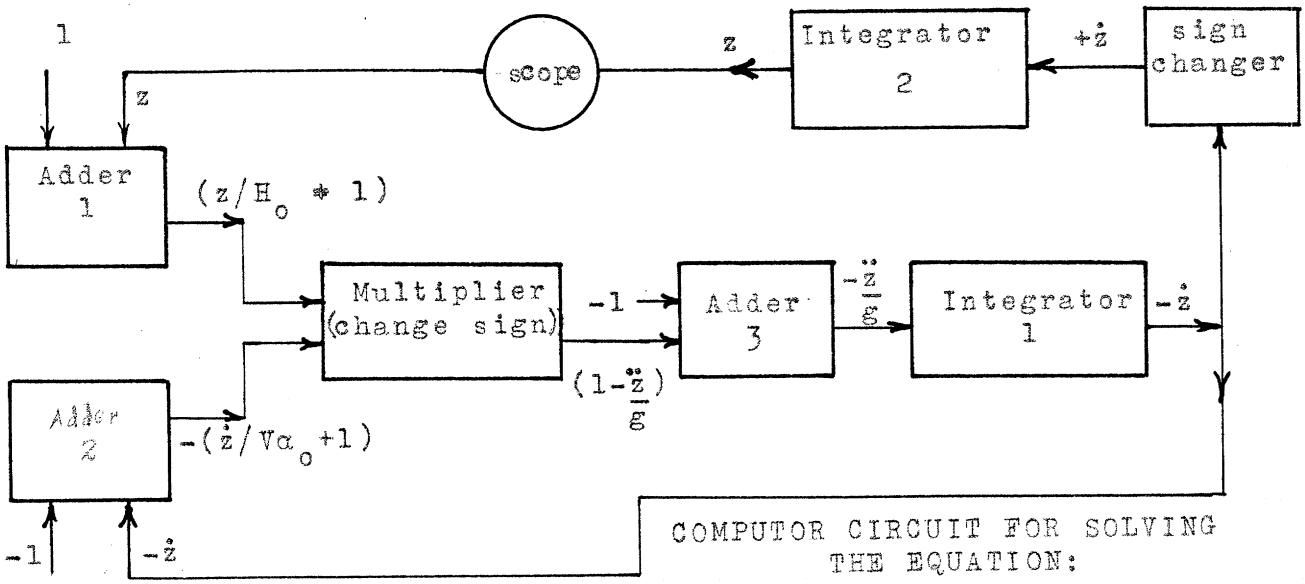

Figure V-4

Linearization:

For manual computation, however, the equation is still difficult to solve because of the non-linear term $z\dot{z}$. The equation my be linearized by the second approximating assumption that $z\dot{z} = 0$.

$$(6) \qquad \frac{\ddot{z}}{g} + \frac{\dot{z}}{V\alpha_o} + \frac{z}{H_o} = 0$$

This equation yields an exact general solution:

$$(6a) \qquad z = c_1 e^{\left[-\frac{g}{2V\alpha_o} - \sqrt{\left(\frac{g}{2V\alpha_o}\right)^2 - \frac{g}{H_o}}\right] t} + c_2 e^{\left[-\frac{g}{2V\alpha_o} + \sqrt{\left(\frac{g}{2V\alpha_o}\right)^2 - \frac{g}{H_o}}\right] t}$$

(damping above critical);

or:

$$(6b) \quad z = e^{-\frac{g}{2V\alpha_o} t} C_1 \cos(qt - \phi)$$

where: $$q = \sqrt{\frac{g}{H} - \left(\frac{g}{2V\alpha_{1_o}}\right)^2}$$

(Damping below critical).

The solution of equation (6) is investigated in Chapter VI, section A.

Validity of Linearization:

The results of the linear analysis are expected to hold qualitatively for the non-linear case. The extent of their quantitative validity should be investigated. Consider again equation (5):

$$(5) \quad \frac{\ddot{z}}{g} + \left(\frac{z}{H_o} + 1\right)\left(1 + \frac{\dot{z}}{V\alpha_o}\right) = 1$$

When expanded this becomes:

$$\frac{\ddot{z}}{g} + \frac{\dot{z}}{V\alpha_o} + \frac{z}{H_o} + \left(\frac{\dot{z}}{V\alpha_o}\right)\left(\frac{z}{H_o}\right) = 0$$

If the solution were of the form $z = z_o \cos(\omega_n t - \phi)$ with ω_n of the order of 2π (see Chapter VI, section A) then reasonable maximum values of the terms in the equation would be:

$$\frac{\ddot{z}}{g} = \frac{z_o \omega_n^2}{g} \approx \frac{(z_o)(6)^2}{32.2} \approx z_o \quad ,$$

$$\frac{\dot{z}}{V\alpha_o} = \frac{z_o \omega_n}{V\alpha_o} \approx \frac{(z_o)(6)}{4} \approx z_o \quad ,$$

$$\frac{z}{H_o} = \frac{z_o}{H_o} \approx \frac{1}{1} = z_o \,,$$

$$\frac{z}{V\alpha_o} \cdot \frac{z}{H_o} \approx z_o^2$$

Typical values of the variables have been entered (from the linear analysis of Chapter VI) to show that all linear terms are of the order z_o, while the non-linear term is of the order z_o^2. Therefore, only for the case of very small motions (less than 1/10th chord) is the linearizing assumption warrented.

The effect of waves:

If the hydrofoil system moves through surface waves instead of smooth water, two properties of the waves will have important effects on the resulting motions: (1) the height of the wave profile will increase the hydrofoil depth; and (2) the orbital motions of the waves will affect the angle of attack.

If the wave trough is a distance i below the smooth water level, and if the wave height (trough to crest) is ζ, then the depth h in expression (e) becomes:

(e') $$h = h_o + z + (\zeta - i).$$

If the vertical velocity of a water particle is v_p (positive downward), then angle of attack in figure V-2 is decreased by v_p/V, and expression (b) becomes:

(b') $$\alpha = \alpha_o + \frac{\dot{z}}{V} - \frac{v_p}{V} .$$

Equation (5) is now written:

$$\frac{\ddot{z}}{g} + \left[\frac{z + (\zeta - i)}{H_o} + 1\right] \cdot \left[1 + \frac{\dot{z}/V - v_p/V}{\alpha_o}\right] = 1$$

Values of ζ and v_p are available from Chapter IV.

B. Two-Degrees of Freedom

The analysis for a two-degree-of-freedom variable area system is performed on plate 1, Appendix A. It is assumed that the hydrofoils have a fixed angle with respect to the boat, and that they are geometrically similar. The hydrofoils extend sufficiently far above the surface that their tips are never immersed. The straight-line simplification of figure V-3 is employed for each foil. The possibility of there being more or fewer foils forward than aft, and of the chord and initial angles of attack of the after foils being different from those forward are included in the analysis. The position of the center-of-gravity is also as yet undetermined.

Equilibrium Conditions:

The hydrofoil system is first considered at rest (dotted figure, PLATE 1) with water approaching it with velocity V, and the equations of static equilibrium (a) are written.

Expressions for the steady-state values of various parameters are listed as expressions (b).

Equations of Motion:

The system is next considered in motion in waves. It is shown in a general position in the solid figure. The hydrodynamic expressions for lift now take the forms

(c). The expressions for depths H_1 and H_2 follow directly from the large diagram. In computing the angle of attack of a hydrofoil the increase in angle due to the upward vertical velocity, v, of the water relative to the foil must be considered. v is made up of a component due to the downward velocity of the hydrofoil minus a component due to the downward velocity v_p of the local water particles in orbital motion. (The latter effect was discussed in Chapter IV, where expressions for both v_p and ζ are presented.)

Equations (d) are the dynamic equations of motion.

Two steps are shown in the process of non-dimensionalizing equations (d) and of substituting the expressions (b) and (c) in their proper places. The final result is equations (7) which are to be integrated to find the motions of the system.

C. Dimensional Analysis

A dimensional analysis is most easily accomplished directly from equations (7) which are already entirely in terms of dimensionless ratios. Further reduction is necessary, however, because the numerators and denominators of nearly all the ratios will be varied separately.

Throughout this analysis it is important to keep in mind two important physical relations which do not appear explicitly in the equations. One is the likelihood of cavitation and/or ventilation, which is implied by large values (of the order 1.0) of the "cavitation index", $\sigma_o = \frac{L/S}{p_a}$ (see Chapter III). The other is the interrelation between the various wave properties -- length, height, and group-velocity. (This interrelation is developed in Chapter IV).

The two different non-dimensional forms of equations (7) will now be developed. In one, time will be retained in dimensional form (seconds). In the other a non-dimensional time-unit will be used. The relative merits of the two forms will be discussed, and the reasons for adopting the first form in the calculating program will be explained.

Form Having Dimensional Time:

In this form all lengths are divided by a characteristic length of the system: namely, the chord of the forward

hydrofoils, c_i.[1] This division is readily accomplished by invoking the condition that hereafter all symbols for length in equation (7) represent those lengths measured in chords. In other words, the symbol ℓ, for example, hereafter represents the ratio of length to chord.

Only one additional change is made to convert equations (7) to the form (7a); the last bracket in each equation is multiplied inside by $\frac{\alpha_{20}}{\alpha_{10}}$, and outside by $\frac{\alpha_{10}}{\alpha_{20}}$. The first form is then:

(7a)

$$\frac{\ddot{z}}{g} + \frac{x_2}{\ell}\left[1 + \frac{z - \frac{x_1}{\ell}\ell\theta + (\zeta_1 - i)}{H_{10}}\right]\left[1 + \frac{\ell\theta}{\ell\alpha_{10}} - \frac{x_1}{\ell}\frac{\ell\dot{\theta}}{V\alpha_{10}} + \frac{\dot{z}}{V\alpha_{10}} - \frac{v_{p_1}}{V\alpha_{10}}\right] + \frac{x_1}{\ell}\frac{\alpha_{10}}{\alpha_{20}}\left[1 + \frac{z + \frac{x_2}{\ell}\ell\theta + (\zeta_2 - i)}{H_{20}}\right]\left[\frac{\alpha_{20}}{\alpha_{10}} + \frac{\ell\theta}{\ell\alpha_{10}} + \frac{\dot{z}}{V\alpha_{10}} + \frac{x_2}{\ell}\frac{\ell\dot{\theta}}{V\alpha_{10}} - \frac{v_{p_2}}{V\alpha_{10}}\right] = 1$$

$$\left(\frac{k_0}{\ell}\right)^2\frac{\ell\ddot{\theta}}{g} - \frac{x_1 x_2}{\ell^2}\left[\quad''\quad\right]\left[\quad''\quad\right] + \frac{x_1 x_2}{\ell^2}\frac{\alpha_{10}}{\alpha_{20}}\left[\quad''\quad\right]\left[\quad''\quad\right] = 0$$

To obtain numerical solutions to equations (7a) numerical values for the following parameters must be stated: $V\alpha_{10}$, $g\ell\alpha_{10}$ (now in chords), H_{10}, H_{20} $\frac{\alpha_{10}}{\alpha_{20}}$, $\frac{x_1}{\ell}$, ζ_1, ζ_2, v_{p_1}, v_{p_2}, i. Stating ζ_1 and ζ_2 implies stating all the various wave parameters -- N, ψ, b, C, etc. -- and, therefore, implies that ζ_1 and ζ_2 be based on a wave system of known dimensions to insure reasonable values. For this reason among others, quick conversion between dimensional and non-dimensional forms is important.

---

[1] The chord is chosen as the basic length because it is convenient to think in terms of the ratios, z/c, ℓ/c, H/c, etc. It is also the dimension on the basis of which the relation between σ and H was developed in Chapter II.

(Note that g is in chords per second - squared.) Conversion of the solutions to dimensional form may be accomplished if the dimensional values are known for c_1 and for any <u>one</u> of the following: α_{10}, ℓ, V, $\sqsubset_o$. For then the dimensional amplitudes of motion can be calculated by multiplying the non-dimensional values by c_1; the remaining values of α_{10}, ℓ, V, and $\sqsubset_o$ can be deduced from $V\alpha_{10}$, $\ell\alpha_{10}$, and from the expression:

$$\sqsubset_o = \frac{L/S}{p_a} = \frac{\frac{\rho}{2} \frac{C_L}{\alpha} V^2 \alpha_{10}}{p_a}$$

Dimensional values for all the wave parameters can be obtained from their appropriate relations. It is noted in particular that frequencies, damping rates, and other time-functions can be read directly in second-units.

<u>Form Having Non-dimensional Time</u>:

In deriving this form, the basic units of measure are taken as length (c_1), weight, and velocity. Time is a derived quantity. A period of time, τ, in non-dimensional units is defined by the relation:

$$\tau = \frac{t}{V/C_1} .$$

(i.e. one τ-unit is the time required for the system to move ahead one chord.)

The conversion to c_1 length units has already been performed in equations (7a). The conversion to τ time units will therefore be made from these equations.

The "dot" derivatives with respect to t become "prime" derivatives with respect to τ . For example:

$$\frac{\dot{z}/c_1}{V/c_1} = \frac{1}{V/c_1}\frac{d(z/c_1)}{dt} = \frac{d(z/c_1)}{V/c_1\, d(\frac{\tau V}{c_1})} = \frac{d(\frac{z}{c_1})}{d\tau} = z'$$

For convenience a new quantity, g' is defined by:

$$g' = \frac{gc}{V^2}$$

The second form of the equations is thus:

$$\frac{z''}{g'} + \frac{\chi_2}{l}\left[1 + \frac{z - \frac{\chi_1}{l}l\theta + (\zeta_1 - i)}{H_{10}}\right]\left[1 + \frac{l\theta}{l\alpha_{10}} + \frac{z'}{\alpha_{10}} - \frac{\chi_1}{l}\frac{l\theta'}{\alpha_{10}} - \frac{v_{p_1}}{\alpha_{10}}\right] + \frac{\chi_1}{l}\frac{\alpha_{10}}{\alpha_{20}}\left[1 + \frac{z + \frac{\chi_2}{l}l\theta + (\zeta_2 - i)}{H_{20}}\right]\left[\frac{\alpha_{20}}{\alpha_{10}} + \frac{l\theta}{l\alpha_{10}} + \frac{z'}{\alpha_{10}} + \frac{\chi_2}{l}\frac{l\theta'}{\alpha_{10}} - \frac{v_{p_2}}{\alpha_{10}}\right] = 1$$

(7b)

$$\left(\frac{k_g}{l}\right)^2\frac{l\theta''}{g'} - \frac{\chi_1\chi_2}{l^2}\left[\quad''\quad\right]\left[\quad''\quad\right] + \frac{\chi_1\chi_2}{l^2}\frac{\alpha_{10}}{\alpha_{20}}\left[\quad''\quad\right]\left[\quad''\quad\right] = 0$$

To obtain numerical solutions to these equations numerical values must be given for the same parameters as for (7a) except that "$V\alpha_{10}$" and "g" are replaced by "α_{10}" and "g'".

To deduce dimensional quantities from the resulting dimensionless solutions requires knowing dimensional values for either c_1, V, or ℓ_o. (V and ℓ_o are related by α_{10} as before, and V and c_1 are related by g' in the definition: $g' = \frac{g\, c_1}{V^2}$.

An additional conversion to time in seconds is necessary to interpret solutions to (7b).

It is noted that the ratio $\ddot{z}/g$ -- or $\ddot{\zeta}/g'$ -- describes the acceleration condition completely, regardless of the units employed.

Comparison of Forms (7a) and (7b):

The same number of parameters occurs in each form of the equations so that the same number of solutions will be required to cover a given range of parameter-variation, whichever form of the equations is used.

In interpreting non-dimensional results it was found that if frequent change in the chord size was made, the form (7b) was much easier to use. On the other hand, if chord size were held constant quicker conversion to dimensional cases could be made from the form (7a).

In the present, preliminary program -- particularly in the section dealing with ocean waves -- it was desired to make continuous checks with dimensional systems to assure reasonable values of the parameters.

Furthermore, since the effect of chord change formed only a small part of the calculating program, the form (7a) was used.

Whenever it is desired to compare solutions based on two different chord sizes, or to extend results to other chord sizes, each solution should be converted to non-dimensional time. In addition the condition should be invoked that g' and α_{10} be the same, and that the systems

be geometrically similar. It then follows that for a given chord size V, ℓ, L/S, etc. will all be the same for both systems.

(There is another purely operational reason for preferring form (7a). This is that changes in the quantity V were made easily in the adders which were pre-calibrated. Changes in g' would necessarily have been made in the integrators and would have required repeated calibration.)

D. Linearization -- Two Degrees of Freedom

The first step in solving equations (7) is to study the possibility of linearizing. Linearization is easily accomplished, merely by dropping all products of the variables z, $\ell\theta$, and v_p and their derivatives. The result is equations 8:

$$\frac{\ddot{z}}{g}+\frac{\chi_2}{\ell}\left[\frac{z-\frac{\chi_1}{\ell}\ell\theta+(\zeta_1-i)}{H_{10}}+\frac{\ell\theta}{\ell\alpha_{10}}+\frac{\dot{z}}{V\alpha_{10}}-\frac{\chi_1}{\ell}\frac{\ell\dot{\theta}}{V\alpha_{10}}-\frac{v_{p1}}{V\alpha_{10}}\right]+\frac{\chi_1}{\ell}\left[\frac{z+\frac{\chi_2}{\ell}\ell\theta+(\zeta_2-i)}{H_{20}}+\frac{\alpha_{10}}{\alpha_{20}}\left(\frac{\ell\theta}{\ell\alpha_{10}}+\frac{\dot{z}}{V\alpha_{10}}+\frac{\chi_2}{\ell}\frac{\ell\dot{\theta}}{V\alpha_{10}}-\frac{v_{p2}}{V\alpha_{20}}\right)\right]=1$$

$$\left(\frac{k_{cg}}{\ell}\right)^2\frac{\ell\ddot{\theta}}{g}-\frac{\chi_1\chi_2}{\ell^2}\left[\quad\text{"}\quad\right]+\frac{\chi_1\chi_2}{\ell^2}\left[\quad\text{"}\quad\right]=0$$

The validity of this linearization -- like that of the single-degree system, page 65 -- depends upon the size of the neglected product terms.

In general the variable $\ell\theta$ is likely to be of the same order of magnitude as z. If in addition ℓ is of the order of 20 chords and ζ of the order of 1 chord, then the following ratios are all of the order z:

$$\frac{z}{H},\quad \frac{\ell\theta}{H},\quad \frac{\zeta}{H},\quad \frac{\theta}{\alpha_{10}},\quad \frac{\ell\dot{\theta}}{V\alpha_{10}},\quad \frac{\dot{z}}{V\alpha_{10}}.$$

$\frac{\alpha_{20}}{\alpha_{10}}$ is in general of order 1.

It is therefore seen that again linearization is warrented only for very small motions and very small waves.

Some special attention will now be given to the

term $\frac{v_p}{V\alpha_{10}}$, which represents the effect of orbital motions of water-particles upon the true angle-of-attack.

In a first approximation:

$$\frac{v_p}{c} = \pi \frac{b}{\lambda} e^{\frac{-2\pi h}{\lambda}}$$

(See Chapter IV.) The largest value of b/λ anticipated is 1/10, and when the foil is quite near the surface h/λ may be very small, so the expression may be written:

$$\frac{v_p}{c}_{max} \approx \frac{\pi}{10} e^{o} \approx .3.$$

The expression for $\frac{v_p}{V\alpha_{10}}$ then becomes $\frac{v_p}{V\alpha_{10}} \approx \frac{.30}{V\alpha_{10}}$.

This relation is plotted in figure V-5 for waves of two lengths and for a range of $V\alpha_o$ borrowed from TABLE 1. It is seen that orbital motions are of first order importance even for moderate speeds (40fps).

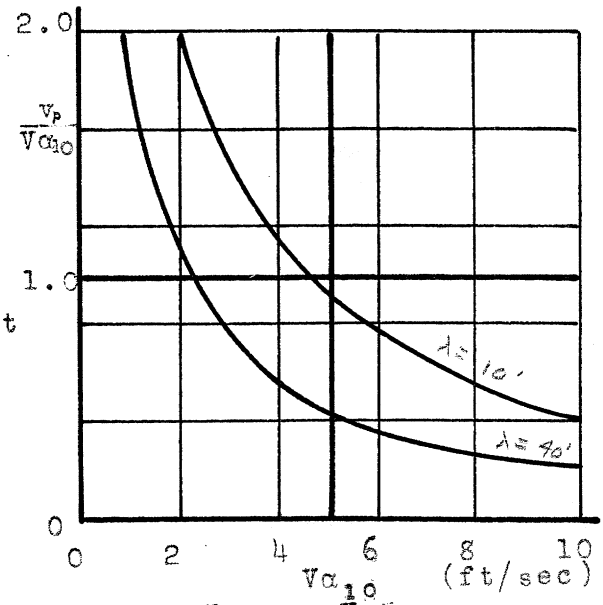

Figure V-5

Although the linearizing assumption is valid only for very small motions, it is probable that the results of a linear analysis will prove qualitatively indicative of the motions to be expected, and of the effects of the various

parameters. For this reason, Mr. Frederick Imlay in 1947 made a preliminary linear study based upon equations similar to equations (6). Mr. Imlay's results were published as NACA Technical Report 1285.[1]

As a link between Mr. Imlay's work and the present program, several linear calculations were made on the electronic differential analyzer by this author. The results of these, together with a review of Mr. Imlay's conclusions, are presented in the Discussion of Results, Chapter VII, Part 1.

---

[1] Reference 12

Part II

VARIABLE ANGLE OF ATTACK SYSTEMS

A. The Problem of Incidence Control

For hydrofoil systems traveling at very high speeds it may be necessary -- for reasons of efficiency and ventilation-prevention -- to control the angles of attack of the hydrofoils.

For such systems stability could be maintained entirely by the incidence-control, as will be shown, so that it would be unnecessary to employ area-variation. The foils would therefore be completely submerged under normal operation, and the lift-depth relation would be as shown by the curves of FIGURE 1, instead of by FIGURE 2. In the first approximation, the lift can be considered constant with depth.

As a first step in studying the performance of incidence-controlled systems, the derivation of PLATE 1 will be modified so that it will apply to a hydrofoil system having flat foils which may be set automatically to any desired angle with respect to the boat. It will be assumed that lift is independent of depth. This assumption is exactly analogous to the replacement of the σ -- h curve in PLATE 1 by a straight line. But in the present case it makes the problem linear.

With this assumption, σ_1 is always equal to σ_{10}

so that $L_1/L_{10} = \alpha_1/\alpha_{10}$, and equations (7) take the form (7C), PLATE 2.

The only other modification which must be made on PLATE 1 is the addition to the expressions for angle of attack of terms representing the incidence-settings, $\Delta\alpha_s$, from the control system. These additions are made in equations (c'), PLATE 2.

A control system can now be set up to furnish the required values of $\Delta\alpha_s$ to maintain the hydrofoil system at any desired depth.

B. An Automatic Control System

The control system has two main parts: one to control the front hydrofoils and one to control the rear foils. (In a study including lateral motions it will undoubtedly be necessary to control each front foil separately.)

The purpose of the control system under study is to control the depths of the front and rear hydrofoils. To this end it will be necessary to measure these depths. More precisely, it is necessary to measure the difference between the actual depth and that which is desired.

The method of depth-measurement will not be specified at this point. It is anticipated, however, that the measuring elements may have dynamic characteristics of inertia, damping, and "spring forces". It is assumed in the first analysis that these may be represented by "equivalent constants" m_{m1}, B_{m1}, and K_{m1} for the forward foil element, and m_{m2}, B_{m2}, and K_{m2} for the after foil element.

It may be possible to measure depth with respect to the water surface at some point ahead of the foil, thus giving early warning of sudden changes in water-level (waves). This possibility has been incorporated

into the analysis by using the symbol ζ_{1e} in place of ζ_1 in computing depth.

It is convenient to measure all quantities from a reference level represented by equilibrium conditions at some operating speed, as in PLATE 1. Deviations in depth from those in PLATE 1 will be denoted by Δh. Any desired deviation in operating depth from the equilibrium depth will be denoted by Δh^*.

The output signal from the depth-measuring device is given the symbol y. Its reference level is also chosen at the point of equilibrium conditions at the (specified) operating speed. Thus when $h = h_o$, $y = o$. If there were no dynamic effects in the measuring device, y would merely be proportional to $(h - h_o)$:

$$y_1 = k_{11} \Delta h_{1e},$$

$$y_2 = k_{12} \Delta h_{2e}.$$

(k_{11} and k_{12} are constants of the depth-measuring system. The second subscripts, 1 and 2, refer as usual to the forward and after hydrofoils, respectively.) When the dynamics of the measuring system are considered, y_1 and y_2 are to be found from equations (e) PLATE 2.

The control element must receive a signal indicating the difference between actual depth and desired depth -- that is, to $\Delta h^* - \Delta h$:

$$h^* - h = (h^* - h_o) - (h - h_o) = \Delta h^* - \Delta h.$$

y represents Δh, so the desired signal, u, is obtained by comparing y with Δh^*, as in equations (f), PLATE 2.

A typical control system is represented by equations (g). (The k's are constants of the control system.)

The control elements chosen contain the possibility of "proportional", "derivative", and "integral" control. In other words, if the deviation of a foil from its desired position is called its "error", then the angle of attack may be varied according to the error, to the derivative of the error, and to the integral of the error. (Derivative control is useful in anticipating errors before they actually occur and hence contributes a stabilizing effect. Integral control is effective in preventing steady state errors.)

The error of <u>both</u> foils is fed into each control element, because it may be desirable to consider the position of both foils, before specifying the control of either.

The dynamics of setting the angle of attack of a foil have not been considered, because it is believed that good control will require sufficient power to insure a positive setting of foil angle. In other words,

the force applied in setting the angle must be very large compared with any hydrodynamic forces which might oppose the setting.

A cardinal reason for requiring incidence-controlled hydrofoils is the importance of preventing cavitation loadings by maintaining the angle of attack always below a certain value. To be entirely effective, therefore, the incidence-control system described above should be refined to include a method of measuring the true angle of attack continuously, and of preventing it from exceeding any specified value.

D. A Particular Case -- the Hook System[1]

An automatic hydrofoil control system has been invented and developed which is ingeneous, strikingly simple, and reportedly highly effective. It will now be described, on the basis of the foregoing analysis.

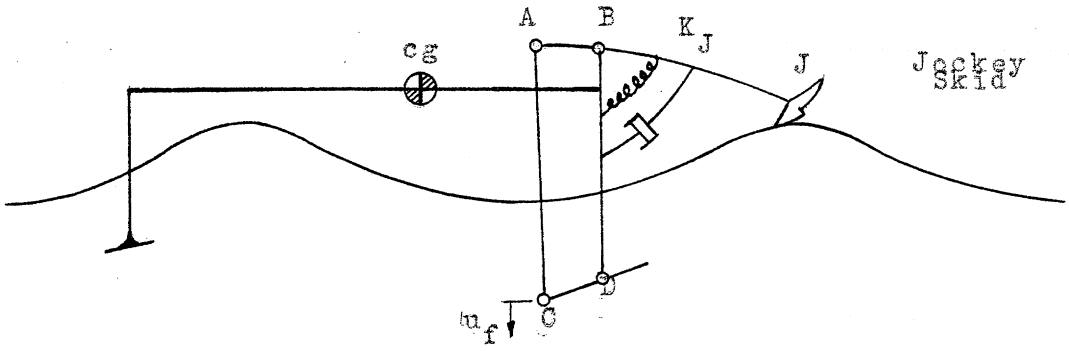

Figure V-6

The system is shown in Fig. V-6. The depth-measuring mechanism is the planing "Jockey skid" which receives an (upward) force, dependent upon the position of the forward foil with respect to the water surface at the skid. This measuring device thus incorporates the "early warning" feature mentioned earlier.

Bar AJ is pivoted about B and is presumed to have inertia. It is possible for the jockey to sink into the water surface, or to leave it entirely. A spring K_J is provided to hold the jockey to the surface.

[1] The inventor is Mr. Christopher Hook, Cowes, Isle of Wight, England

Thus the unit consisting of bar AJ and the jockey is held in a spring system. The equivalent spring constant of the system is non-linear, but in the first analysis may be considered to have just two values, depending on whether the jockey skid is in or out of the water. The resulting spring force is shown in Fig. V-7. The value of d is altered by the operator of the boat, by changing the tension in spring K_J.

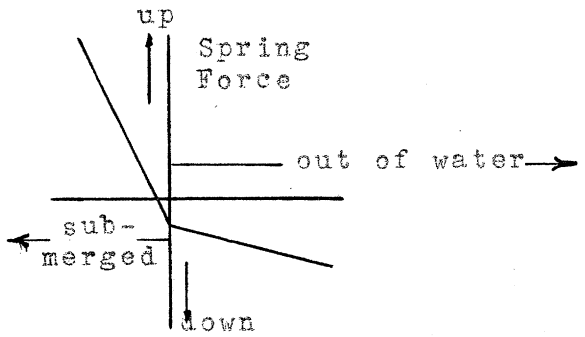

Figure V-7

A dash-pot is fixed to bar AJ as shown, to introduce damping into the system. This bar will therefore act as the forward depth-sensing element described in Section B. The motion of point A is y_1, which is given by the first equation (e), PLATE 2.

If the motion of point C is denoted by u_1, then angle of attack is simply proportional to u_1. In other words, the control element of the Hook system consists of only proportional control. However, it must be remembered that the advanced position of the jockeys provides some anticipation of future error -- a function similar to that performed by the derivative controller.

In Equations (f), u_1 is obtained from y_1 by comparing y_1 with the desired depth. In the Hook system this operation is tacitly performed by rod AC. Therefore to change desired depth (at a given speed) the length of AC is altered.

The angular position of the rear foil is fixed. Its angle of attack is altered by appropriate changes in the trim of the boat.

The Hook System has been under development for several years, and has a number of additional features to recommend it, which are outside the scope of the present discussion of longitudinal motions. In particular, the methods of preventing ventilation have been given careful thought.

Chapter VI

APPROACH TO SOLVING THE EQUATIONS OF MOTION

Introduction

The task of obtaining solutions to the general non-linear equations of motion (7) will be undertaken in Chapter VII. In the present chapter several preliminary steps will be taken in preparation for that task.

The first step -- made in section A of this chapter -- is to study the linearized form of the equation of motion of a hydrofoil system having only one degree of freedom. It is found that important information regarding damping and natural frequency may be obtained from this analysis.

In section B the linearized equations of a hydrofoil system having two degrees of freedom are studied under some simplifying conditions. Additional information about the natural frequencies is gained, and some stability limitations of the system are predicted.

Finally in section C the method of obtaining the non-linear solutions is discussed, and the differential analyzing equipment is described.

A. Linear Analysis of a Hydrofoil System Having One Degree of Freedom

Equation (5) (Chapter V-A) is the same as that of the classical mass-spring-dashpot system. It will be instructive to pursue this analogy further. The two systems are shown in figure VI-1.

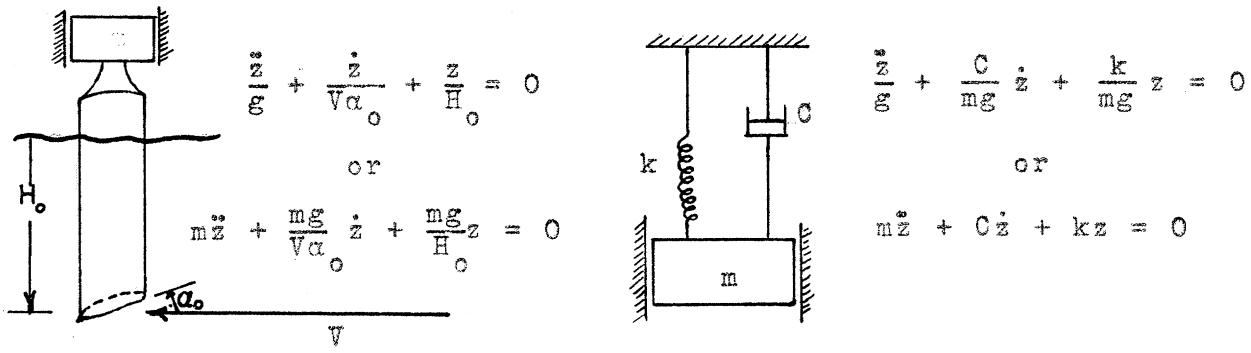

Figure (VI-1)

The hydrofoil system of mass, m, [1] has a "spring constant", $\frac{mg}{H_o}$, and a "dashpot constant", $\frac{mg}{V\alpha_o}$. The time constant for sub-critical damping is $\tau_c = 2V\alpha_o/g$ seconds. (That is, free vibrations of the system will damp to $1/e^{th}$ their value in $\frac{2V\alpha_o}{g}$ seconds.) The undamped natural frequency of the system is $\omega_n = \sqrt{\frac{g}{H_o}}$. (This is also the bobbing frequency of a prismatic floating block.)

Natural Frequency:

The natural frequency of a system is always important if the system is to be subjected to periodic disturbances.

[1] Change in "effective mass", due to motion of a certain small mass of water, has been neglected.

Since ocean waves are sinusoidal, the natural frequency of a hydrofoil system becomes very important. It will be shown in the next chapter that a low natural frequency is desirable.

The undamped natural frequency is $\omega_n = \sqrt{\frac{g}{H_o}}$ $(f_n = \frac{\omega_n}{2\pi})$, which decreases with increasing H. (This relation is shown in Fig. VI-2.) When high damping exists, the natural frequency is

$$q_n = \sqrt{\frac{g}{H_o} - \left(\frac{g}{V\alpha_o}\right)^2}$$

which is lower than ω_n, and is decreased by increasing damping.

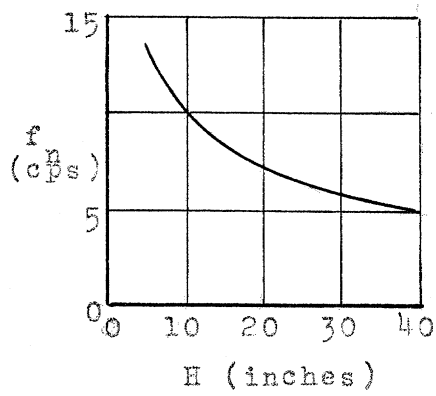

Figure VI-2

Damping:

Critical damping occurs when $\left(\frac{mg}{V\alpha_o}\right)^2 = 4m^2 \frac{g}{H_o}$

or

(a) $$(V\alpha_o)^2 = \frac{gH_o}{4}$$

It will now be shown that critical damping is likely to occur for large, deep, lightly-loaded hydrofoils and for high speeds.

The first step is shown in Fig. VI-3 where the relation (a) is plotted. The plot is left in dimensional form for ease of interpretation. (For a dimensional analysis of the problem, see Chapter V, part C.) Next some values

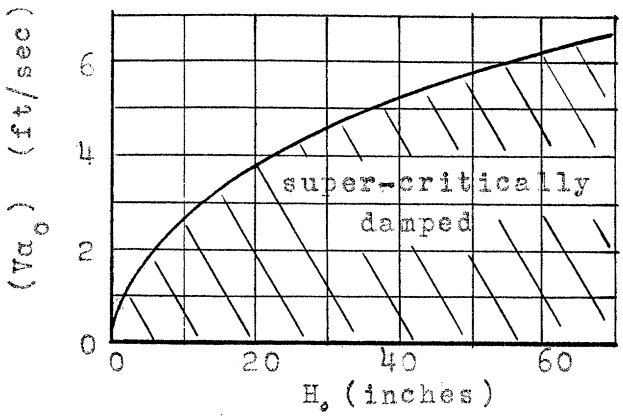

Figure VI-3

of $V\alpha_o$ which are likely to occur will be calculated. Finally the quantity H will be investigated.

Three values of reasonable foil-loading are chosen (on the basis of Chapter III). Then, from the basic relation defining C_L --

$$L = C_L \frac{\rho}{2} V^2 S = \frac{C_L}{\alpha} \alpha \frac{\rho}{2} V^2 S \text{ --}$$

a formula for α_o is obtained:

$$\alpha_o = \frac{L/S}{\frac{\rho}{2} \frac{C_L}{\alpha} V^2} \approx \frac{1}{3} \frac{L/S}{V^2}$$

(The value of $\frac{C_L}{\alpha}$ is taken from graph II-7.) Values of $V\alpha_o$ occurring at various speeds can now be calculated and are shown in TABLE 1, Appendix A.

The values of H for which critical damping occurs have been read from figure VI-3, and are listed in the last column of the table. It is seen that critical damping is likely to occur for deep hydrofoils, high speeds, and light loadings.

Depth:

It has been shown that both high damping and a more desirable natural frequency result from larger values of the depth of submergence, H_o. The methods of increasing H_o will therefore be reviewed.

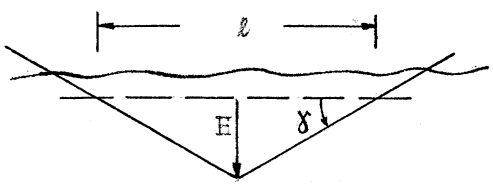

Figure VI-4

From figure VI-4 a geometric relation for H_o can be seen:

$$S = \ell c = (2H_o \cot \gamma)c$$

$$H_o = \frac{S}{2c} \tan \gamma$$

Three methods of increasing H_o are available: (1) increase dihedral, (2) decrease chord, (3) increase foil area. Method (3) implies either (a) increasing total load, or (b) decreasing load per unit area.

The methods of increasing H are illustrated in figure VI-5.

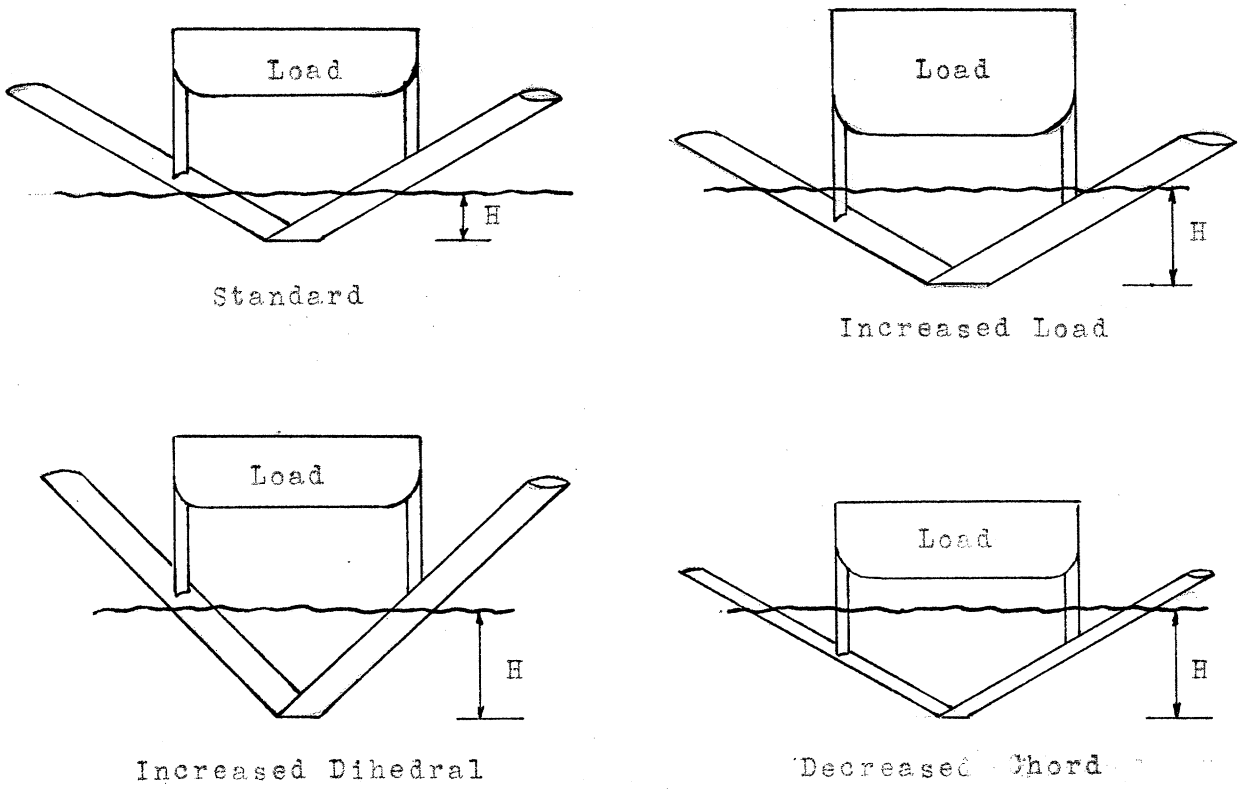

Figure VI-5

Each one, of course, involves serious practical limitations. Load and chord size are strictly limited by strength considerations. High dihedral produces higher profile drag, because a greater true area of hydrofoil is necessary to support a given load.

Summary:

The one-degree-of-freedom, linear analysis indicates that to obtain high damping and low natural frequency, deep hydrofoils should be employed. Deep hydrofoil operation can be obtained by using the highest dihedral, the smallest chord, and the lightest loadings per unit area consistant with other structural and operational considerations. Damping is expected to increase with speed (provided loading is unchanged).

B. Linear Analysis of a Hydrofoil System Having Two Degrees of Freedom

A thorough study of the characteristic properties of the linear, two-degree-of-freedom equations is contained in reference 12. In particular, the roots of the stability equation and the response of the system to step functions were calculated.

It was decided that the purpose of the present study -- to learn the effects of a wide range of parameters -- would be best served by carrying out the less accurate, but more rapid machine calculations.

However, the divergent boundaries and, under certain particular conditions (which happen to be important), the natural frequencies of the system can be quickly found. These two calculations will now be demonstrated.

Divergent Boundaries:

A "divergent boundary of stability" of a system is defined as a set of conditions for which the system is in neutral equilibrium: if the conditions are changed slightly in one direction, the system will be unstable, while if they are changed in the other direction, it will be stable.

The divergent boundaries can be easily found, because when the system is in a neutrally stable condition, a set of equilibrium equations can be written with the system in an arbitrary position. In the linear case the coordinates describing the arbitrary position can be eliminated from these equations, leaving the relation between the parameters

of the system which must hold for neutral equilibrium.

The relation for calculating the location of the divergent boundaries is found by the analysis shown on plate 3. Equations (a) and (b) are the same equilibrium conditions which were found in Chapter V, part 1-B.

For the system to be in equilibrium in an arbitrary position (z,Θ) the lift on each hydrofoil must be the same as it was in the initial equilibrium position. This condition is expressed by equations (c). All of the constant terms in equation (c) can be eliminated by dividing by L_o, and only the variables are left: equations (d).

When equations (d) are linearized the products $\Delta\alpha_1$, $\Delta\sigma_1$, and $\Delta\alpha_2$, $\Delta\sigma_2$ are dropped. The result is equations (e).

The straight line assumption of Figure 2 is applied to relate σ and H. (This assumption is discussed at the end of Chapter 2.) The quantity H is the depth below the hypothetical surface. The values of ΔH and $\Delta\alpha$ are evident from the arbitrary position of the system shown. Substituting these values into equations (e) results in equations (f). (Lengths z, ℓ, x_1, x_2, and H_{1O} are understood to be measured in terms of c_1. H_{2_O} is measured in terms of c_2. This is done so that a single relation between σ and H will hold for all hydrofoils.)

The arbitrary coordinates z and Θ can be eliminated from equations (f), giving equation (g). Relations (a) and (b) can then be used to transform equation (g) to the final form (h).

DETERMINING THE CONDITIONS FOR WHICH A HYDROFOIL SYSTEM WILL BE IN NEUTRAL EQUILIBRIUM

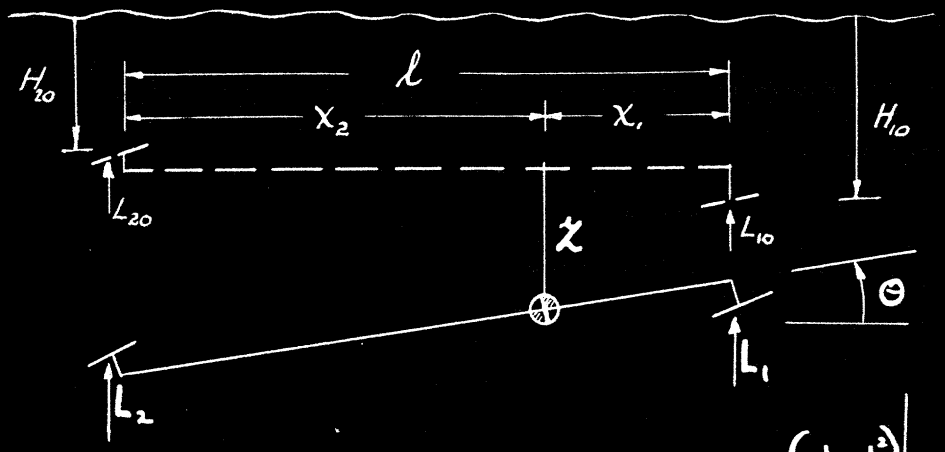

$$L_{10} X_1 = L_{20} X_2$$

$$\frac{L_{10} X_1}{L_{20} X_2} = 1 = \frac{\eta_1 \frac{\rho}{2} V^2 \left(\frac{C_L}{\alpha} S\right)_{10} \alpha_{10}}{\eta_2 \frac{\rho}{2} V^2 \left(\frac{C_L}{\alpha} S\right)_{20} \alpha_{20}} \frac{X_1}{X_2}$$

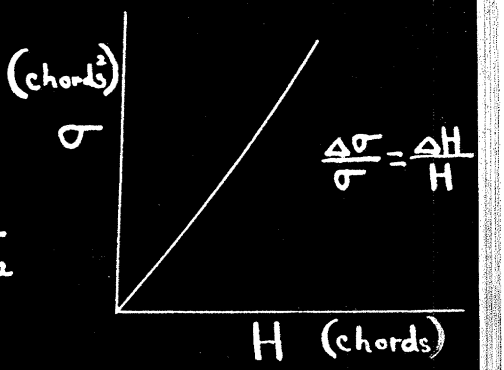

$$\frac{\Delta\sigma}{\sigma} = \frac{\Delta H}{H}$$

(a) $$\left(\frac{\eta_1}{\eta_2} \frac{c_1^2 \sigma_{10}}{c_2^2 \sigma_{20}}\right) \frac{\alpha_{10}}{\alpha_{10}} \frac{x_1}{x_2} = 1$$

$$\frac{\sigma_{10}}{\sigma_{20}} = \frac{c_1}{c_2} \frac{H_{10}}{H_{20}}$$

(H measured in chords.)

(b) $$x_1 + x_2 = l$$

(c) $$\begin{cases} L_1 = L_{10} \\ L_2 = L_{20} \end{cases}$$

(d) $$\begin{cases} \dfrac{L_1}{L_{10}} = \dfrac{\sigma_1}{\sigma_{10}} \dfrac{\alpha_1}{\alpha_{10}} = 1 \\ \dfrac{L_2}{L_{10}} = \dfrac{\sigma_2}{\sigma_{20}} \dfrac{\alpha_2}{\alpha_{20}} = 1 \end{cases}$$

$$\Delta\alpha_1 = \alpha_1 - \alpha_{10}$$

$$\Delta\sigma_1 = \sigma_1 - \sigma_{10}\,, \text{ etc.}$$

Drop products $\Delta\alpha\,\Delta\sigma$:

(e)
$$\begin{cases} \dfrac{\Delta\sigma_1}{\sigma_{10}} + \dfrac{\Delta\alpha_1}{\alpha_{10}} = 0 \\ \dfrac{\Delta\sigma_2}{\sigma_{20}} + \dfrac{\Delta\alpha_2}{\alpha_{20}} = 0 \end{cases}$$

(f)
$$\begin{cases} \dfrac{c_1 z - c_1 x_1 \theta}{(c_1 H_{10})} + \dfrac{\theta}{\alpha_{10}} = 0 \\ \dfrac{c_1 z + c_1 x_2 \theta}{(c_2 H_{20})} + \theta \end{cases}$$

(g)
$$\left(\frac{1}{\alpha_{20}} + \frac{c_1 x_2}{(c_2 H_{20})}\right) = \left(\frac{c_1 H_{10}}{c_2 H_{20}}\right)\left(\frac{1}{\alpha_{10}} - \frac{c_1 x_1}{(c_1 H_{10})}\right)$$

(h)
$$\frac{x_2}{l} = \frac{1}{1 + \frac{n_2}{n_1}\left(\frac{c_2}{c_1}\right)^3 \frac{H_{20}}{H_{10}}\left[1 + \frac{1}{H_{20}}\alpha_{20}\right]}$$

Equation (h) expresses the position of the center of gravity for the system to be in neutral equilibrium. If center of gravity positions aft of that given by equation (h) are used, a small displacement of the system from equilibrium will result in divergent motions.

The location of the divergent boundary as computed from equation (h) is shown in figure VI-6 for three values of the parameter, $\frac{n_1}{n_2} \cdot \left(\frac{c_1}{c_2}\right)^3 \cdot \frac{H_{1_o}}{H_{2_o}}$, which will be given the symbol r. It is seen that when this parameter is small, the location of the divergent boundary is much further aft than when it is large. However, it should be remembered that the parameter in question is closely connected with that location of the center of gravity for which the load is equally distributed among the foils.

As an illustrative example, suppose that the chords and normal depths of all foils are the same. The parameter under consideration then becomes simply n_1/n_2, the ratio of the number of foils forward to the number aft. Then if all foils are to be loaded equally, the center of gravity must be located so that x_2/x_1 equals n_1/n_2; if there are two after foils and only one forward foil, the center of gravity must be two-thirds of the way aft.

Since it may be important to have nearly equal load distribution in some cases, the distance between the center of gravity position giving equal load distribution and that giving divergence may be of interest. This distance is shown in figure VI-7. It is seen that on this basis (of permissible departure from the cg position of equal load distribution)

Figure VI-6

CONDITIONS FOR NEUTRAL STABILITY

The System will be unstable if $\frac{x_1}{\ell}$ lies to the right of the curve

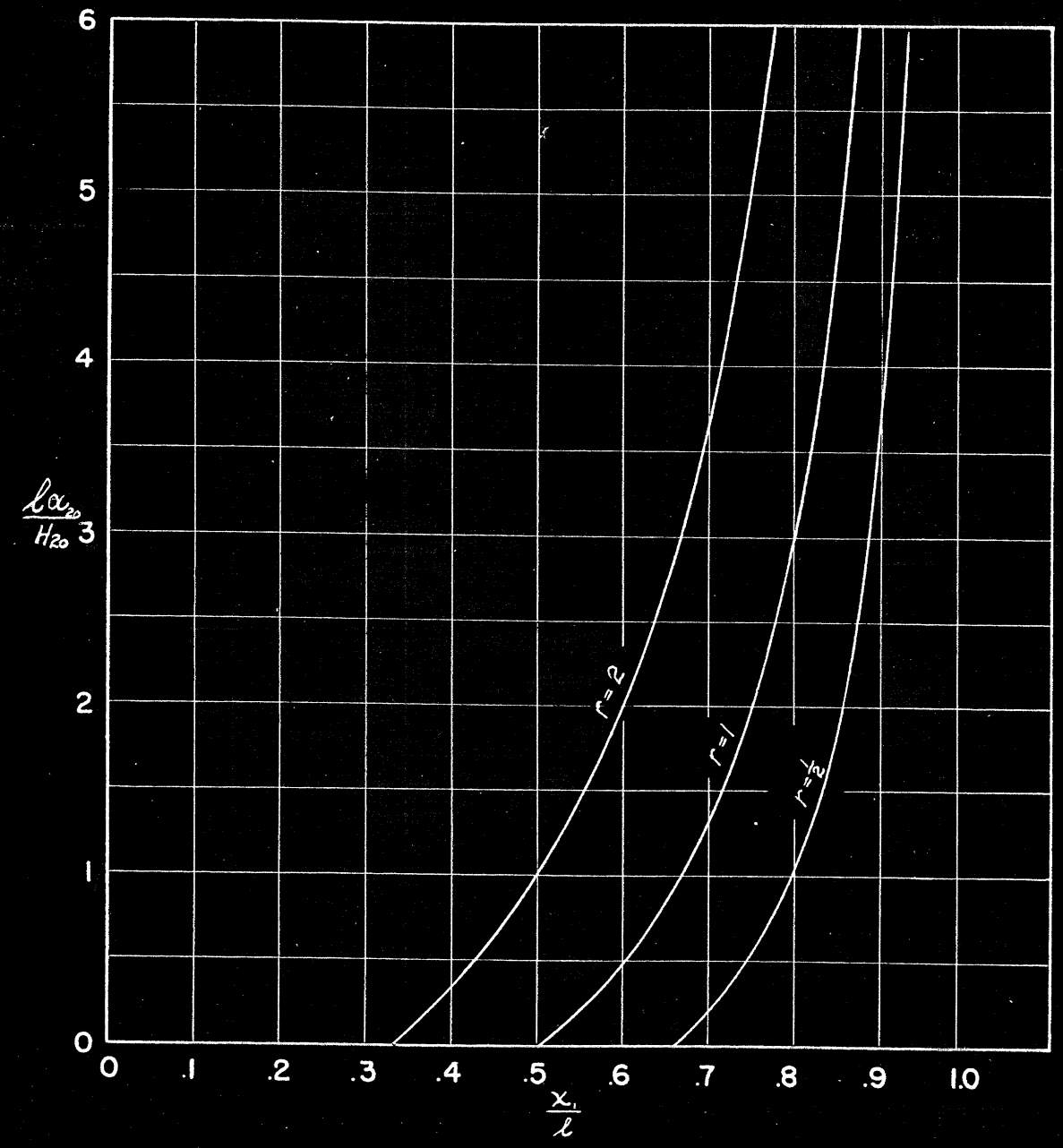

CONDITIONS FOR NEUTRAL STABILITY

HYDROFOIL SYSTEM HAVING TWO DEGREES OF FREEDOM

Figure VI-7

The System will be unstable if $\frac{\Delta x_2}{l}$ is above the curve

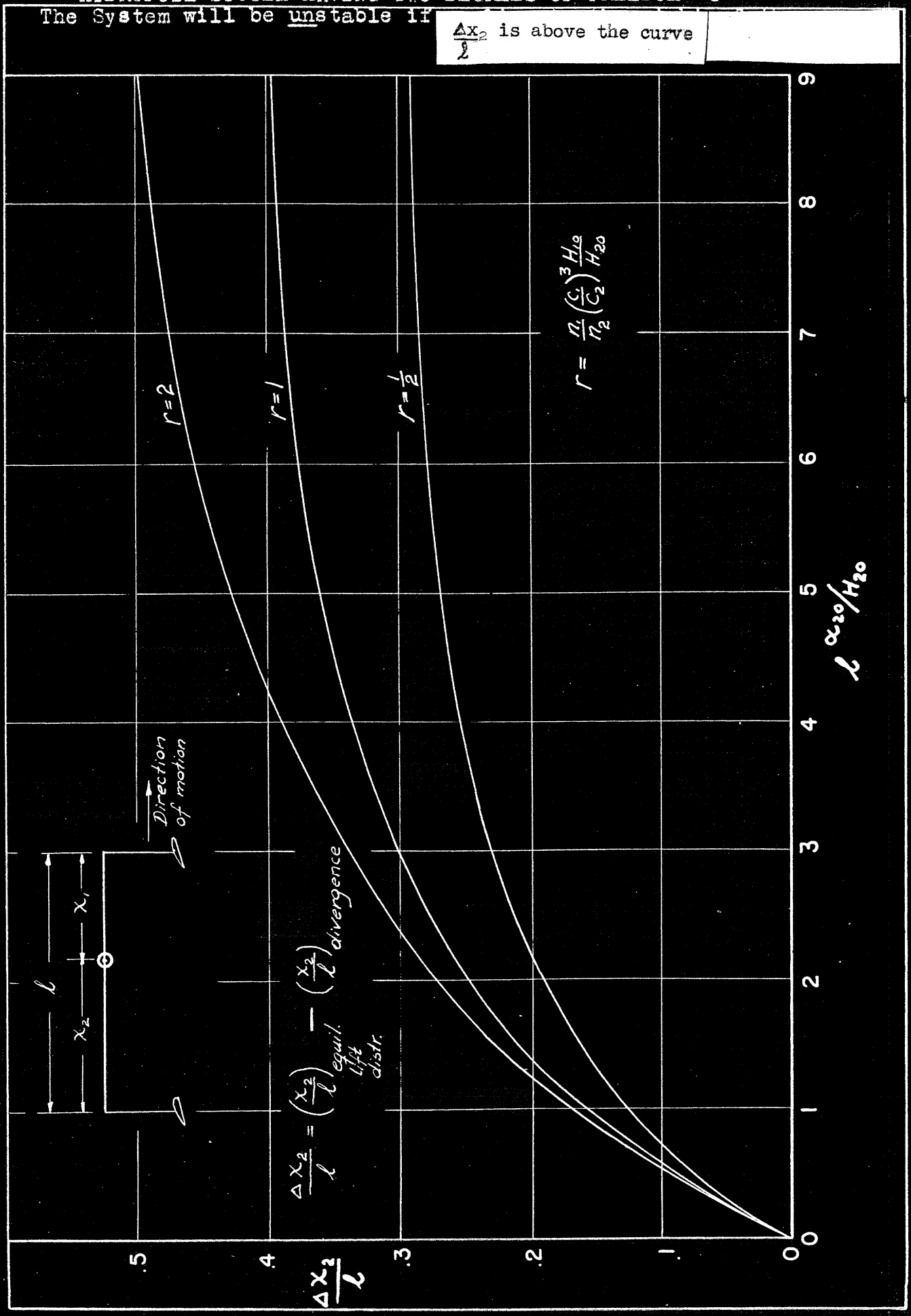

large values of parameter r are advantageous.

Both figures VI-6 and VI-7 show the very important part played by the ratio $\frac{l\alpha_{2_o}}{H_{2_o}}$ in determining the after divergent boundary. In general it is expected that several factors other than center of gravity location -- particularly ventilation and strength considerations -- will prescribe the depth H_{2_o} within close limits. Similarly, the maximum useable value of α_{2_o} is closely limited by the possibility of ventilation. At high speeds α_{2_o} must be very small. It is therefore desirable -- and at high speeds imperative -- that the length of the hydrofoil system be made as great as possible.

It is believed that figures VI-6 and VI-7 may be useful design curves in predicting stable locations of the center of gravity. They will be discussed again in Chapter VII.

Natural Frequencies:

The natural frequencies of the undamped, linearized, two-degree-of-freedom system can be quickly found for the particular case that the pitching and rising motions of the system are uncoupled. This means that pitching (θ only[1]) or rising (z only) oscillations can persist independently of each other. Since the condition of uncoupling is met for the important case that all foils bear the same load, the uncoupled system has been analyzed.

---

[1] In the coordinate system z, θ, a pure pitching motion implies that the center of gravity is stationary, while the system pitches about the center of gravity.

PLATE 4

Each applied force may be broken down into two sets of forces, each of which excites a natural mode:

(e)

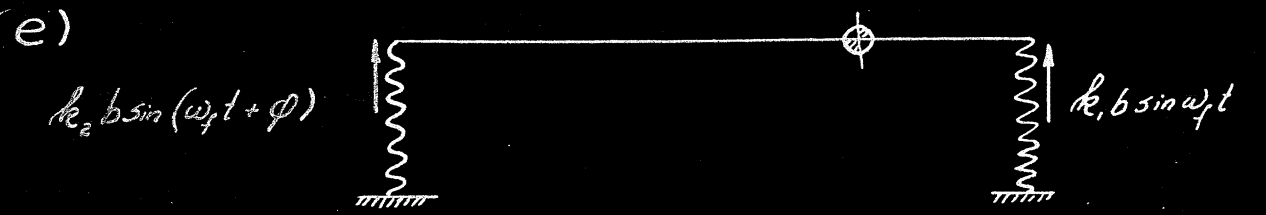

=

(e')

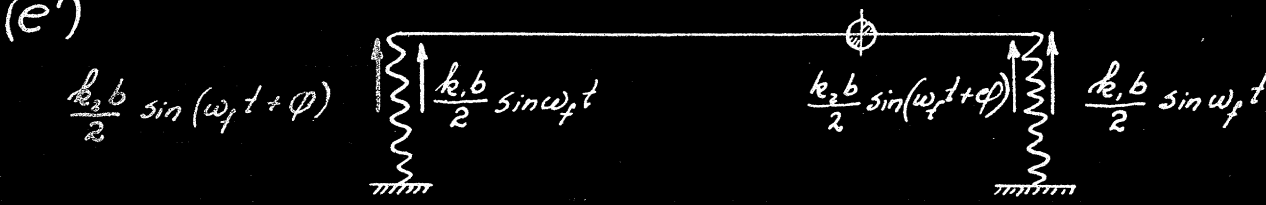

+

(e")

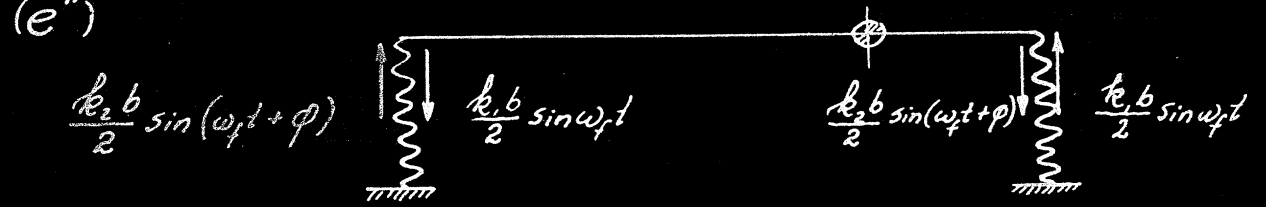

(f)

$$\begin{cases} \dfrac{z}{b} = \dfrac{1}{2}\left[\dfrac{\left(\frac{k_1}{k_1+k_2}\right)}{1-\beta_1^2} \sin \omega_f t + \dfrac{\frac{k_2}{k_1+k_2}}{1-\beta_1^2} \sin(\omega_f t + \varphi)\right] \\ \dfrac{l\theta}{b} = \dfrac{1}{2} \dfrac{1}{1-\beta_2^2}\left[\dfrac{k_1 x_1}{k_1 x_1 + k_2 x_2} \sin \omega_f t + \dfrac{k_2 x_2}{k_1 x_1 + k_2 x_2} (\sin \omega_f t + \varphi)\right] \end{cases}$$

$$\beta_1 = \frac{\omega_f}{\omega_{n_1}} \qquad \beta_2 = \frac{\omega_f}{\omega_{n_2}}$$

FINDING THE NATURAL FREQUENCIES

OF AN UNCOUPLED SYSTEM HAVING TWO DEGREES OF FREEDOM

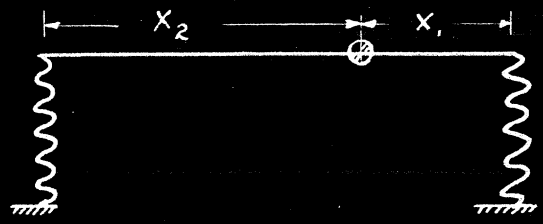

$k_2 = x_1 \frac{mg}{H}$ $\qquad k_1 = \frac{\Delta L_1}{\Delta H} = \frac{L_1}{H} = \frac{\frac{x_2}{l} mg}{H} = x_2 \frac{mg}{H}$

(a) Condition for uncoupling : $k_1 x_1 = k_2 x_2$.

(b)
$$\begin{cases} m\ddot{z} + (k_1 + k_2) z = 0 \\ mx^2 \ddot{\Theta} + (k_1 x_1^2 + k_2 x_2^2)\Theta = 0 \end{cases}$$

(c) Rise: $(\omega_n)_1 = \sqrt{\frac{g}{H_0}}$

Pitch: $(\omega_n)_2 = \sqrt{\frac{x_1 x_2}{k_g^2}} \sqrt{\frac{g}{H_0}}$

(d) $\left(\frac{k_g}{l}\right)^2 \frac{\omega_{n_2}^2}{\omega_{n_1}^2}$

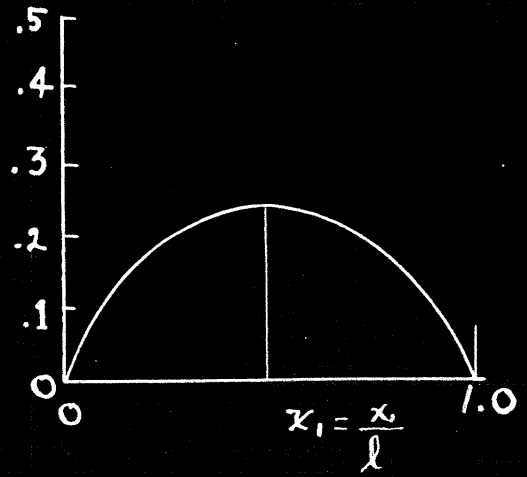

(e)

The system is shown schematically in plate 4, where the hydrofoils have been replaced by equivalent springs, in the manner of section A of this chapter. The effect of omitting damping will be discussed later.

The equivalent spring constants k_1 and k_2 are similar to the spring constant for the one-degree system discussed in section A. If all foils are at the same depth (h), the condition for uncoupling of the pitching and rising motions is that:

(a) $$k_1 x_1 = k_2 x_2$$

When this is true a unit displacement z, for example, will cause no moment about the center of gravity. Similarly, a rotation, Θ, will cause no net vertical force on the center of gravity.

Equations (b) are the equations of motion for the free (uncoupled) oscillations. Each equation can be solved for the appropriate natural frequency, with the results (c).

The natural frequency in rise is the same as in the one-degree-of-freedom case (part A). The pitch frequency differs from the rise frequency by the factor $\sqrt{\frac{x_1 x_2}{k_g^2}}$. Relation (d) is a plot of the ratio of pitch-frequency to rise frequency (multiplied by (k_g^2/ℓ^2), as a function of center of gravity location. For large radii of gyration (k_g/ℓ) the pitch frequency will be very much smaller than the rise frequency. For small values

of (k_g/ℓ) the pitch frequency may be of the same order of magnitude as the rise frequency.

It will be shown (Chapter VII, part I) that when k_g/ℓ is small the pitching motions are heavily damped, so that the natural frequency in pitch is unimportant. For large k_g/ℓ the damping may be small, in which case the natural frequencies calculated for the undamped case will differ little from the damped natural frequencies.

It is concluded that for oscillatory motion the natural frequency of pitching will be lower than that of rising. This fact will be important in understanding the motion in waves.

Motion in Waves:

Some useful information about motion in waves can be quickly deduced, because the wave shapes are sinusoidal in character(Chapter IV). The passage of a hydrofoil system through waves corresponds to a displacement of the bottom ends of springs k_1 and k_2 by the amount of the wave height, ζ. It can be easily shown that this is equivalent to applying forces of $k_1\zeta_1$ pounds and $k_2\zeta_2$ pounds to the upper ends of the springs.

In a uniform wave pattern the spring deflections ζ_1 and ζ_2 would have the same maximum amplitude, and would differ from each other only by a constant phase

angle. Consequently, a similar statement would hold for the equivalent forces applied to the upper ends of the springs.

Consider first the simplified case that the waves are pure sine waves of amplitude b. Then the equivalent forces acting on the system are as shown in the first of figures (e). (ϕ is the phase angle.) By superposition, the black force in figure (e) can be broken up into the sum of the two black forces in figures (e') and (e"). The red force in (e) can be similarly broken up. But the force system (e') (red and black) will cause only a vertical motion of the bar, but no rotation. The force system (e") will cause only rotation about the center of gravity (z = 0). The total rise of the system under forces (e) can therefore be calculated from (e') which acts like a single-degree-of-freedom system. Similarly, the total pitch of the system can be calculated from (e"). The results are expressions (f).

Expressions (f) contain the familiar factors $(1 - \beta_1^2)$ and $(1 - \beta_2^2)$, which represent the magnification in motion when resonance is approached.

C. Method of Obtaining Non-Linear Solutions

Form of the Equation:

The advisability of retaining the equation in the form (7a)[1] -- rather than multiplying out all of the terms -- is recognized at the outset. If the expressions in brackets are multiplied together, a total of twenty-eight variable terms results in each equation (i and l are constants), eighteen of which are products of variables. But if form (7a) is retained, the bracket terms in the first equation are identical with those in the second. In this arrangement, therefore, there are only ten variable terms in each equation and it is necessary to perform a total of only two multiplications.

Choice of Integrating Equipment:

In deciding upon a method of integrating equations (7a) the basic purpose of the thesis was reviewed. This purpose is to study the possible motions of the hydrofoil systems under a wide range of sea conditions and to study the effects of many system variables. In a preliminary study of this type a high degree of accuracy did not seem essential. Further, the data available on lift and ventilation characteristics of hydrofoils was of limited accuracy. It was therefore decided that prime consideration in selecting the method of integrating the

[1] Page 70.

equations should be given to speed of solution rather than to accuracy.

There were available three methods of integration: (1) by means of manual, stepwise calculation, (2) by means of the large MIT Differential Analyser, and (3) by means of a smaller, electronic differential analyser.

After a few trial calculations, it was decided that the tedious trial and error procedure necessary for manual integration was too time-consuming to permit the large number of solutions necessary -- even if only a moderate degree of accuracy were preserved.

The MIT Differential Analyser could produce solutions having a very high degree of accuracy and without the fatigue of manual integration, but it was estimated that fifteen minutes would be required for each solution. (This is the time between changing a variable and seeing its effect.) The expense in man-hours required to operate the machine would also have been very large.

The smaller electronic differential analyser was still under development at the time the equations were ready for solution, but this machine offered some important advantages. Foremost of these was the principle on which it operates of presenting solutions sixty times per second. Thus as system parameters, forcing functions, and initial conditions are varied, their effect on the entire solution can be seen instantaneously. Many

solutions can thus be obtained in a short time and an entire range of variation of a parameter can be investigated at one "sitting". Another important advantage of the electronic machine was its comparitively low-operating expense -- about twenty-five dollars per day (excluding the operators time).

With its advantages this machine had some attendant disadvantages. The errors introduced by the linear components of the machine were found to be between five per cent and ten per cent, but the errors introduced by the multipliers were estimated to be at least fifteen per cent, and were later found to be of the order of twenty to twenty-five per cent. Since the equipment was in the early stages of development, considerable electronic difficulty was anticipated. This apprehension was more than justified.

However, the speed of solution offered by the electronic differential analyzer seemed to suit it so well to the need of covering a large range of many variables that it was decided to begin the solutions on that machine.

Description of the Electronic Differential Analyzer:

No attempt will be made in this thesis to describe or evaluate the electronic aspect of the equipment[1]. However, a tabulation of the analyzing units available and of their mathematical capabilities will facilitate discussion of the application of the machine in solving equations, (7a), page 70.

1. Information on this aspect can be found in reference 20.

The equipment consists of several each of the following units: adders, integrators, multipliers, square-wave generators, triangle wave generators and arbitrary function generators.

Briefly, voltages are employed to represent the variables in the problem. Each unit of the machine consists of two sets of terminals. To one set are applied the voltages representing input functions. Voltages representing the output functions then appear at the other set.

Time is the independent variable in the present problem. Consequently, all quantities are presented (on the oscilloscope) as functions of time. The time of solution (1/100th of a second) is chosen to represent a specific problem-time. The oscilloscope then pictures what happens during the specified time-interval.

Adders:

If a unit is designated as an "adder", then it consists of electronic circuits such that if voltages are applied to each of its input terminals, another voltage representing their sum will occur at the output terminals.

Actually the input terminals of the adder are not connected directly to the adder circuit. Instead, there is a separate attenuating stage between each input and the adder circuit, and an amplifying stage between the circuit and the output of the adder unit. Thus, if one

input to the adder unit is x, any portion of x --- from .1x to 80x -- may be added to the other inputs. (In analyzer parlance a "gain" may be applied to each input before the inputs are added.)

Integrators:

The terminals to the integrator units lead through an amplifying stage to an integrating circuit whose output voltage is the time-integral of its input voltage. Each integrator unit contains a square-pulse generator so that the level of the output voltage may be set at any desired value. This is the mathematical equivalent of setting the "constant of integration" or "initial conditions" of the problem. This ability to set initial conditions at will and to observe the results instantaneously comprises a great advantage of this type of computing equipment.

Both the adder and integrator circuits happen to have the characteristic that their output is negative. That is the adder output is (-) the sum of the inputs, and the integrator output is (-) the integral of the input. Because of this feature any adder or integrator may be used as a sign-changer. (In the case of the integrator a small external circuit change must be made).)

Function Generators:

A single unit serves either as a multiplier or a function-generator.

When used as a function-generator, the unit presents

an output voltage which is any arbitrary function of its input voltage. (The arbitrary function is introduced into the unit in the form of a black-paper mask, cut to the desired shape.) In this problem two function-generators were used to supply the instantaneous value of the wave height above each foil. Therefore, the input to the function generators was a signal proportional to time (i.e.)a "triangle" wave: 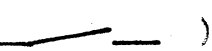). The mask was cut in a series of trochoidal shapes. The output voltage then had the desired wave-form. The frequency of the output -- i.e. the number of waves traversed during the solution time -- could be varied by changing the slope of the input signal. Wave height was varied by means of the amplifier at the input to an adder.

Multipliers:

When used as a multiplier, the unit presents an output voltage proportional to each of the two voltages applied at its input terminals. Thus the output represents the product of the inputs to some scale. The scale -- i.e. the amount of the output variable represented by a unit voltage is of course arbitrary. But once the scale has been chosen, the scale of both of the input variables, and hence, of all other variables in the system, is specified.

Circuit Synthesis:

A schematic layout of the differential analyzer control panel is shown in Fig. VI-8. A part of the network used in solving equations (5) is shown for demonstration purposes. One loop of the network will be traced.

Since the loop is a closed one, the starting point is arbitrary. Begin, for example, by assuming that a voltage representing $\ddot{z}$ is available. This voltage is applied at the input of integrator number 1. The output of integrator 1 will then be proportional to $-\dot{z}$. This quantity is integrated again by integrator 2, giving signal $i_2 z$, proportional to z.

Adder 1 has been chosen to form the sum H_1. Since one component in this sum is z, signal $i_2 z$ is applied to one input of adder 1. The other inputs are connected to the other quantities in the sum H_1.

The output of adder 1 is therefore proportional to H_1. This quantity is entered at one input to multiplier 1, and a signal proportional to α_1 is entered at the other input, so that the output of multiplier 1 is proportional to the product $H_1 \cdot \alpha_1$.

This product is added to a similar product -- $H_2 \cdot \alpha_2$ -- obtained from multiplier 2. When these products are properly added their sum is proportional to $\ddot{z}$, according to the equation being solved. This output is, therefore, the quantity assumed to be available at the outset, and may be connected to the input of inte-

grator 1, closing the loop.

The entire network for the solution of equations (7a) is shown in Fig. VI-9. The symbols preceeding the output quantity of each unit (e.g. a_1, i_3, etc.) are the proportionality constants, dependent upon the gain of the unit. They must, of course, be properly adjusted according to the requirements of the equation and the limitations of the electronic equipment. In particular, the proportionality constants of the multipliers -- and of the units to which they are connected -- must be very carefully chosen.

Solutions obtained from the electronic differential analyzer, as set up in Fig. VI-9, will be presented in Chapter VII, part 3.

$\frac{\ddot{z}}{p^2 g} = -\frac{x_2}{l}\left[f_1 + \frac{f_2}{r}\right] + 1$		$f_1 = \frac{H_1}{H_{10}} \frac{\alpha_1}{\alpha_{10}}$	$f_2 = \frac{H_2}{H_{20}} \frac{\alpha_2}{\alpha_{20}}$
$\frac{H_1}{H_{10}} = \frac{z}{H_{10}} - \frac{x_1}{l} \frac{l\theta}{H_{10}} + \frac{(\xi_1 - i)}{H_{10}} + 1$			

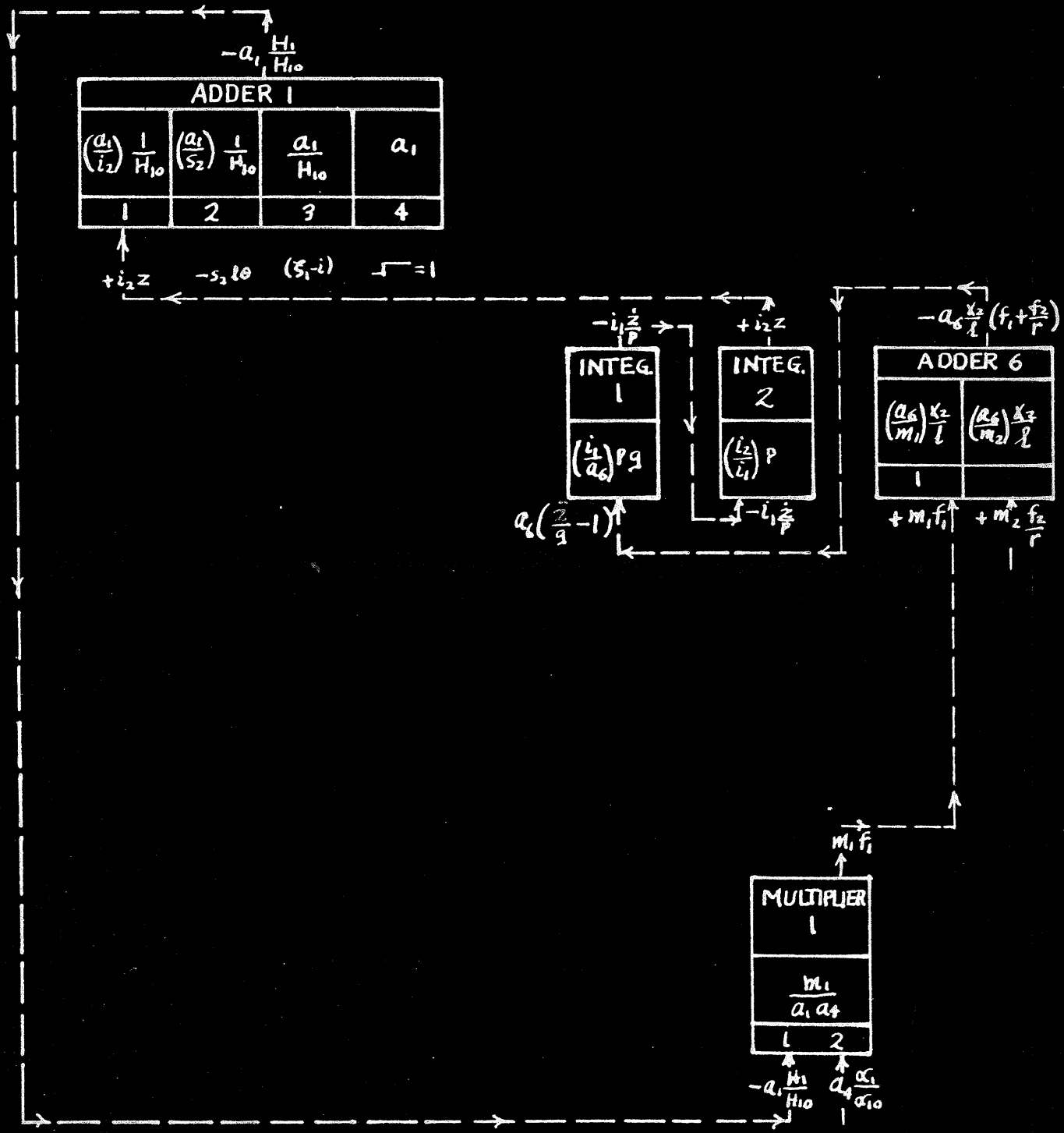

DIFFERENTIAL ANALYZER SETUP FOR SOLVING EQUATIONS (7)

Figure VI - 9

$\frac{\ddot{z}}{p^2 g} = -\frac{x_2}{l}\left[f_1 + \frac{f_2}{r}\right] + 1$	$\frac{\left(\frac{k_g}{l}\right)^2 l\ddot{\theta}}{\frac{x_2}{l} p^2 g} = -\left[-\frac{x_1}{l} f_1 + \frac{x_2}{l}\frac{f_2}{r}\right]$	$f_1 = \frac{H_1}{H_{10}}\frac{\alpha_1}{\alpha_{10}}$	$f_2 = \frac{H_2}{H_{20}}\frac{\alpha_2}{\alpha_{10}}$
$\frac{H_1}{H_{10}} = \frac{z}{H_{10}} - \frac{x_1}{l}\frac{l\theta}{H_{10}} + \frac{(\zeta_1 - i)}{H_{10}} + 1$	$\frac{\alpha_1}{\alpha_{10}} = \frac{\dot{z}}{pV\alpha_{10}} - \frac{x_1}{l}\frac{l\dot{\theta}}{pV\alpha_{10}} + \frac{l\theta}{l\alpha_{10}} + 1$		
$\frac{H_2}{H_{20}} = \frac{z}{H_{20}} - \frac{x_2}{l}\frac{l\theta}{H_{20}} + \frac{(\zeta_2 - i)}{H_{20}} + 1$	$\frac{\alpha_2}{\alpha_{10}} = \frac{\dot{z}}{pV\alpha_{10}} + \frac{x_2}{l}\frac{l\dot{\theta}}{pV\alpha_{10}} + \frac{l\theta}{l\alpha_{10}} - \frac{\alpha_{20}}{\alpha_{10}}$		

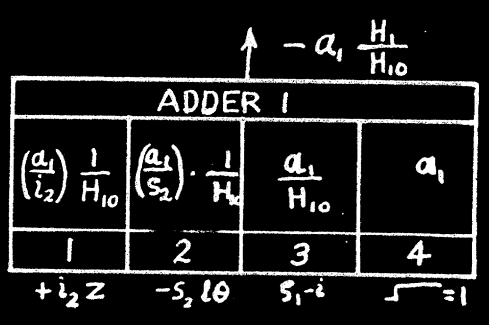

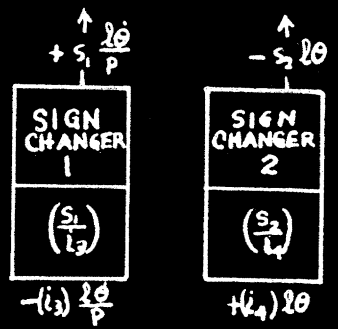

Note: Soln. Time = represents P seconds.

(All derivates on this page are with respect to t/p.)

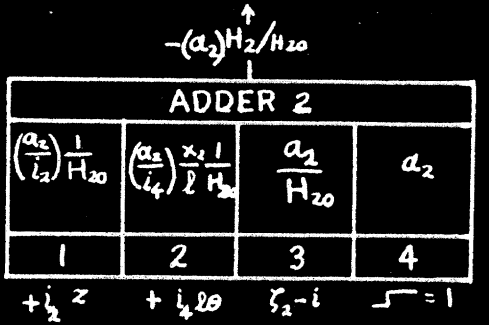

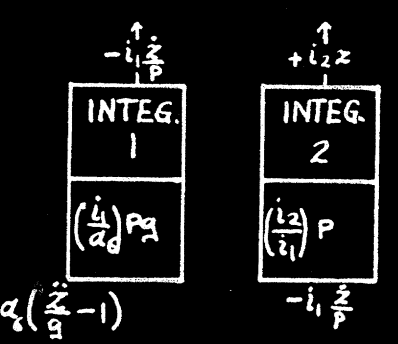

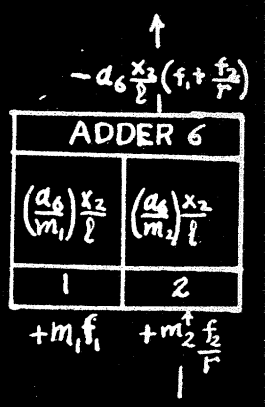

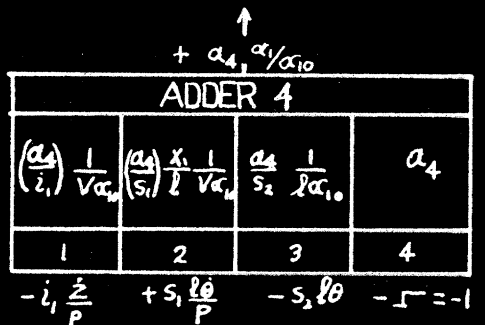

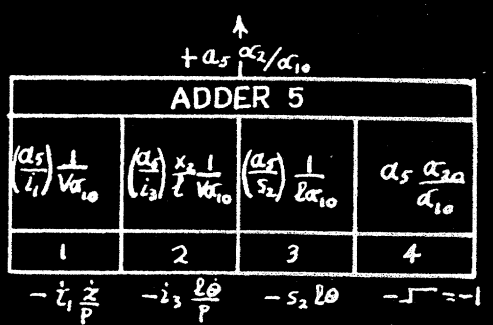

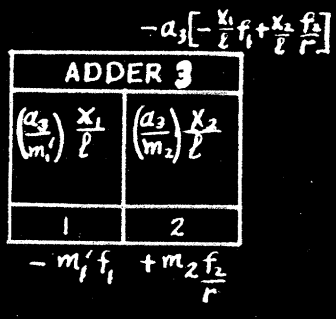

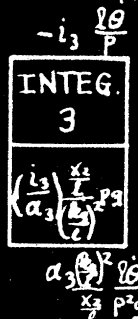

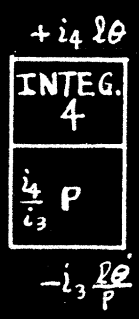

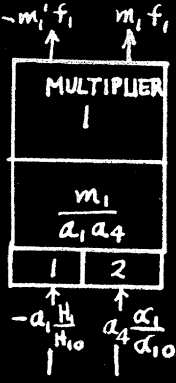

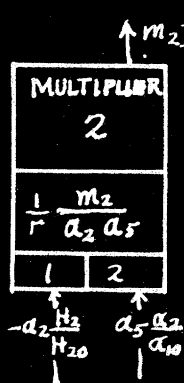

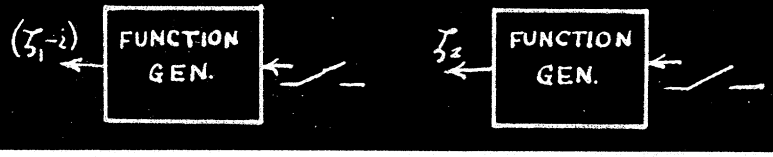

CHAPTER VII

RESULTS OF CALCULATIONS

Differential Analyzer Solutions to the Equations of Motion of a Hydrofoil System Having Two-Degrees-of-Freedom.

Part 1: LINEAR SOLUTIONS

Preliminary solutions to the linearized equations of motion were obtained to serve three main purposes: 1) They form a link between the present study and the earlier work of Mr. Frederick Imlay[1]; 2) They furnish a preview of the degree of importance of three of the major hydrofoil-system parameters; 3) They make possible some comparison between linear and non-linear solutions.

Procedure:

With the first of these purposes in mind, the initial calculations were made for a system similar to one studied by Mr. Imlay. Dimensionally this system consisted of two equal hydrofoils of 1.5 inch chord and 30-degree dihedral, spaced ten chords apart. The weight of the system was 8-1/4 pounds and the radius of gyration was two-thirds of a boat length (6.67 chords). The equilibrium depth of the foils was such that the projected area of each was 6 square chords, and the foil tips were considered to pierce the surface always. The forward speed

[1] Reference 12

was 20 feet per second. The center of gravity position was a variable.

The dimensionless parameters in the linearized equations were set up on the differential analyzer to represent this system. The responses to a step change in load were obtained for many values of center of gravity position, and the solutions were compared with those of Imlay.

Next, these solutions were repeated for two values of boat-length and for two radii of gyration. Thus, the inter-effects of center of gravity location, boat-length, and radius of gyration were available for preliminary study.

Discussion of Results:

The results of the linear, two-degree-of-freedom calculations are presented in figures VII-1 and VII-2. Each of the traces in these figures is a copy of the oscilloscope trace representing the motion z or $\ell\,\theta$ when the other parameters in the system were as noted. (It is recalled that z is the downward displacement of the c.g. and θ the pitch angle. ℓ is the boat length in chords.)

Figure VII-1 shows the response of the system when it is subjected to a sudden vertical force[1]. The length of the system is 10 chords, and the center of gravity

[1] The force applied was equal to the original weight of the system. However, the relative amplitudes of force and resulting motion are the quantities of interest; absolute amplitudes are unimportant because the system is linear.

location is noted next to each trace. The solid traces show the differential analyzer solutions, while the dotted traces show the corresponding manual calculations of Imlay.

Comparison of Manual and Machine Calculations:

The manual calculations are, of course, the more accurate, and should be considered the standard for comparison. The machine calculations are seen to be in reasonably good agreement with the manual calculations for those cases where the motions are stable. ($\frac{x_1}{\ell}$=.35, $\frac{x_1}{\ell}$ = .43.) The machine solutions were found to be highly sensitive to the various gain settings near each of the unstable boundaries. Thus, when $\frac{x_1}{\ell}$ = -.2, the machine response was an unstable oscillation, even when no forcing function was applied. Imlay's calculations of stability roots indicated neutral stability at this point. The natural frequencies of machine and manual calculations are in good agreement at all points.

It is concluded that the machine calculations are reliable in the stable region, but predict the unstable borders with some error.

Center of Gravity Position:

The combined effects of center of gravity position, length, and radius of gyration are shown in figure VII-2 which displays all of the linear calculations made.

The effect of center-of-gravity position on stability is clearly demonstrated. Consider first the

system of length 10 chords, shown in column 1, The limits of stable operation are between $\frac{x_1}{\ell} = .2$ and $\frac{x_1}{\ell} = .5$. The instability at $\frac{x_1}{\ell} = -.2$ is oscillatory. At $\frac{x_1}{\ell} = 0$ a stable response is obtained, still highly oscillatory. As the center of gravity is moved aft, the damping becomes more and more effective, until at $\frac{x_1}{\ell} = .5$ no oscillation takes place (damping is super-critical). However, operation at $\frac{x_1}{\ell} = .5$ is indicated to be quite dangerous because of proximity to the region of unstable divergence.

The conclusion is that, <u>for this system</u>, if a smooth (non-oscillatory) ride is desired, without the danger of a sudden dunking, the center of gravity should be placed between two-tenths and four-tenths of the way back from the forward hydrofoil.

<u>Boat Length:</u>

The effect of boat length on stability can be seen in figure VII-2 by comparing column 2 with column 1.

The advantage of a "long" system (i.e. one having a large length-to-chord ratio) over a short system is clear and emphatic. The longer boat has a markedly greater range of stable c.g. positions. (Imlay has calculated the boundaries of the stable region at $\frac{x_1}{\ell} = -.9$ and $\frac{x_1}{\ell} = +.7$ for $\ell/c = 20$, as compared with $\frac{x_1}{\ell} = -.15$ and $\frac{x_1}{\ell} = +.5$ for $\ell/c = 10$.) What is more important, the motions of the long system are more highly damped at any positive value of $\frac{x_1}{\ell}$. This decisive importance of having the ratio ℓ/c

as large as possible will be demonstrated repeatedly by the results of the non-linear calculations.

Radius of gyration:

The motions in column 2, figure VII-2 are the responses of a system whose length is twice that of the system in column 1. In the third column of figure L-2 are shown the responses of a system having the same length as the system in column 2, and the same radius of gyration as the system in column 1. A comparison of columns 2 and 3 showns that decreasing the radius of gyration effects an important additional improvement in performance. The improvement is not so great, however, as the initial improvement due to increased length.

Divergent Boundaries:

The divergent boundaries of the system were defined in Chapter VI, section B, and were predicted in figure VI-6. The system represented in figure VII-1 has a small value of $\ell\alpha_{20}$ (about .35 chords), and a value of r = 1. From figure VI-6 divergence should first occur when x_1/ℓ is about .56. This is shown to be closely the case in figure VII-1.

Natural Frequency:

In section A of chapter VI it was shown that the natural frequency in rise of a variable-area hydrofoil system was given by $f_n = \frac{1}{2\pi}\sqrt{\frac{g}{H_0}}$ in the absence of

damping. Heavy damping was shown to decrease the natural frequency. In section B it was shown that for large radii of gyration the natural frequency of pitching would be much less than that of rising. The frequency at which the system will perform a particular combination of the two motions would therefore appear to be somewhat less than the rising frequency.

For the system shown in figure VII-1 the value of H_o is 2.61 inches, for which the above formula gives f_n = 1.94 cycles per second. A fair amount of pitching is seen to take place in figure VII-1, and the frequency of oscillation is about 1.5, which is reasonable on the basis of the above discussion.

Summary:

The differential analyzer solutions of the equations of motion of a linearized two-degree-of-freedom system predict the motions of the system with acceptable accuracy. The prediction of the unstable limits of operation appears to be subject to error.

An increase in the length-to-chord ratio markedly increases the region of stable operating conditions and effects greatly improved performance under given operating conditions.

Decreasing the radius of gyration of the system further expands the region of stable operation and further improves performance under given conditions.

The divergent boundaries and frequencies of the vibration of the system are in good agreement with the predictions of Chapter VI.

The conclusions indicated by the differential analyzer solutions regarding the motions of the system, ranges of stability, and the effects of the length-chord ratio and radius of gyration are all in agreement with the conclusions expressed by Imlay in reference 12 .

The responses of the linear system to sinusoidal disturbances --particularly ocean waves-- could easily have been obtained in the same manner as the responses to step-loadings have been. However, the time available for analysis was limited, and it was decided that results of greater usefulness could be obtained by concentrating on the physically more valid non-linear equations.

However, the conclusions reached in the linear investigations of Chapter VI and the results of linear calculations just discussed will be referred to frequently in analyzing the non-linear results which are presented in the next section.

Part II: SOLUTIONS TO THE NON-LINEAR EQUATIONS OF MOTION OF A HYDROFOIL SYSTEM HAVING TWO DEGREES OF FREEDOM

At this point in the development the linear approximation of the equations of motion are discontinued. Henceforth, the solutions obtained will be limited in validity largely by the accuracy of the calculating methods, rather than by the form of the equations.

It should be pointed out, however, that there remain two approximating assumptions: (1) the relation bebween lift and depth has been replaced by a straight line (FIGURE 2); and (2) the effects of orbital motions of water particles in waves have been neglected.

The performance of hydrofoil systems in the most general sea conditions will be approached in three stages; First, the performance in smooth water will be studied; second, the motions will be observed when the system has reached steady state conditions in a uniform wave pattern; and finally, the calculated transient performance of a large number of systems in the worst feasible sea conditions will be presented.

Transient Motions in Smooth Water:

In this section calculations will be discussed which correspond to making tests on a boat under calm water conditions. The boat is assumed to be moving at constant speed, and is given various displacement from equilibrium. The resulting motions are then observed.

Procedure:

The performance of the non-linear, two-degree-of-freedom system in smooth water (i.e. in the absence of surface waves) was most easily studied on the differential analyzer by varying the initial conditions of the equations of motion and observing the transient response of the system. Electronically, this was done by means of the square-pulse generators built into each integrator (see Chapter VI, section C). Physically, this corresponds to giving the boat initial values of pitch angle, pitch velocity, displacement (from the equilibrium position), and vertical velocity, and then observing the resulting motions.

The transient responses of many hydrofoil systems to many different sets of initial conditions were observed. In addition, one standard set of initial conditions was chosen to which the response of the system was recorded as each of the system-parameters was varied over a large range.

"Standard Response":

The choice of a "standard" set of initial conditions was necessarily somewhat arbitrary. The main requisites were that the conditions be physically reasonable, and that both pitching and rising motions be excited. In addition, it was desired to cause motions large enough that their characteristics could be easily detected, and

at the same time not so large as to overload (electrically) the components of the analyzer.

With regard to physical reasonability, particular attention should be given to the fact that the solutions will be considerably in error whenever a hydrofoil comes completely out of the water. (This is shown clearly in FIGURE 2, where the straight-line approximation becomes increasingly inaccurate for negative depths.) It was therefore decided that the initial conditions should be such as not to cause either hydrofoil to come out of the water.

After many trials the following set of initial conditions was adopted: $z = +1$, $\ell\theta = -1$, $\dot{z} = 0$, $\dot{\theta} = 0$. In other words, the center of gravity is pushed down one chord. The boat is rotated about the center of gravity until its forward foils are one chord deeper than the after foils. The boat is then released from rest[1], and its motions are observed. For convenience, the response of a system to this set of initial conditions will hereafter be referred to as the "standard response" of the system. (It is understood that this "standard" is quite arbitrary.

---

[1] It is recalled that the boat is "at rest", with respect to the coordinate system adopted, and water is moving past it with constant velocity, V.

Method of Recording Data:

With the analyzer set up as explained in Chapter VI-C it was possible to present on the oscilloscope any of the following quantities: z, $\dot{z}$, $\ddot{z}$, θ, $\dot{\theta}$, $\ddot{\theta}$, $\frac{\alpha_1}{\alpha_{10}}$, $\frac{\alpha_2}{\alpha_{10}}$, $\frac{H_1}{H_0}$, $\frac{H_2}{H_0}$. Of particular interest in this study were displacements z and θ, which describe the motions of the system; acceleration $\ddot{z}$, which will be important in stress calculations and in compact considerations; angles of attack $\frac{\alpha_1}{\alpha_{10}}$ and $\frac{\alpha_2}{\alpha_{10}}$, which determine likelihood of cavitation and ventilation; and depths $\frac{H_1}{H_{10}}$ and $\frac{H_2}{H_{20}}$, which will indicate when the solutions are in error because of either foil being out of water, and which are also important in predicting likelihood of ventilation.

By far the simplest method of recording so much information in a short time was to photograph the oscilloscope screen. The procedure, then, was to set the machine to solve the equations under a desired set of conditions. The oscilloscope was then connected in sequence to the terminal whose voltage represented each of the quantities of interest. A plot of the desired quantity vs. time then appeared stationary for the oscilloscope, and could be photographed. (Usually several quantities were photographed on a single film.)

Figure VII-3 is a typical set of oscilloscope photographs, picturing the "standard response" of a two-degree-of-freedom, non-linear system. The distance marked

"solution time" on photo 1a represents 1-1/4 seconds. Other scale factors are indicated.

Photo 3a shows the initial-condition settings: $z = +1$, $\ell\theta = -1$. The period of free oscillation can be estimated: $T = 1$ second. A strong "restoring-spring" action is shown by the fact that the center of gravity (z) moves only slightly below its initial value, in spite of the large initial downward pitch angle ($\ell\theta$). The natural effect of the pitch attitude in directing the displacement is evident in the picture.

Photo 3b pictures the values of $\frac{\ddot{z}}{g}$, $\frac{\dot{z}}{10}$, and $\frac{\ell\dot{\theta}}{10}$. (This scale was chosen for $\dot{z}$ and $\ell\dot{\theta}$ because $V\alpha_{10}$ is approximately 10, and it is the ratio of $\frac{\dot{z}}{V\alpha_{10}}$ and $\frac{\ell\dot{\theta}}{V\alpha_{10}}$ which is important. A comparison of photo 1b with pictures of $\frac{\alpha}{\alpha_{10}}$ will thus indicate the effect of vertical velocities on true angle of attack.)

The acceleration of the center of gravity during response is initially downward. As the lowest position is reached the acceleration is, of course, upward. Except for the initial instant the acceleration varies between $-.2g$ and $+.2g$.

In comparing $\frac{\dot{z}}{10}$ with $\frac{\alpha}{10}$ (VII-3c) it should be remembered that $\frac{\dot{z}}{10}$ is plotted positive upward, and $\frac{\alpha}{\alpha_{10}}$ positive downward. The contribution of $\dot{z}$ to α is evidently large. $\frac{\alpha_1}{\alpha_{10}}$ varies between .65 and 1.25, and $\frac{\alpha_2}{\alpha_{10}}$ between .85 and 1.1. It was shown in chapter III that

these values are well within the safe region, from the cavitation standpoint.

Photo VII-3d shows the depth of each foil (measured from the hypothetical surface, about 1/2 chord below the real surface). In this case, neither foil comes dangerously close to the surface at any time.

Importance of Non-linearities:

A typical series of pictures, taken to show effects additional to those available from "standard" responses, is shown in figure VII-4.

In this particular series the effect of the non-linear character of the problem was studied. The initial value of z was varied, all other initial conditions being zero.

Were the equations linear, the first two responses of figure 2 should be mirror images of each other, and all the remaining responses should differ from the first by only a scale factor. The effect of the non-linear terms on the general shape of the response is evident. The first two responses are, in fact, different in basic character. The most striking effect is the great increase in "stiffness" of the system as the free water-surface is approached.

Copies of several hundred photographs like those in figures SWP-1 and 2 are presented throughout the remainder of this thesis. (see for example, figure VII-5)

The effects of a number of boat-parameters are clearly shown by the smooth-water results. These will now be discussed in turn.

Effect of cg Location:

The effects of center-of-gravity location, $\frac{x_1}{\ell}$, on the transient motions of a hydrofoil system are shown under a number of different conditions in figures VII-5 to 7. (All of the figures show the "standard response" of the system - see page 122.) The most stringent limitations on $\frac{x_1}{\ell}$ are shown in the third column of figure VII-7. The case shown is for a short boat (ℓ = 10 chords) with two foils forward and one aft. The system is stable only when $\frac{x_1}{\ell}$ is very close to .33. For a more stable arrangement, such as that shown by column 1, figure VII-6, a very wide range of values for $\frac{x_1}{\ell}$ will be most satisfactory depending to some extent on which foil arrangement is used. This is shown in the other columns of figure VII-6. For the arrangement of two foils aft and one forward ($n_1/n_2 = 1/2$) the most desirable response appears to be attained when $\frac{x_1}{\ell}$ = .5. For the other two arrangements -- one forward, one aft, or two forward, one aft -- this position is too near the divergent boundary. A value of $\frac{x_1}{\ell}$ nearer to .33 must be used, despite the more oscillatory motion which will result.

The maximum limit placed on $\frac{x_1}{\ell}$ by the occurrance of divergent instability is indicated in each of the columns of figures VII-6 and VII-7. A comparison of these values

with the divergent boundaries predicted from the linear analysis of Chapter VI-B (see figure VI-6) shows that the linear predictions always offer more leeway than is found to exist in the non-linear results. In other words, the center of gravity must always be placed well forward of the divergent boundaries shown in figure VI-6. However, the importance of having a "long boat" stressed by figure VI-6 is borne out by figures VII-6 and 7.

Effect of Length:

As with the linear calculations, the effect of the ratio ℓ/c is found to be of controlling importance. This is shown clearly in figure VII-5. For the shortest boat studied ($\ell/c = 10$) only center of gravity locations very near the one-third point result in stable motions. For $\ell/c = 20$ the range is increased to $0 < \frac{x_1}{\ell} < .8$. For any given cg location an increase in length is seen to improve performance greatly.

Effect of Speed:

The cardinal importance of the velocity, V, with which the hydrofoil system moves through the water is shown for the first time in figures VII-8, 9, and 10. The central column in each of these figures is the same, while the two outside columns provide comparitive responses when one parameter is changed. The parameters changed are: for VII-8 -- length; for VII-9 -- loading; and for VII-10 -- arrangement.

All of the above figures show that as speed is increased the amplitude of the response increases rapidly, and that the amount by which oscillations are damped is not increased in proportion. Evidently the "spring-stiffness" of the system is decreased by increased speed, until eventually at some speed the system is unstable for the initial conditions shown.

In figure VII-8 it is seen that a short boat will become unstable at a relatively low speed -- less than 80 feet per second. The medium-length boat is still stable at high speed, but its motions are quite large. The motions of the long system are shown to be quite stable for the entire speed range studied.

The effect of foil loading is shown in figure VII-9. The lightly loaded system will evidently become unstable for speeds slightly greater than 80 feet per second. The more heavily-loaded systems remain barely stable even for the top speed studied (160 feet per second). It is important to notice that the "spring-stiffness" of the system definitely increases with loading. In other words, a lightly loaded boat undergoes much larger transient motions than a heavily loaded boat. (It is not necessarily more stable, however.) The only important effect of foil -arrangement evident for the particular center of gravity location shown in figure VII-10 is that the spring-stiffness of the system is greater for the arrangement having two hydrofoils aft and one forward ($n_1/n_2 = 1/2$).

Part III: SOLUTIONS TO THE NON-LINEAR EQUATIONS OF A HYDROFOIL SYSTEM HAVING TWO DEGREES OF FREEDOM -- PERFORMANCE IN WAVES

Introduction

Purpose:

The purpose of this, the largest section of the program is to study the performance of hydrofoil systems in the worst feasible sea conditions. This study was deemed necessary, because, as all water-travelers know, one's chances of encountering the "worst sea conditions feasible" -- even on a short excursion-- are very high. The steady-state performance of a system, while interesting and informative, is expected to lead to a sense of false security, because the steady-state is likely to be seldom-reached in normally confused seas.

Method:

The first step in studying performance under the worst sea conditions is to discover what these worst conditions are. Four primary wave parameters will be studied: (1) wave-height, b, (2) the depth of the hydrofoils as they enter a wave, H_I (measured in chords); (3) the frequency with which waves are encountered, N(waves per second); and (4) the "phase" between the position of the front and rear foils in a wave at any instant, ψ. The last quantity is

equal to the ratio of boat-length to wave length, where wave-length is measured in the direction of travel .

It is recognized that the above quantities are quite inter-related. If the frequency, boat-speed, and boat-length are known, for example, then the phase is known. However, the term $\ell\alpha_{10}$ will be used instead of boat-length, and the term $V\alpha_{10}$ will be used instead of speed. In this way several lengths and speeds (under different loading conditions) can be represented by a single pair of values for $\ell\alpha_{10}$ and $V\alpha_{10}$. (A tabulation of the loadings, speeds, and boat lengths represented by various pairs of these parameters is given in TABLE 1.) The applicability of the results to each of the conditions represented by a given pair -- $\ell\alpha_{10}$ and $V\alpha_{10}$ -- will be determined at the end of the analysis.

The important possibility of traveling at some arbitrary angle with the wave system is, of course, implied, when all of the wave parameters are varied separately.

With regard to physically reasonable wave shapes, it is noted that the wave profile will be steepest for straight upwind or downwind travel. Under these conditions the wave length is given by FIGURE 4 for stated values of V and N. The wave height, b, should be compared with this wave length, λ , to see whether the wave steepness, b/λ , is reasonable. (For example, long waves having b/λ greater than one-tenth have been shown in Chapter IV to be unreasonable.)

In order to find the worst feasible[1] combination of the four wave parameters, the following procedure was followed: (1) the parameters H_i, ψ, and N were each varied separately, and the worst feasible values of each were determined. (2) The effect of each of the hydrofoil-system parameters was studied, always under the worst combination of wave-parameters, as determined in step (1). (In other words, the boat was assumed to be operating in the worst cross-wind direction.) (3) The same procedure was followed as in (2), except that the boat was assumed to be moving directly upwind or downwind, and the appropriate value of N was calculated in each case. The data taken included the largest wave-height, b, which could be negotiated by the system under study, without instability. Plots of these maximum values of b against the various system-parameters show the effect of each parameter. As always, the criteria for stable performance included the necessity for both stable motion and sub-cavitation loading.

Calculating Procedure:

Because of the very large number of solutions it was necessary to perform in order to carry out the ob-

---

[1] The term "feasible" is used to preclude such unlikely conditions as negative values of i (the whole boat is out of water), or negative phase angles (the rear foils hit each wave before the front ones do.)

jectives of this section of the calculating program, the careful development of a calculating technique was necessary. The technique was based on several considerations.

First, it was necessary to consider the accuracy of the differential analyzer. It has been mentioned in Chapter VI that the probable error of the machine when set up to solve the general non-linear equations (7) was of the order of twenty to thirty percent -- as great as some of the effects it was desired to measure. However, the "precision" with which the machine will repeat a given solution (if the machine settings are unchanged) is very high. It was, therefore, possible to observe the effect of changing a given set of parameters with considerable consistency, even though the absolute values of the solutions may have been very much in error, provided the particular parameters under observation were changed in a systematic manner, and provided no other settings were changed. This means that the effects of the entire range of values of each set of parameters had to be calculated at a single "sitting".

The next consideration was the number of values a given set of parameters should be given in order to obtain a satisfactory indication of their effects. A typical set of parameters was the group: $V\alpha_{10}$, $\ell\alpha_{10}$, $\frac{b}{H_o}$, ψ. This group specified the simultaneous values of speed, length, loading per unit area, wave height and phase. For this

particular set more than one hundred solutions were obtained in one calculating session (of about 10 hours). In these cases, however, only one or two motion characteristics were desired - for example, the maximum angle of attack, or the highest waves which could be stably negotiated.

In some cases it was desired to measure as many as twelve motion characteristics for each solution. In these cases special consideration had to be given to the method of recording. (It was, of course, impossible to make as many solutions as when only one or two quantities were measured.) Photographing each solution would have been prohibitively time-consuming. Instead, the important numerical values were read from the oscilloscope and plotted directly on graph paper. Typical important numbers were the maximum values of z and $\frac{\alpha_m}{\alpha_o}$, and the minimum depth. Graphs VII-11, 12 and 13 represent samples of this plotting technique.

Finally, the order in which the parameters in a given set were varied had to be considered, so that a minimum of time was expended in covering the desired range of values.

Altogether it is estimated that in this section of the non-linear calculating program about 90 solutions were obtained in which from ten to twelve characteristics were measured, about 50 solutions were obtained in which three

or four characteristics were measured, and over three-hundred solutions were obtained in which only one or two characteristics were measured.

These solutions will now be discussed.

A. General Discussion of Results

Although nearly all the solutions in this section were recorded graphically, as described in the preceeding paragraphs, two typical solutions were photographed in their entirety, in order to show clearly the meaning of the various numbers which were recorded.

The photographs are shown in plates 5 and 6.[1] The solutions pictured are for common values of the various boat parameters, and for an average wave height (three chords), wave frequency (two cycles per second), and phase (.4). One set of photographs shows the steady-state motions of the boat in these waves, and the other shows the transient motions which result when the boat is started into the waves from a position near the wave crest.

Waves:

The first group of photographs shows the oscilloscope trace of the waves to which the system was (electronically) subjected. The first trace (a) is the wave pattern felt by the forward hydrofoil), and the second trace (b) is the pattern felt by the after hydrofoil. The phase between the two traces (ψ) is .4 in this case. This implies that the physical boat represented is traveling across the waves in such a manner that the length of the boat is four-tenths the distance from one wave crest to the next. (An expanded view of the waves is superimposed on these traces to show

[1] Appendix A

the wave shape in detail.)

Motions:

The next group of pictures displays the coordinates z and θ -- which define the path of the boat -- and the acceleration, $\frac{\ddot{z}}{g}$.

The steady state performance of the system is remarkable. In waves three chords high, the center of gravity moves less than one-third of a chord, and the boat pitches less than one and one-quarter degrees (for a boat length of twenty chords)! (It will be shown that for a phase nearer 0 or 1.0 the motion of the center of gravity would be slightly greater, and the pitching slightly less.) A boat displaying such steady motions in waves would surely find a ready market.

However, the transient calculations (second column) tell a different story. When the boat enters the wave system at a level near the wave crest it takes an initial plunge of the same magnitude as the wave height (z trace, figure c'). Furthermore, it attains a pitch angle of nearly nine degrees. ($\ell\theta$ trace, (α')). In these respects the boat is no better than a displacement craft.

It is noted that after the initial plunge the craft makes a quick recovery and returns to the steady state motion. It is therefore the initial plunge which should be observed in measuring the severity of the motion. In recording the data the maximum values of z and $\ell\theta$ were plotted.

Unstable Motions:

If the wave height were increased from the value shown, all other quantities being unchanged (including the initial depth), a value of wave height would finally be reached for which the boat would not recover itself at the bottom of the first trough. This could be observed by watching the z trace, which would continue downward after the first wave, instead of recovering as it does in the photograph. The maximum wave height for which the z-trace showed a recovering motion was termed the "limiting wave height for stable motions". This limiting wave height was the primary quantity recorded in a large section of the subsequent calculations.

Accelerations:

The last trace on plate 5 is the acceleration, measured in the form $\ddot{z}/g$. In the steady-state the acceleration varies between .8g upward and .6g downward, neither of which should be uncomfortable, except that the rapidity (twice per second) might be annoying[1]. But in the transient motion the sharp recovery at the first wave trough (z-trace, c') results in a large upward acceleration (2.2 g's) and a sudden change in acceleration (jerk) of over thirty g's per second. Although physiological data is not available on the point, it seems likely that this would be uncomfortable.

The acceleration characteristics recorded in the

[1] It is suggested that physiological research on the combined ranges of z, $\dot{z}$, $\ddot{z}$, (and other pertinent quantities) which are comfortable would be most useful to designers of vehicles of all types.

remaining calculations were the maximum values of $\ddot{z}/g$ and $\ddot{z}/g$. (These nearly always occurred near the first wave trough.)

Depth of Submergence and Angle of Attack:

These two quantities -- shown in pairs in Plate 6-- should be studied together, because it is particular ranges of their combined values which invite ventilation. (See Chapter III).

In interpreting the depth traces it is noted that thay are presented as the ratios of depth to equilibrium depth, where both are measured from the hypothetical surface assumed in approximating FIGURE 2. (See Chapter II, section C). It is recalled that this hypothetical surface is about .4 chords below the true surface. Thus, in the traces shown the zero ordinate corresponds to the hypothetical surface, while the true surface is $\frac{.4}{H_o} = .3$ divisions below the zero ordinate. (The ordinates of the depth traces can be converted to chords by multiplying by H_o, which is 1.33 in this case.)

It has been shown in Chapter III that ventilation will probably occur when the cavitation index $\sigma = \frac{L/S}{p_a}$ becomes about .8 for deep hydrofoils (deeper than one chord), but that ventilation is likely even for small values of σ, if the depth is less than 1/2 chord. From the preceeding paragraph this means that ventilation is likely whenever the depth trace has a negative value. Ventilation is also

likely at any depth for very high loadings.

The magnitude of the loading -- i.e. the value of -- has been shown to depend only on angle of attack. The ratio of maximum loading to initial loading is therefore equivalent to the ratio of α_{max} to α_o, which can be taken directly from the photograph for each foil.

$$\frac{C_{max}}{C_o} = \frac{(L/S)_{max}}{(L/S)_o} = \frac{\alpha_1}{\alpha_{10}}_{max} \quad \text{or} \quad \frac{\alpha_2}{\alpha_{10}}_{max}$$

As has been explained, the set of parameters used to specify a given hydrofoil system are $V\alpha_{10}$, $\ell\alpha_{10}$, rather than V, α_{10}, and ℓ. In this way each pair of parameters ($V\alpha_{10}$, $\ell\alpha_{10}$) actually represents systems having several combinations of the parameters V, α_{10} and ℓ. For example, the system under discussion has the values:

$$V\alpha_{10} = 9.6,$$

$$\ell\alpha_{10} = 4.$$

This pair of parameters may be considered to represent either of the two systems:

$V = 20$ ft/sec, $\ell = 20$ chords, $\alpha_{10} = 11.5^\circ$,
$L/S = 240$ lb/ft^2

or

$V = 40$ ft/sec, $\ell = 40$ chords, $\alpha_{10} = 5.7^\circ$,
$L/S = 480$ lb/ft^2.

(Any number of other systems could also be represented, of course, but two will suffice for illustration.) In general, when any one of the four quantities listed above

is given, the system is defined.

The important fact to note from the above tabulation is that the value of the initial loading, L/S, depends on which of the several systems represented is designated. To be specific; if the first set of parameters is designated, then:

$$C_o = \frac{240}{2120} = .11,$$

From FIGURE 3, the value of $\frac{\alpha_{cav}}{\alpha_o}$ [1] under these conditions is considerably greater than 2.0. (It is shown on page 45 that ventilation and cavitation seem to occur under about the same conditions, provided the foil is submerged at least one chord.) If, on the other hand, the second set of parameters is designated, then:

$$C_o = \frac{480}{2120} = .22,$$

for which FIGURE 3 gives:

$$\frac{\alpha_{cav}}{\alpha_o} = 1.7 \quad .$$

To summarize: if the first set of parameters is designated, ventilation will probably occur when the ratio $\frac{\alpha_1}{\alpha_{10}}$ exceeds about 3. If the second set is designated, then ventilation is likely if the ratio $\frac{\alpha_1}{\alpha_{10}}$ exceeds 1.7. In any case, ventilation is likely if $\frac{H}{H_o}$ becomes negative.

---

[1] It is presumed in this example that α_o is the design angle of attack of the system -- i.e. that $\alpha_o = \alpha_{design}$.

Ventilation of Forward Foils:

Consider now the traces in plate 6 of $\frac{H_1}{H_{10}}$ and $\frac{\alpha_1}{\alpha_{10}}$. For the steady-state motions the depth of the hydrofoil is approximately equal to the height of the wave over it, since the foils follow a nearly straight path. The foil does not appear to be in serious danger of ventilation due to close approach to the surface at any point. Furthermore, the maximum value of the ratio $\frac{\alpha_1}{\alpha_{10}}$ is only 1.2, which would certainly not produce danger of ventilation for any reasonable initial angle of attack. So again the steady-state picture is one of remarkably smooth, trouble-free operation.

But again the transient picture holds much less promise. First, the forward foil -- which has entered the wave pattern near the crest of the first wave -- is carried out of the first wave into the air, completely free of the surface. It then falls freely for a short distance (see the z trace, figure c'), and enters the water again (near the wave trough) with a large downward velocity. This causes a very large value of the angle of attack, on a hydrofoil which is already thoroughly aerated. The result will almost certainly be ventilation, a sudden loss of lift, and a motion much more severe than that shown by the z trace of figure c'. Moreover, if it is the second system tabulated (on the previous page) which is under consideration, then the maximum value of $\frac{\alpha}{\alpha_o}$ (2.6) is great enough to cause cavitation and probably ventilation regardless of the condition of aeration.

After Foils:

So far, only the forward hydrofoil has been under discussion. Actually it is the foil whose failure would be most dangerous to the operation of the boat. Also, from the results of the discussion of divergent boundaries in Chapter VI the center of gravity is likely to be so placed that the forward foils have a loading equal to, or slightly greater than the rear foils. However, the operation of the after foils has been carefully watched throughout all the calculations.

In the sample set of calculations under discussion, the configuration of the system is such that the after foils have an initial loading only half that of the forward foils. (This is evident in trace i, because the equilibrium value about which the ratio $\frac{\alpha_2}{\alpha_{20}}$ is varying is .5, rather than 1.0.) Even in the transient response (figures h', i'). There is evidently no danger whatever of ventilation from overloading. Furthermore, the motion of the system is such that the rear foil does not come within one-half chord of the (true) surface at any point. Therefore, in the particular system under observation the danger of ventilation lies solely with the forward foils.

In recording the results of the subsequent data, the maximum values of $\frac{\alpha_1}{\alpha_{10}}$ and $\frac{\alpha_2}{\alpha_{20}}$, and the maximum and minimum depths were noted for each hydrofoil.

Summary:

Plates 5 and 6 are photographs of the oscilloscope

screen of the differential analyzer, when the non-linear, two degree-of-freedom equations are being solved for a typical set of boat and wave parameters.

Under the conditions shown, it is seen that the steady-state motions of the system are remarkably smooth; the motions of the boat are almost imperceptable, the accelerations are small, and the hydrofoils are never in danger of cavitating or ventilating.

In contrast, the transient performance of the system when entering the same waves from a position near the crest of a wave is probably intolerable in several respects. First, the rising and pitching motions of the system in the first wave are of the same order of magnitude as the wave height; second, the rate of acceleration at the first wave trough is very large; and third, the forward hydrofoil comes completely out of the water over the first wave trough, becomes thoroughly aerated and then plunges back into the water at a very high true angle of attack, so that it will almost certainly lose most of its lifting capacity abruptly because of ventilation.

The degrees of severity of these undesirable characteristics of performance have been recorded for the calculations which are to be reviewed in the remainder of this chapter. Specifically, the values of the following quantities have been recorded:

z_{max} - the maximum departure of the center of gravity of the system from equilibrium,

$\ell\theta_{max}$ - the maximum and minimum angles of pitch,

$\frac{\ddot{z}}{g}_{max}$ - the maximum acceleration of the center of gravity,

$\frac{\dddot{z}}{g}_{max}$ - the maximum rate of acceleration,

$\frac{H_1}{H_{10}}_{max}$ and $\frac{H_1}{H_{10}}_{min}$ the maximum and minimum depths of the forward and after hydrofoils,

$\frac{H_2}{H_{20}}_{max}$ $\frac{H_2}{H_{20}}_{min}$

$\frac{\alpha_1}{\alpha_{10}}_{max}$ The maximum angles of attack of the hydrofoils. (Note was usually made of the relative occurances of maximum angle and minimum depth. However, these two almost always took place at about the relative times shown in plates 5 and 6.

$\frac{\alpha_2}{\alpha_{10}}_{max}$

It should be mentioned that the performance of an actual hydrofoil craft would not perform the disastrous motions indicated by the second columns of plates 5 and 6: the use of "booster" foils, and ultimately the hull would serve to prevent motions any more severe than those of a planing-hull craft. However, when such measures come into play the hydrofoil system is no longer carrying out its designed function, and the performance must be considered unsatisfactory.

B. The Effect of Initial Depth

The results of some studies of the effect of initial depth in a wave system upon the resulting transient motions are shown in Figs. VII-11, 12, and 13. The data in these graphs were plotted directly from the oscilloscope of the differential analyzer. Each graph shows the simultaneous effects of the parameter being varied on the values of z, $\ell\theta$, $\frac{\alpha_1}{\alpha_{10\ max}}$, $\frac{\alpha_2}{\alpha_{10\ max}}$, H_1, H_2, $\frac{\dot{z}}{g}$, and $\frac{\ddot{z}}{g}$. In figure VII-11 theinitial depth is varied in wave systems of two heights. In Figs VII-12 and 13 two extreme values of initial depth are used, and wave height is varied. The "worst" initial depth will be selected on the basis of the following effects of initial depth.

Effect on z:

The amount a hydrofoil system will move when placed in waves of given height at a given speed will, of course, depend very much on the initial depth which the system is given. The degree of dependence is shown in Figure VII-11a. When the system is started at about the same level as the wave trough very small motions - characteristic of the steady state - take place. When the system is started at a point deeper than the trough, the system responds by returning upward (negative z) to about the trough level. For the depths investigated (3 chords below the trough in this case) this returning motion was quite stable. (It seems likely that the returning motions for very deep

hydrofoils would be less and less dependent on the wave condition at the surface, and could, therefore, be predicted satisfactorily on the basis of smooth-water performance.) When the system is started at a position up near the wave crest, a sudden downward motion results. This motion is quite dependent on wave height, and does, in fact, become unstable as the wave size increases and as the starting position approaches the crest more and more closely. It is the high initial position, then that is dangerous. This can be seen more clearly in Figs. VII-12a, and VII-13a, where wave height is the parameter varied. In Fig. VII-12 the boat is always started at the wave-trough level. It is seen that even for very high waves (9 chords) the motion is not very great. There is certainly no instability indicated. In Fig. VII-13 the system is always started one chord below the wave crest. It is seen that the system can negotiate only small waves (2 or 3 chords high) without instability. The danger of starting near the wave crest is confirmed. The implication of this result is, of course, that the mean steady-state position of the hydrofoil system is a short distance below the wave trough. The very smooth steady-state performance has already been contrasted with the very rough transient performance in the preceeding General Discussion.

(Unfortunately an exact comparison of Figs. VII-12 and 13 is not possible, because the data in VII-2 were taken at a higher forcing frequency, which will be

shown to result in more favorable motions and less favorable loadings. However, the qualitative comparison is valid.)

Depths less than one chord below the wave crest were not investigated thoroughly, because it seemed unlikely that a boat would get into a position where its foils were practically out of water at the top of a wave.

Effect on Loading:

The maximum value of the ratio $\frac{\alpha}{\alpha_o}$ is a measure of the maximum loading the foil will receive. For foils which were initially lightly loaded, cavitation and ventilation may not threaten until the maximum angle of attack becomes two or three times as great as the initial angle: But for foils which are already heavily loaded, values of the ratio $\frac{\alpha}{\alpha_o}$ only slightly greater than 1 may result in cavitation. (See chapter III). The effect of initial depth on $\frac{\alpha}{\alpha_o}$ is shown clearly in Fig. VII-11b. For all initial points deeper than a point just below the wave trough the maximum value of $\frac{\alpha}{\alpha_o}$ is constant, only slightly greater than 1. But if the initial point is shallower than the trough the ratio increases rapidly as the surface is approached.

In Figs. VII-12b and 13b the effect of wave height on the ratio $\frac{\alpha}{\alpha_o}$ is shown for trough-level and near crest-level starting positions, respectively. When the system is started at trough-level the ratio is small, even for very high waves, and could probably be tolerated with-

out cavitation by most systems. But with the high starting position fairly small waves (two to three chords high) may cause intolerable values of the ratio.

Effect on Depth of Submergence:

It has been explained in the General Discussion that for a given foil-loading the likelihood of ventilation occuring becomes much greater as the foil approaches the free surface. In fact, if the foil is less than about one-half chord submerged (i.e. if H/H_o becomes negative), ventilation will probably take place even for rather light loading.

In Figs. VII-11c, 12c, and 13c the maximum and minimum depths reached by the hydrofoils shown for the various conditions studied. The ordinate in these graphs is the ratio of depth to equilibrium depth, both depths being measured to the hypothetical surface discussed in Chapter II-C. Fig. VII-11c shows the effect of initial depth on minimum depth, for one wave height. Figs. 12c and 13c show the effect of wave height on minimum depth when the initial depth is at trough-level, and at one chord below crest-level respectively. The qualitative interpretation of 11c is that if the initial depth is greater than a certain level, the minimum depth will always have the same, safe value. From Fig. 12c, if the system is started at trough level the foils will just reach the mythical surface - i.e. will be just safe - for small waves. For larger waves they will be in danger of ventilation.

From Fig. 13c systems started near the crest will reach a dangerious minimum depth in smaller waves.

In evaluating the likelihood of ventilation indicated by Fig. VII-12c, as compared with the likelihood indicated by Fig. VII-13c, the combined effects of surface proximity and loading should be considered. On this basis it is clear that the conditions of 13c - where $\frac{H}{H_o}_{min}$ decreases rapidly and $\frac{\alpha_i}{\alpha_{10}}_{max}$ increases rapidly with wave height - are very much more likely to produce ventilation that the conditions of 12c. In other words, the system started near the crest of the wave is much more likely to suffer ventilation than a system started near the trough.

Effect on Acceleration:

The acceleration and rate of acceleration values are shown in graphs d of Figs. VII-11, 12 and 13.

The effect of depth on the acceleration of the center of gravity (Fig. 11d) is quite similar to its effect on angle of attack: for large depths the maximum acceleration had a moderate value which is independent of depth. For shallow depths the acceleration increases rapidly with approach to the wave crest (represented by $H_i/H_o = 0$. (The reason for this behavior has been investigated in the General Discussion.)

The increase in maximum acceleration with wave height is slow, almost linear, for the system started near the wave trough (Fig. 12d). But for the system started

near the wave crest (Fig. 13d), the acceleration increases very rapidly with wave height, reaching intolerable values for rather small waves.

The rate of acceleration in all cases is seen to vary in complete coincidence with the acceleration itself, and to have a value about ten times the acceleration. Quantitative interpretation of the rate of acceleration is not possible at this time. It is included in the hope that it may be useful in future psyiological and structural considerations.

Summary of the Effect of Initial Depth:

It has been shown that from every conceivable point of view the starting position high in the wave crest is the very worst possible. On the grounds that it is unlikely that a hydrofoil system would find itself higher in a wave crest than its normal equilibrium depth in smooth water, the value of $H_i/H_o = 1$ has been chosen as the worst "feasible" starting position.

C. The Effect of Phase

The "Phase" between a hydrofoil system and a wave system has been defined as the ratio of hydrofoil system length to wave length in the direction of travel. In other words, it is the per cent of a given wave which the forward hydrofoil has traversed at the time that the after hydrofoil enters that wave[1].

It is evident that by proceeding at various angles cross-wise in the waves, a boat could have any of a large range of phases with respect to the waves. There is of course an upper limit on the phase which is its value when the boat is going at right angles to the waves. This limiting phase is given by:

$$\psi = \frac{\ell}{\lambda} = \frac{\ell}{b} \cdot \frac{b}{\lambda} .$$

To evaluate the range of values that ψ will have for a given wave height, b, the largest and smallest values of ℓ and b/λ are entered:

$$\psi_{max \quad largest} = \frac{40}{b} \quad \frac{1}{10} = \frac{4}{b}$$

$$\psi_{max \quad smallest} = \frac{10}{b} \quad \frac{1}{40} = \frac{.25}{b}$$

(The minimum value of phase can be very small if the boat runs almost parallel to the waves. The question of lateral stability of course becomes important in this case. In the present preliminary investigation it has been necessary to study the effect of small phases on longitudinal motions

[1] It is appreciated that this definition of phase is somewhat unconventional. It has been adopted because of the considerable convenience it afforded in the calculating program.

without considering lateral motions. It is suggested that future studies might consider the combined lateral and longitudinal motions resulting from traversing waves in a nearly parallel direction.)

In order to obtain a thorough understanding of the effects of phase on hydrofoil system performance, systems of several configurations, having a large range of lengths and operating over a large speed range in waves of many sizes were studied. Three of the major characteristics of motion were observed: maximum displacement, maximum loading (measured by observing true angle of attack), and maximum acceleration. Altogether, about 220 solutions to the equations were obtained in this section -- over 90 of them in one eight-hour period.

Effect on Stability:

In the first group of calculations the measured quantity was the maximum wave height b/H_{max} which a system could negotiate without having unstable motions of the type discussed on page 138. The results of these calculations are shown in Figs. VII-14 to 17.

The boat parameters varied were $V\alpha_{10}$ and $\ell\alpha_{10}$, from which corresponding values of velocity (v), boat length (ℓ), angle of attack (α_{10}) and loading (L/S) were calculated. (Refer to TABLE I.)

In Fig. VII-14 the results of varying boat lengths are shown for two frequencies of wave encounter. The conclusions which can be drawn are that (1) the worst phase is between .4 and .6; (2) long boats are much more stable than short boats; (3) phase is more important

in determining the stability of long boats than of short boats; (4) the results shown for N = 2 are about the same as for N = 1.

The last conclusion was important in determining the calculating procedure, because it was considerably easier to observe results for N = 2 than for N = 1. But it was known from the linear calculations of natural frequency and from the non-linear smooth water data that the natural frequency of the system was between 1 and 1.7 cycles per second. Partly on the basis of Fig. VII-14 it was decided to proceed with the succeeding calculations at N = 2. Further justification of this decision will be found in section D on the effect of frequency of wave-encounter.

All of the calculations in Figs VII-14 to 17 were made at one time with the same machine set-up. They may therefore be related to each other with considerable precision, as explained on page 133, even though the absolute values of these results may be in error by about 20 per cent.

All of the calculations shown in these graphs were made at a frequency of wave-encounter of two per second.

One conclusion indicated by all of the graphs is that a system is usually least stable for phases greater than about .5. As phase decreases below .4 the system is stable for higher and higher waves, but as phase is increased above .6, the allowable wave height remains near the minimum value. Physically this means that if the after

foils do not start down the wave until the forward foils have proceeded to the wave trough or beyond, a stable recovery is less likely than if the after foils follow down the wave profile close behind the forward foils.

Fig. VII-15 shows the combined effects of boat length and phase for an average speed and foil loading. It is seen that the maximum negotiable wave height is increased at every value of phase by lengthening the boat.

Fig. VII-6 shows the effect of hydrofoil loading on stability as phase is varied. The graph indicates that heavily loaded foils lead to more stable motions. However, stability of motion is secondary to the possibility of ventilation in considerations of foil loading. This possibility will be studied under the effects on angle of attack.

Fig. VII-17 depicts the effect of speed on stability of motion for a system of average length and loading. This effect is by far the most significant of those studied. First, the waves negotiable at small phases are more than twice as high as for large phases (greater than .4). Second, while reasonable wave heights can be traversed at low speeds, at the highest speed studied the system is barely stable in smooth water!

Fig. VII-18 presents a variation of the preceding results. Here the wave height is constant and the amplitude

of motion is recorded. The amplitude is seen to be greatest at about $\psi = .5$ (The two systems observed differ in several ways, and their results should not be compared quantitatively with each other.

Effect on Loading:

Results of studies of the effect of phase on the maximum values of true angle of attack -- a measure of loading -- are presented in Figs. VII-19 through 23. These results are for various representative combinations of the system parameters. The first three graphs (19 through 21) were all obtained for $x_1/\ell = 1/3$ (the center of gravity one-third the way aft). The results shown in these graphs are qualitatively similar. When the phase, ψ, is near 0, $\frac{\alpha_1}{\alpha_{10}}$ and $\frac{\alpha_2}{\alpha_{10}}$ are both at their maximum values and are approximately equal. As ψ increases $\frac{\alpha_1}{\alpha_{10}}$ drops 20 to 30 percent and becomes about constant for ψ larger than about .4. It is concluded that the loading on the forward foil is always the most dangerous, and is at its worst value for very small values of phase. Observations of maximum loading made when $\psi > .4$ may be 30 per cent too low.

In Fig. VII-22 x_1/ℓ is 2/3, and the relative values of $\frac{\alpha_1}{\alpha_{10}}$ and $\frac{\alpha_2}{\alpha_{10}}$ differ from the corresponding relation when x_1/ℓ was 1/3; the two ratios are now practically equal for all phases. They have their maximum value at ψ near zero, as before. Then they both drop to

about 30 per cent of that value when ψ reaches .4. It is concluded that in this case the forward and after foils are in equal danger of ventilating. As before, the smallest phase is the worst.

Effect on Acceleration:

The effect of phase on acceleration is shown in Fig. VII-23 for several representative values of the variables. It is seen that the acceleration, like the angles of attack, is always greatest near $\psi = 0$, drops to some minimum value between $\psi = .2$ and .3 and becomes approximately constant for $\psi > .3$. (The curves in this graph were each calculated at a different time, and so should be compared only on a qualitative basis.)

Summary of the Effect of Phase:

The maximum negotiable waves are the smallest, and the motions of the system the worst for $\psi > .5$, best for ψ near zero.

The worst hydrofoil loadings occur for ψ near zero and the least serious loadings occur for ψ greater than .3.

The worst accelerations occur under the same conditions as the worst loadings.

It is concluded that to anticipate the performance of a system the motions and stability characteristics should be observed at $\psi = .5$, and the loadings (angles of attack) and accelerations should be observed at $\psi \approx 0$.

D. The Effect of Frequency of Wave-Encounter

General Discussion:

It is well known that if a dynamic system is "forced" by some function of sinusoidal character, and if the damping in the system is not preponderately large, then the amplitude of the resulting motions will depend very strongly on the frequency of the impressed force. The motion will be most severe when the forcing frequency is near a natural frequency of the system.

It is further known that for a linear system the resulting motion will also be sinusoidal in character, and will have the same frequency as the forcing function. That is, the motion will be given by some relation of the form:

$$x = A \sin (\omega_f t - \phi) + B \sin 2(\omega_f t - \phi) + \ldots$$

where ω_f is the forcing frequency.

Differentiation of the above relation yields a similar expression for the velocity $\dot{x}$, except that all terms are multiplied by the frequency, ω_f. In other words, in sinusoidal motions the velocity is proportional to the frequency. Similarly, the acceleration is proportional to frequency-squared.

These facts have important application to the present problem, because although the system under study is non-linear, it is being forced by a sinusoidal function (the ocean waves) so that the above results are certainly expected to hold in an approximate manner.

Of particular importance are the implications regarding the accelerations and the angles of attack of the system.

The acceleration of the hydrofoil system (center of gravity) will be proportional to the maximum amplitude of the motion of the center of gravity, and approximately proportional to the square of the forcing frequency. A plot of acceleration vs. frequency should, therefore, be approximately parabolic, except that a peak should appear near each resonance because of the increased amplitude of motion.

The angle of attack of the hydrofoils is a strong function of the rising and pitching velocities of the system, and will therefore be proportional to the maximum amplitudes of rise and pitch, and to the first power of the frequency. Consequently, the plots of angle of attack vs. frequency are expected to be nearly linear, except for peaks at resonance.

Natural Frequency:

The natural frequency of the hydrofoil system has been studied on a linearized basis in Chapter VI, and has been observed in the transient responses of the linear and non linear systems in the present Chapter.

It was shown in Chapter VI that, except for very small radii of gyration, the natural frequency rising is always higher than the natural frequency of pitching. It was further shown that for the system which will be studied

throughout most of this chapter -- one having a normal running depth of 8.67 inches -- the natural frequency is about one cycle per second. This value was approximately confirmed in the linear transient calculations (part 1 of this Chapter). The non-linear transient calculations showed that the natural frequency was actually a function of the amplitude of motion and other characteristics, but that it was in the range between 1 and 1.7 cycles per second.

Damping:

It was shown in Chapter VI, part A that the damping of the system increases as $V\alpha_{10}$ decreases - i.e. as speed is increased for a given loading, or as loading is decreased at a given speed. It was also shown that damping is increased as normal running depth is increased. (Refer to TABLE I.)

To summarize the above general discussion, it is expected that the worst motion will occur for forcing frequencies near one cycle per second. It is expected that the worst accelerations and foil-loadings will occur at high forcing frequencies. It is expected that damping will be more effective at high speeds, light loadings, and deep normal running positions.

The frequency at which waves are encountered, in cycles per second has been given the symbol N.

Effect on Stability of Motion:

The procedure for calculating the effects of frequency, N, on the stability of motion was similar to the procedure used in the case of the phase. The motions of the system were studied over a range of frequencies for a wide range of speeds, boat-lengths, and foil-loadings.

As before, the quantity measured was the maximum wave height the system could negotiate without having unstable motions. The boat parameters varied were $V\alpha_{10}$ and $\ell\alpha_{10}$. Again, all of the calculations were completed in a single calculating session. (In this case only about forty solutions were obtained.) The results may therefore be compared to one another with considerable precision, although the numerical accuracy of the data may be very poor.

To illustrate the calculating procedure the results obtained are presented in Figure VII-24 in the form in which they were recorded. For each run the waves were adjusted to give a phase of .6, in accordance with the conclusion of the previous section that this phase would lead to the least stable motions. The waves were then set at such a level that the boat "entered" them at a depth of 1.73 chords[1] below the wave-crest, as recommended by the studies of initial depth effects. At each

[1] i.e. The starting depth below the wave crest was equal to the equilibrium depth in smooth water.

frequency this process was repeated for increasing wave heights, until finally the motion of the boat became just unstable. This wave height was then recorded in Fig. VII-24.

The type of symbol used in the figure denotes the value of $V\alpha_{10}$. (Refer to the legend on the graph.) The number within the symbol is the value of $\ell\alpha_{10}$. (Clearly the values of speed, frequency of encounter, boat length, and phase are inter-related. However, it was found to be more fruitful to study the effects of frequency alone, the other parameters being held constant.)

In general, smaller values of $V\alpha_{10}$ mean higher speed. (This can be seen from TABLE 1 by noting the values of $V\alpha_o$ for constant loading at increasing speed.) Similarly, for constant speed and loading, the higher values of $\ell\alpha_{10}$ imply longer boats. A qualitative understanding of the effects of speed and length may therefore be obtained directly from Fig. VII-24.

The squares and triangles represent low speeds. It is seen that at low speeds the effect of frequency is very strong. For the "triangle-4" series[1], for example, the negotiable wave height is doubled in going from N = 2 to N = 3.5. But for the higher speeds, represented by the circles and diamonds, the effect of a change in frequency is very much less. It is suggested that

[1]Representing, for instance, the conditions: V = 20 ft/sec, ℓ = 20 chords.

the greater importance of approaching resonance (N = 1) at low speeds may be due to a lower effective damping at low speeds which was anticipated in the general discussion of frequency.

The effect of length may be investigated because the increasing progression of numbers in each symbol represents increasing boat-lengths. As with every previous investigation of the effect of length, the longer boats are always able to negotiate higher waves than the shorter boats. However, the qualitative effect of frequency seems to be independent of boat length, all the curves in the "square" family being of one shape, for example, and all the curves in the "circle" family being of another shape.

The most important information to be gained from Fig. VII-24 is of course the effect of approach to resonance. A resonance is expected at $N \approx 1$. Unfortunately, the time scales used on the differential analyzer were such that it would have been necessary to change to a completely different machine set-up to cover the range of frequencies between 1 and 2. Since such a change-over would mean sacrificing completely the comparitive precision available on a single machine set-up, it was decided that extrapolation to the lower frequencies would be a more valid procedure. This extrapolation is performed by the dashed extensions of the

curves in Fig VII-24. These extensions seem clearly to indicate that there is not very much difference between theperformance at N = 1 and that at N = 2 for any of the systems investigated. With this justification - and because the machine time-scales were such that observations of higher frequency waves was much easier than observation of low frequency waves - most of the remainder of the calculations on "worst" conditions were preformed with N = 2. It is believed that conditions close to the most dangerous were thus produced.

The exact break-down of Fig. VII-24 for particular values of V, ℓ, and α_{10} will be discussed in section E on the effects of speed.

Effect on loading:

As usual, the loading of the hydrofoils was studied by measuring the ratio of maximum angle of attack to equilibrium angle of attack. A number of calculations were made for a given system during one calculating session, so that the results may be compared with each other. The system chosen had two hydrofoils forward and one aft, and its cg. was 1.3 of the way aft.

The system was always started into the waves at the depth of 1.73 chords below the wave crest, and the phase was always made zero. Although a phase of zero would probably never be actually encountered, very small phases are possible. It was therefore believed that

loadings calculated with zero phase would represent an upper limit to the worst loadings which might occur in actual operation.

The choice of zero phase, together with the choice of system mentioned above, happen to represent a special case; pure rising motion of this particular system happens to be a natural mode of oscillation. With zero phase, the waves excite only this mode, so that no pitching motions take place (It is indicated by previous observations that if the phase had been increased from zero and pitching motions excited the loadings obtained would have been less severe.)

The results of loading calculations are shown in Figs. VII-25 and 26. In 26 a relation is available between $\frac{\alpha_m}{\alpha_o}$ and wave height(b/H_o) at one frequency. (Because of the absence of pitching motions explained above, the value of $\ell\alpha_{10}$ does not affect the results in Fig 26. Further, $\alpha_1 = \alpha_2$, so that it is not necessary to plot both.) It is seen that for constant values of $V\alpha_{10}$ (constant speeds) the curve of $\frac{\alpha_m}{\alpha_o}$ vs b/H_o is approximately a straight line. This relation was found to hold for a number of other representative systems at other frequencies. (See for example Figs. VII-11 and 29.) This fact suggests good approximate results might be obtained -- and the number of variables reduced by one -- by using a new variable: the slopes of Fig. 26. The new variable is given the symbol Λ :

$$\Lambda = \frac{\partial \frac{\alpha_m}{\alpha_o}}{\partial \frac{b}{H}}$$

There is no justification for carrying this approximation beyond the point where $\frac{\alpha_m}{\alpha_o}$ becomes greater than about 3.5.

Graph 25 shows that under the conditions imposed the value of $\frac{\alpha_m}{\alpha}$ increases rapidly with N until about N = 3, and then levels off to a constant value. This is not in good qualitative agreement with the results of calculations under some other conditions -- for example, those shown in Figs 29a and b. In Fig. 29a it appears that a leveling-off may take place at some higher frequency -- say N = 6. In Fig. 29b no leveling-off appears likely. It is suggested that the quantitative inter-relation between amplitude of motion and frequency -- the two factors largely responsible for the value of α_m -- is different from one system to another, so that the point of leveling- off is also quite different.

It seems reasonable that α_m must approach a constant value for some high frequency, because the hydrofoil system will be unable to follow very high-frequency waves, and will merely drop from its initial position to some new equilibrium position without regard for the wave shape. (This motion would be similar to the transient motions in smooth water studied in part II.)

Returning to Fig. 25, it has been thought desirable to generalize the results of this graph to a limited extent by making use of the new variable Λ. The first step was to plot the solid curve in Fig. 27 of Λ vs. N. This curve contains the same information as Fig. 25 except that

it should hold for any value of b/H_o (so long as $\frac{\alpha_m}{\alpha_o}$ does not exceed about 3.5.) Next values of Δ for other $V\alpha_{10}$'s were plotted at N = 4. Finally the dotted curves were sketched in with the same general shape as the solid curve. (The dotted curves represent a very approximate extrapolation.)

The results of Fig. 27 have been replotted in different form in Fig. 28 to show more clearly the effect of speed. (It is recalled from TABLE 1 that low values of $V\alpha_{10}$ represent high speeds.) It is clear that the danger of high loading increases rapidly with speed.

Unfortunately time did not permit more extensive calculations of the effects of frequency on loading. However, the results obtained show definitely that the worst values of $\frac{\alpha_m}{\alpha_o}$ occur for (1) high speeds, and (2) high frequencies, probably above some leveling-off value (in this case N = 4 cycles per second).

Effect on Acceleration:

Two isolated sets of calculations on the effect of frequency on acceleration are presented in Fig. VII-30. The curves are approximately parabolic in shape as expected. The accelerations attained for frequencies greater than 3 cycles per second would be severe even if experienced statically. But the rates of accderation are enormous, and may well prohibit completely operation on all but the smallest waves at high frequencies.

Summary Effect of Frequency:

The frequency of wave encounter has an important effect on the size of waves which may be negotiated without danger of unstable transient motions. This effect is great at low speeds, and less important at high speeds. In all cases the danger is, of course, greatest near the natural frequencies of the system. However, it is found that the motions of the system at N = 2 will closely predict the motions at the natural frequency, which is between one and 1.7 cycles per second for the system studied.

Frequency of encounter plays an important role in determining the maximum value of the ratio $\frac{\alpha_m}{\alpha_o}$. This effect is more important at high speeds. In all cases $\frac{\alpha_m}{\alpha_o}$ increases rapidly with frequency for low frequencies, and then reaches a nearly constant value at some high frequency.

The acceleration and rate of acceleration increase rapidly with frequency, and may reach prohibitively large values for relatively low frequencies (say 3 or 4 cps) and moderate wave heights (2 chords).

E. The Effect of Speed

General Discussion:

As the speed of a boat traveling in a given wave pattern is increased, all of the quantities studied so far change in some definite inter-related manner. The effects of changing each of the parameters separately have been investigated, and it is now desired to study their combined effect under more realistic circumstances.

Even at this stage it is found necessary to make some approximating assumptions. First, it will be assumed that the phase has always the worst value. Actually, of course, if speed, frequency of encounter, and boat length are known, the phase is determined. In selecting the worst phase the chance is taken that the predicted performance will be less favorable that the actual performance. In the case of stability of motion the worst phase is .6 . But it has been shown that the results are about the same for all phases greater than .4. Therefore, error is incurred only for small phases. In the case of loading it has been seen that for all phases above .4 the loading is about constant, and differs by only about 20 or 30 per cent from the worst loading (at zero phase). So again the error incurred by assuming a fixed phase is not too great.

In studying theperformance of a boat in a given wave pattern it is certainly important to consider the possibility that the boat may travel at any arbitrary angle

with respect to the waves. In the case of the sailboat, for example, it will in fact be necessary. On the other hand, it will be of interest to know what the performance will be when the boat proceeds directly into or away from the wave pattern.

Therefore, three cases will be considered: (1) the hydrofoil system is proceeding directly upwind (into the waves); (2) the system is proceeding directly downwind; (3) the system is traveling at approximately the least favorable angle with the wave pattern. From the study of the effect of frequency of wave encounter it seems evident that this least favorable angle will be one which gives a frequency of encounter near the natural frequency of the system. For reasons previously explained, a frequency of two cycles per second has been chosen.

Effect of Stability of Motion:

The calculations of performance at constant frequency were easier to perform, and are easier to explain. They will therefore be discussed first.

Figure VII-24 is used directly. A vertical line is drawn at N = 2; all the necessary data lies on this line. To interpret this data continuous reference is made to TABLE 1. For example, if the value of $(b/H_o)_{max}$ is desired for a speed of 40 feet per second, foil loading of 480 pounds per square foot, and length of 20 chords, TABLE 1 indicates that the 2 symbol should be read (2 means $V\alpha_{10} = 9.6$, $\ell\alpha_{10} = 2.$) and the corresponding value of (b/H_o) is .7.

The results of the calculations thus made are shown in Figure VII-31 to 33. In 31 the effect of length is seen to have its usual predominat importance. It is unlikely that high-speed operation of short boats is feasible. In Figs. 32 and 33 the effect of initial loading is investigated. Higher foil loading results in higher permissible waves, as far as stability of motion is concerned, but no positive conclusions can be made until the dynamic foil-loading has been investigated. One negative conclusion can be drawn, however; high-speed operation with loadings as light as 240 pounds per square foot is probably not feasible.

When the boat is proceeding directly into or away from the waves, the frequency is given (for given values of speed and wave length) by FIGURE 4. When the frequency has been found, the value of $(b/H_o)_{max}$ can be read from Fig. VII-31 in the manner outlined above.

The stability of motion in cross-wave operation is compared with that in direct upwind or downwind operation in Fig. VII-34. It is seen that in traveling upwind the increase in forcing frequency (away from resonance) accompanying increased speed is important enough to offset completely the destablizing effect of high speed which was observed in the constant frequency tests and in the smooth water transients. Eventually, as has been explained, the frequency becomes so high that there is no possibility of response to the wave profile, but only the question of transients due to changes in average height which can be

understood from the transient responses in smooth water. Eventually, therefore, the boat must suffer the high-speed instabilities indicated by Figs. VII-8, 9, and 10. But for a given boat these will come at higher speeds for upwind operation than for cross-wave travel.

Downwind operation is seen in Fig. VII-34 to have exactly the same characteristics as upwind operation, except that the frequency of encounter is now somewhat lower, and the motion correspondingly somewhat less stable. (This comparison of upwind with downwind performance is quite incomplete because orbital motions of the water particles have not been considered.)

The effects of boat length and foil loading are shown in Figs VII-35 and 36 respectively, to be qualitatively the same for upwind travel as they were for the constant-frequency case. It appears, however, that lighter foil loadings can be used in small waves at considerably higher speeds.

In Figs. VII-34, 35, and 36 the ratio of wave length to wave height was assumed to be 10 to 1. This is a very steep wave, but it is likely to occur in the height-range being considered (under two feet for the 5" chord system). It might be expected at first thought that less steep waves would lead to more favorable motions. However, Fig. VII-37 shows that the lower forcing frequencies experienced in longer waves is of controlling importance, and travel in less steep waves is actually less stable.

The above observation regarding the effect of wave steepness again is not conclusive, because the effect of the orbital motions of the water particles has not been included. It is recalled from Chapter IV that the velocity of orbital motion is directly proportional to wave steepness.

On page 169 the question was raised whether serious error resulted from the assumption of constant phase. To make the argument more conclusive, the calculations of Fig VII-31 were repeated using the data on effect of phase obtained in Section C, and computing the correct phase for each calculation. The results were found to be in good qualitative agreement with Fig. VII-31, except that the curves did not drop so sharply with speed, because of the effect of more favorable phase with increasing speed. These results are not presented in graph form, because they may not be compared quantitatively with the other results in this section.

Effect on Hydrofoil Loading:

The best available information for predicting the maximum loading on the foils as speed is increased is contained in Figs. VII-25, 26, and 27.

It is recalled that these figures represent a very special set of operating conditions, and therefore, that a considerable amount of extrapolation was necessary to make the data applicable to other conditions. No evaluation of the quantitative accuracy of these extrapolations was possible, but there was evidence that they were qualitatively sound.

It was found most perinent to present the information about dynamic foil loading and cavitation in a form corresponding to that used in Figs VII-31 through 37 - namely, as plots of the wave height which will cause cavitation as a function of speed, under various conditions. Again it is emphasized that the incipience of cavitation may not in itself cause instability of motion, but that it is indicative of the probability of ventilation which does usually result in erratic motions. Since much more data is available on cavitation conditions, the calculations are based thereon. (The correlation between ventilation and cavitation is discussed in Chapter III.)

The data of Figs. VII-25, 26, and 27 are put into the desired form via the following steps: (1) several sets of curves like those of Fig. 26 are derived for other values of

N from Fig. 27 (these are a definite extrapolation); (2) a value of C_D is chosen in FIGURE 3; (3) for each speed and equilibrium loading (L/S) the value of $V\alpha_{10}$ is read from TABLE 1; (4) the value of (α_m/α_{10}) which will cause cavitation is calculated (as explained below); (5) this value is entered into Fig. 28 (or one of the derived sets of curves for values of N other than 4) to obtain the wave height (b/H_o) which will cause cavitation.

Some elaboration is necessary on the considerations involved in choosing a vlaue of C_D (step 2, above). For any given speed, C_D represents the camber of the hydrofoil profile.

It is recalled that operation of a given foil at constant speed is represented by the straight lines in FIGURE 3. It is clear that for a given speed a foil with high camber can be operated at much higher loadings per unit area without cavitation than can a foil with low camber. On the other hand, if a large range of variation in angle of attack is to be had, (i.e. a large range of α_m/α_{10}) and at the same time if α_{10} is to be near the design angle of attack, a low value of C_D must be used.

Since it has already been seen that operation at very low foil loadings result in unstable motions at high speed, it is necessary that some compromise be made between high C_D -- to permit high initial foil loading -- and low C_D -- to permit large variation in angle of attack.

Once the value of C_D has been chosen the value of C_{cav} is found from FIGURE 3 at the intersection of the constant C_D line with the cavitation curve. This may then be compared with the equilibrium loading, L/S, from step (3) (above) to find the value of α_m/α_{10} which will give cavitation because:

$$\frac{\alpha_m}{\alpha_{10}} = \frac{(L/S)_{cav}}{(L/S)_o} = \frac{C_{cav}\, P_a}{(L/S)_o}$$

Some results of the calculations just explained are presented in Figs. VII-38, 39, and 40. In all the figures it is seen that operation in moderate waves at low speeds is possible without the danger of cavitation, but that at high speeds only very small waves can be negotiated. The degree to which this general limitation holds varies with the foil camber, frequency of wave encounter, and foil loading.

The effect of camber -- represented by C_D -- is shown in Fig. V-8. It is seen that cavitation-free operation is possible in higher waves if a high-camber foil is used ($C_D = .5$). However, the table in Fig. 38 states that if $C_D = .5$, the equilibrium lift coefficient must be less than one-half the design value (for the case shown that L/S - 480 psf). But operation at an angle of attack so much below the design angle will generally be inefficient, and it will be necessary to use a lower value of C_D. For operation at the design lift coefficient, C_D

should be .22. In this case the waves which could be traversed without cavitation would be very small. It is probable that some compromise would again be reached. A compromise value of C_D = .35 has been taken as an example in the succeeding calculations.

The effect of frequency of wave encounter is shown in Figure VII-39. For the particular case from which these curves were derived there would be little change as N increased above N = 4, as is clear from Fig. N-4. In any event, it is seen that at high speeds the frequency of encounter becomes less important. A curve indicating the conditions under which the hydrofoil will probably stall is shown in Fig. 39 as a reminder that there is a low-speed as well as a high-speed limitation on loading conditions. The limit in this case indicates that for speeds below 40 feet per second lighter loadings muct be used.

In Fig. 40 the operating of foils of <u>given design</u> (given value of C_D) is depicted for various loadings. In other words, at a particular speed a foil profile is chosen which is designed to carry about 800 pounds per square foot, in this case, and then loading on this profile is varied, and the angle of attack varied accordingly. Under these circumstances lighter loadings are seen to lead to less likelihood of cavitation. However, lighter loadings are seen to lead also to operation farther and farther below the design lift coefficient, and therefore to less and less efficient operation. It is probable

that some minimum operating lift coefficient will be evident for each profile design, so that for a particular design it would be pertinent to study the effect of varying load when the ratio of operating C_L to design C_L is near its minimum, efficient value.

Summary - Effect of Speed:

It is shown that increasing the speed of a hydrofoil boat rapidly reduces the ranges of boat and wave parameters for which the performance will be stable.

The general effect of speed on the performance of a hydrofoil system can be best understood by comparing its effect on the two most important performance criteria: nearness to unstable motions and nearness to cavitation.

In the results of the calculations performed, these criteria are shown as the maximum wave-height which the system could encounter at each speed without experiencing either unstable motion or cavitation. In each particular case, the very worst feasible circumstances of encounter (i.e. frequency, phase, and initial depth in the waves) were assumed.

Representative results of the calculations on motion stability and cavitation are shown by Figs. VII-33 and 40 respectively. In both figures a hydrofoil system which has been well-designed (on the basis of the preceeding analysis) is studied for different hydrofoil loadings. In particular, a large length-chord ratio is assumed. It is seen that light loadings reduce the likelihood of cavitation,

but lead to unstable operation at moderate speeds. On the other hand, heavy loadings result in more stable motions, but cause cavitation at moderate speeds. (Finally, the foil loading at low speeds is limited by stalling - Fig VII-39.)

It is concluded that a light loading should be used for low speeds (e.g. below 40 fps),and that some intermediate loading (on the order of 500 lb per sq. ft.) is indicated for higher speeds. (This loading should be such that the limitation on wave height due to instability of motion is about the same as that due to cavitation.)

All of the above analysis has been based on the assumption that the best hydrofoil profile would be used at each speed. It is assumed that for a boat operating over a large speed range the foil profile will be designed for the maximum operating speed, and that as speed is varied the loading will be made to follow the desired pattern by a suitable combination of area-reefing and angle-of-attack adjustment.

F. EFFECT OF RUNNING DEPTH

It has been seen repeatedly -- particularly in Section B of this chapter on the effect of initial depth -- that when the lowest point of the hydrofoils is somewhat below the wave trough on entering a wave, the resulting transient motions are very much more stable than when the lowest point is above the trough.

This observation suggests that hydrofoils whose running depth is normally deeper will produce more stable motions in any given set of waves.

In this section calculations were made for the specific purpose of verifying this suggestion.

A system having common values of the various parameters was subjected to the usual transient motions in waves of a single height (which happened to be 17.7 inches). The total load on the system was not changed, but the running depth of the hydrofoils was varied by changing the angle of attack.

The results of the calculations are shown in Fig. VII-41. The usual characteristics of performance are plotted: maximum amplitude of motion, maximum dynamic loading, depth of submergence, and acceleration.

It is seen that for the shallow depth (3.3 inches) the performance is quite intolerable in every respect. The system comes out of the water 5 inches, then drops a distance greater than the wave height. The dynamic loading is guaranteed to produce ventilation, and the

acceleration is 3 g's at a rate of 30 g's per second.

In sharp contrast, when the running depth is 10 inches, the system does not come of water, the motion is only 9 inches, the loading is entirely safe, and the acceleration is less than one g. Furthermore, it is apparent that if the running depth were increased to the magnitude of the wave-height the motion would be very small and the loading and acceleration almost negligible. The very great importance of operating the hydrofoils at a depth near the wave height is clear.

It is true of course, that the maximum operating depth will be governed by several other considerations, particularly the depth of the water and the strength of the foils. This section simply points out the importance of using the greatest depth possible.

G. THE TIETJENS SYSTEM

The hydrofoil system designed by Dr. Tietjens, and described in the Intorudction of this thesis, differs from the general system shown on PLATE 1, only in that the after hydrofoil is flat, so that its lifting force does not vary with depth.

The equations of motion of this system were written by abridging the equations of PLATE 1 so that the lift on the rear foil was proportional only to angle of attack. One set of solutions to these equations was obtained, for an arrangement which had been shown to be most desirable in the general case: $x_1/\ell = 1/3$; $\ell\alpha_{10} = 4$, $V\alpha_{10} = 9.6$. The area of the after foil was taken to be three-tenths that of the forward foil in accordance with pictures of the Tietjens boats.

The results of these calculations are shown in Fig. VII-42 where the effect on performance of increasing wave height is shown. This figure is quite similar to Fig. VII-13 as regards the hydrofoil and wave parameters used. Comparison of these two figures shows that there exists also a very close similarity in the qualitative performance of the two systems. (Only in one instance is there marked difference: the after hydrofoil of the original system undergoes about the same dynamic loading as the forward foil, but in the Tietjens system the after foil appears to get very little dynamic loading.)

It is unfortunate that time limitations did not

permit further numerical study of this system -- particularly of the effects of center of gravity location and area distribution. However, it is suggested that the strong similarity of performance of the two systems furnishes some grounds for extending the results of calculations on the general system qualitatively to the Tietjens system. In particular, the conclusions regarding stable center of gravity locations and running depth should apply.

The pertinent conclusions reachedwere that center-of-gravity locations too near the forward hydrofoil lead to undesirable transient oscillations, and that the height of the waves which can be smoothly traversed is about the same as the running depth of the foils. The Tietjens system (Fig. I-2e) has a very shallow draft and its center of gravity is almost directly over the forward hydrofoil. The German-built boats are reported to have had unstable characteristics, particularly in waves.

G. SUMMARY OF RESULTS

In this section of the calculating program it was desired to determine theprobable performance of a hydrofoil system under the worst sea conditions likely to be encountered. The main criterion for performance was the maximum height of waves which could be stably negotiated without either cavitation (or ventilation) or unstable motions. Accelerations, depth, and other quantities were also calculated.

Although the absolute accuracy of the differential analyzing equipment was not high, its precision of repitition was good, so that the effects of varying one parameter at a time could be closely observed.

In a typical analysis it was shown that the steady-state performance of a hydrofoil system in a given set of waves could be remarkably good (with the center of gravity motion as little as one-tenth the wave-height), and yet the response under reasonable transient conditions in the same waves could be quite intolerable. The necessity for the transient study was thus confirmed.

It was found that the depth at which the hydrofoil system entered a set of waves was of predominent importance in determining the resulting transient. Shallow initial entries produced the worst motions in every respect, while entry at all depths greater than the wave height resulted in a quite stable return to the steady state.

The ratio of boat-length to wave-length (phase) was found to be of some importance: the motions are least stable when this ratio is about .4, and are about the same for all values of the ratio greater than .4. On the other hand, the loadings and accelerations become worst for very small values -- near zero.

As expected, the motions of the system become much more violent when the waves are encountered at approximately a resonant frequency of the system. The foil loading (which is a strong function of vertical velocity) and the acceleration are proportional to both the amplitude of motion and the frequency, and therefore increase rapidly with frequency of encounter until some frequency is reached for which the system cannot follow the waves at all. The system then merely undergoes the transient motions accompanying any change in mean water height.

It was found that the effect of frequency of encounter on the motions of the system was much more pronounced at low speeds than at high speeds. It is suggested that this may be due to a higher effective damping at high speeds, which was predicted in Chapter VI-A. The degree to which frequency of encounter affected the performance was found to be nearly independent of the length of the system. (Long boats at slow speeds were

of course always the most stable.)

To find the worst motions possible as a function of speed, the system was assumed to be moving cross-wind so as to encounter the waves at approximately the worst combination of frequency and phase. The resulting calculations show that increasing the speed at which the system operates markedly reduces the ranges of the various system and wave parameters for which stable performance will be obtained.

As usual the system becomes less stable as its length is decreased. At high speed this limitation is so stringent that operation of systems less than 20 chords in length will probably be out of the question.

The choice of equilibrium loading per unit area of the hydrofoils is much more limited at high speeds. It is found that a high loading results in more desirable motions, but gives rise more quickly to dynamic loadings of cavitation magnitude. For very light initial loading the motions are unstable. An intermediate loading must therefore be very carefully chosen. In this regard a careful selection of foil profile for the speed anticipated is very important.

If operation directly upwind or downwind, instead of cross-wind, is possible, the performance of the system will be markedly better at high speeds, with

upwind operation offering the greatest improvement.

It was clearly demonstrated that if hydrofoils can be made to operate at a depth as great as the wave height to be encountered, good performance can be expected, but if the operating depth is appreciably less, severe transient motions will probably result.

Brief calculations on the Tietjens system (flat instead of dihedral foil aft) indicate performance very much like that of the all-dihedral system, from which it is suggested that most of the conclusions reached in this thesis would apply also to the Tietjens system.

CHAPTER VIII

CONCLUSIONS

It is believed that a number of pertinent conclusions regarding the design of hydrofoil systems and their operation on ocean waves are warrented by the results presented in Chapters VI and VII.

First, some recommendations regarding the choice of the various hydrofoil system dimensions will be presented. Then some predictions of operating characteristics in waves will be made. Finally, some notes will be submitted on the problem of designing high speed hydrofoil craft.

Center of Gravity Location:

The center of gravity must be located within specific limits for stable operation. The range of stable positions may be increased by careful selection of other parameters of the system which will be discussed. In general, for a given configuration the best center of gravity location is somewhat forward of the position which would result in equal load per unit area on all hydrofoils. As the center of gravity is moved forward from this point, the motions of the system will become increasingly oscillatory, and will finally display unstable oscillation. As the center of gravity is moved aft the "spring-stiffness" of the system will decrease, so that

although the motions are more highly damped the system is also less inclined to return to equilibrium and will finally exhibit unstable divergence.

Length:

A "long" hydrofoil system - i.e. one having a large ratio of length to chord - will be superior in every respect to a "short" system. Increasing the length of a system will increase the speed at which it can operate, the magnitude of the seas it can negotiate, and the region of permissible center of gravity locations. It will also greatly improve the performance under any given set of conditions.

Radius of Gyration:

The ratio of the radius of gyration of a hydrofoil system to its length should be made as small as possible. In general, decreasing radius of gyration has the same favorable effects as increasing length.

Speed:

As the speed of a hydrofoil system is increased its performance becomes less stable in every respect. In particular, the "spring-stiffness" of the system is decreased, and the tendency to cavitate and ventilate is greatly increased. The first effect causes the system to make wider and wider excursions from its equilibrium position in response to a given disturbance. The second effect will ultimately result in violent sudden dipping

of the various foils in a random fashion.

Hydrofoil Loading:

At low speeds (below 30 feet per second) the loading per unit area of the hydrofoils will necessarily be light,(less than 300 lb/ft^2) because the angle of attack will be limited by the stall angle.

At intermediate speeds (in the neighborhood of 50 feet per second) a fairly large range of loadings can be used satisfactorily. The lower limit of this range is a loading of 200 lb/ft^2, because very light loadings result in the same sort of decrease in "spring-stiffness" as high speeds, and therefore in a divergent type of instability. The upper limit of the range is about 1000 lb/ft^2. (one-half an atmosphere) because of the important danger of cavitation and ventilation.

At high speeds (over 100 feet per second) the limits of permissible loading become very much more stringent: loadings which are too light will lead quickly to unstable motions, while loadings which are too heavy will cause early cavitation and ventilation. It appears that the loading must be held closely in the neighborhood of 600 lb/ft^2.

Operating Depth:

The hydrofoils should be designed to operate at as great a depth as stuctural and operational conditions permit. (An increase in depth can be effected by reducing

chord, reducing angle of attack, increasing dihedral or increasing total load.

The principle reason for desiring deep hydrofoils is the greatly improved performance of the system in waves. In general, if the smooth-water running depth of the hydrofoils can be made at least as great as the height of the largest waves to be encountered, the very undesirable motions described in Chapter VII, Part III, will be almost entirely avoided. Instead, a remarkably smooth ride may be expected, with motions of the order of one-fifth the wave height.

Increasing the operating depth has two other important effects; (1) for straight-dihedral foils the natural frequency is lowered, which is generally advantageous because it decreases the probability of encountering waves at a resonant frequency; (2) The effective damping of the system is increased.

Increasing depth also tends to reduce the "stiffness" of the system, but this effect is considered secondary in this case.

Effects of Main Wave Properties:

The transient performance of a hydrofoil system in waves may be very much worse than the indicated steady-state performance. Of cardinal importance in determining the motions of the system in a wave is the elevation at which it enters the wave: the higher (nearer the wave-crest) the

worse the motions.

In general, the magnitude of the motions and of the angles of attack, depths of submergence, accelerations, etc., all increase in approximately direct proportion to the wave height.

The frequency at which waves are encountered has roughly opposite effects on the amplitudes of motion and on dynamic foil loading: Low frequencies (near resonance) cause large motions, but only moderate dynamic loadings, while higher frequencies cause smaller motions but higher loadings. As frequency is increased, a value is eventually reached for which the system responds very little to the waves, and undergoes only the transient motions of following changes in mean surface level or those due to other disturbances.

The ratio of boat length to wave length (called the "phase" in this thesis) is of considerable importance in determining the type of motions the boat will have. If this ratio is near zero the motions will be largely rising, with little pitching. If the ratio is near one-half, less rising but much more pitching takes place. The result is that the motions are greater (and become unstable sooner) when the phase is near one-half, but the angles of attack (and therefore the dynamic loadings) reach more severe values when the phase is near zero.

At high speeds upwind operation will be preferable to cross-wave travel.

High Speed Design:

It is clear that for operation at high speed a careful design of all of the components connected with the loading per unit area of the hydrofoils is imperative. Of particular importance are the choice of foil profile and camber, and of operating angle of attack -- which will probably be somewhat below the design angle. It is believed that a careful study of the factors presented in Figure 3 will be of considerable help in this selection.

It is quite possible that the operation of rigid hydrofoil systems in the very high speed regime may be impracticable. First, the stiffness of the system becomes so small at high speeds that additional control may be necessary. But more important, when it is realized that at 160 feet per second the maximum permissible (cavitating) angle of attack of the foils is about one-half degree, it is evident that a very highly-developed form of incidence control may be required.

Closure:

This thesis has presented what is hoped to be an extensive study of the theoretical performance of rigid hydrofoil systems which obtain their stability from variation of the submerged area of the foils.

As originally conceived, the thesis was to have included also a study of incidence controlled-systems (i.e. systems which obtain stability by variation in angle of attack,) including such specific examples as the Hook and Grunberg

systems. The preliminary derivations for this study are indicated in Chapter V, Part II.

However, the time required to complete the analysis of rigid systems was much longer than anticipated, so that with great regret it was necessary to discontinue the parallel analysis of incidence-controlled systems.

It has been conclusively shown that the control of angle of attack becomes critically important at high speed. It is therefore hoped that a complete analysis of hydrofoil systems having automatic incidence control can be made in the near future.

APPENDIX A

PRIMARY RELATIONS

FIGURE 1

LIFT ON HYDROFOILS NEAR A FREE SURFACE

SUMMARY OF EXPERIMENTAL DATA

$$\left(\frac{\partial C_L}{\partial \alpha}\right)_{th} = 4.54$$

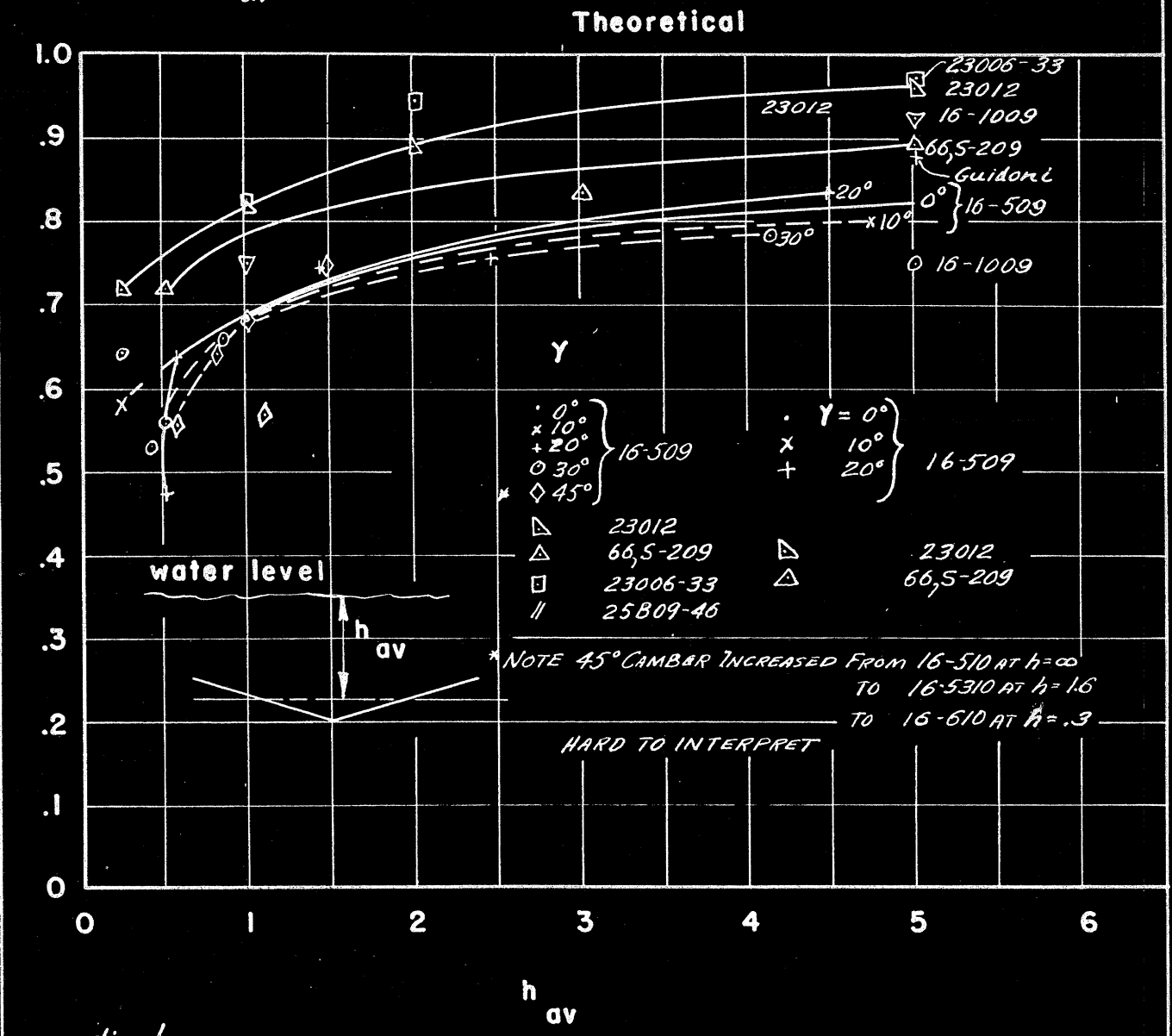

ordinate:

$$R_t = \frac{\left(\frac{\partial C_L}{\partial \alpha}\right)_{meas.}}{\left(\frac{\partial C_L}{\partial \alpha}\right)_{th}}$$

FIGURE 2

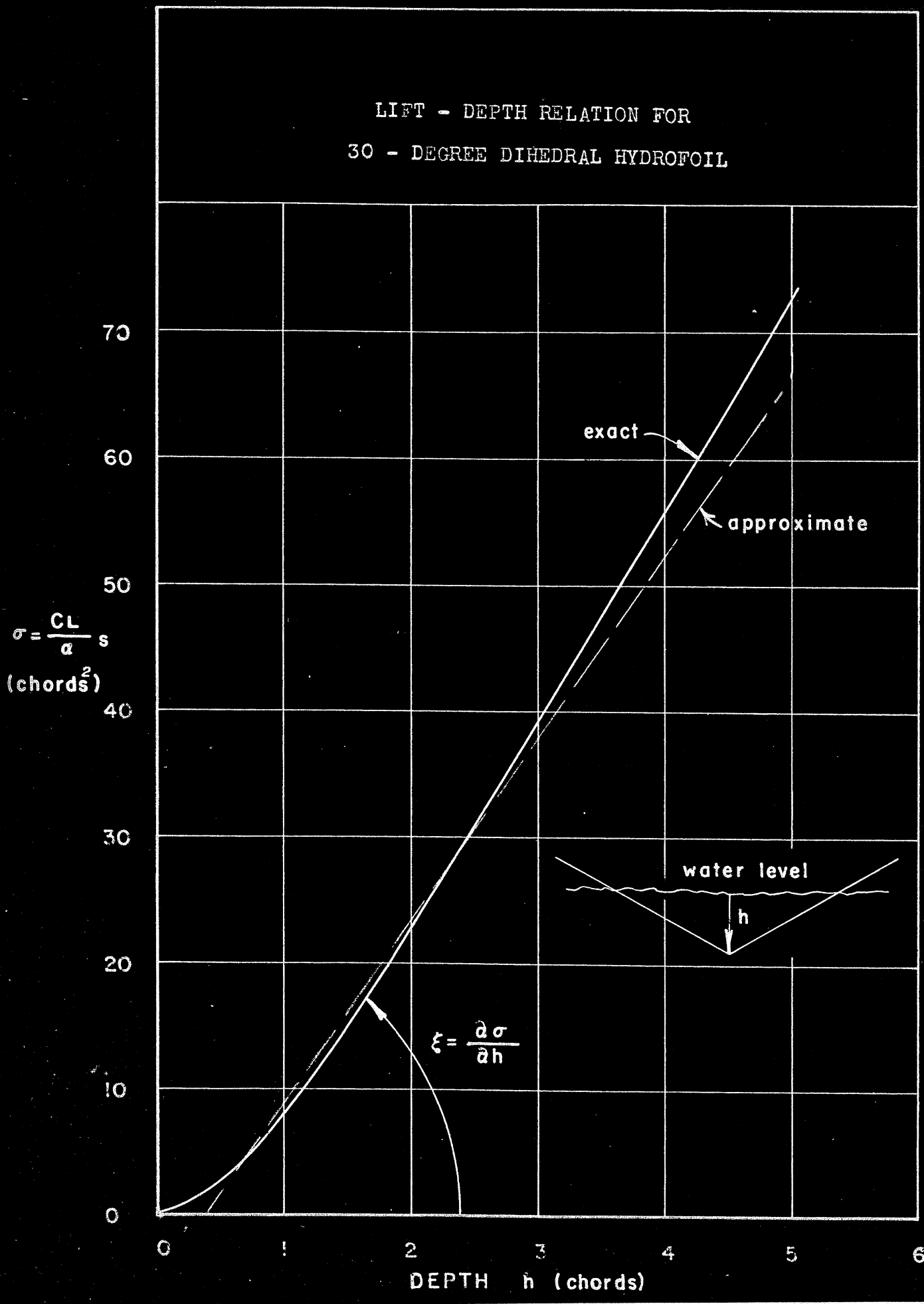
LIFT - DEPTH RELATION FOR
30 - DEGREE DIHEDRAL HYDROFOIL
exact
approximate
water level
h
$\xi = \frac{\partial \sigma}{\partial h}$
$\sigma = \frac{CL}{\alpha} s$
(chords^2)
70
60
50
40
30
20
10
0
0
1
2
3
4
5
6
DEPTH h (chords)

CAVITATION CONDITIONS FOR 16 - SERIES HYDROFOILS

FIGURE 3

EQUATIONS (2), (3), (4)

RELATIONS BETWEEN WAVE PARAMETERS

$$(2) \qquad \zeta = \frac{b}{2}\left[1 - \cos\frac{2\pi x}{\lambda} + \frac{1}{2}\frac{\pi b}{\lambda}\cos\frac{4\pi x}{\lambda} - \frac{3}{8}\left(\frac{\pi b}{\lambda}\right)^2 \cos\frac{6\pi x}{\lambda}\right]$$

$$(3) \qquad \frac{v_p}{C} = \mp \frac{\pi b}{\lambda}\left\{\left[1 - \frac{5}{8}\left(\frac{\pi b}{\lambda}\right)^2\right] e^{-\frac{2\pi}{\lambda}(h_{1o}-i+\frac{b}{2})}\right\} e^{-\frac{2\pi z}{\lambda}} \sin\frac{2\pi x}{\lambda}$$

$$(4) \qquad C^2 = \frac{gb}{2}\,\frac{1 + (\pi b/\lambda)^2}{\pi b/\lambda}$$

ζ	Wave profile height (measured positive upward from trough).
b	Maximum wave height (measured from trough to crest).
x	Horizontal position in wave (measured from trough).
$h_{1o}-i$	Distance from wave trough to equilibrium depth to hydrofoil 1.
C	Wave velocity.
g	Acceleration of gravity.
λ	Wave length.

Sign of EQUATION 3: − if x is measured positive upwind,
+ if x is measured positive downwind.

V_p

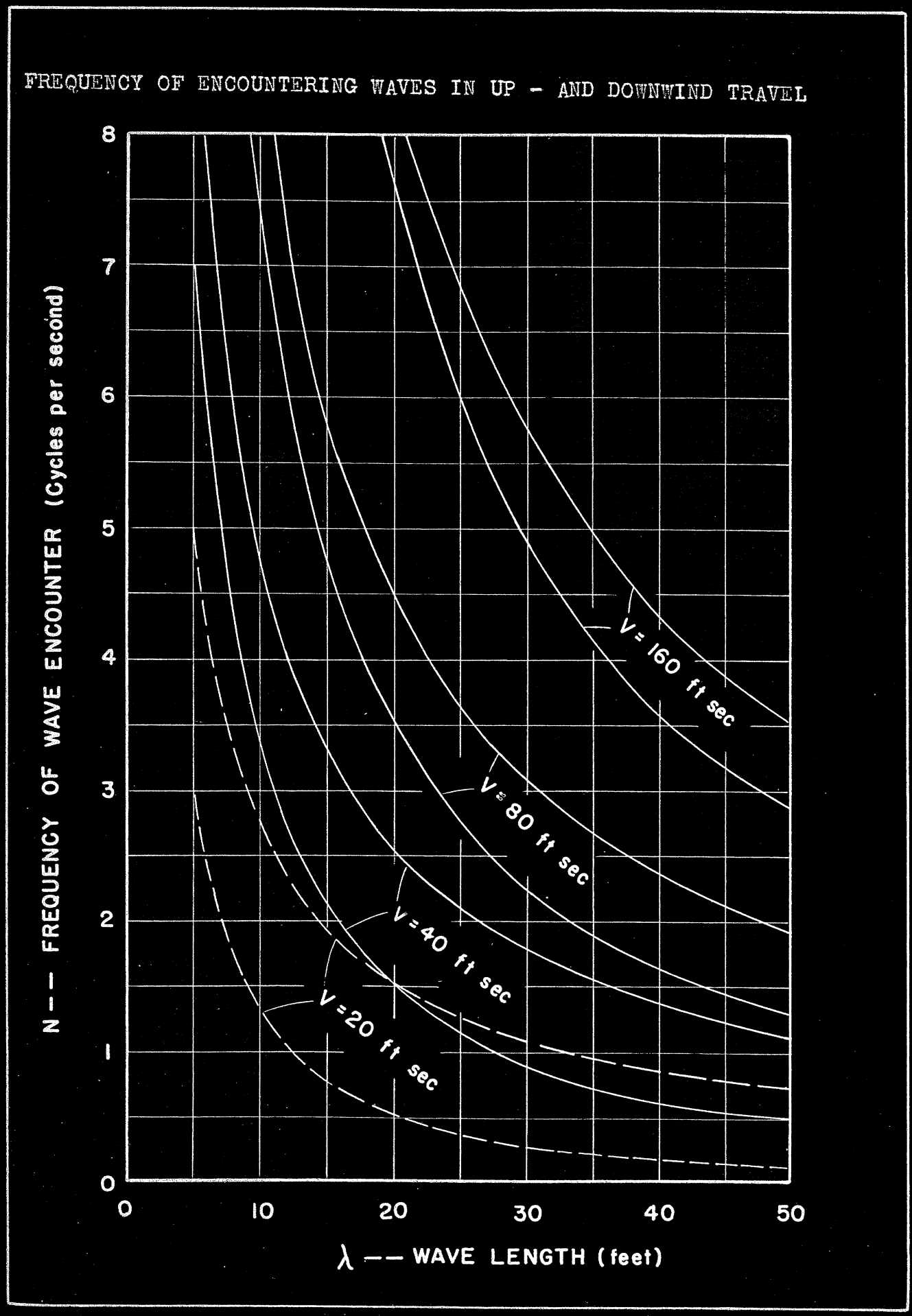
FREQUENCY OF ENCOUNTERING WAVES IN UP - AND DOWNWIND TRAVEL
N -- FREQUENCY OF WAVE ENCOUNTER (Cycles per second)
λ -- WAVE LENGTH (feet)
0
1
2
3
4
5
6
7
8
0
10
20
30
40
50
V = 160 ft sec
V = 80 ft sec
V = 40 ft sec
V = 20 ft sec

DERIVATION OF THE EQUATIONS OF MOTION OF A RIGID HYDROFOIL SYSTEM HAVING FREEDOM TO PITCH AND RISE

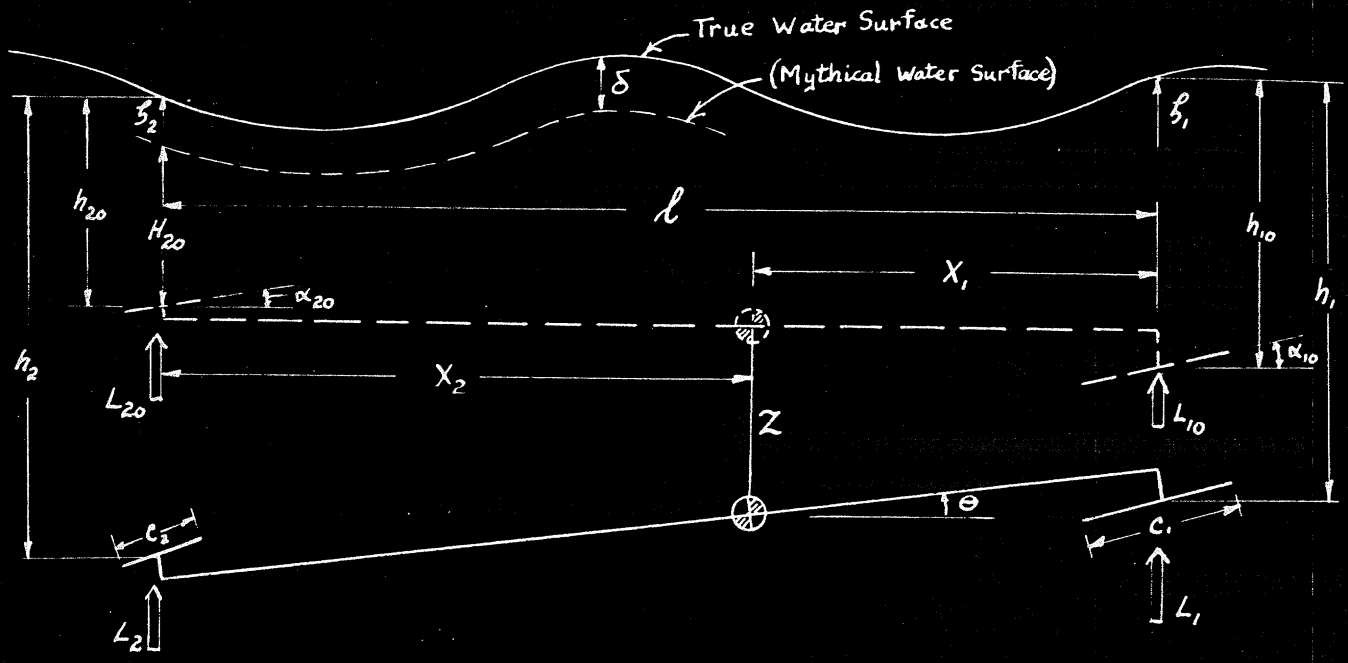

EQUATIONS OF EQUILIBRIUM:

$$(a)\quad \begin{cases} L_{10} + L_{20} = mg \\ L_{10} X_1 = L_{20} X_2 \end{cases} \qquad \text{or:} \quad \frac{L_{10}}{mg} = \frac{X_2}{l}, \qquad \frac{L_{20}}{mg} = \frac{X_1}{l}$$

STATIC LIFT EXPRESSIONS:

$$(b)\quad \begin{cases} L_{10} = n_1 \frac{\rho}{2} V^2 c_1^2 \sigma_{10} \alpha_{10} \\ L_{20} = n_2 \frac{\rho}{2} V^2 c_2^2 \sigma_{20} \alpha_{20} \end{cases}$$

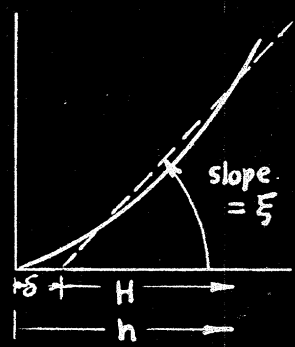

$$\sigma = \frac{c_1}{\alpha} S$$

Approximating Assumption: $\sigma = \xi(h-\delta) = \xi H$

Then: $\frac{\sigma}{\sigma_0} = \frac{\xi H}{\xi H_0} = \frac{H}{H_0}$

$$\frac{L_{10}}{L_{20}} = \frac{X_2}{X_1} = \frac{n_1}{n_2} \left(\frac{c_1}{c_2}\right)^2 \frac{\sigma_{10}}{\sigma_{20}} \frac{\alpha_{10}}{\alpha_{20}}$$

HYDRODYNAMIC EXPRESSIONS:

$$(c)\quad \begin{cases} \dfrac{L_1}{L_{10}} = \dfrac{n_1}{n_1}\dfrac{\frac{\rho}{2}V^2 c_1^2 \sigma_1 \alpha_1}{\frac{\rho}{2}V^2 c_1^2 \sigma_{10} \alpha_{10}} = \dfrac{\sigma_1}{\sigma_{10}}\dfrac{\alpha_1}{\alpha_{10}} = \dfrac{H_1}{H_{10}}\dfrac{\alpha_1}{\alpha_{10}} \\ \dfrac{L_2}{L_{20}} = \dfrac{n_2}{n_2}\dfrac{\frac{\rho}{2}V^2 c_2^2 \sigma_2 \alpha_2}{\frac{\rho}{2}V^2 c_2^2 \sigma_{20} \alpha_{20}} = \dfrac{\sigma_2}{\sigma_{20}}\dfrac{\alpha_2}{\alpha_{20}} = \dfrac{H_2}{H_{20}}\dfrac{\alpha_2}{\alpha_{20}} \end{cases}$$

$$\begin{cases} \dfrac{H_1}{H_{10}} = 1 + \dfrac{z - x_1\theta + (\zeta_1 - i)}{H_{10}} \\ \dfrac{H_2}{H_{20}} = 1 + \dfrac{z + x_2\theta + (\zeta_2 - i)}{H_{20}} \end{cases}$$

$$\begin{cases} \dfrac{\alpha_1}{\alpha_{10}} = 1 + \dfrac{\theta}{\alpha_{10}} + \dfrac{\dot z/V}{\alpha_{10}} - \dfrac{x_1\dot\theta/V}{\alpha_{10}} - \dfrac{v_{p1}/V}{\alpha_{10}} \\ \dfrac{\alpha_2}{\alpha_{20}} = 1 + \dfrac{\theta}{\alpha_{20}} + \dfrac{\dot z/V}{\alpha_{20}} + \dfrac{x_2\dot\theta/V}{\alpha_{20}} - \dfrac{v_{p2}/V}{\alpha_{20}} \end{cases}$$

$v_1 = \dot z - x_1\dot\theta - v_{p1}$

$v_2 = \dot z + x_2\dot\theta - v_{p2}$

EQUATIONS OF MOTION:

$$(d)\quad \begin{cases} m\ddot z + (L_1 - L_{10}) + (L_2 - L_{20}) = 0 \\ m k_y^2 \ddot\theta - x_1(L - L_{10}) + x_2(L_2 - L_{20}) = 0 \end{cases}$$

$$\begin{cases} \dfrac{m\ddot z}{mg} + \dfrac{L_{10}}{mg}\left(\dfrac{L_1}{L_{10}} - 1\right) + \dfrac{L_{20}}{mg}\left(\dfrac{L_2}{L_{20}} - 1\right) = 0 \\ \dfrac{k_y^2}{l^2}\dfrac{m l\ddot\theta}{mg} - \dfrac{x_1}{l}\dfrac{L_{10}}{mg}\left(\dfrac{L_1}{L_{10}} - 1\right) + \dfrac{x_2}{l}\dfrac{L_{20}}{mg}\left(\dfrac{L_2}{L_{20}} - 1\right) = 0 \end{cases}$$

$$(7)\quad \begin{cases} \dfrac{\ddot z}{g} + \dfrac{x_2}{l}\left(\dfrac{H_1}{H_{10}}\dfrac{\alpha_1}{\alpha_{10}}\right) + \dfrac{x_1}{l}\left(\dfrac{H_2}{H_{20}}\dfrac{\alpha_2}{\alpha_{20}}\right) = 1 \\ \left(\dfrac{k_y}{l}\right)^2 \dfrac{l\ddot\theta}{g} - \dfrac{x_1 x_2}{l^2}\left(\dfrac{H_1}{H_{10}}\dfrac{\alpha_1}{\alpha_{10}}\right) + \dfrac{x_1 x_2}{l^2}\left(\dfrac{H_2}{H_{20}}\dfrac{\alpha_2}{\alpha_{20}}\right) = 0 \end{cases}$$

$$(7)\quad \begin{cases} \dfrac{\ddot z}{g} + \dfrac{x_2}{l}\left[1 + \dfrac{z - \frac{x_1}{l}l\theta + (\zeta_1 - i)}{H_{10}}\right]\left[1 + \dfrac{l\theta}{l\alpha_{10}} + \dfrac{\dot z}{V\alpha_{10}} - \dfrac{\frac{x_1}{l}l\dot\theta}{V\alpha_{10}} - \dfrac{v_{p1}}{V\alpha_{10}}\right] + \dfrac{x_1}{l}\left[1 + \dfrac{z + \frac{x_2}{l}l\theta + (\zeta_2 - i)}{H_{10}}\right]\left[1 + \dfrac{l\theta}{l\alpha_{20}} + \dfrac{\dot z}{V\alpha_{20}} - \dfrac{\frac{x_2}{l}l\dot\theta}{V\alpha_{20}} - \dfrac{v_{p2}}{V\alpha_{20}}\right] = 1 \\ \left(\dfrac{k_y}{l}\right)^2 \dfrac{l\ddot\theta}{g} - \dfrac{x_1 x_2}{l^2}\left[1 + \dfrac{z - \frac{x_1}{l}l\theta + (\zeta_1 - i)}{H_{10}}\right]\left[1 + \dfrac{l\theta}{l\alpha_{10}} + \dfrac{\dot z}{V\alpha_{10}} - \dfrac{\frac{x_1}{l}l\dot\theta}{V\alpha_{10}} - \dfrac{v_{p1}}{V\alpha_{10}}\right] - \dfrac{x_1 x_2}{l^2}\left[1 + \dfrac{z + \frac{x_2}{l}l\theta + (\zeta_2 - i)}{H_{20}}\right]\left[1 + \dfrac{l\theta}{l\alpha_{20}} + \dfrac{\dot z}{V\alpha_{20}} - \dfrac{\frac{x_2}{l}l\dot\theta}{V\alpha_{20}} - \dfrac{v_{p2}}{V\alpha_{20}}\right] = \end{cases}$$

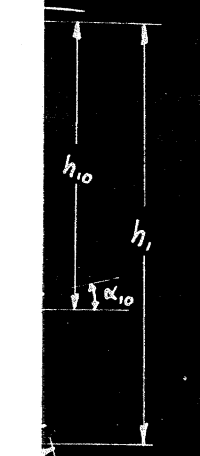

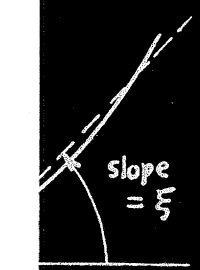

$\delta) = \xi H$

$= \dfrac{H}{H_0}$

PLATE 2

ADDITIONS TO PLATE 1

FOR A HYDROFOIL SYSTEM HAVING INCIDENCE CONTROL

$$(7c)\quad \begin{cases} \dfrac{\ddot{z}}{g} + \dfrac{x_1}{l}\dfrac{\Delta\alpha_1}{\alpha_{10}} + \dfrac{x_2}{l}\dfrac{\Delta\alpha_2}{\alpha_{20}} = 0 \\ \left(\dfrac{kg}{l}\right)^2 \dfrac{l\ddot{\theta}}{g} - \dfrac{x_1 x_2}{l^2}\left[\dfrac{\Delta\alpha_1}{\alpha_{10}} - \dfrac{\Delta\alpha_2}{\alpha_{20}}\right] = 0 \end{cases}$$

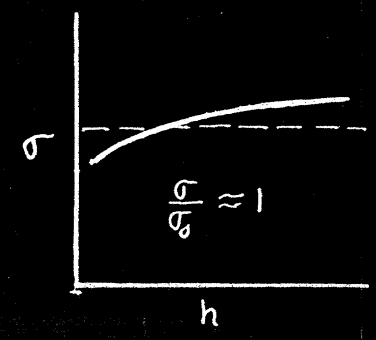

(c.f. Fig. II-7)

$$(c')\quad \begin{cases} \dfrac{\alpha_1}{\alpha_{10}} = 1 + \dfrac{\theta}{\alpha_{10}} + \dfrac{\dot{z}/V}{\alpha_{10}} - \dfrac{\frac{x_1}{l}\dot{\theta}/V}{\alpha_{10}} - \dfrac{v_{p1}/V}{\alpha_{10}} + \dfrac{\Delta\alpha_{1s}}{\alpha_{10}} \\ \dfrac{\alpha_2}{\alpha_{20}} = 1 + \dfrac{\theta}{\alpha_{20}} + \dfrac{\dot{z}/V}{\alpha_{20}} + \dfrac{\frac{x_2}{l}\dot{\theta}/V}{\alpha_{20}} - \dfrac{v_{p2}/V}{\alpha_{20}} + \dfrac{\Delta\alpha_{2s}}{\alpha_{20}} \end{cases}$$

$$(e)\quad \begin{cases} m_{m1}\ddot{y}_1 + B_{m1}\dot{y}_1 + K_{m1}y_1 = k_{11}(K_{m1}\Delta h_{1e}) \\ m_{m2}\ddot{y}_2 + B_{m2}\dot{y}_2 + K_{m2}y_2 = k_{12}(K_{m2}\Delta h_{2e}) \end{cases}$$

$$(f)\quad \begin{cases} u_1 = k_{11}(\Delta h_1^* - \Delta h_{1e}) = K_{m1}\Delta h_1^* - y_1 \\ u_2 = k_{21}(\Delta h_2^* - \Delta h_{2e}) = K_{m2}\Delta h_2^* - y_2 \end{cases}$$

$$(g)\quad \begin{cases} \dfrac{\Delta\alpha_{1s}}{\alpha_{10}} = k_{12}u_1 + k_{13}\dot{u}_1 + k_{14}\int u_1 dt + k_{15}u_2 + k_{16}\dot{u}_2 + k_{17}\int u_2 dt \\ \dfrac{\Delta\alpha_{2s}}{\alpha_{20}} = k_{22}u_1 + k_{23}\dot{u}_1 + k_{24}\int u_1 dt + k_{25}u_2 + k_{26}\dot{u}_2 + k_{27}\int u_2 dt \end{cases}$$

TABLE 1

THE RELATIONS BETWEEN SPEED, LOADING, AND ANGLE OF ATTACK

Speed, V (ft / sec)	Loading, L/S (lb / ft^2)	Angle of Attack, α_{10} (rad.)	(deg.)	$V\alpha_{10}$ (c/sec)	$\ell\alpha_{10}$ ℓ=10	20	30	H_{cr} (in.)
20	240	.2	11.4	9.6	2	4	8	24
	480	.4	22.8	19.2	4	8	16	--
	960	(.8)	(45.6)					
40	240	.05	2.8	4.8	.5	1	2	7
	480	.1	5.7	9.6	1	2	4	24
	960	.2	11.4	19.2	2	4	8	--
80	240	.0125	.7	2.4	.13	.25	.5	1.5
	480	.025	1.4	4.8	.25	.5	1	7
	960	.05	2.8	9.6	.5	1	2	24
160	240	.0031	.18					
	480	.00625	.36	2.4	.06	.13	.25	1.5
	960	.0125	..72	9.6	.13	.25	.5	7

PLATE 5

DIFFERENTIAL ANALYZER SOLUTIONS TO NON-LINEAR EQUATIONS OF MOTION OF A HYDROFOIL SYSTEM HAVING TWO DEGREES OF FREEDOM

DATA:

chord = 5 inches

H_{10} = 1.33 chords

$\ell \alpha_{10} = 4$

$V \alpha_{10} = 9.6$

WAVE SHAPE

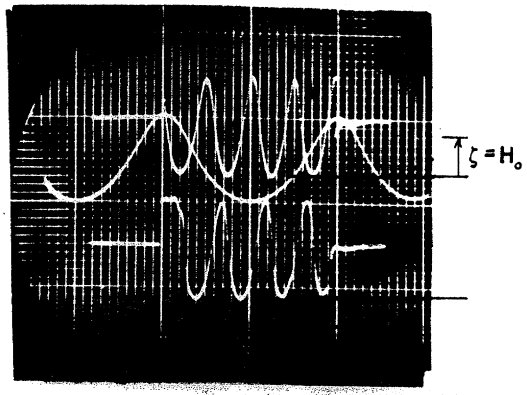

(a) WAVES AT FORWARD HYDROFOILS
(b) WAVES AT AFTER HYDROFOILS

STEADY-STATE PERFORMANCE

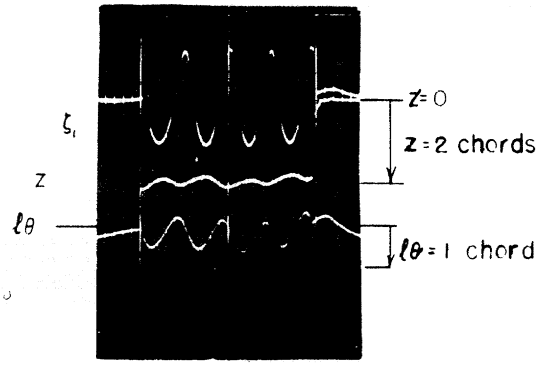

(a) ζ_1 REPEATED
(c) VERTICAL MOTION OF C.G.
(d) PITCHING MOTION ABOUT C.G.

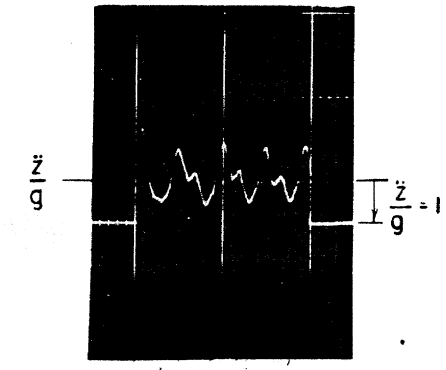

(e) VERTICAL ACCELERATION OF C.G.

TRANSIENT PERFORMANCE

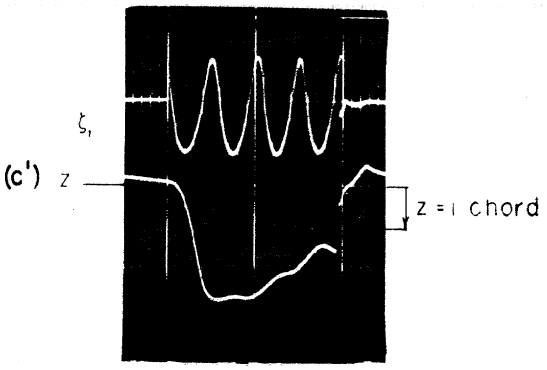

(a) ζ_1 REPEATED
(c') VERTICAL MOTION OF C.G.

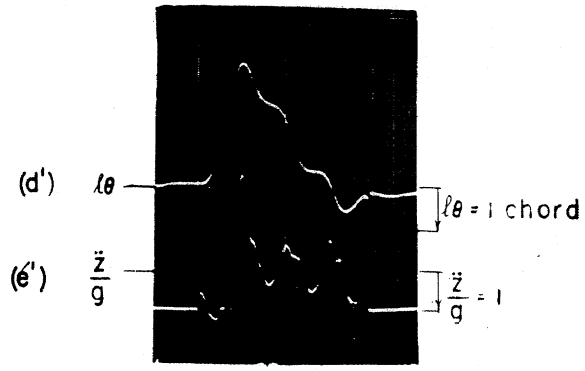

(d') PITCHING MOTION ABOUT C.G.
(e') VERTICAL ACCELERATION OF C.G.

PLATE 6

DIFFERENTIAL ANALYZER SOLUTIONS
(Continued)

STEADY-STATE PERFORMANCE

TRANSIENT PERFORMANCE

(f) $\frac{H_1}{H_{10}}$

(g) $\frac{\alpha_1}{\alpha_{10}}$

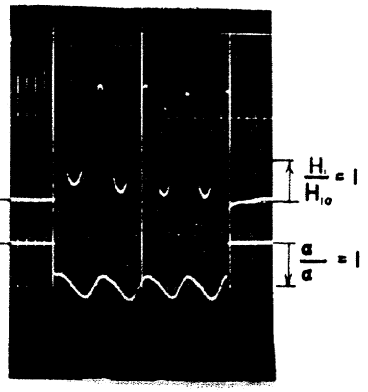

(f') $\frac{H}{H}$

(g') $\frac{\alpha_1}{\alpha_{10}}$

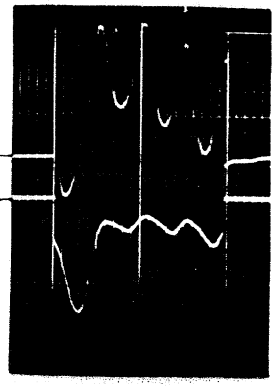

(f) DEPTH OF FORWARD HYDROFOILS
(g) ANGLE OF ATTACK OF FORWARD FOILS

(f') DEPTH OF FORWARD HYDROFOILS
(g') ANGLE OF ATTACK OF FORWARD FOILS

(h) $\frac{H_2}{H_{20}}$

(i) $\frac{\alpha_2}{\alpha_{20}}$

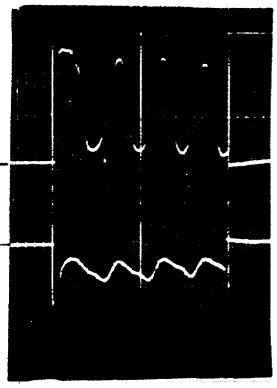

(h') $\frac{H_2}{H_{20}}$

(i') $\frac{\alpha_2}{\alpha_{20}}$

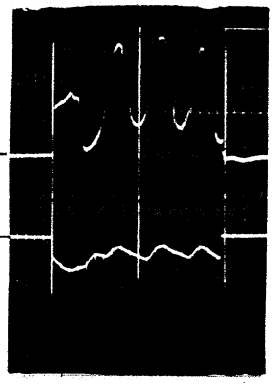

(h) DEPTH OF AFTER HYDROFOILS
(i) ANGLE OF ATTACK OF AFTER FOILS

(h') DEPTH OF AFTER HYDROFOILS
(i') ANGLE OF ATTACK OF AFTER FOILS

APPENDIX B

NUMERICAL RESULTS

SAMPLE OF EXPERIMENTAL HYDROFOIL DATA
AS REPORTED IN NACA WARTIME REPORT L - 758

Figure II-5

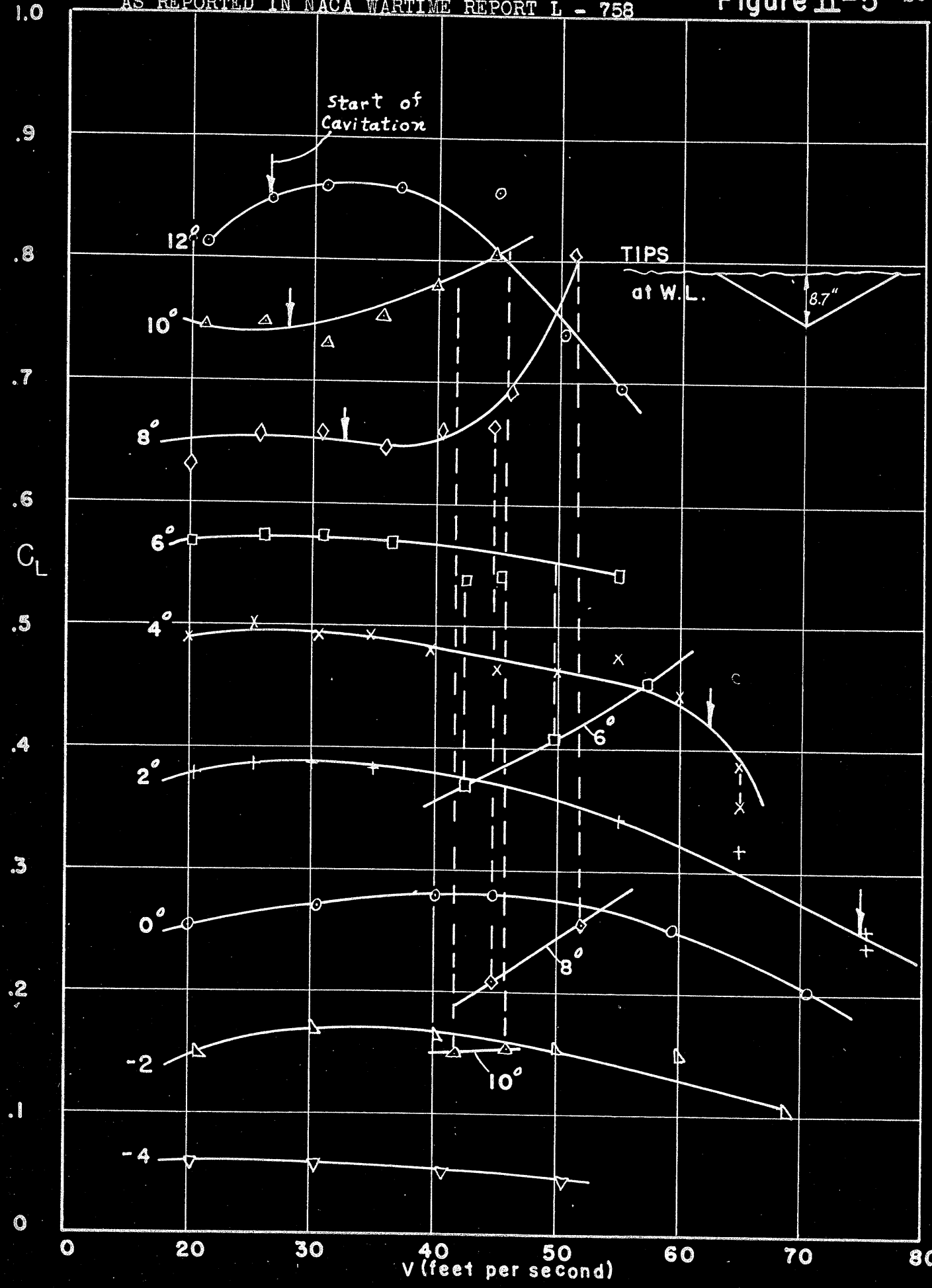

Figure II-6

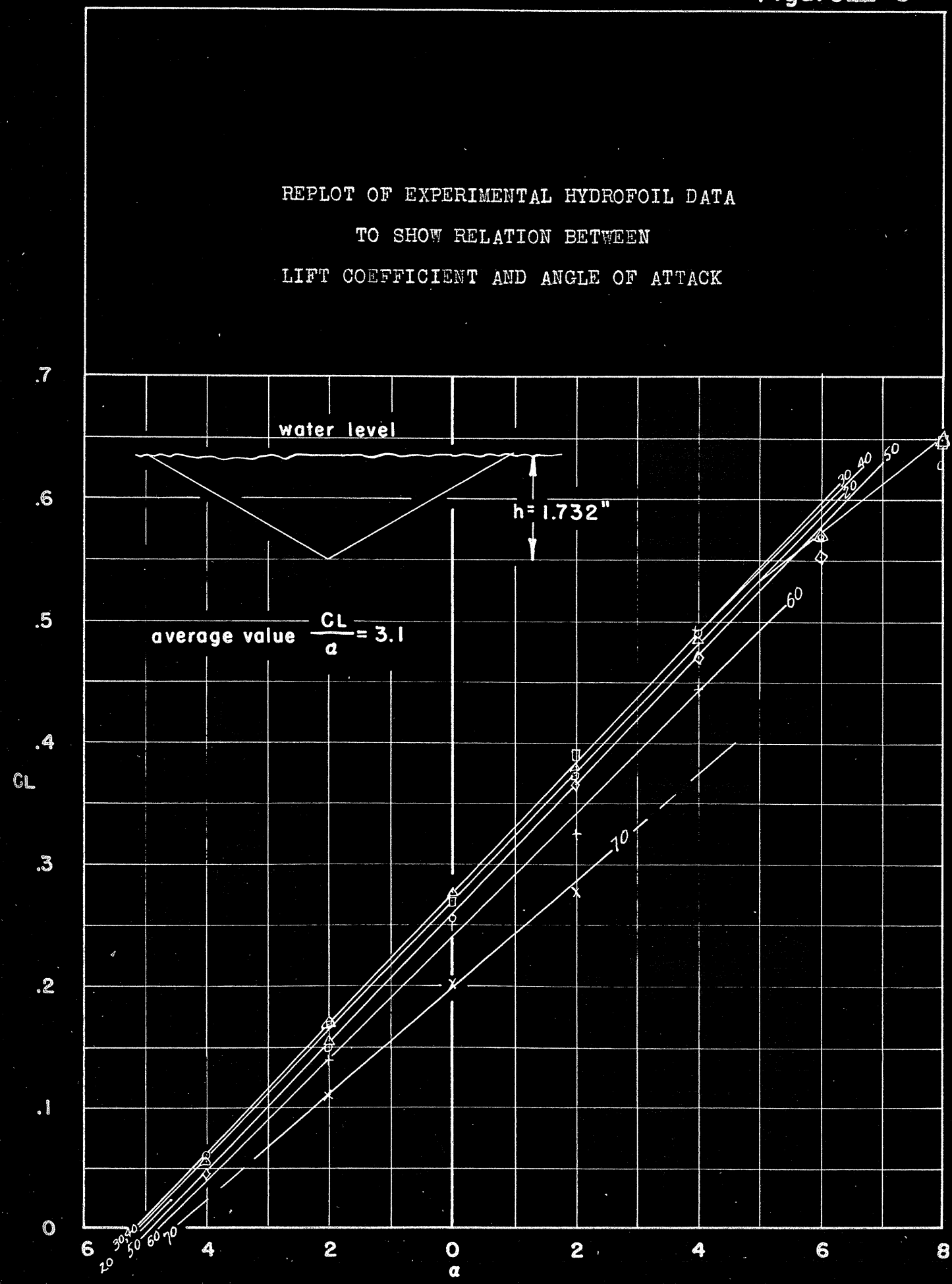
REPLOT OF EXPERIMENTAL HYDROFOIL DATA
TO SHOW RELATION BETWEEN
LIFT COEFFICIENT AND ANGLE OF ATTACK
water level
h = 1.732"
average value CL/α = 3.1
CL
α
.7
.6
.5
.4
.3
.2
.1
0
6
4
2
0
2
4
6
8
20
30
40
50
60
70

SLOPE OF THE LIFT COEFFICIENT -- ANGLE OF ATTACK CURVE FOR FLAT AND 30-DEGREE DIHEDRAL HYDROFOILS BASED ON NACA EXPERIMENTAL DATA

Figure II-7

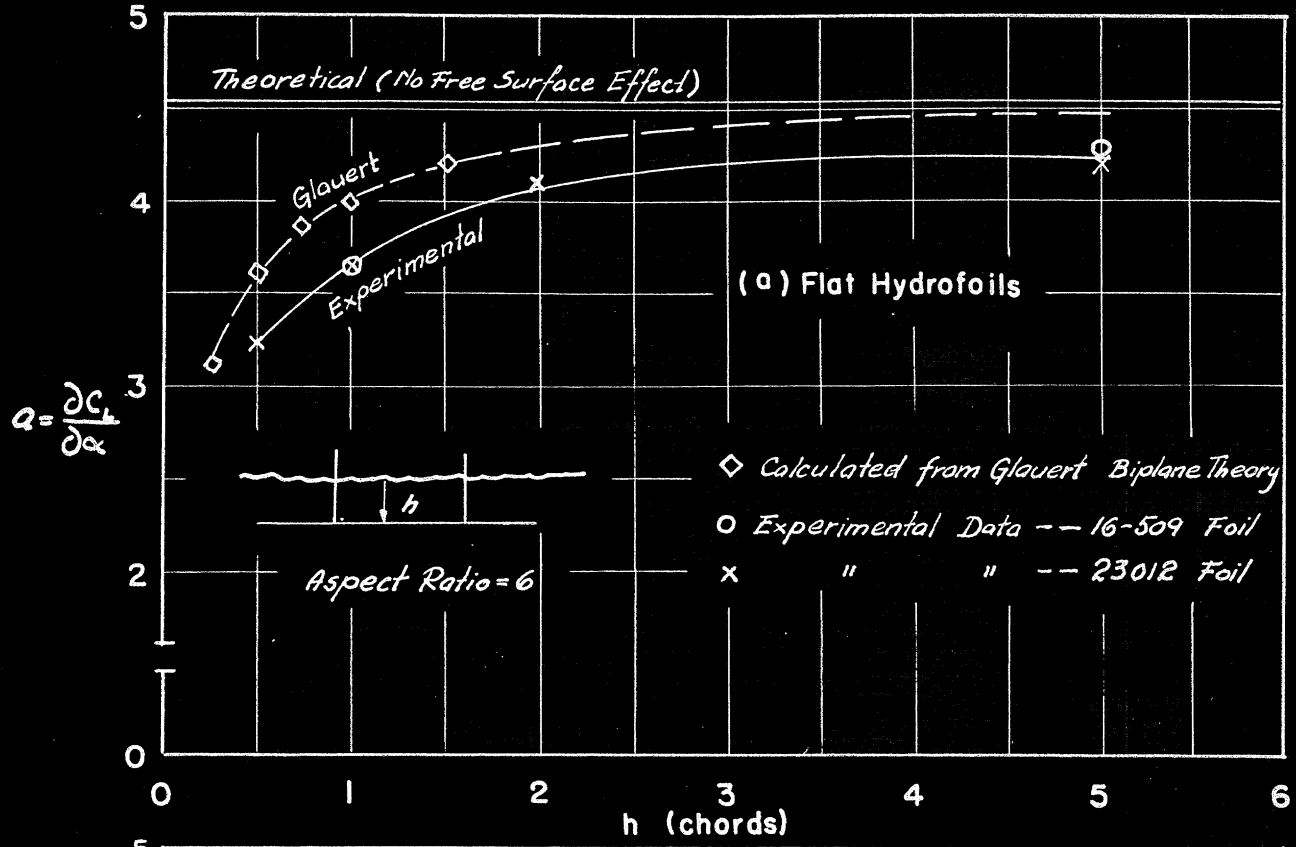

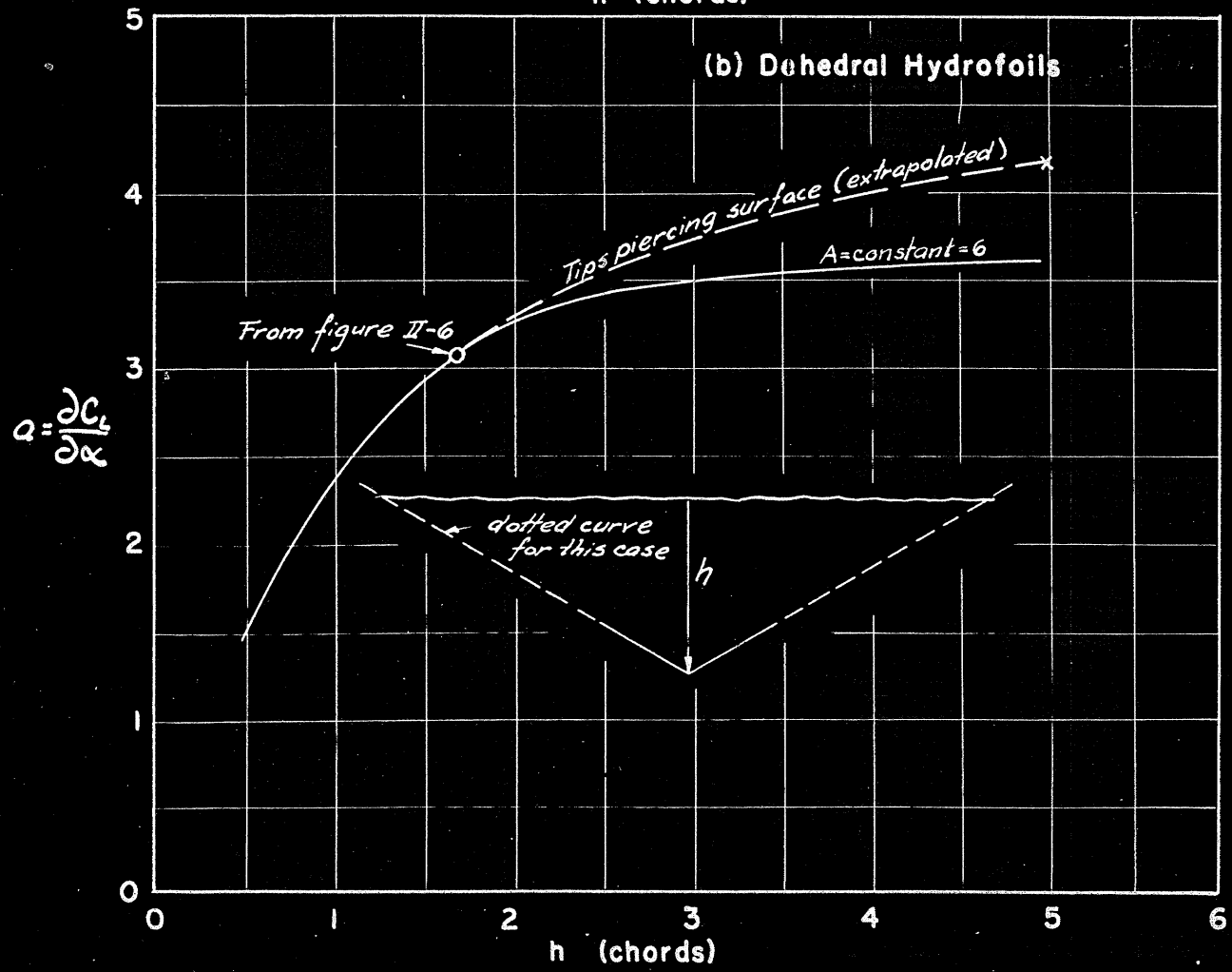

Figure III-2

SUMMARY OF CAVITATION DATA

RECORDED DURING EXPERIMENTAL TESTS OF HYDROFOILS

AT THE NACA TOWING TANK, LANGLEY FIELD, VA.

16-509 Hydrofoils Design Lift Coefficient: $C_L = .5$

(Points Mark Lowest Loading Resulting in Cavitation.)

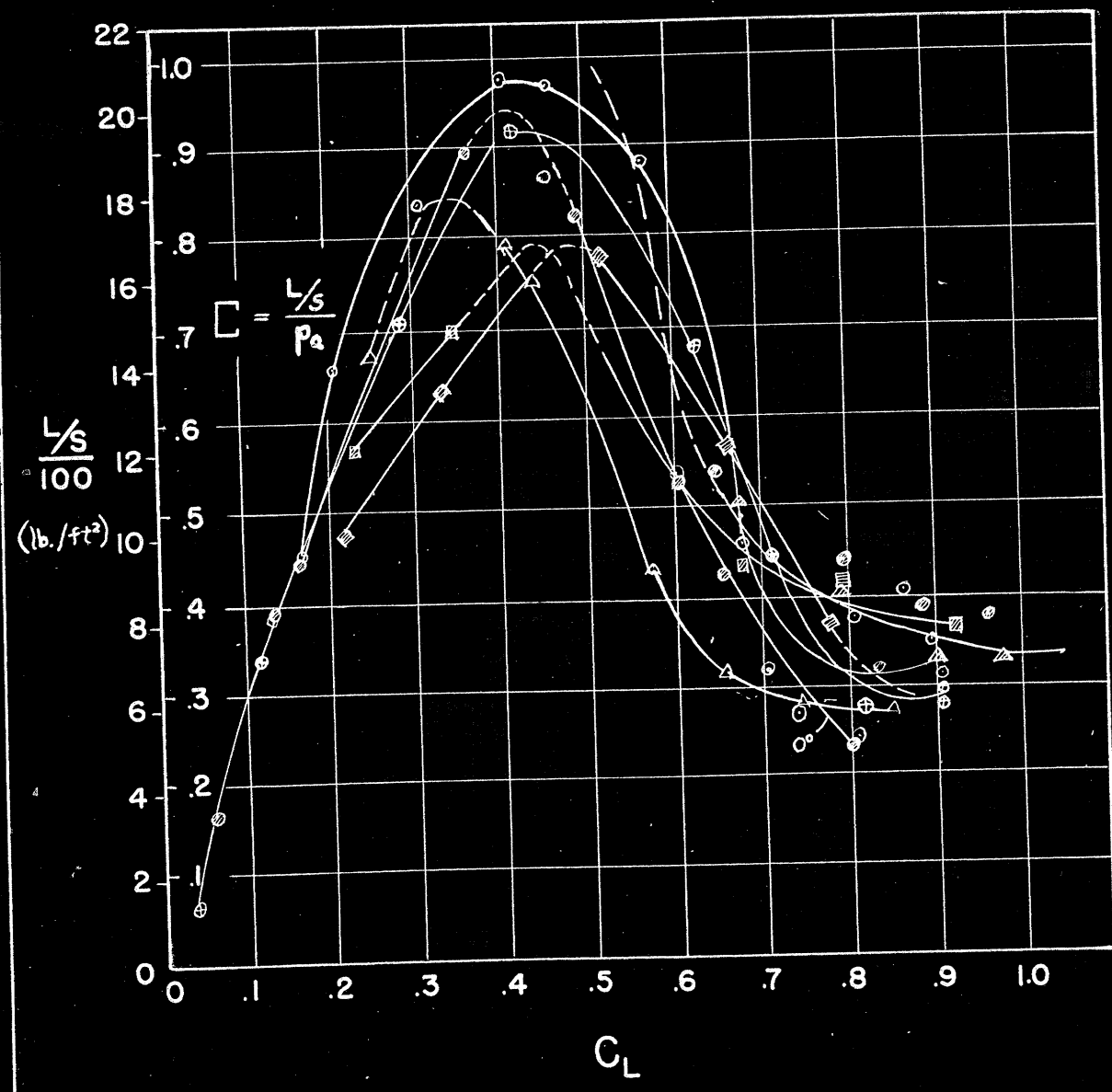

Figure III-3

EFFECT OF DIHEDRAL ANGLE ON CAVITATION CONDITIONS OF HYDROFOILS

Experimental Data on 16-509 Hydrofoils

(Design Lift Coefficient: $C_L = .5$)

From NACA Wartime Report L-758

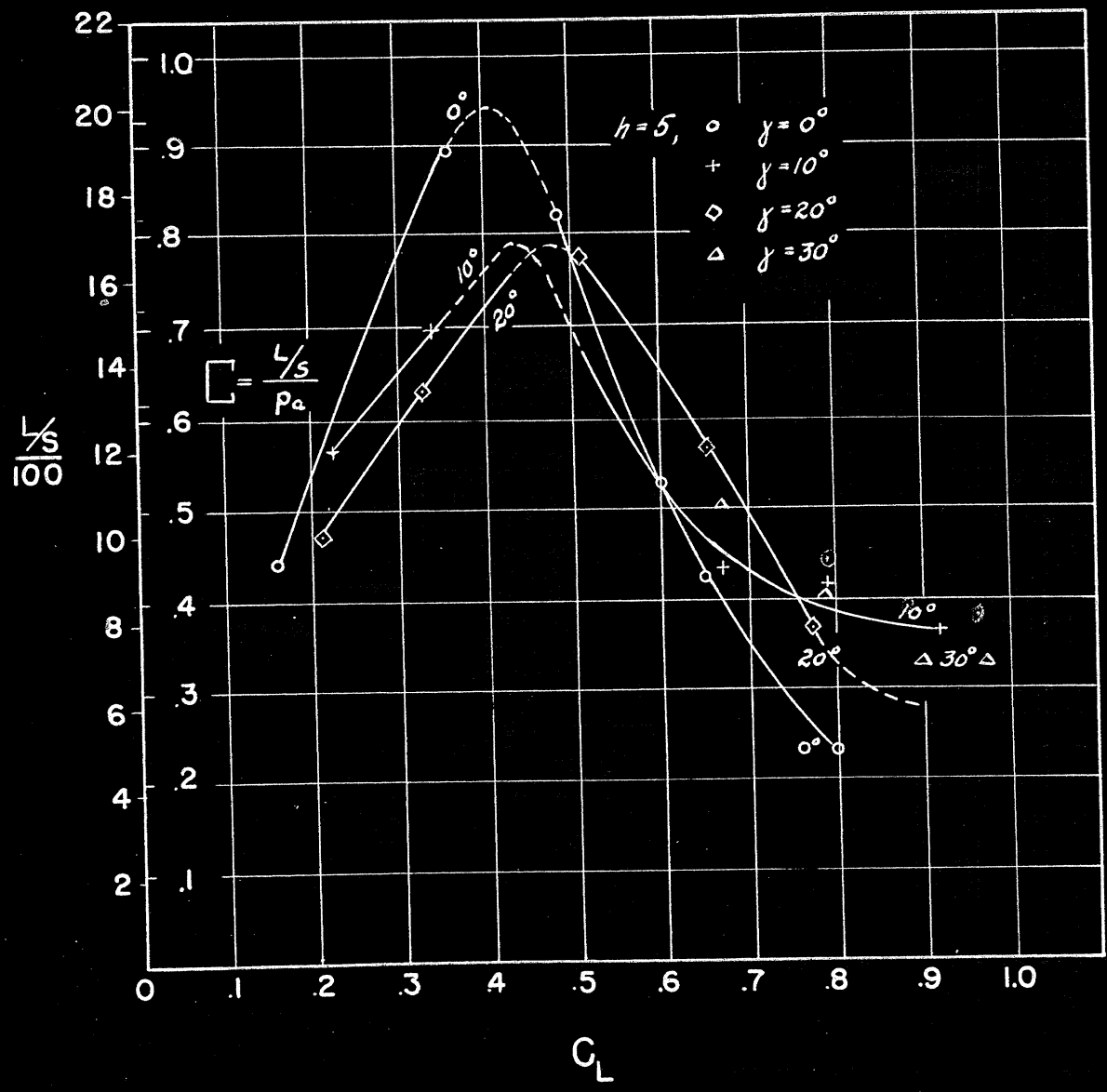

Figure III-4

EFFECT OF DEPTH ON CAVITATION CONDITIONS

OF FLAT HYDROFOILS

Experimental Data on 16-509 Hydrofoils

(Design Lift Coefficient: $C_L = .5$)

From NACA Wartime Report L-766

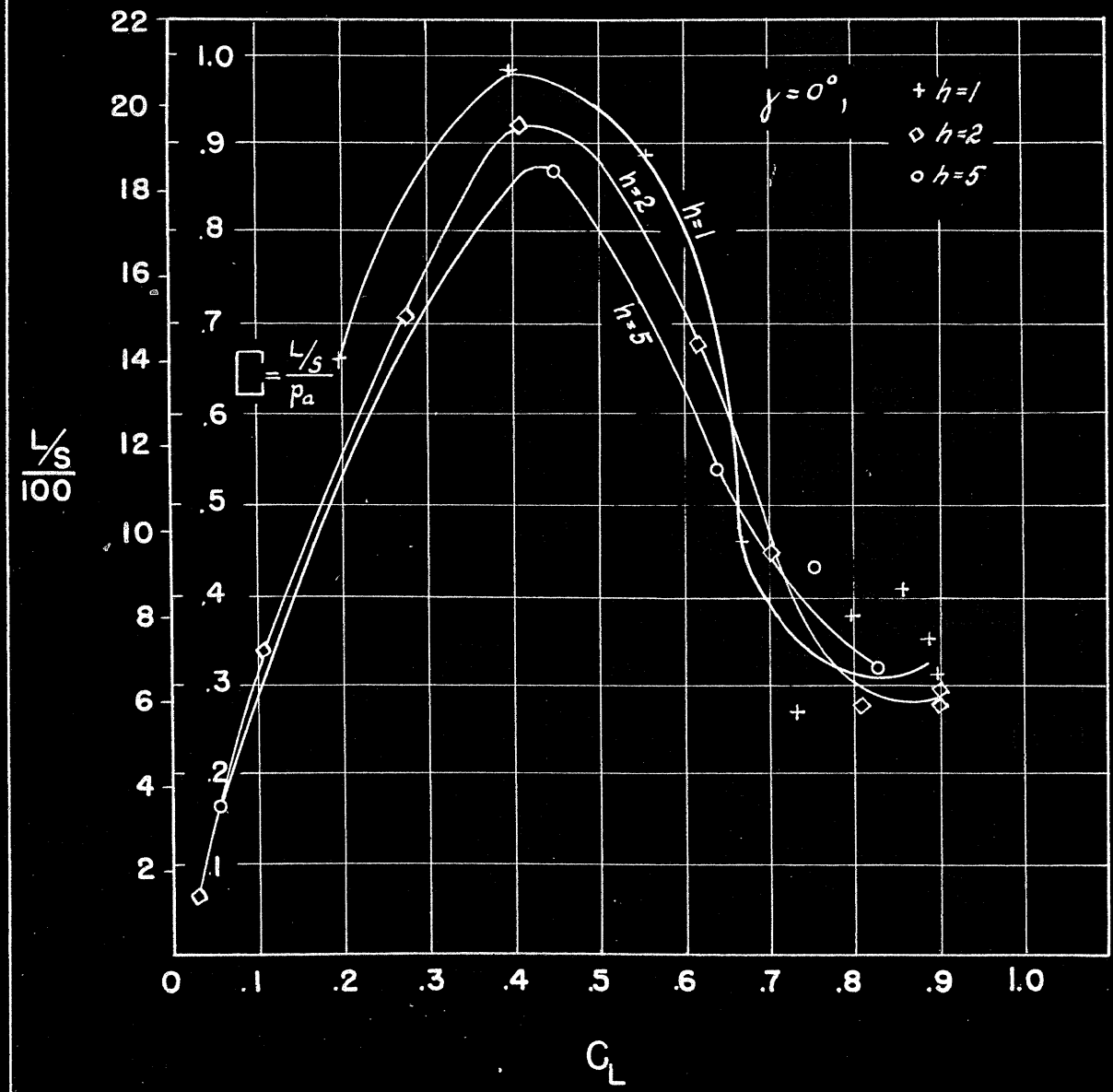

Figure III-5

EFFECT OF DEPTH ON CAVITATION CONDITIONS

OF 30 - DEGREE DIHEDRAL HYDROFOILS

Experimental Data on 16-509 Hydrofoils

(Design Lift Coefficient: $C_L = .5$)

From NACA Wartime Report L-758

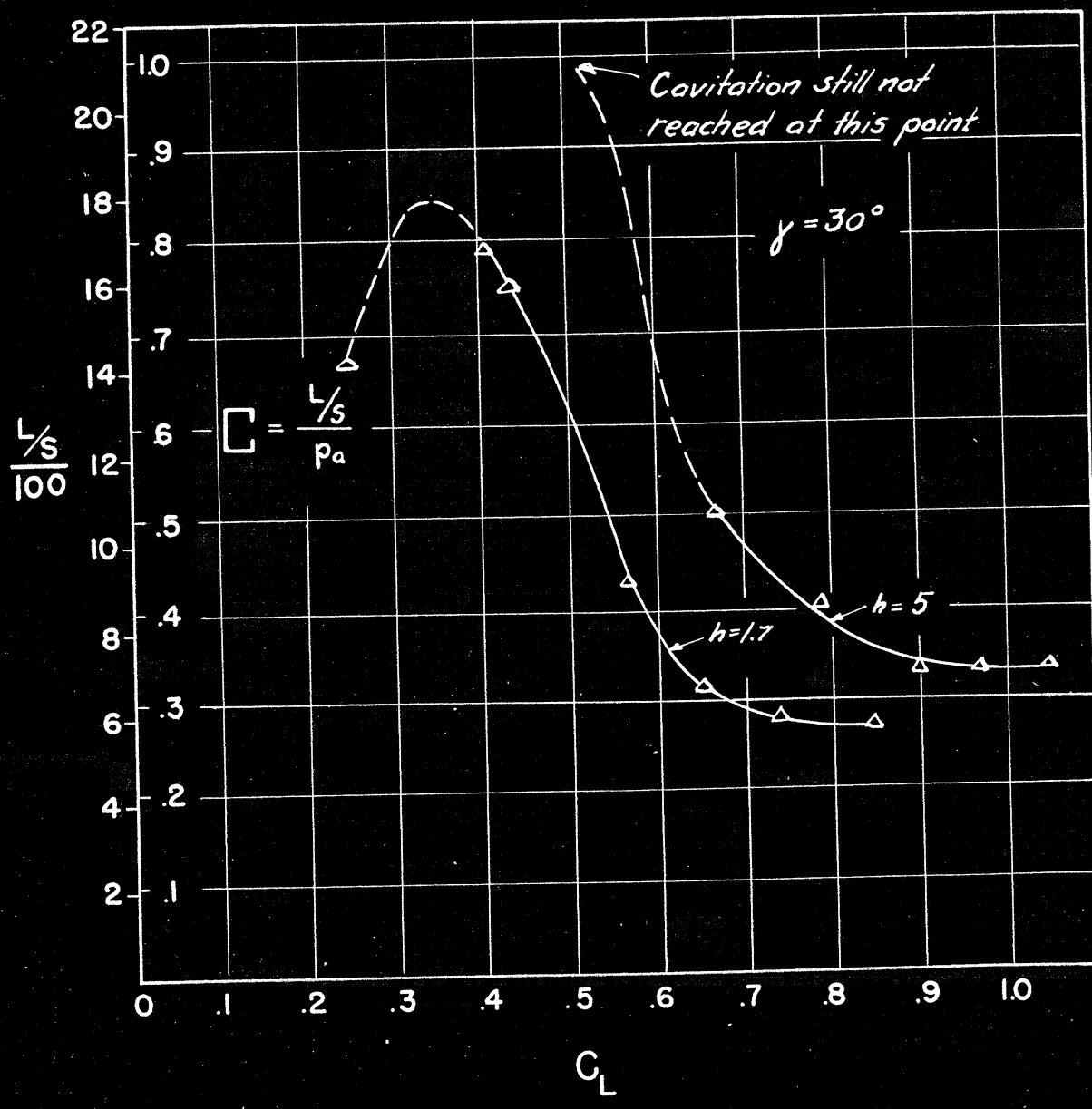

Figure III-6

IMPORTANCE OF SPEED ON CAVITATION CONDITIONS

OF HYDROFOILS

Experimental Data on 16-509 Hydrofoil

From NACA Wartime Report L-758

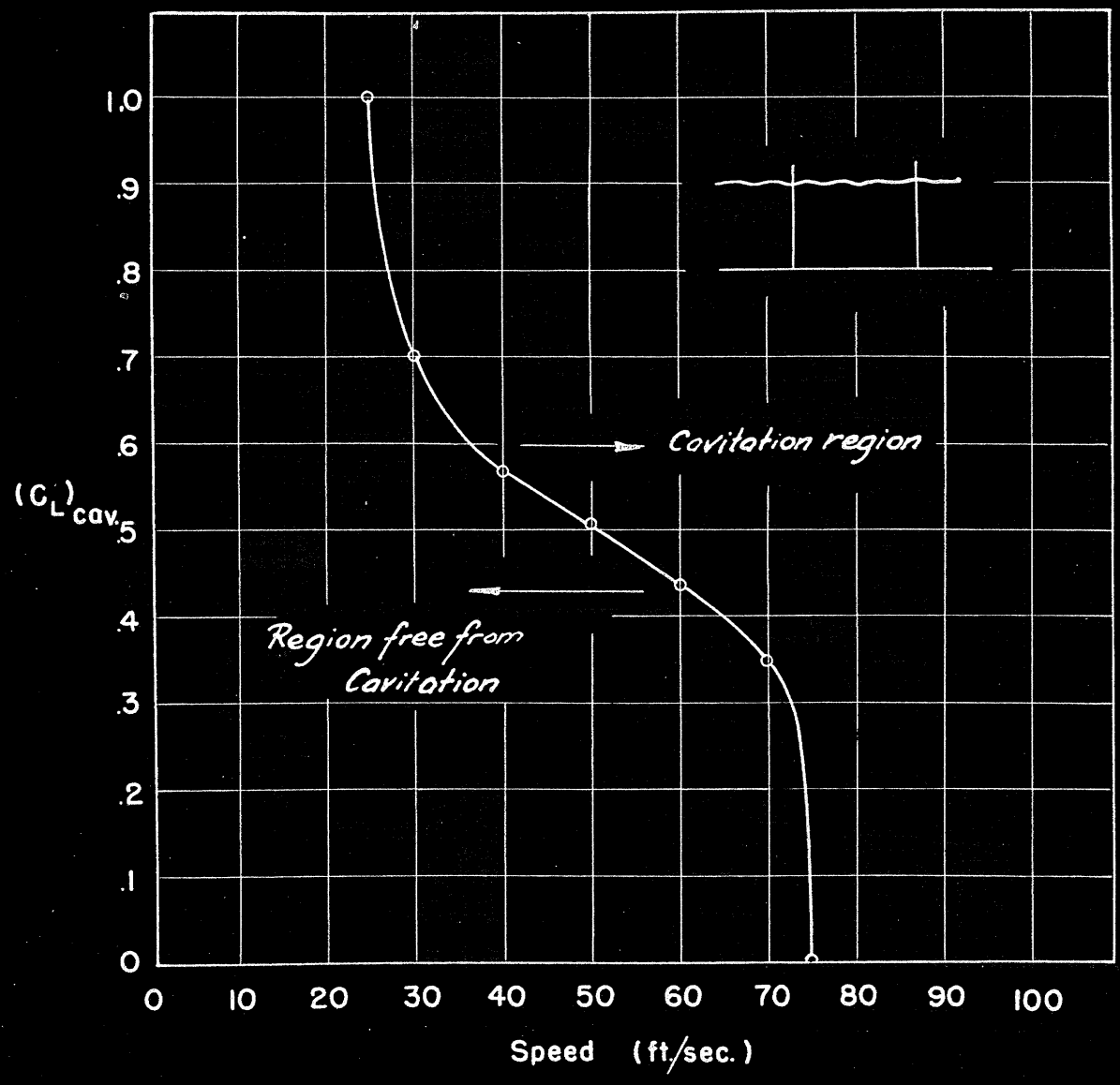

Figure III-7

VENTILATION CONDITIONS FOR 30-DEGREE DIHEDRAL HYDROFOIL

SHOWING IMPORTANCE OF DEPTH

Based on Observation of Double-Valued Lift Coefficients

In Experimental Tests of 16-509 Hydrofoils

NACA Wartime Report L-758

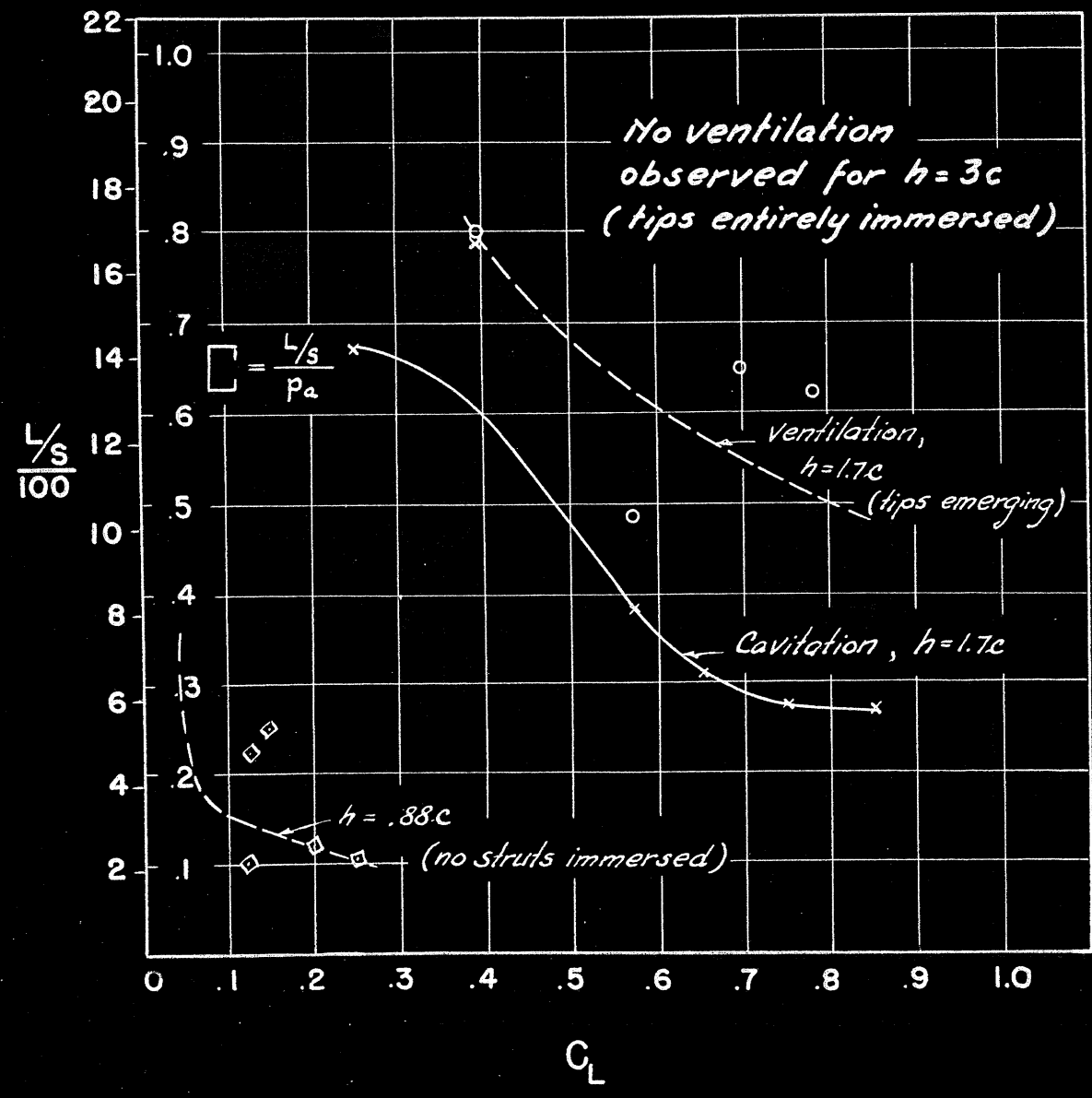

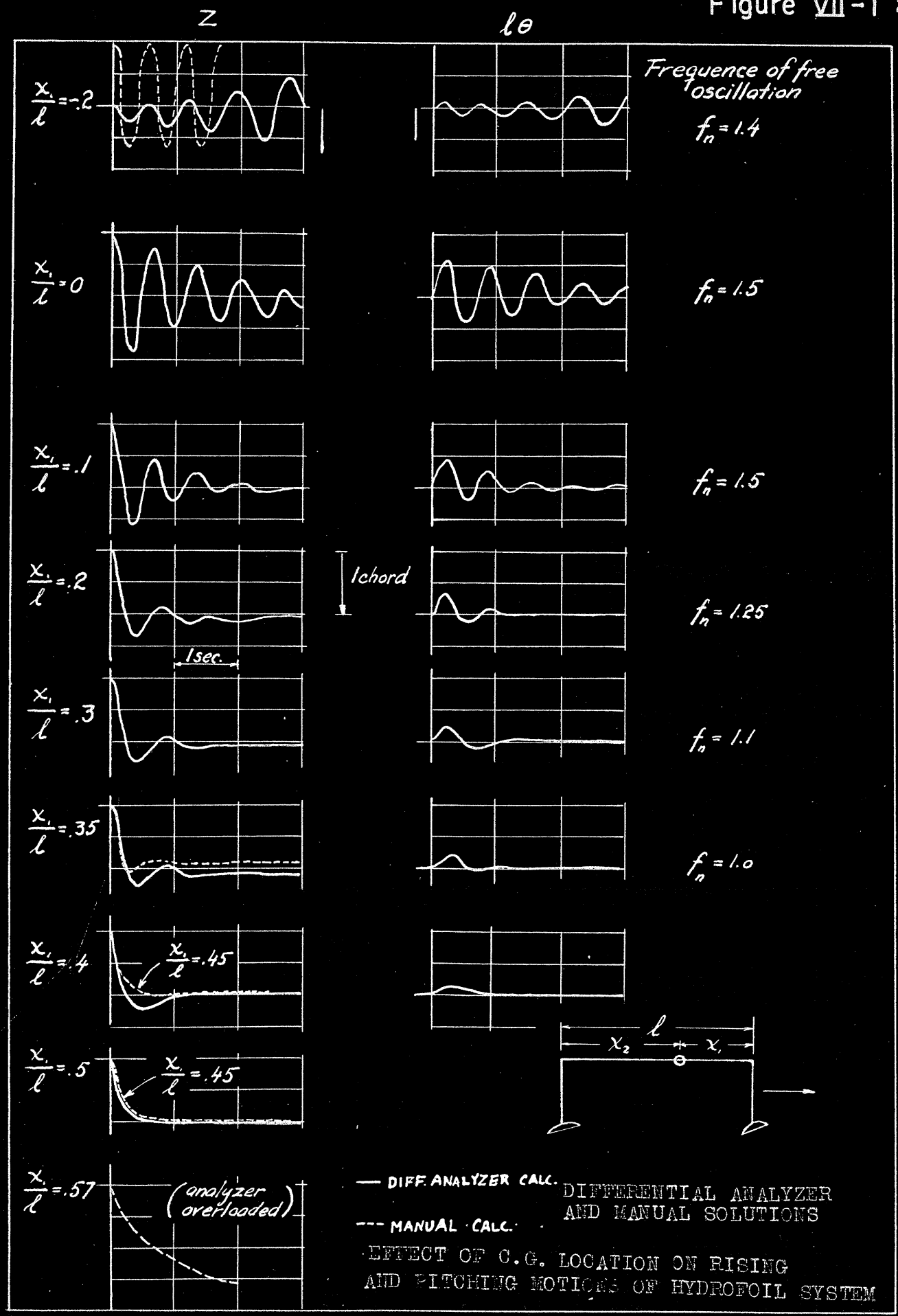
z
lθ
Frequence of free oscillation
x₁/l = -.2
f_n = 1.4
x₁/l = 0
f_n = 1.5
x₁/l = .1
f_n = 1.5
x₁/l = .2
f_n = 1.25
l chord
1 sec.
x₁/l = .3
f_n = 1.1
x₁/l = .35
f_n = 1.0
x₁/l = .4
x₁/l = .45
x₁/l = .5
x₁/l = .45
x₁/l = .57
(analyzer overloaded)
l
x₂
x₁
— DIFF. ANALYZER CALC.
--- MANUAL CALC.
DIFFERENTIAL ANALYZER AND MANUAL SOLUTIONS
EFFECT OF C.G. LOCATION ON RISING AND PITCHING MOTIONS OF HYDROFOIL SYSTEM

Figure VII-2

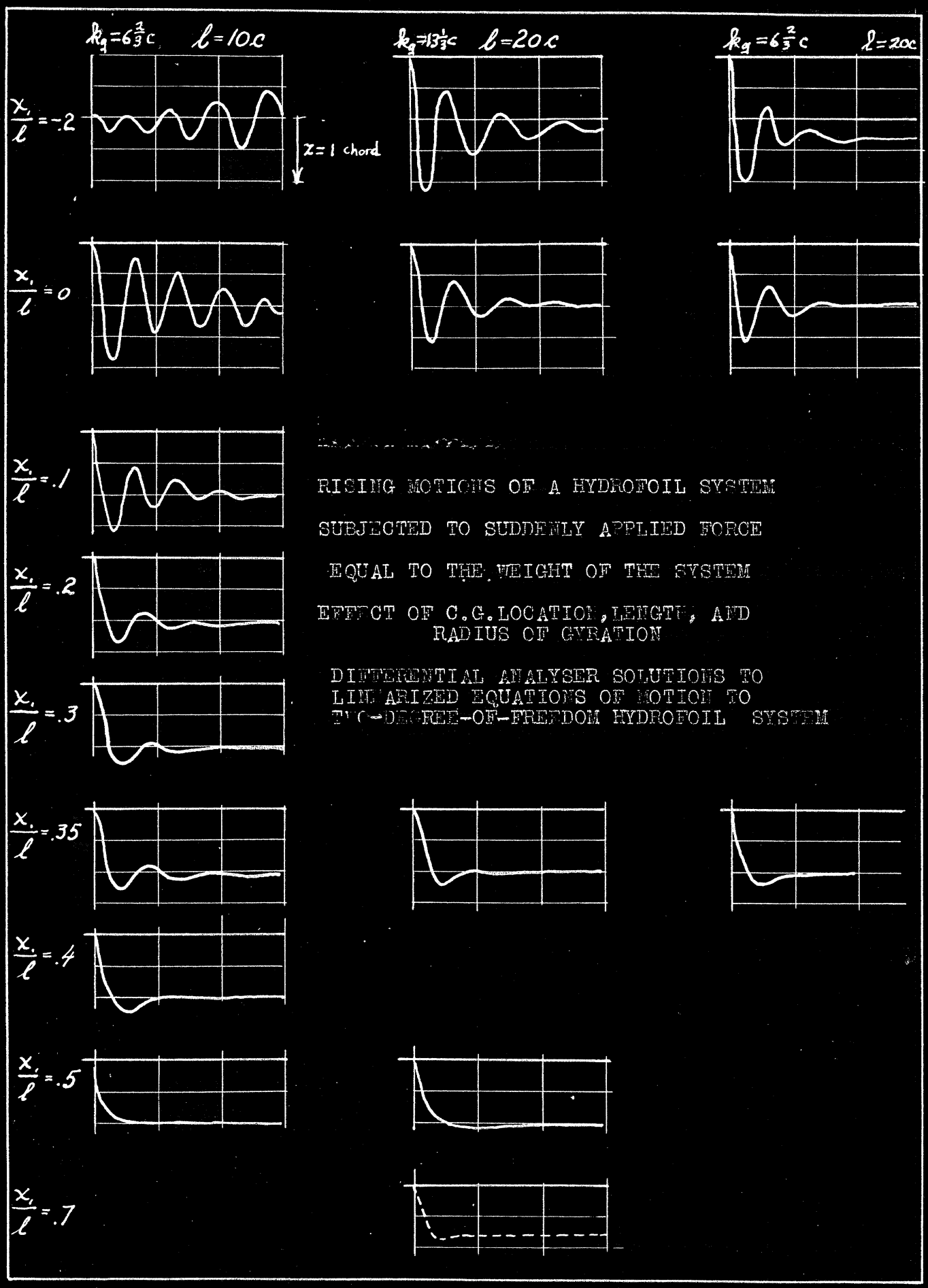

RISING MOTIONS OF A HYDROFOIL SYSTEM

SUBJECTED TO SUDDENLY APPLIED FORCE

EQUAL TO THE WEIGHT OF THE SYSTEM

EFFECT OF C.G. LOCATION, LENGTH, AND RADIUS OF GYRATION

DIFFERENTIAL ANALYSER SOLUTIONS TO LINEARIZED EQUATIONS OF MOTION TO TWO-DEGREE-OF-FREEDOM HYDROFOIL SYSTEM

FIGURE VII-3

TRANSIENT PERFORMANCE CHARACTERISTICS OF HYDROFOIL SYSTEM IN SMOOTH WATER

Differential Analyzer Solutions to non-linear Equations

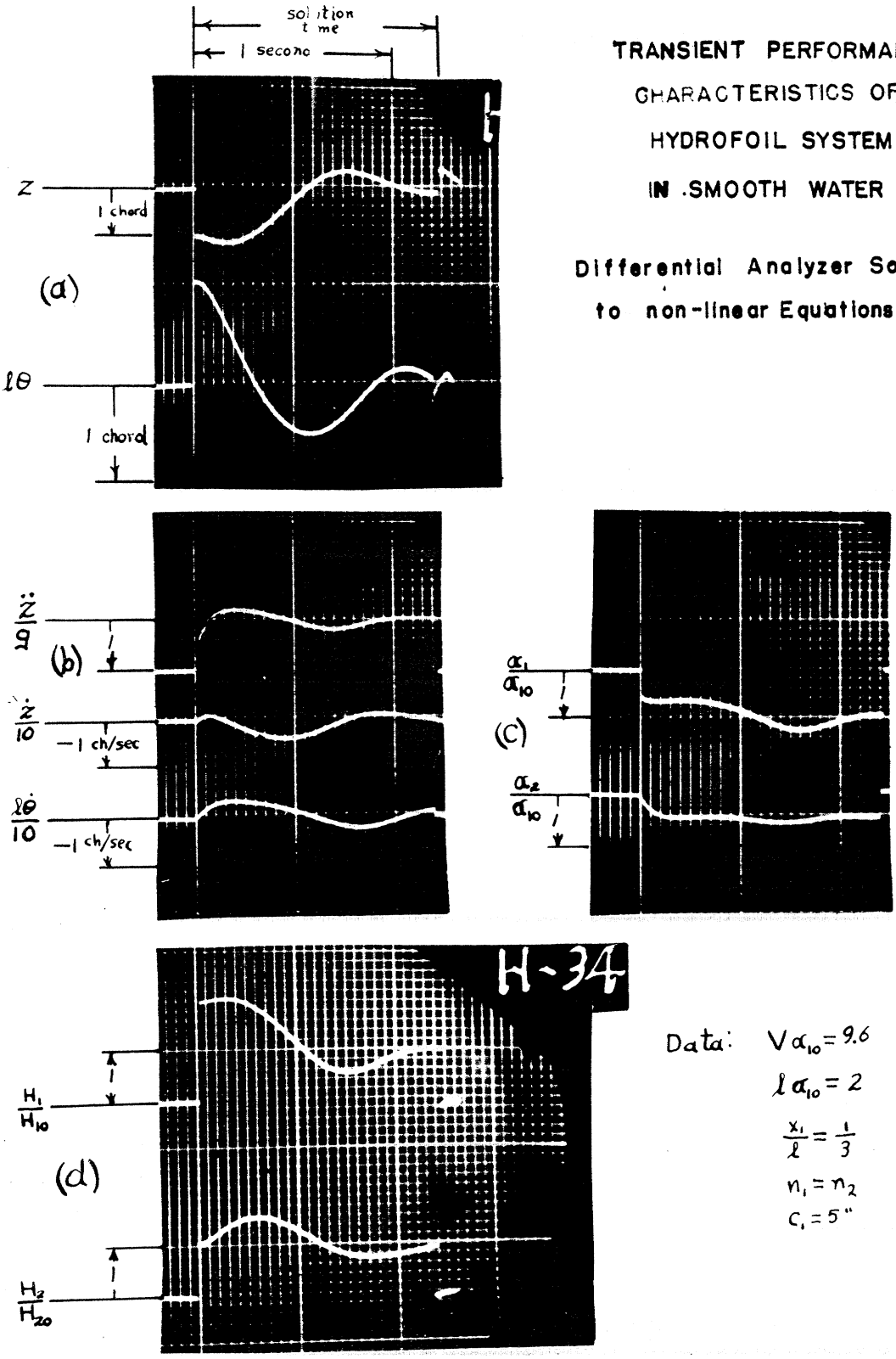

Data: $V\alpha_{10} = 9.6$

$l\alpha_{10} = 2$

$\frac{x_1}{l} = \frac{1}{3}$

$n_1 = n_2$

$c_1 = 5''$

FIGURE VII-4

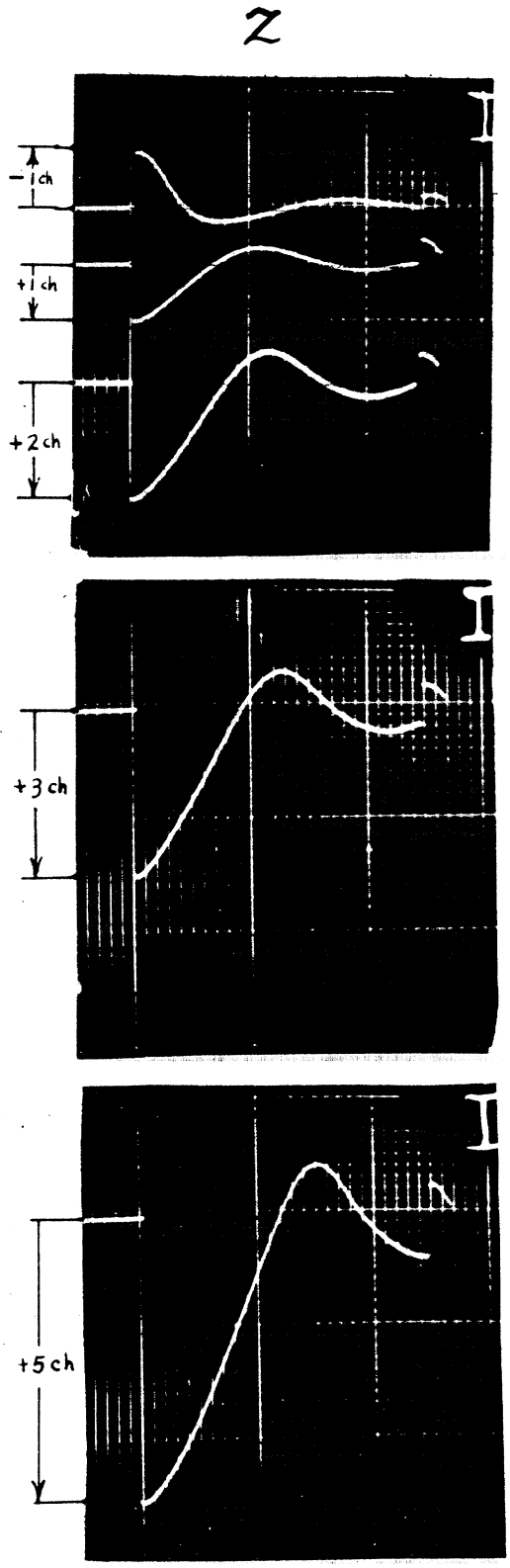

EFFECT OF AMPLITUDE ON MOTIONS OF NON-LINEAR HYDROFOIL SYSTEM

Differential Analyzer Solutions

Figure VII-5

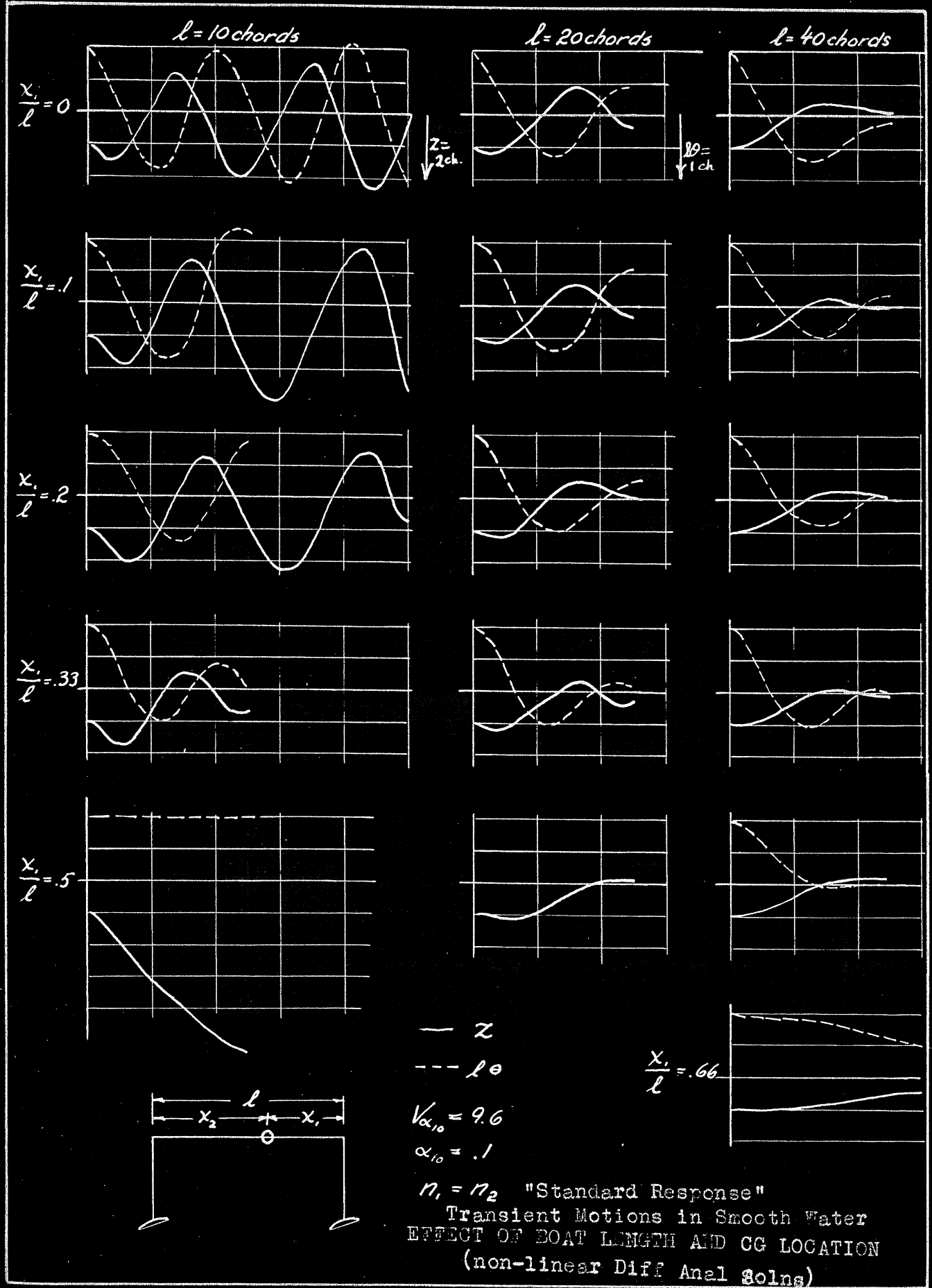
ℓ = 10 chords
ℓ = 20 chords
ℓ = 40 chords
x₁/ℓ = 0
x₁/ℓ = .1
x₁/ℓ = .2
x₁/ℓ = .33
x₁/ℓ = .5
x₁/ℓ = .66
z = 2ch.
lθ = 1ch
— z
--- lθ
Vα₁₀ = 9.6
α₁₀ = .1
n₁ = n₂ "Standard Response"
Transient Motions in Smooth Water
EFFECT OF BOAT LENGTH AND CG LOCATION
(non-linear Diff Anal Solns)
ℓ
x₂
x₁

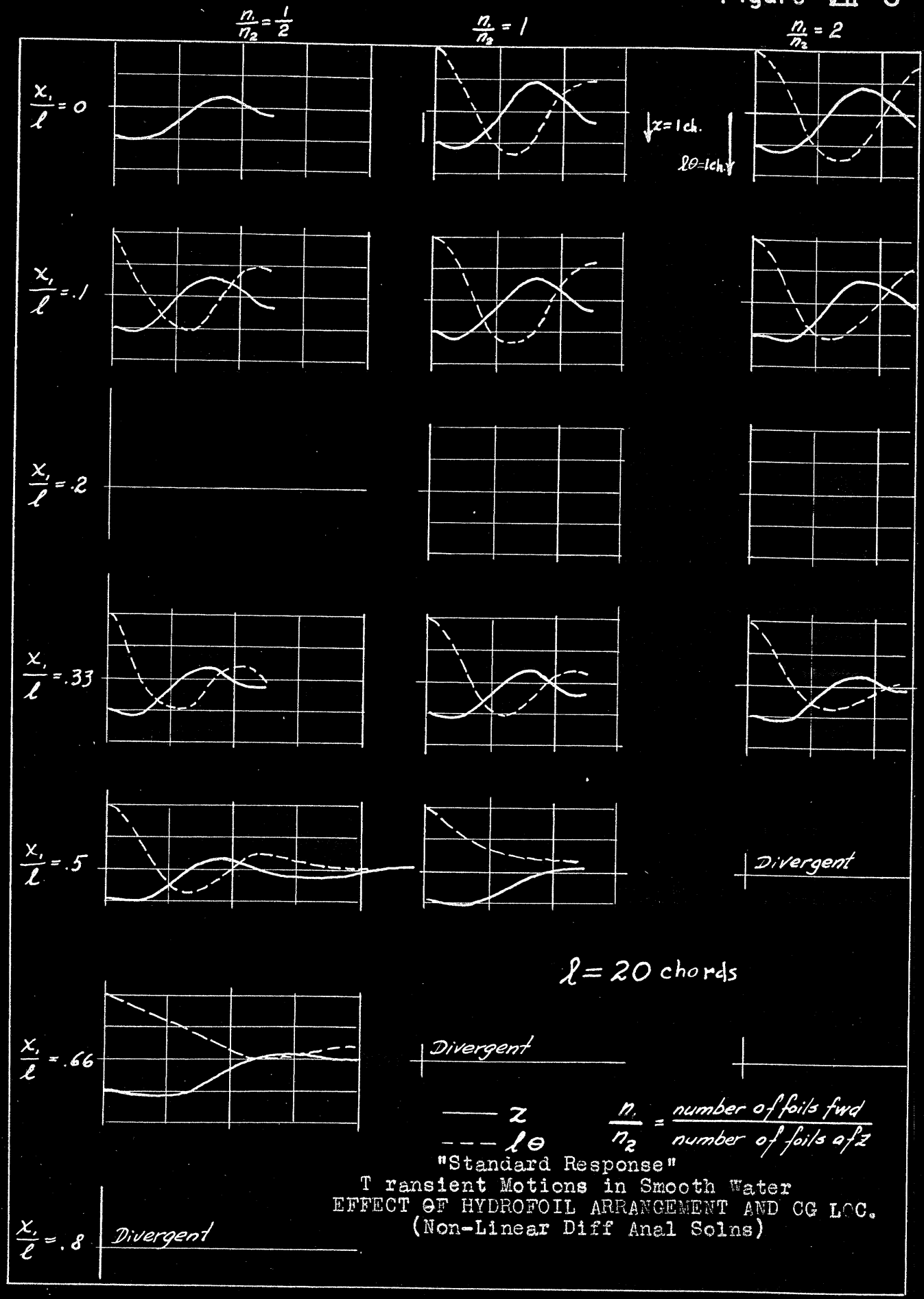

"Standard Response"
Transient Motions in Smooth Water
EFFECT OF HYDROFOIL ARRANGEMENT AND CG LOC.
(Non-Linear Diff Anal Solns)

Figure VII-7

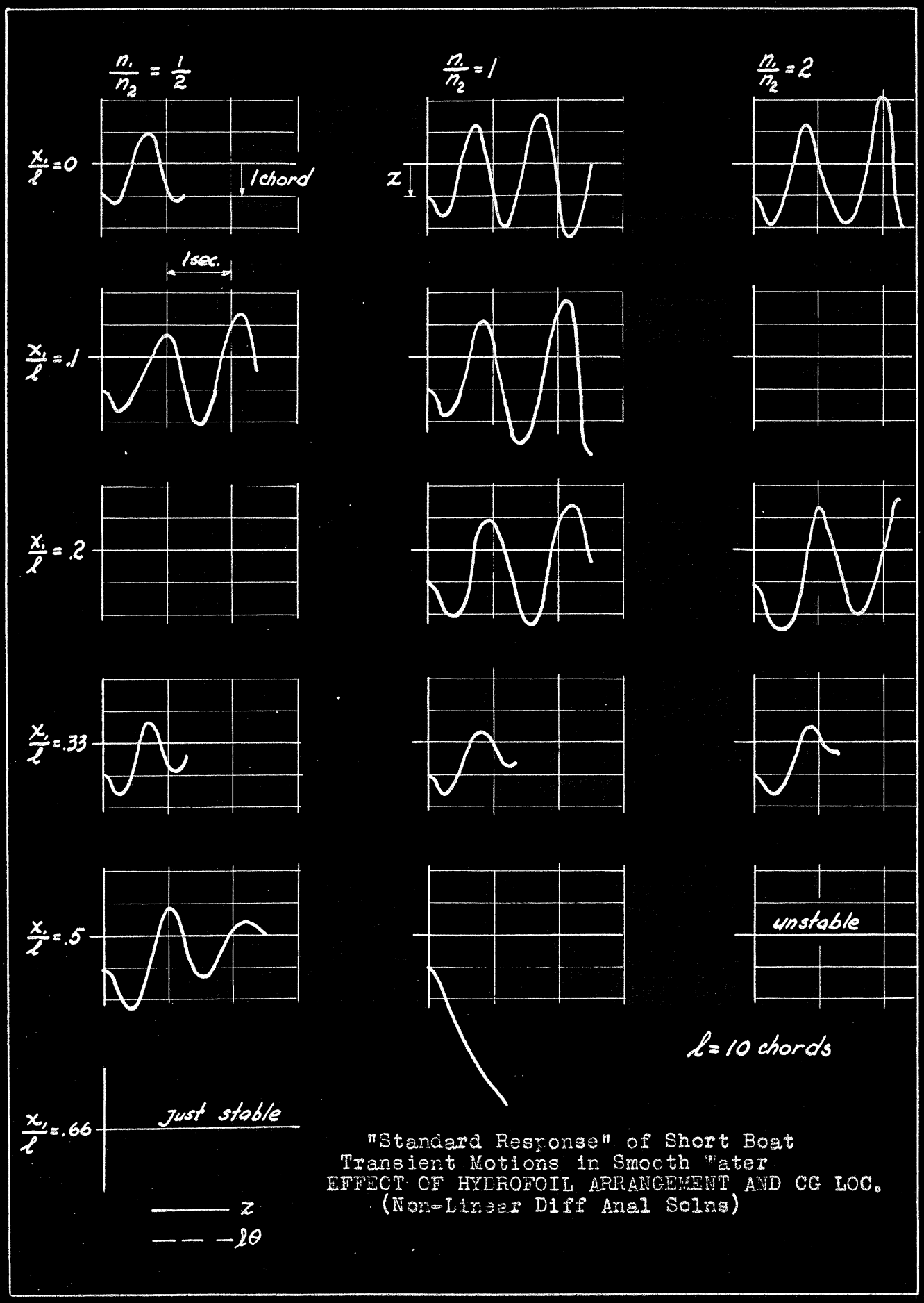

"Standard Response" of Short Boat
Transient Motions in Smooth Water
EFFECT OF HYDROFOIL ARRANGEMENT AND CG LOC.
(Non-Linear Diff Anal Solns)

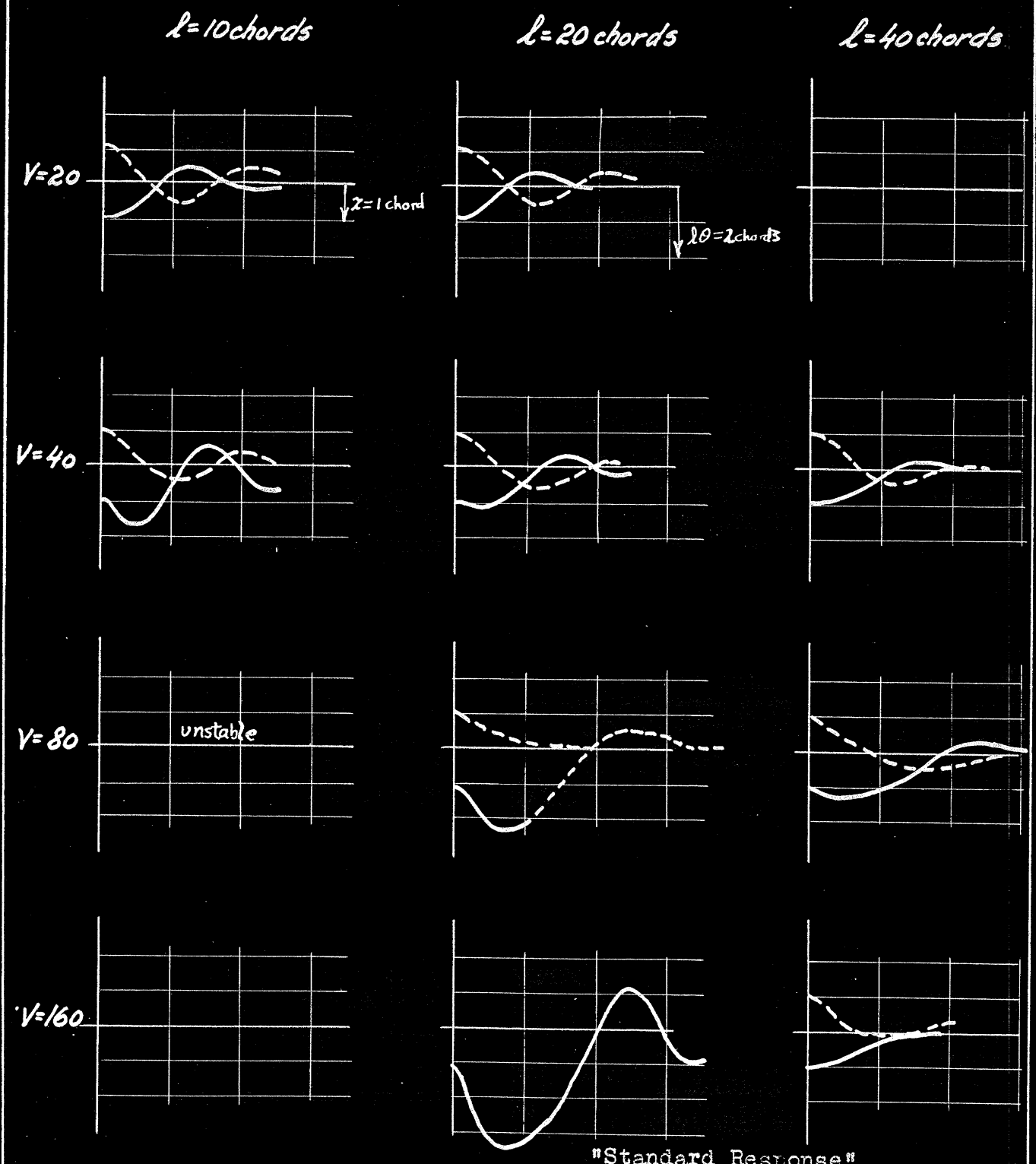

"Standard Response"
Transient Motions in Smooth Water

——— z

– – – lθ

$\Delta/S = 480\ ^{\#}/_{ft^2}$

IMPORTANT EFFECTS OF SPEED AND BOAT LENGTH ON STABILITY

(Non-Linear Diff Anal Sols)

Figure VII-9

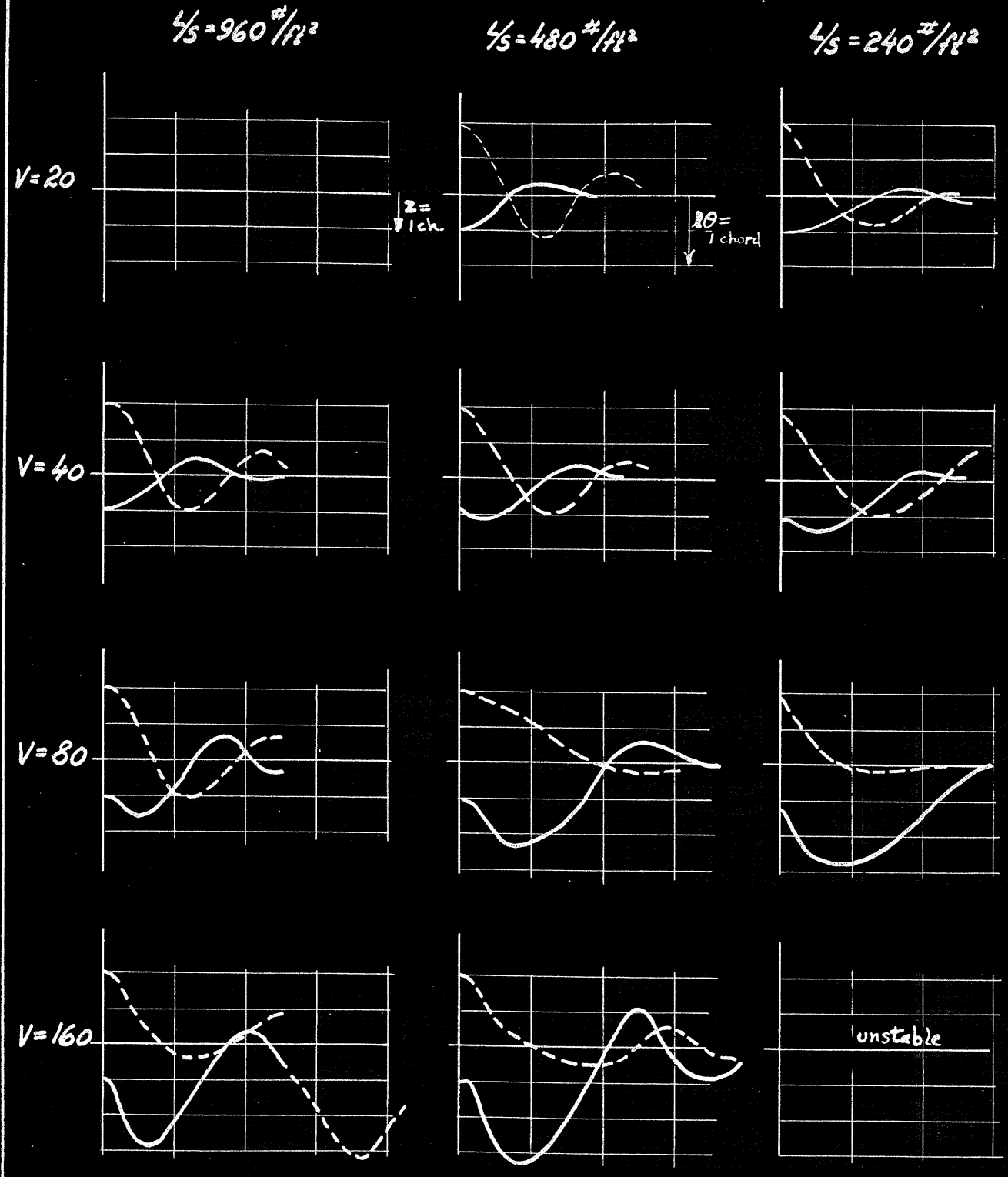

$\frac{x_1}{l} = .33$

$l = 20$ chords

$n_1 = n_2$

"Standard Response"
Transient Motions In Smooth Water
EFFECTS OF SPEED AND
LOADING PER UNIT AREA

(Non-Linear Diff Anal Solns)

Figure VII-10

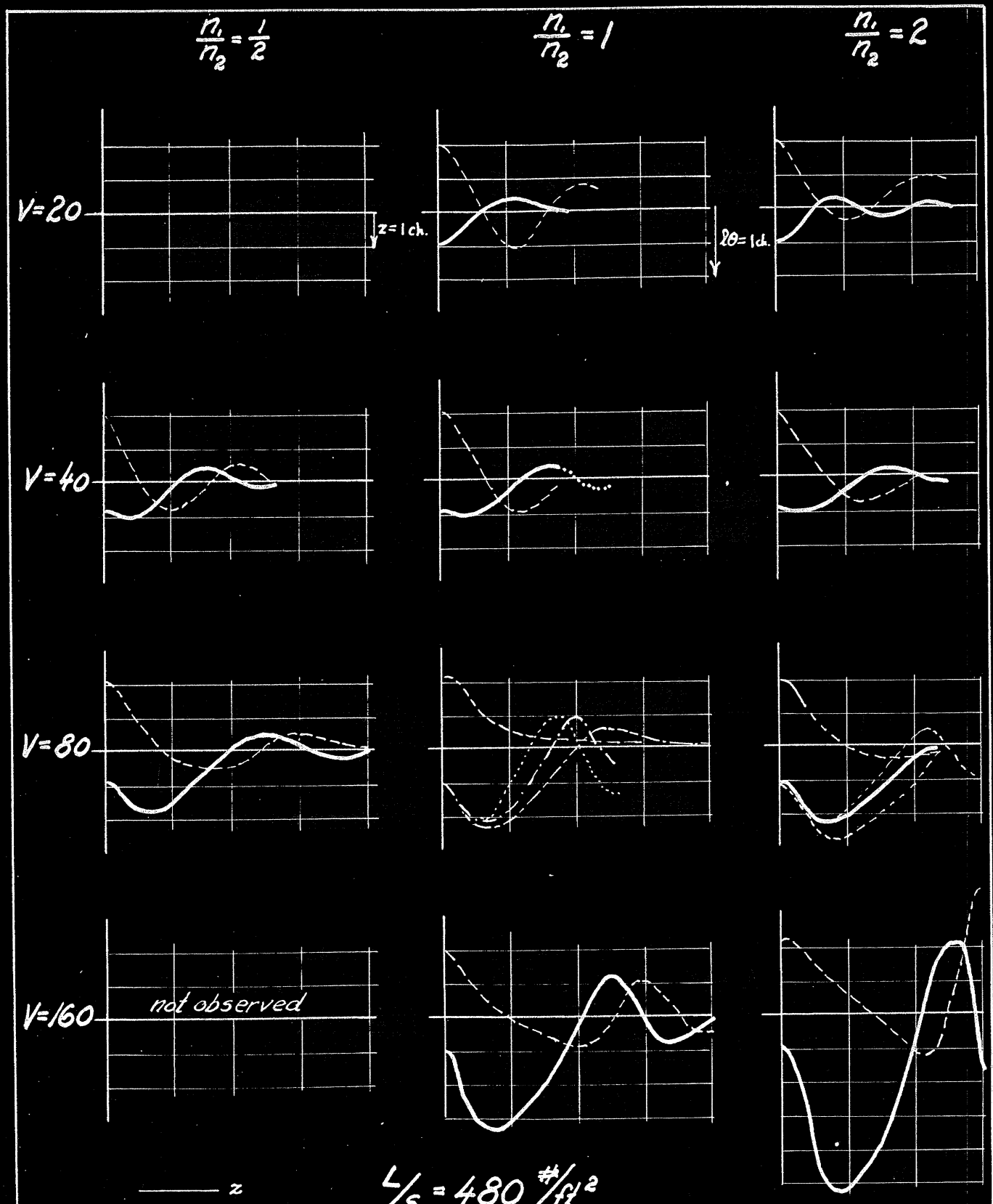

EFFECTS OF SPEED AND HYDROFOIL ARRANGEMENT
(Non- Linear Diff Anal Solns)

Figure VII-11

$V\alpha_{10} = 4.8$

$l\alpha_{10} = 1$

$N = 2$

Transient Motions in Waves
EFFECT OF INITIAL DEPTH OF ENTERING WAVE
ON ALL PERFORMANCE CHARACTERISTICS
(non-linear diff anal solns)

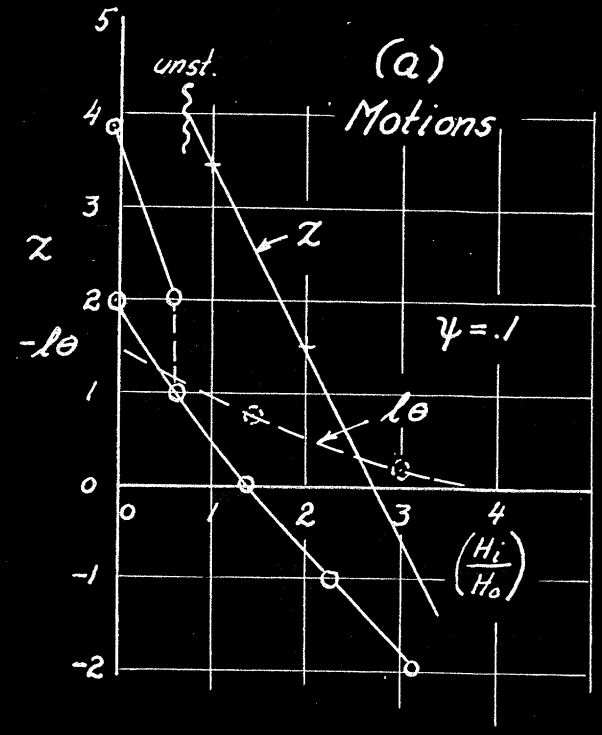

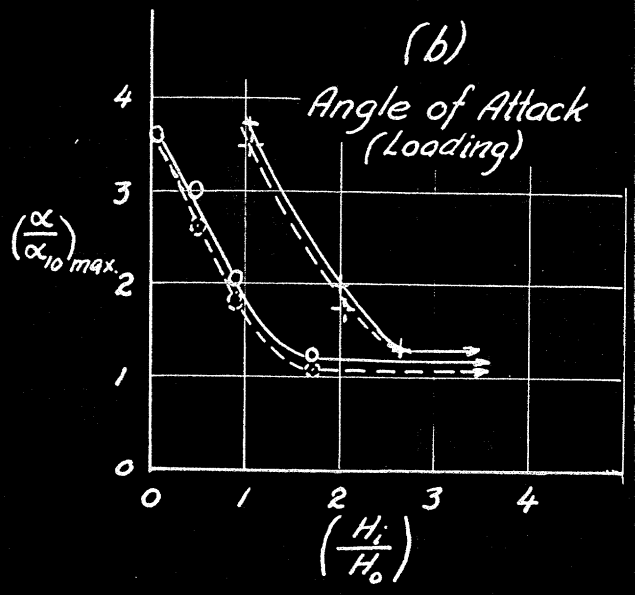

$\odot \frac{b}{H} = 1$

$+ \frac{b}{H} = 2$

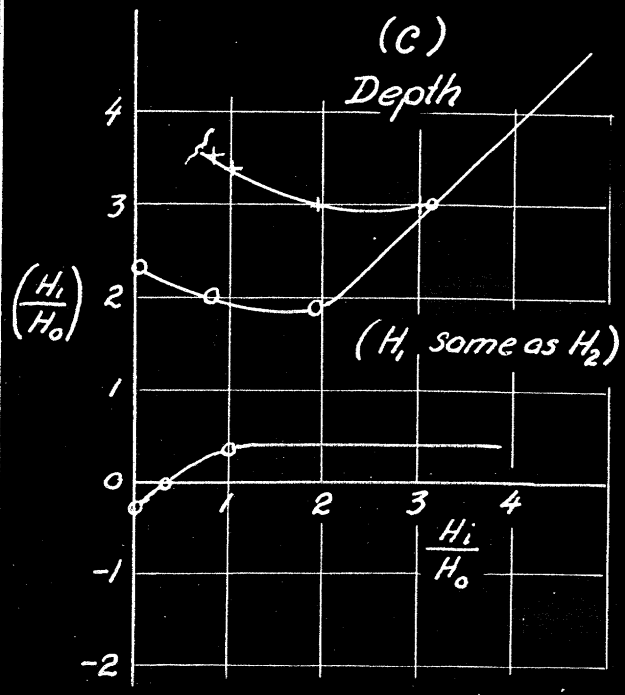

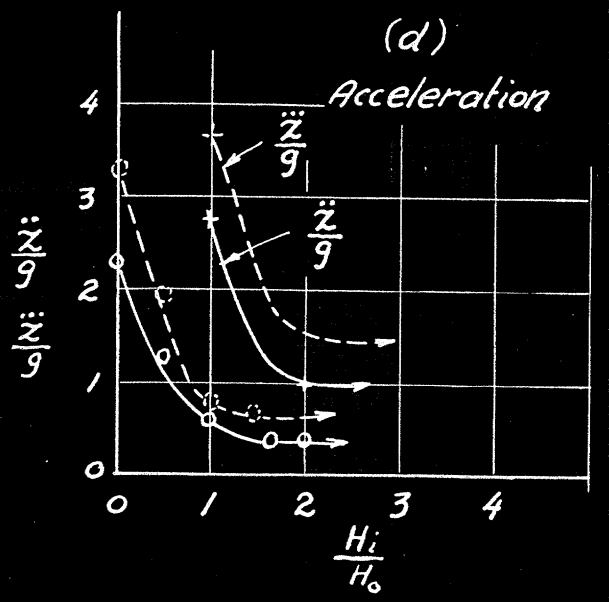

Figure VII - 12

$V\alpha_{10} = 9.6$

$l\alpha_{10} = 1$, $\frac{n_1}{n_2} = 2$

$\frac{x_1}{l} = \frac{1}{3}$

$N = 4$ Transient Motions in Waves
EFFECT OF WAVE HEIGHT ON ALL PERF CHAR IF FOILS ALWAYS ENTER WAVES AT TROUGH LEVEL
(non-linear diff anal solns)

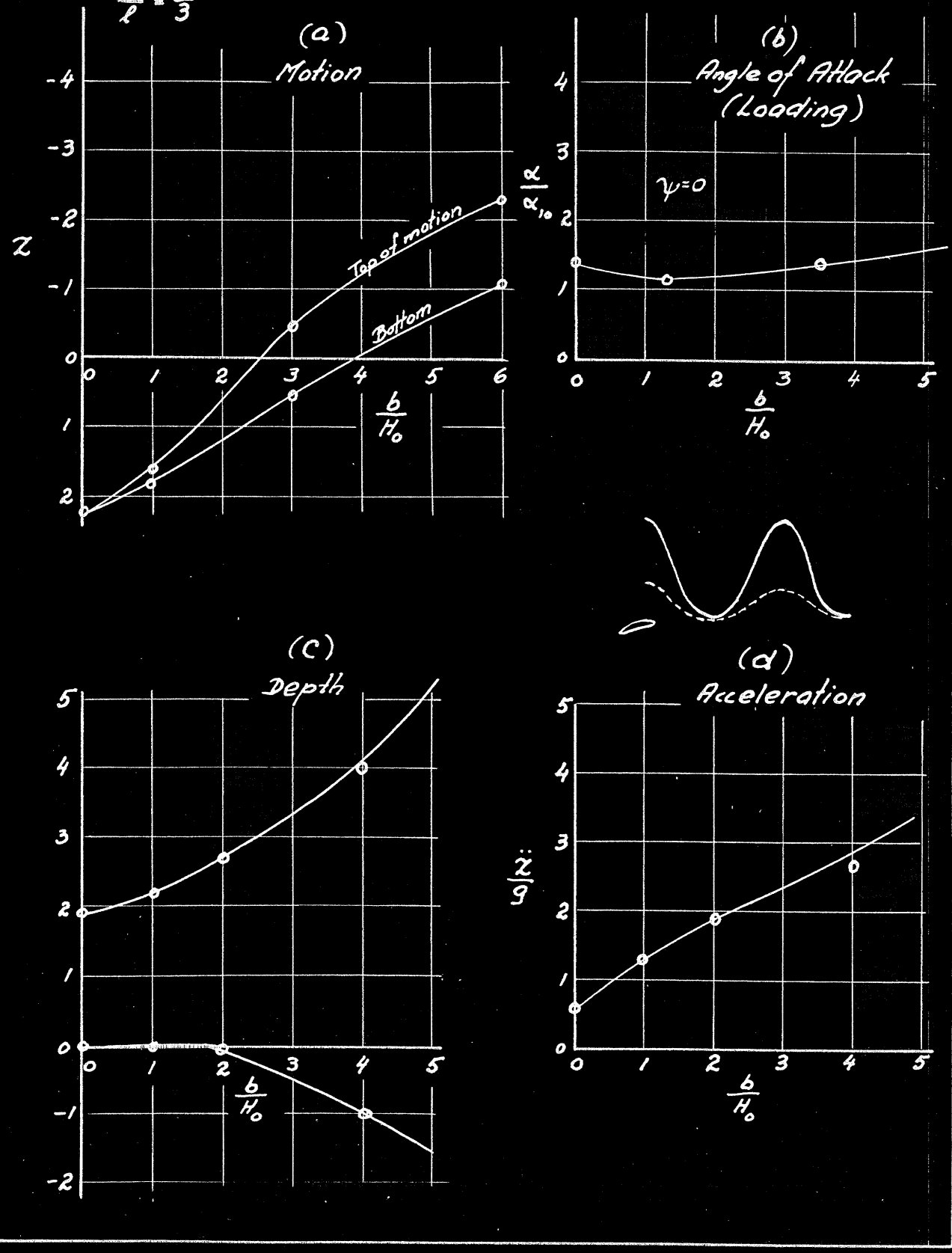

Figure VII-13

Transient Motions in Waves
EFFECT OF WAVE HEIGHT ON ALL PERF CHAR
WHEN FOILS ALWAYS ENTER WAVES
ONE CHORD BELOW WAVE CREST
(non-linear diff anal solns)

$l\alpha_{10} = 2$ $\quad N = 2$

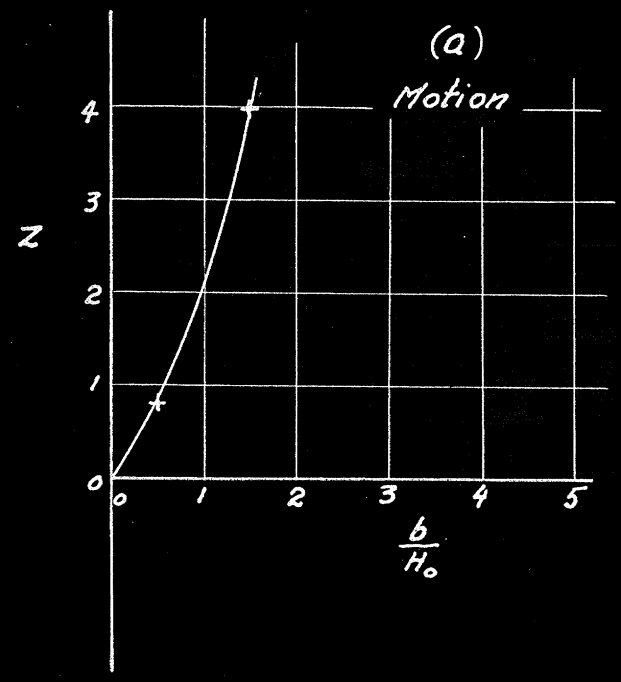

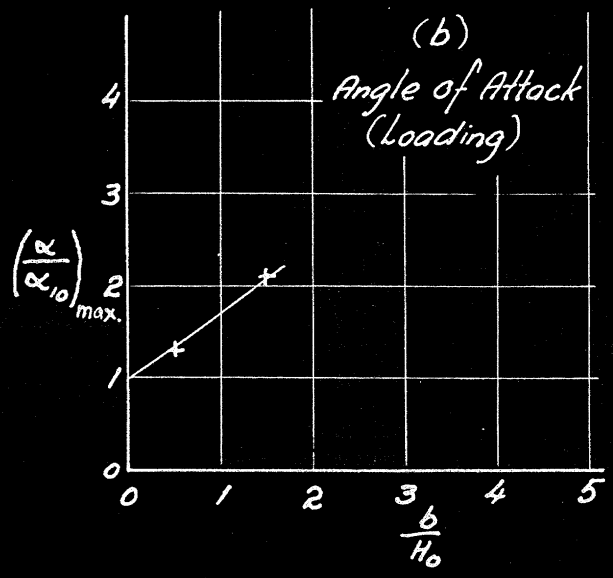

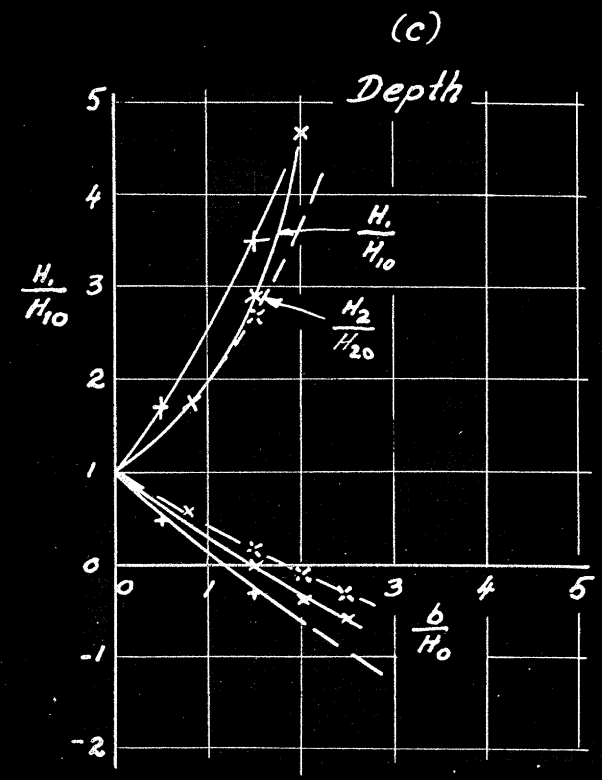

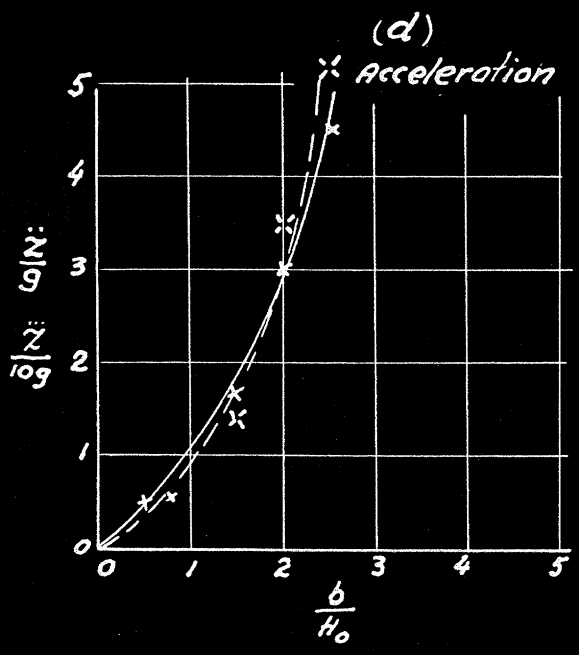

Figure VII-14

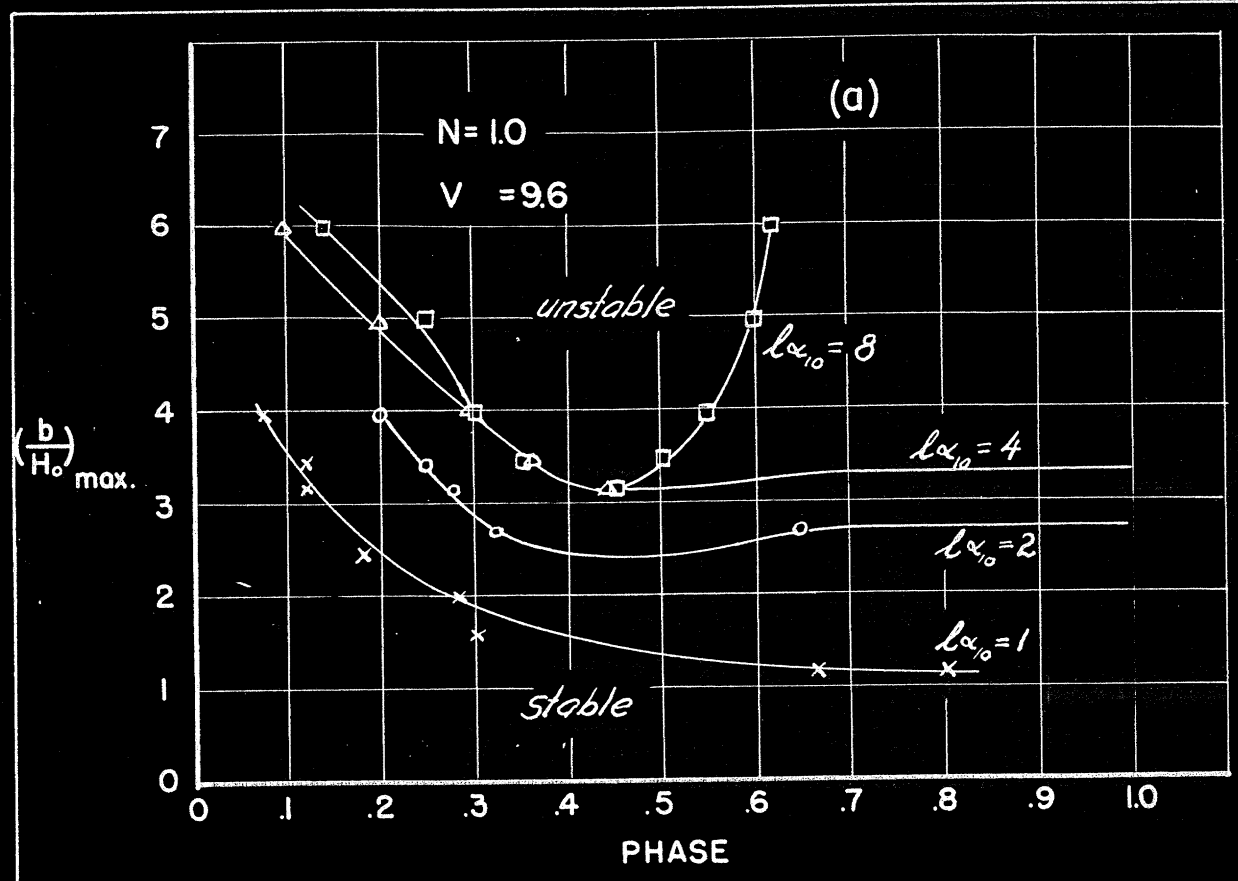

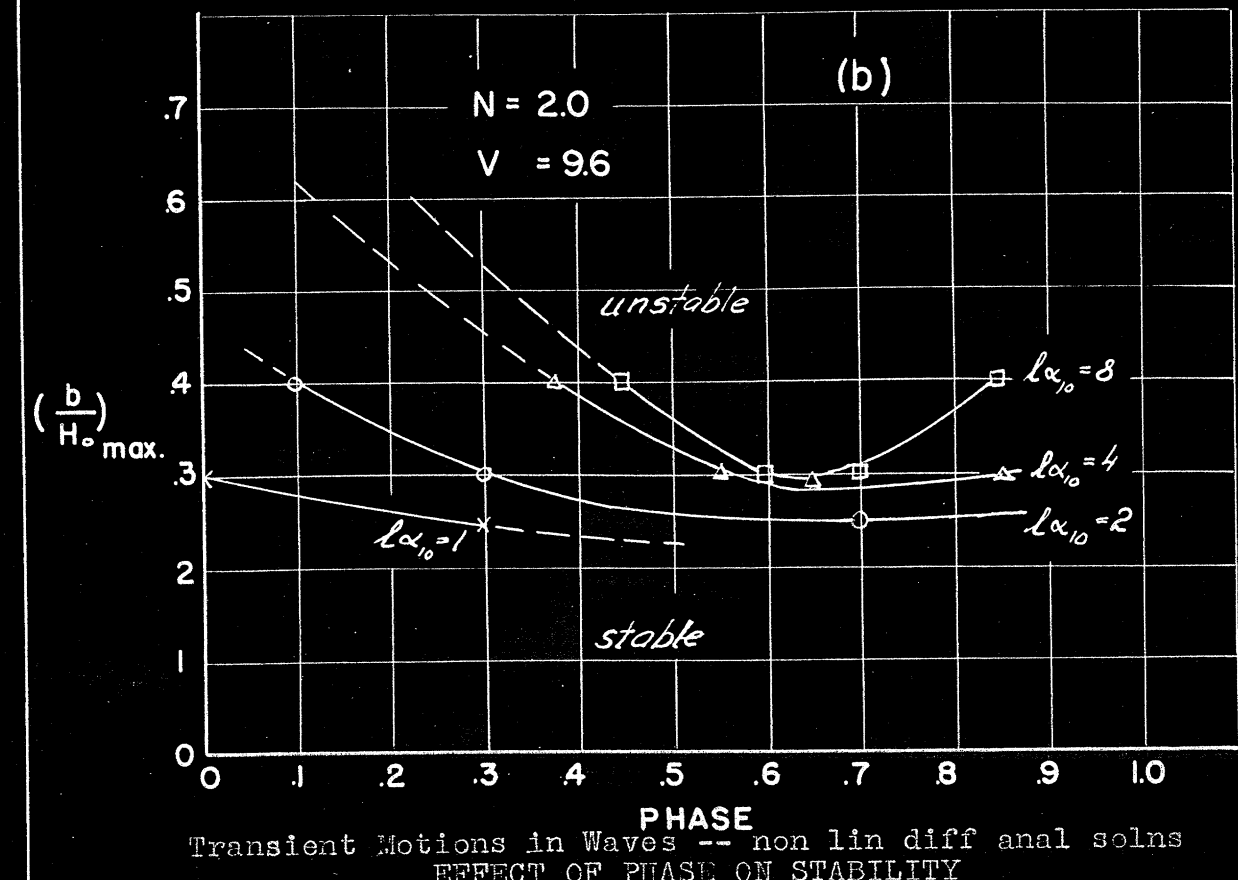

Transient Motions in Waves -- non lin diff anal solns
EFFECT OF PHASE ON STABILITY

Figure VII-15

Transient Motions in Waves -- non-lin diff anal solns

EFFECT OF PHASE ON STABILITY OF MOTION

FOR FOUR LENGTHS AND TWO SPEEDS

(a)

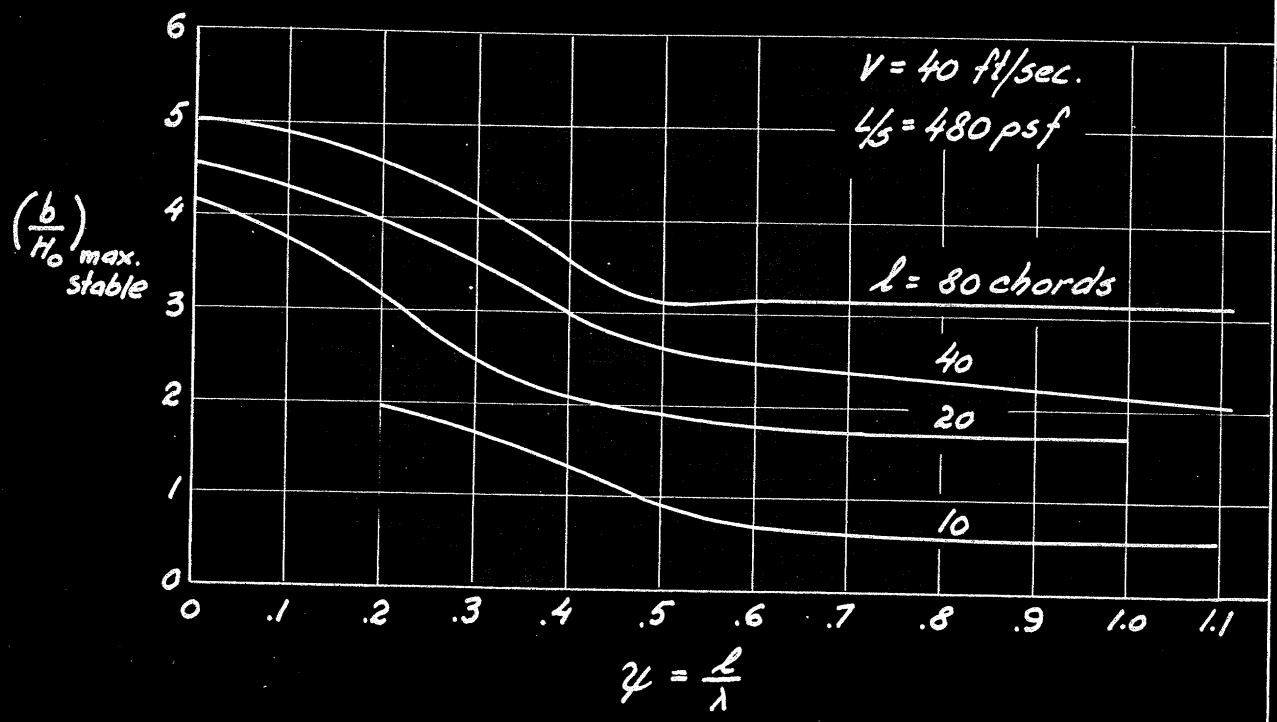

(b)

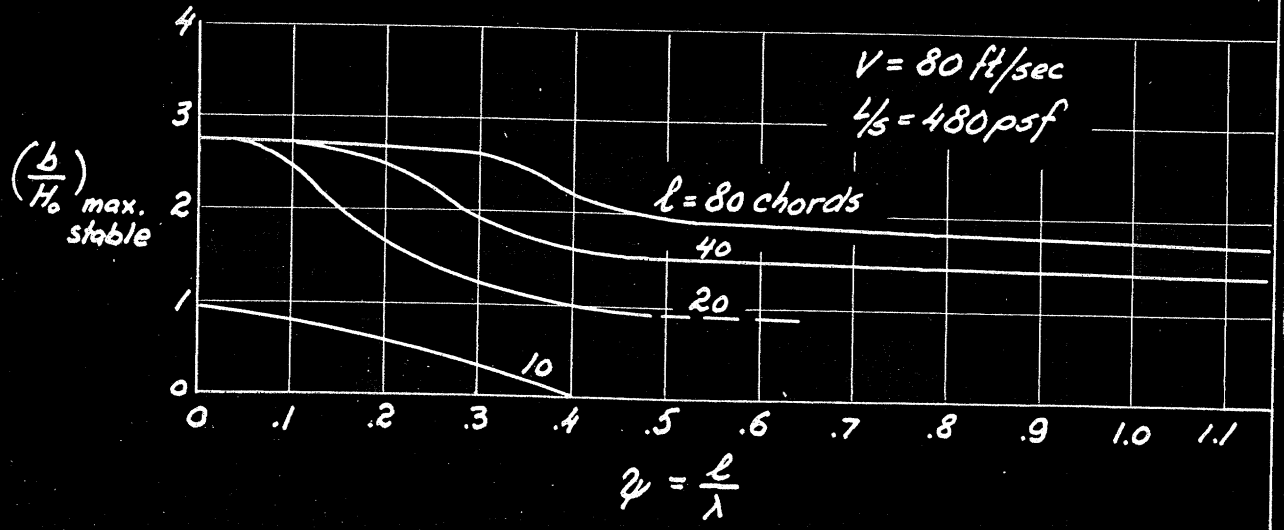

Figure VII-16-17

Transient Motions in Waves -- non lin diff anal solns
PHASE,
COMBINED EFFECTS OF LOADING PER UNIT AREA, AND SPEED
ON STABILITY OF MOTION

VII - 16

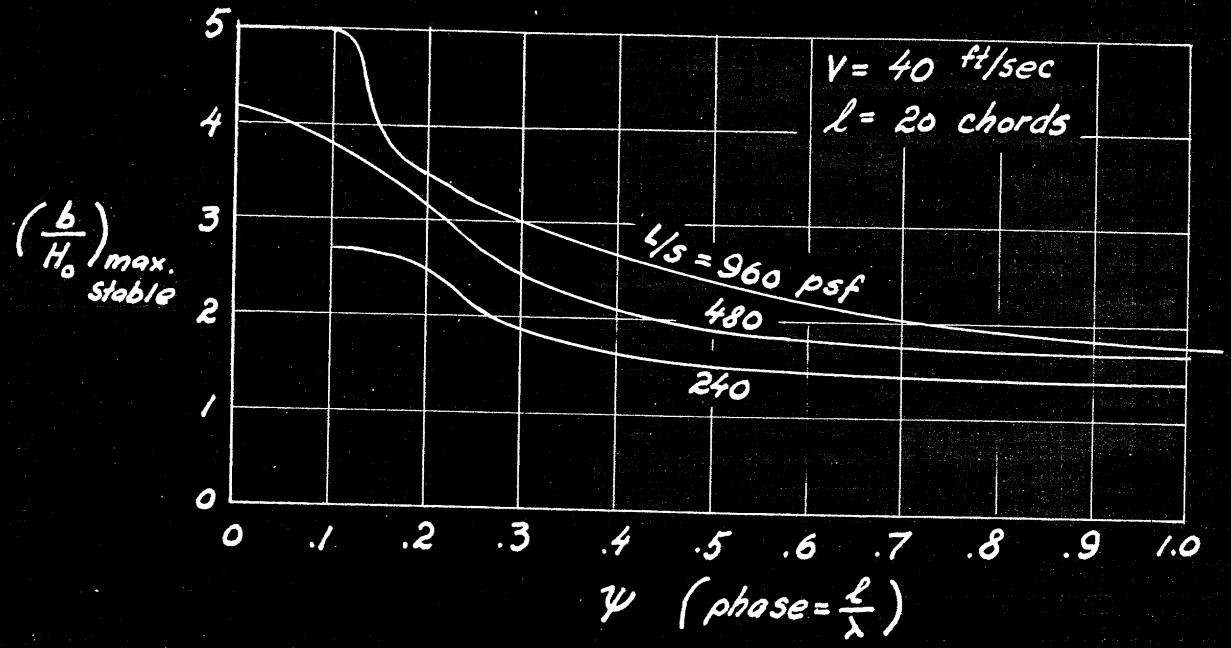

VII - 17

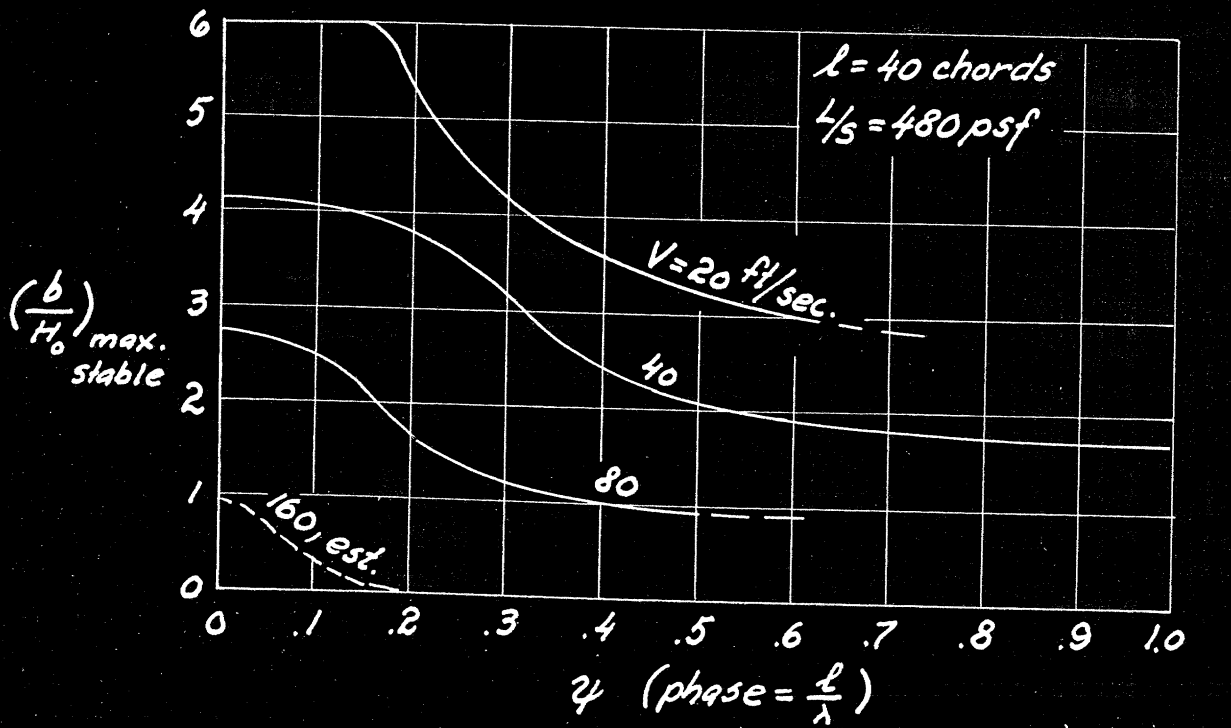

Figure VII-18

Transient Motions in Waves -- non-lin diff anal solns

EFFECT OF PHASE ON AMPLITUDE OF RISING MOTIONS

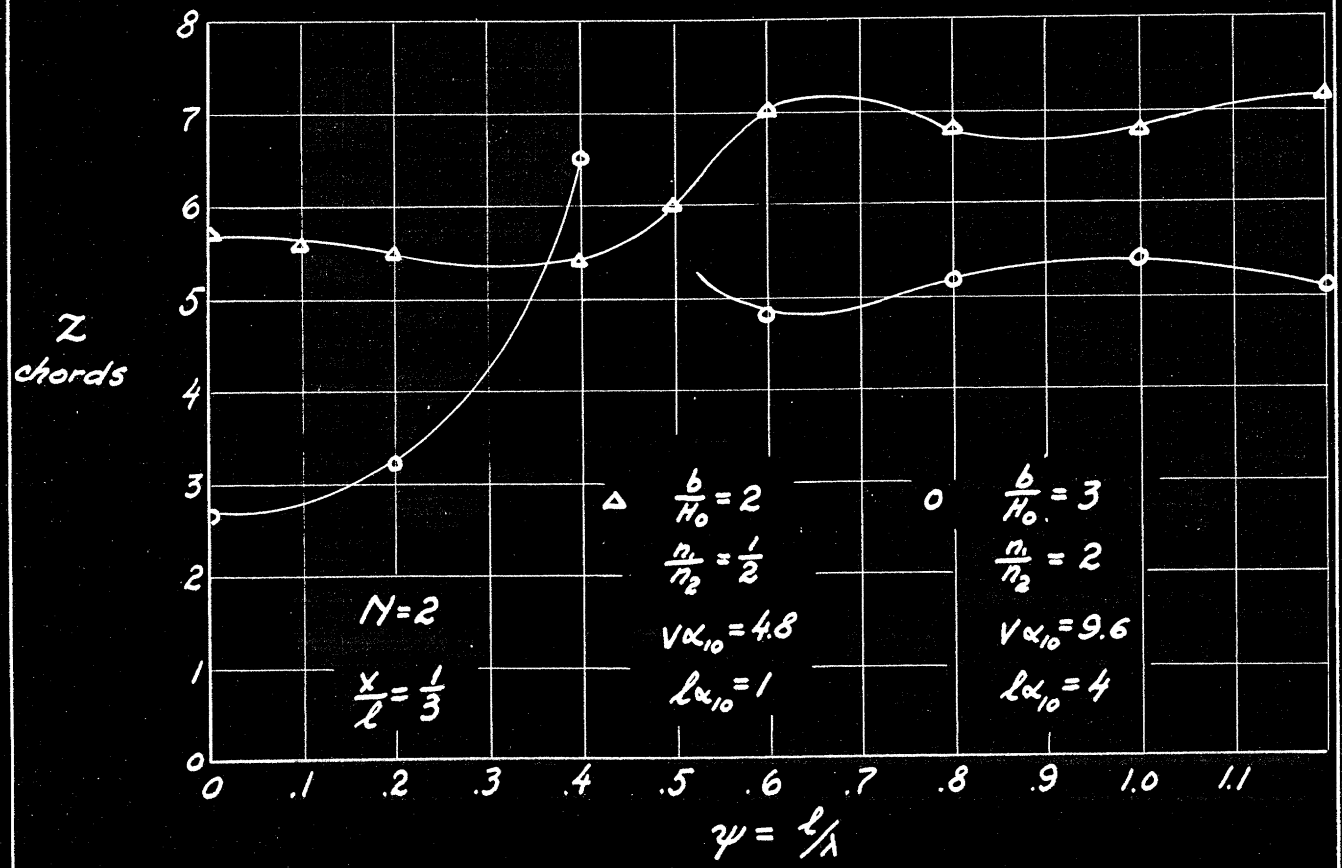

Figure VII - 19-22

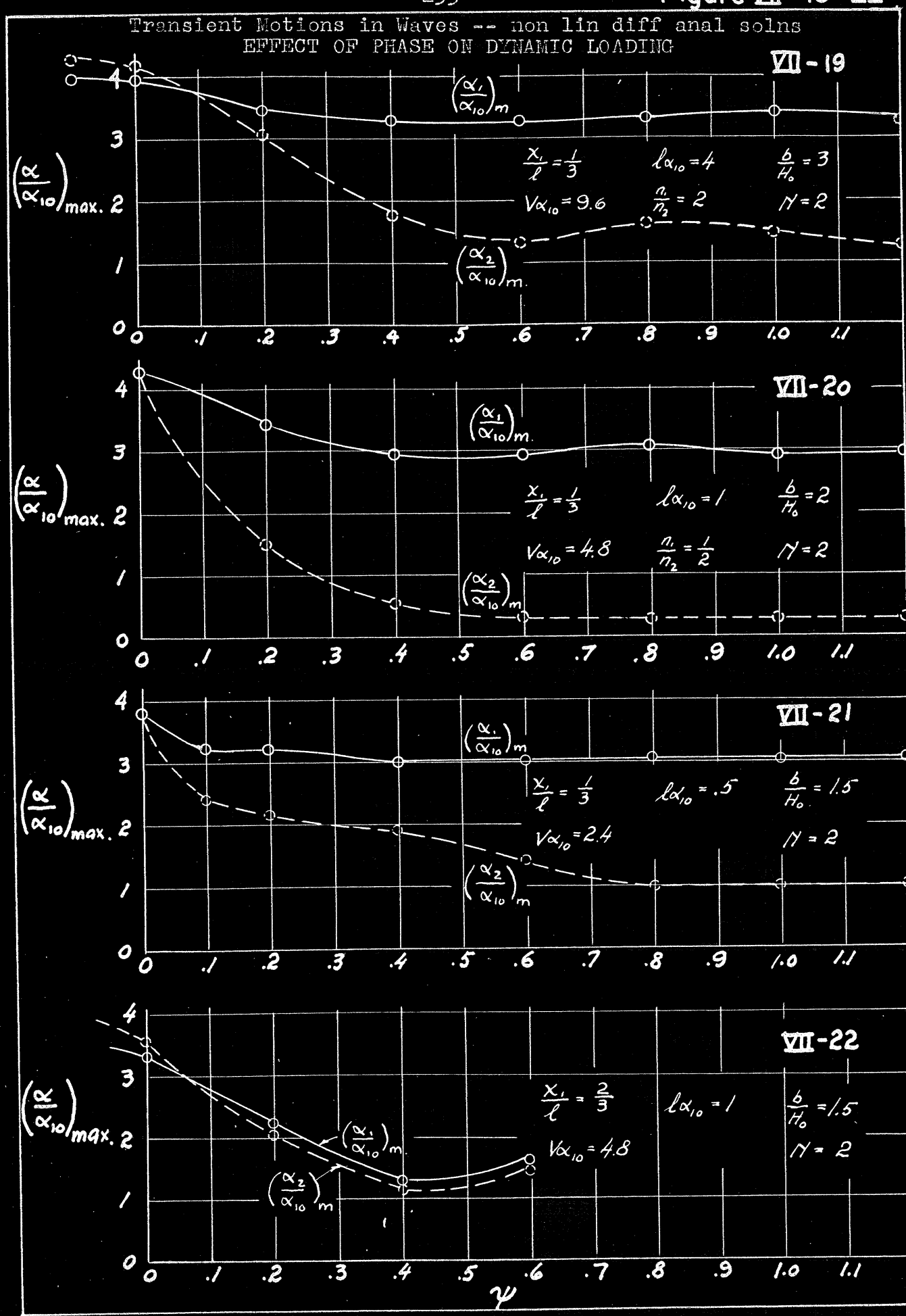

Figure VII-23

Transient Motions in Waves -- non-lin diff anal solns

EFFECT OF PHASE ON ACCELERATION

FOR

FOUR REPRESENTATIVE SETS OF CONDITIONS

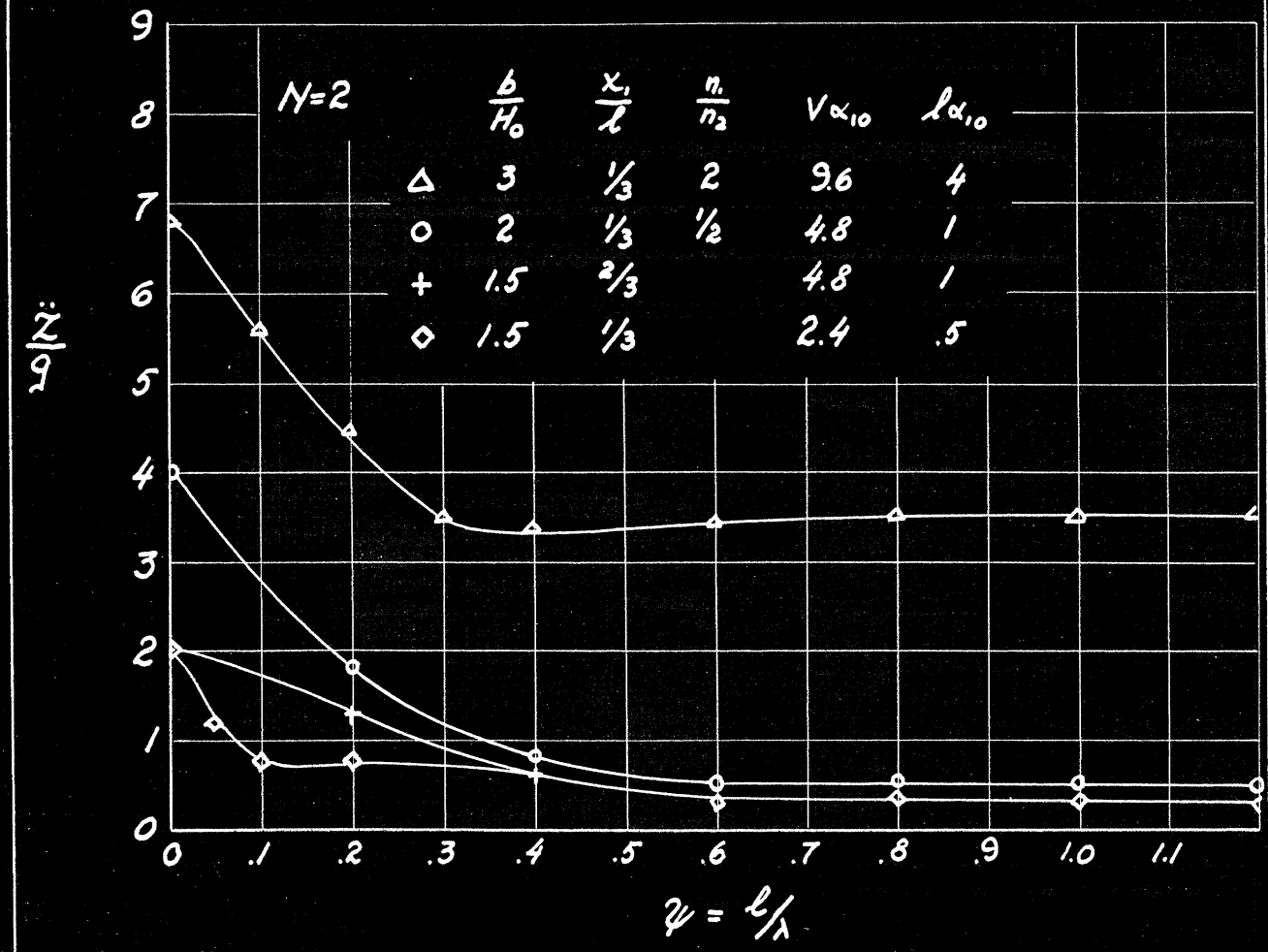

Figure VII-24

Transient Motions in Waves -- non-lin diff anal solns
SUMMARY OF DIFFERENTIAL ANALYZER CALCULATIONS OF
THE EFFECT OF FREQUENCY OF WAVE ENCOUNTER
ON STABILITY OF MOTION

Numbers within symbols are equal to $l\alpha_{10}$

All calculations on this graph were performed with a single diff anal setup, so precision of comparison should be high.

□ $V\alpha_{10} = 19.2$
△ $V\alpha_{10} = 9.6$
○ $V\alpha_{10} = 4.8$
◇ $V\alpha_{10} = 2.4$

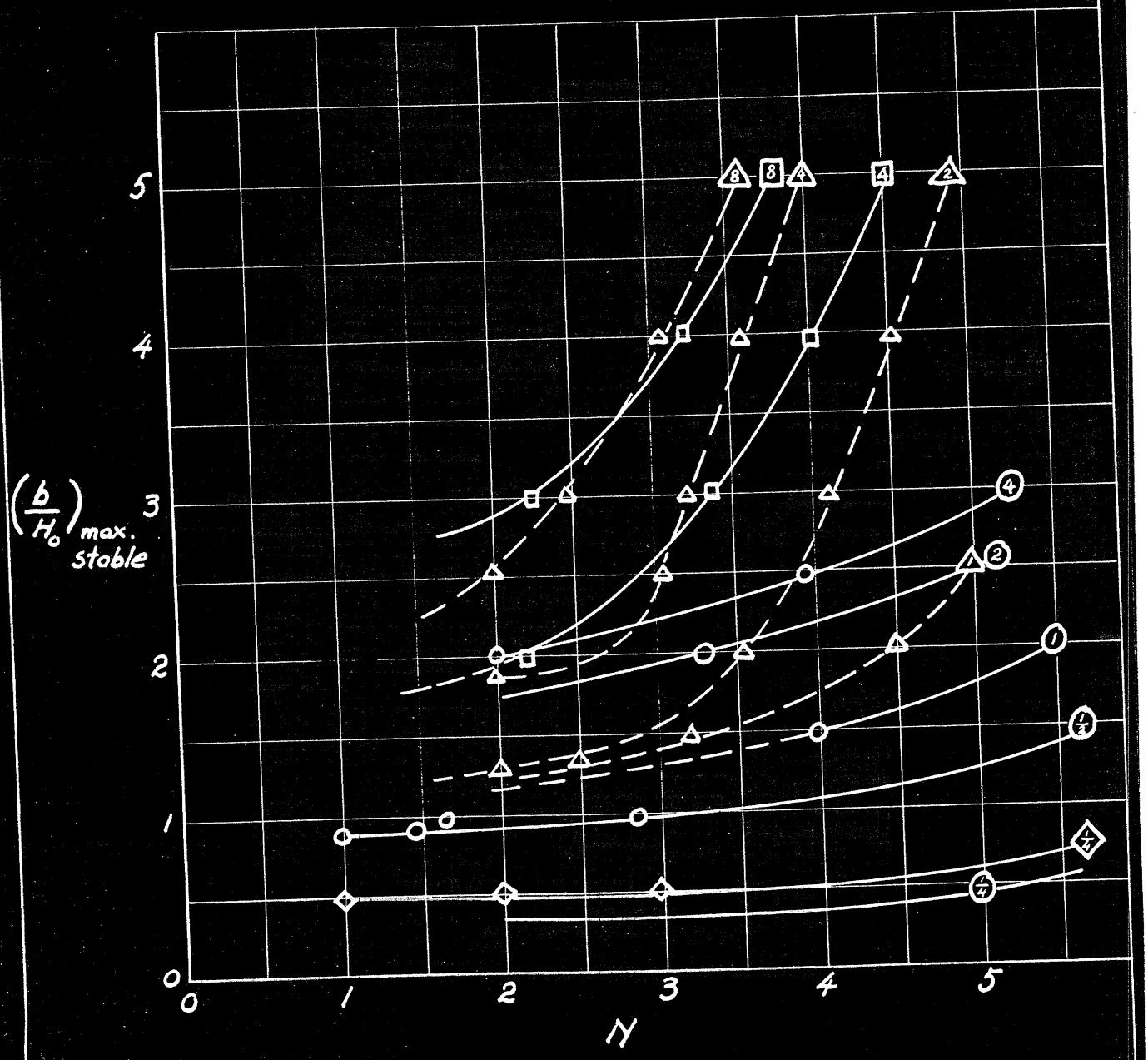

Figure VII-25,26

Transient Motions in Waves -- non-lin diff anal solns
EFFECT OF FREQUENCY OF ENCOUNTER ON DYNAMIC LOADING
(ANGLE OF ATTACK) FOR ZERO PHASE

VII-25

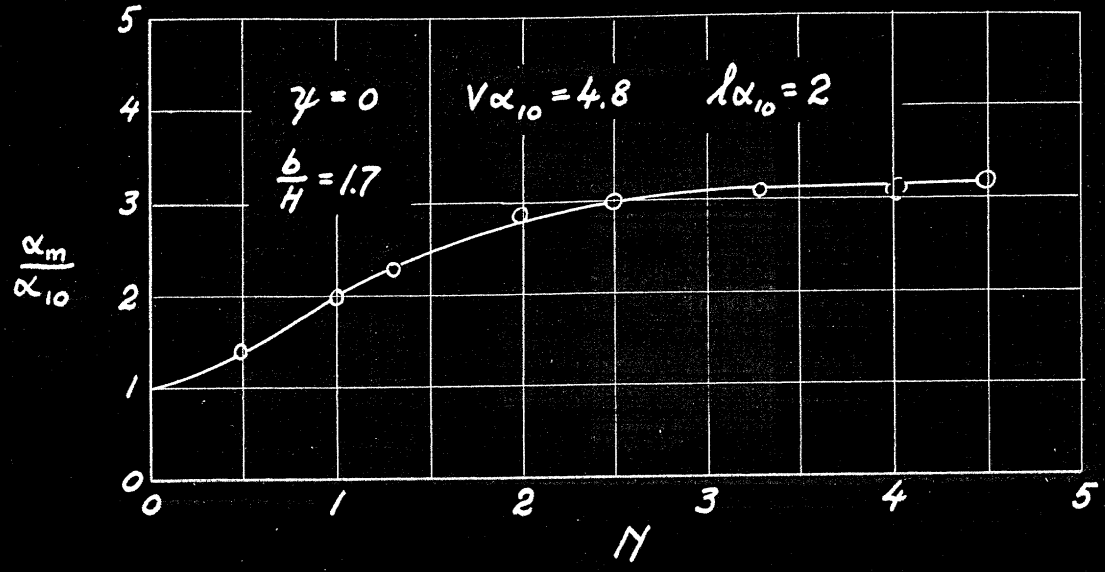

EFFECT OF WAVE HEIGHT ON DYNAMIC LOADING
(MEASURED BY MEASURING ANGLE OF ATTACK)
FOR ZERO PHASE

VII-26

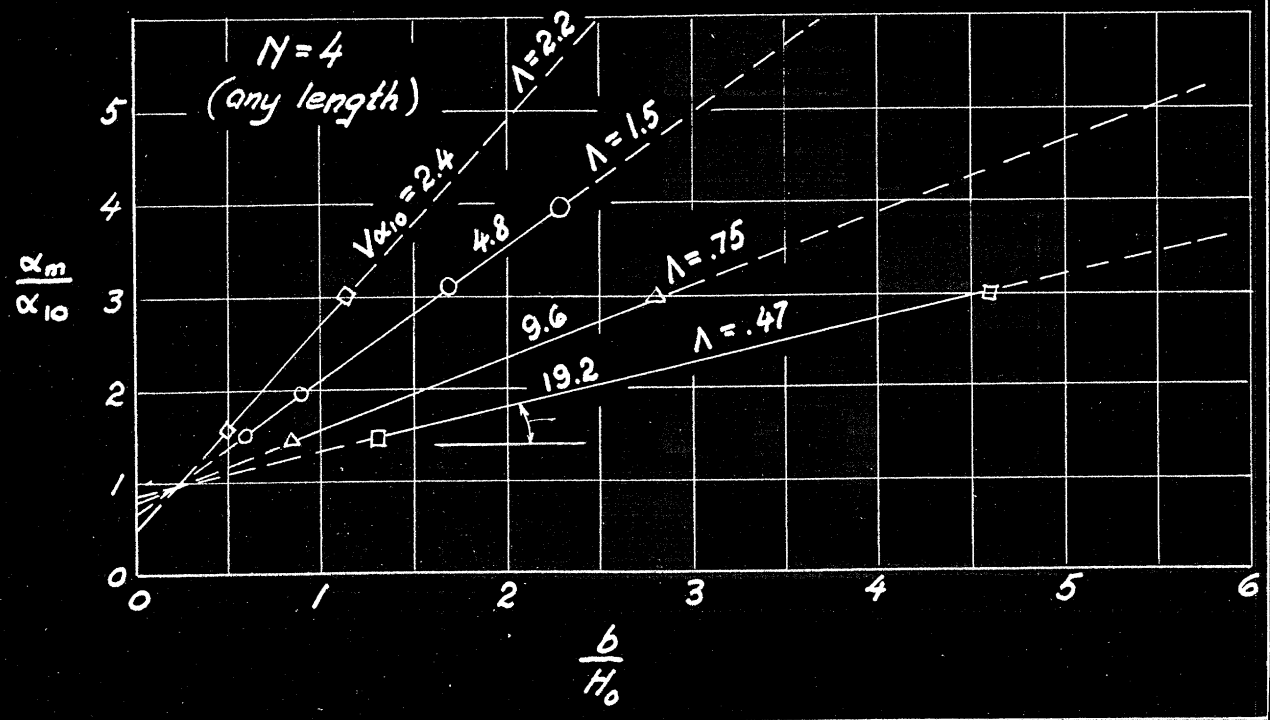

Figure VII - 27, 28

Transient Motions in Waves -- non-lin diff. anal solns
EFFECT OF FREQUENCY OF WAVE ENCOUNTER ON
DYNAMIC LOADING
EXTRAPOLATED FROM FIGURES VII 25 AND VII 26

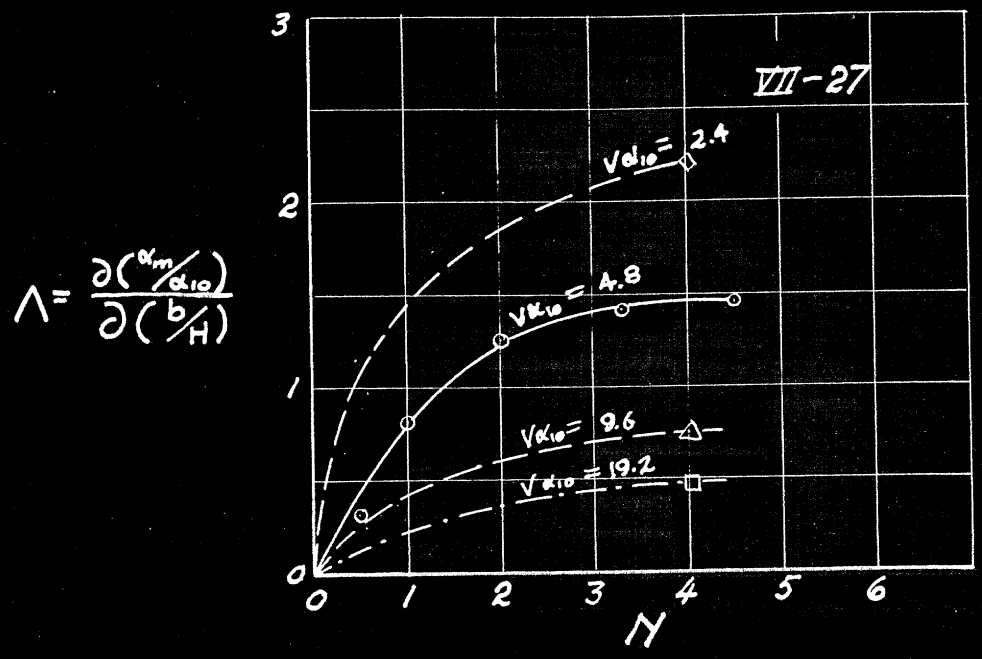

EFFECT OF SPEED ON DYNAMIC LOADING

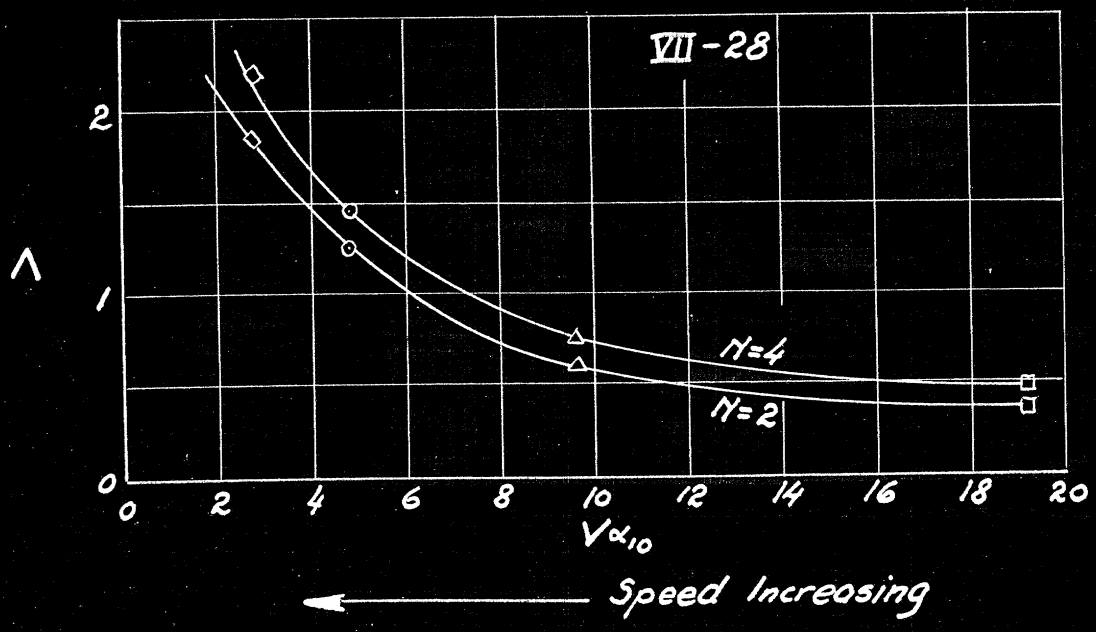

Figure VII- 29, 30

Transient Motions in Waves -- non-lin diff anal solns
EFFECT OF FREQUENCY OF ENCOUNTER ON DYNAMIC LOADING

VII-29

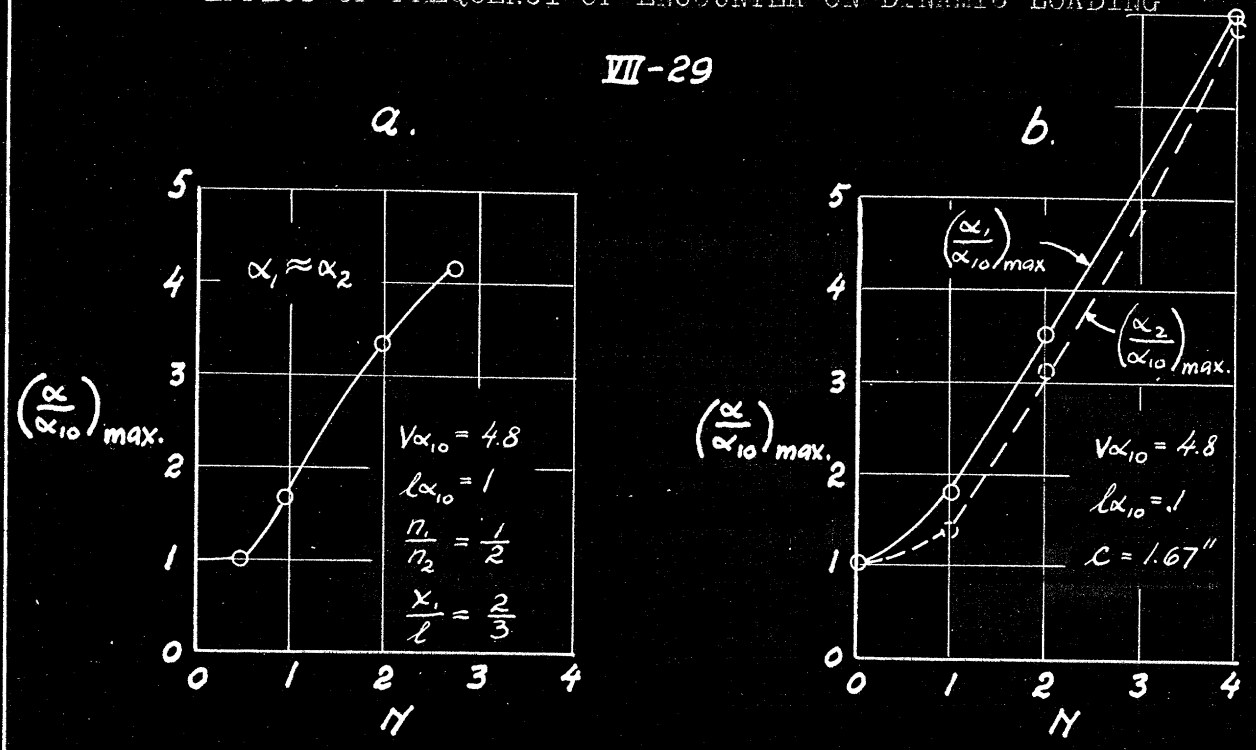

VII-30

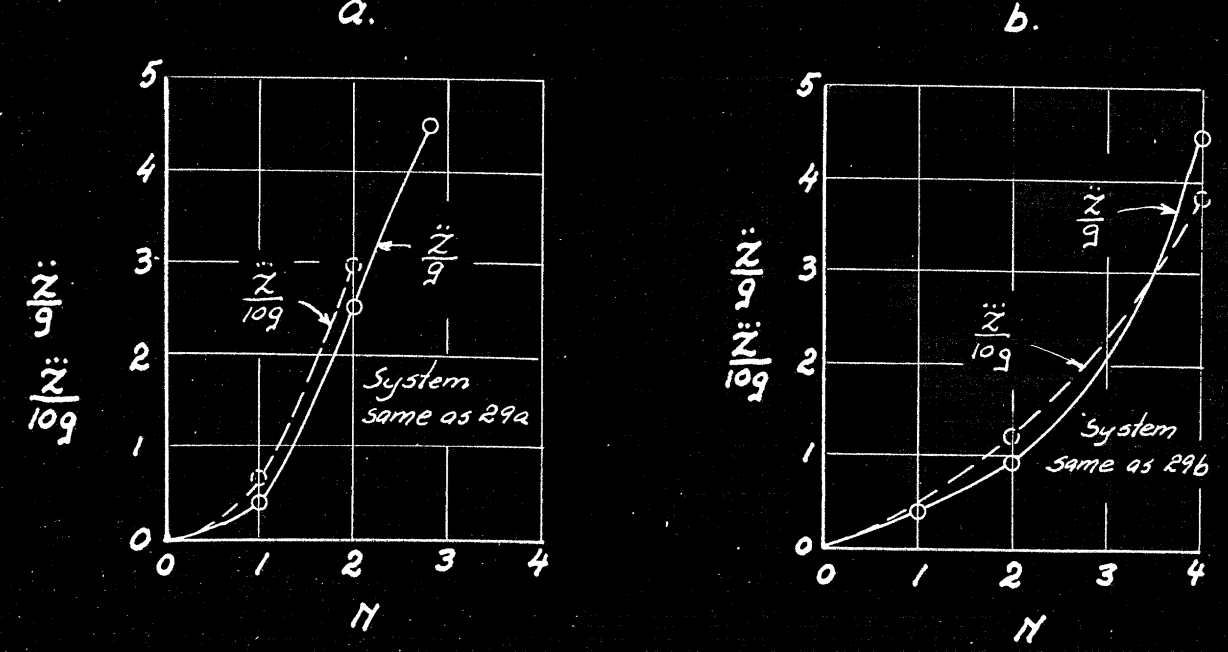

EFFECT OF FREQUENCY OF WAVE ENCOUNTER ON ACCELERATION, AND RATE OF ACCELERATION

Figure VII - 31, 32

COMBINED EFFECTS OF SPEED AND BOAT LENGTH
ON STABILITY OF MOTION

VII -31

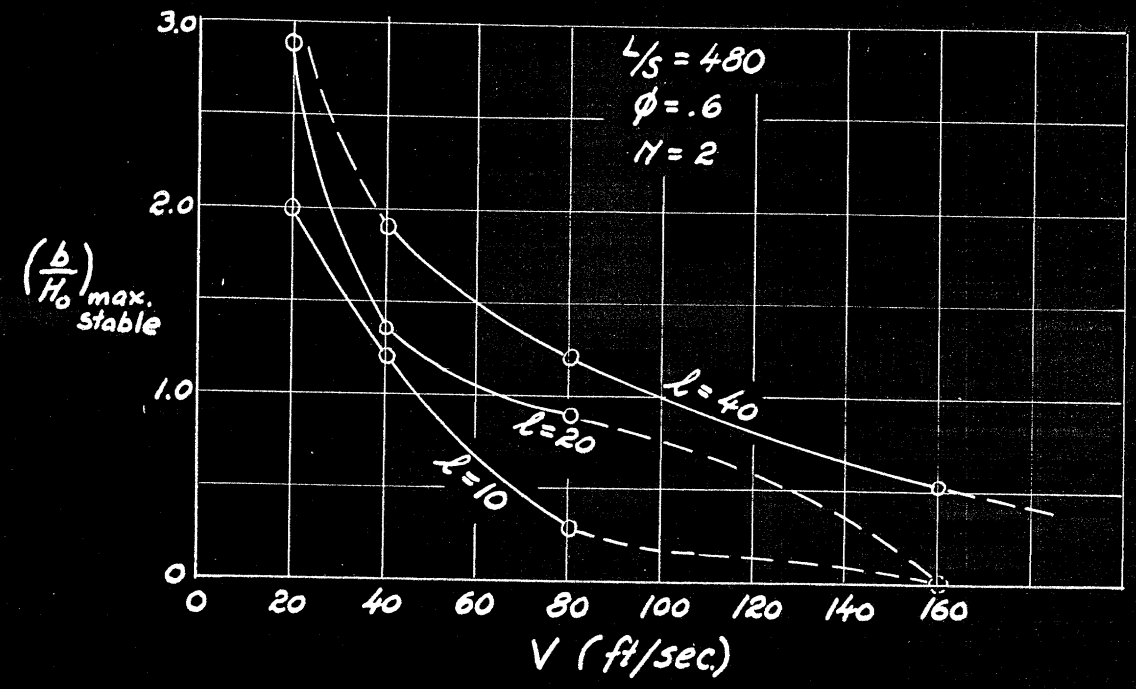

COMBINED EFFECTS OF SPEED AND STATIC LOADING
ON STABILITY OF MOTION
(low frequency of wave encounter)

VII - 32

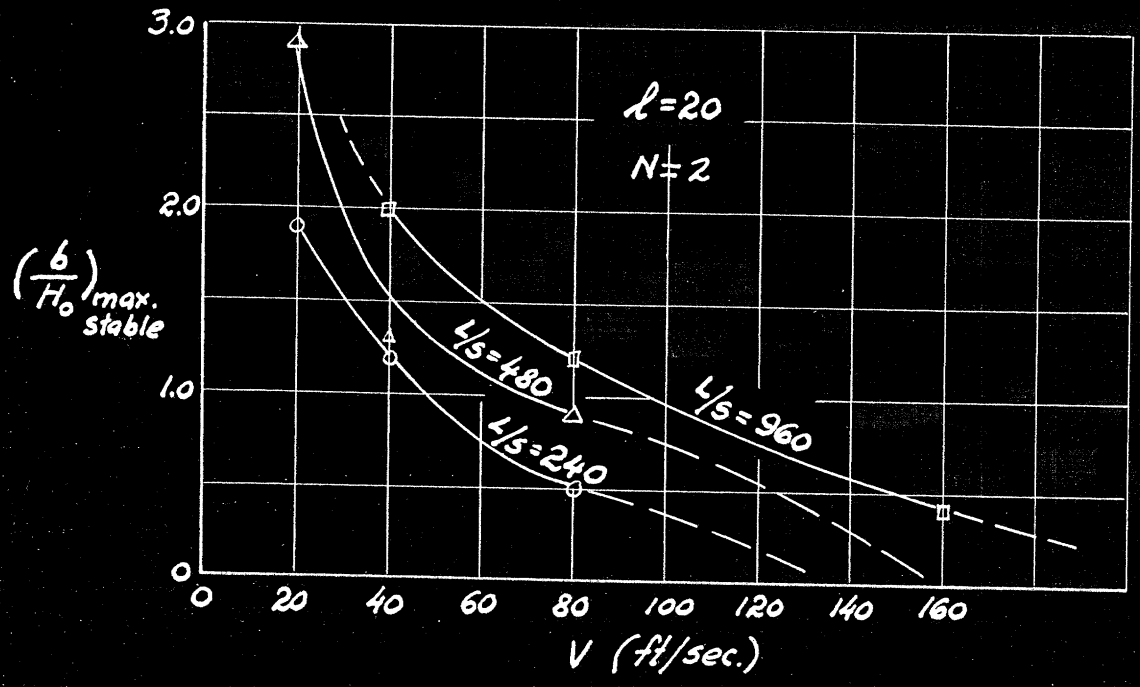

Figure VII – 33, 34

COMBINED EFFECTS OF SPEED AND STATIC LOADING
ON STABILITY OF MOTION
(low frequency of wave encounter)

VII – 33

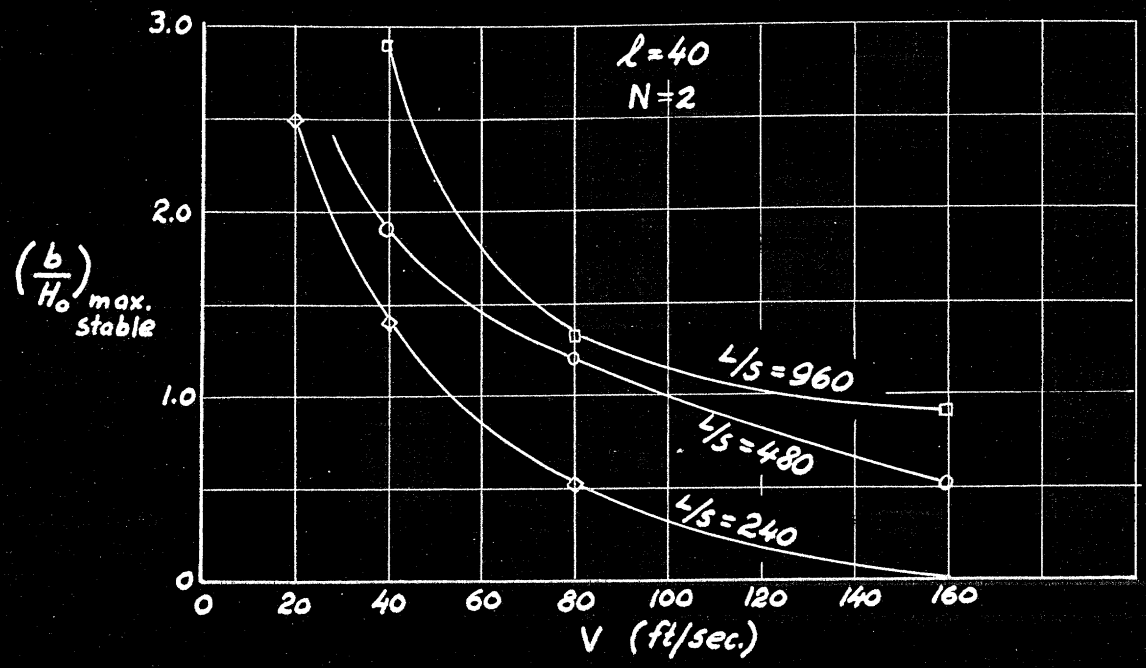

COMBINED EFFECTS OF SPEED AND DIRECTION OF TRAVEL
(Frequency of Wave Encounter)

VII – 34

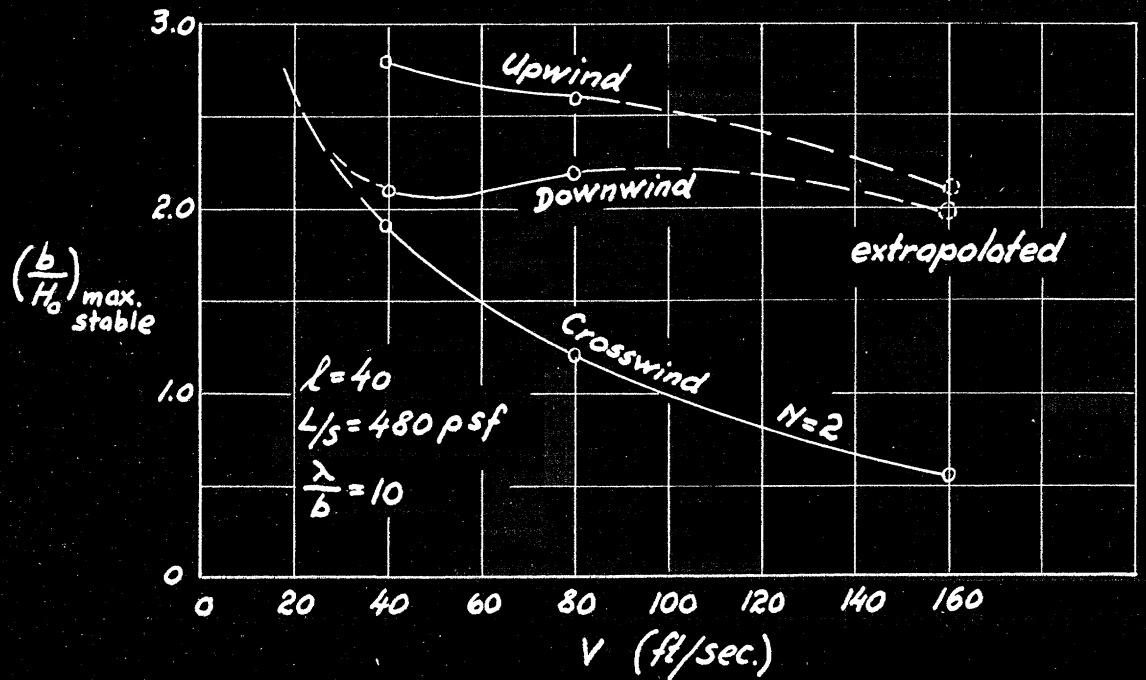

Figure VII - 35, 36

COMBINED EFFECTS OF SPEED AND BOAT LENGTH ON STABILITY OF MOTION VII-35 FOR TRAVEL UPWIND

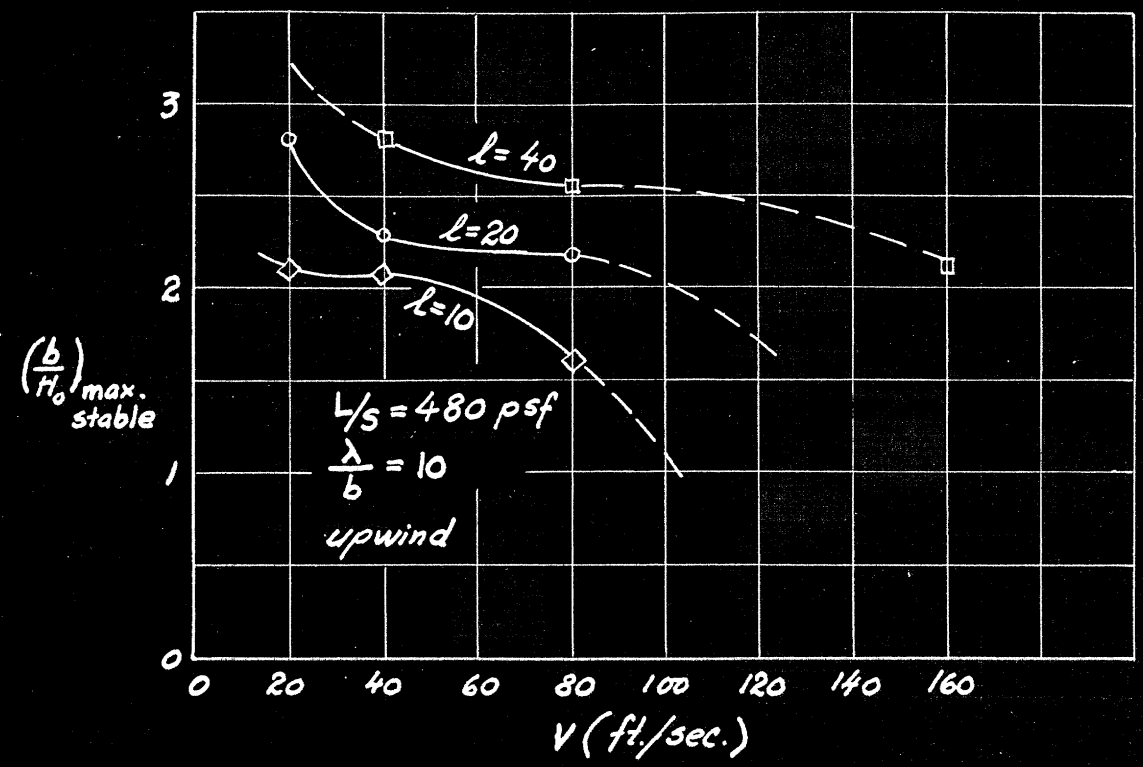

VII-36

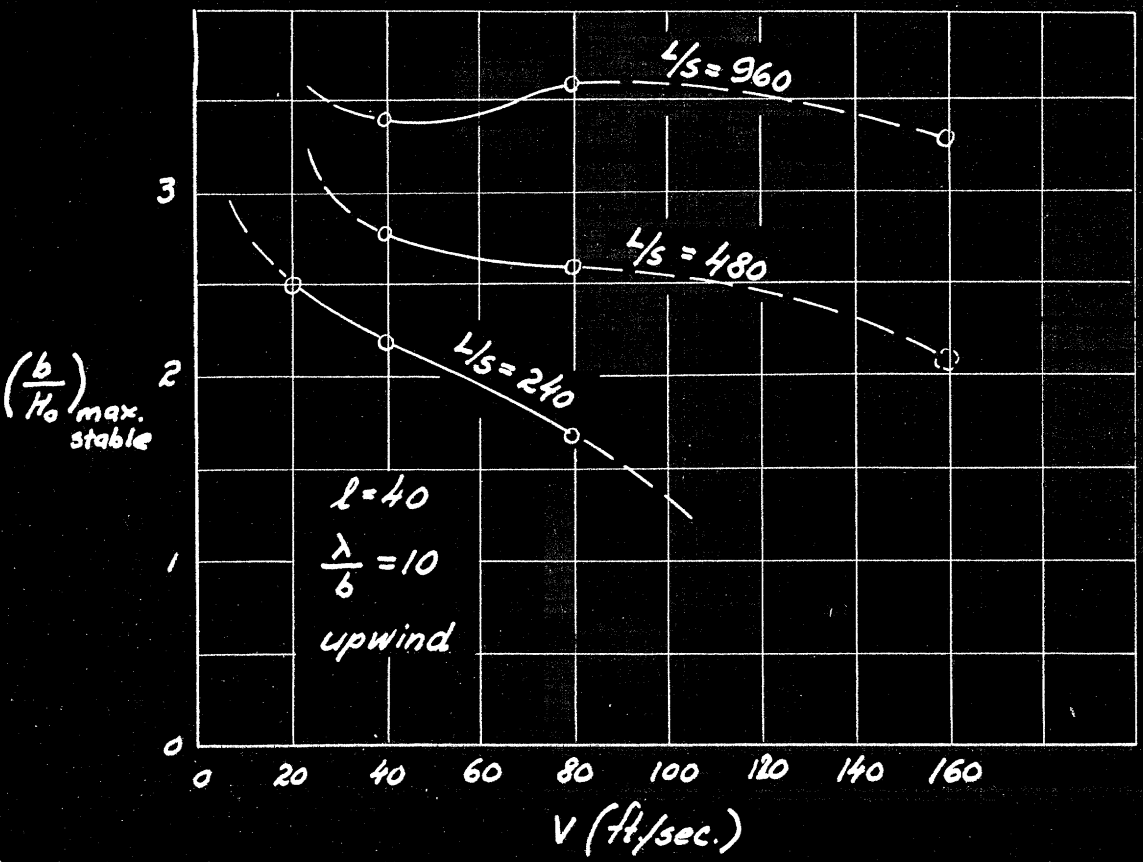

SPEED AND STATIC LOADING

Figure VII – 37, 38

COMBINED EFFECTS OF SPEED AND WAVE LENGTH ON STABILITY OF MOTION (TRAVEL UPWIND)

VII - 37

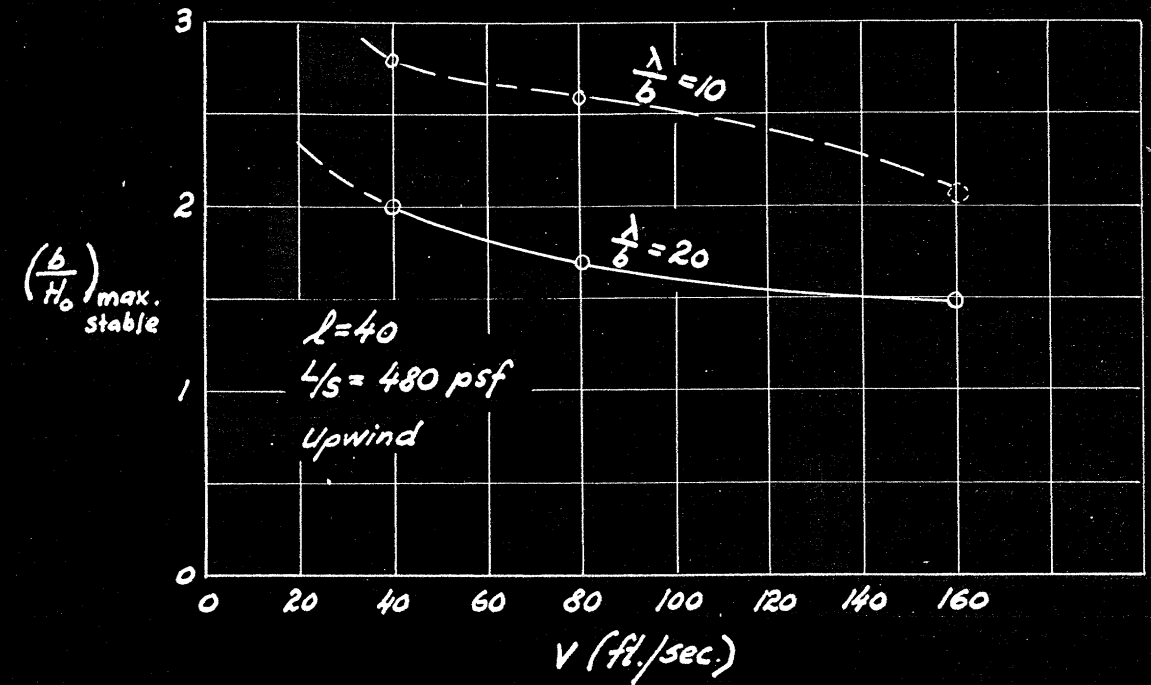

IMPORTANCE OF DESIGN CAVITATION INDEX ON STABILITY OF MOTION

VII -38

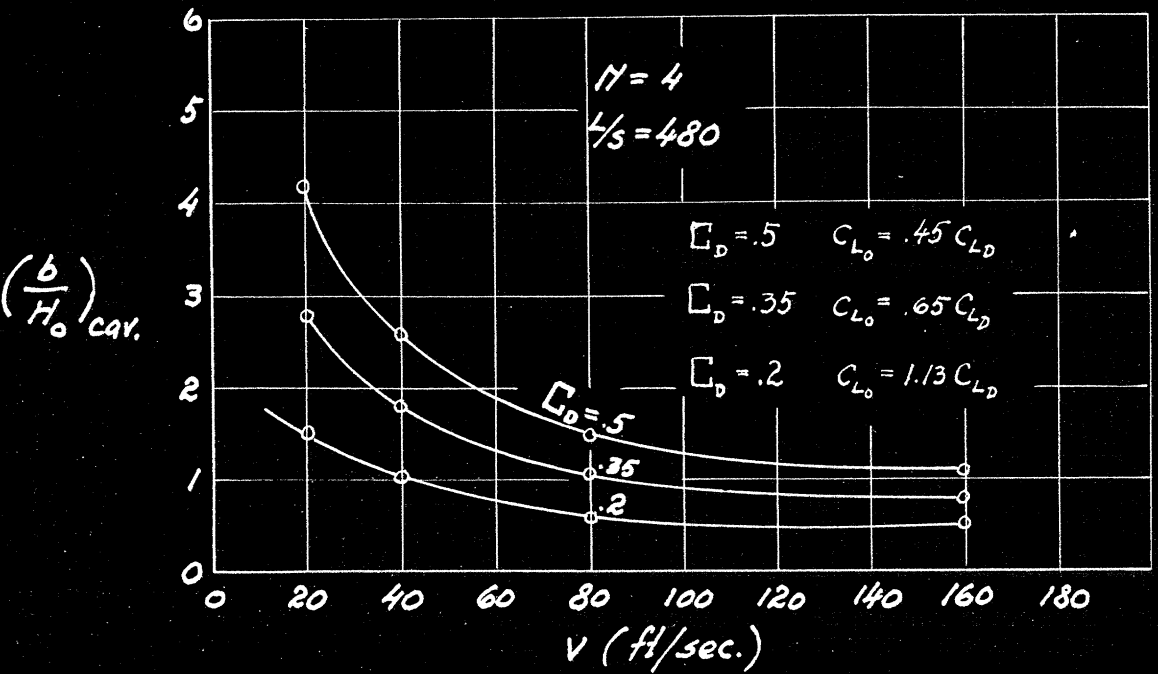

Figure VII – 39, 40

IMPORTANCE OF SPEED AND FREQUENCY OF WAVE ENCOUNTER IN CAUSING A DYNAMIC LOADING WHICH WILL RESULT IN CAVITATION

VII – 39

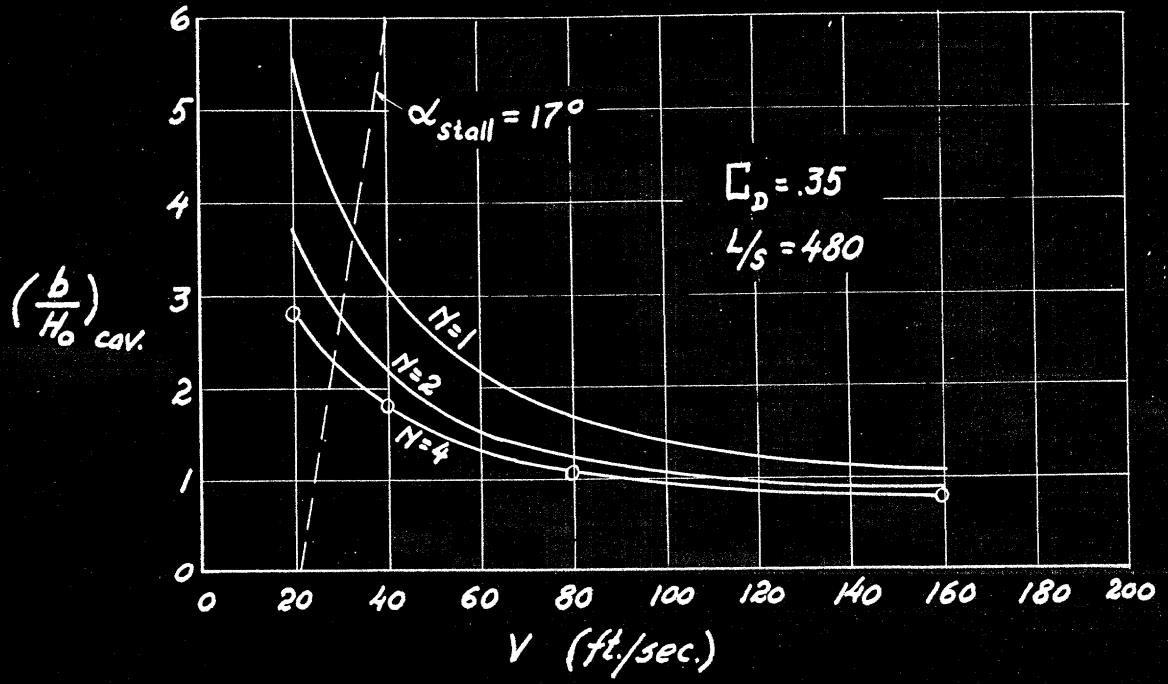

COMBINED EFFECTS OF SPEED AND STATIC LOADING ON PROXIMITY OF THE HYDROFOILS TO CAVITATION

VII – 40

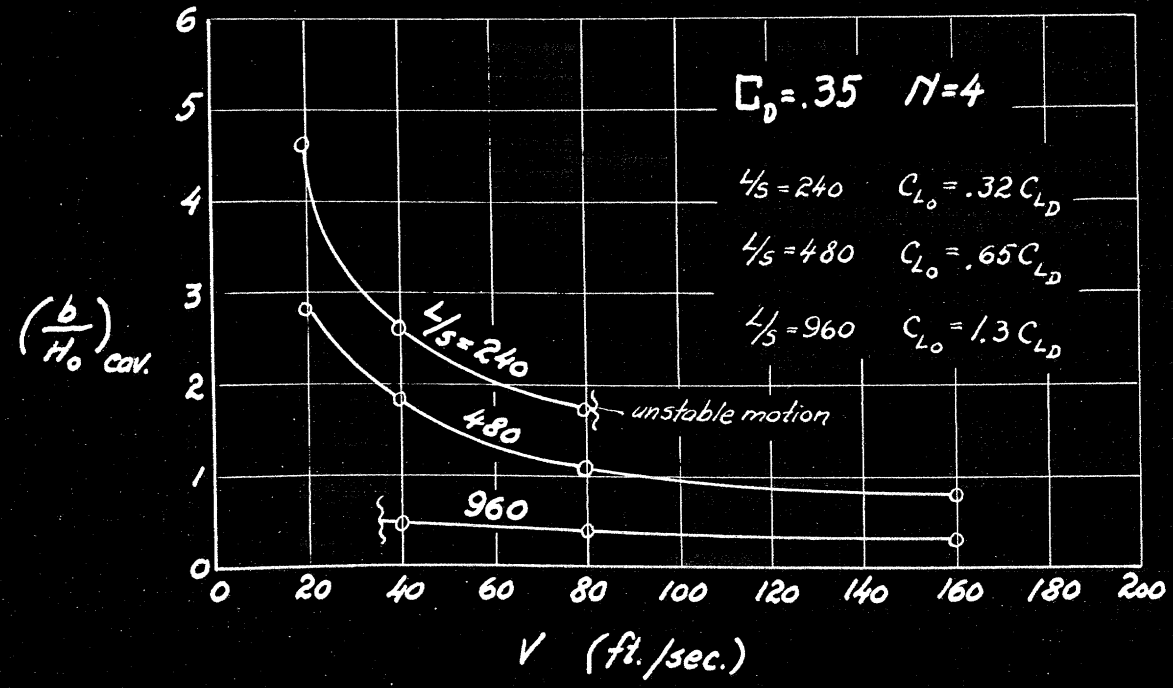

Figure VII-41

THE EFFECT OF RUNNING DEPTH

Equilibrium Depth of System Varied by Changing Angle of Attack.

Wave height: $b = 17.7$ in.

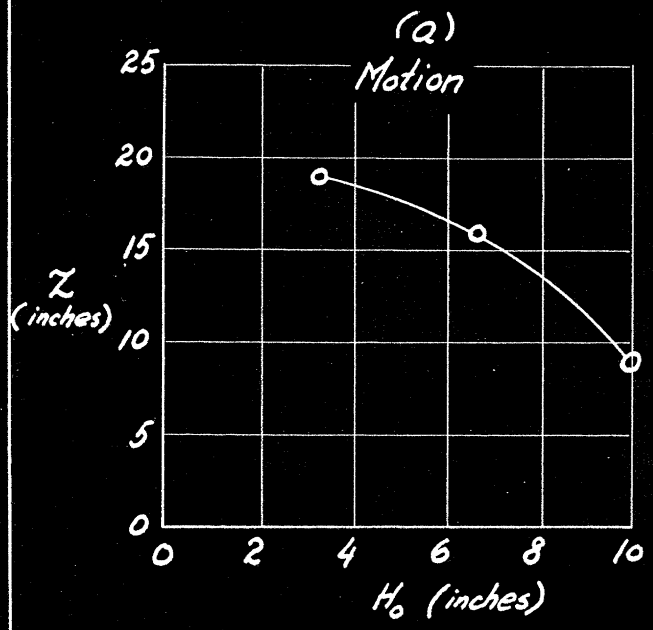

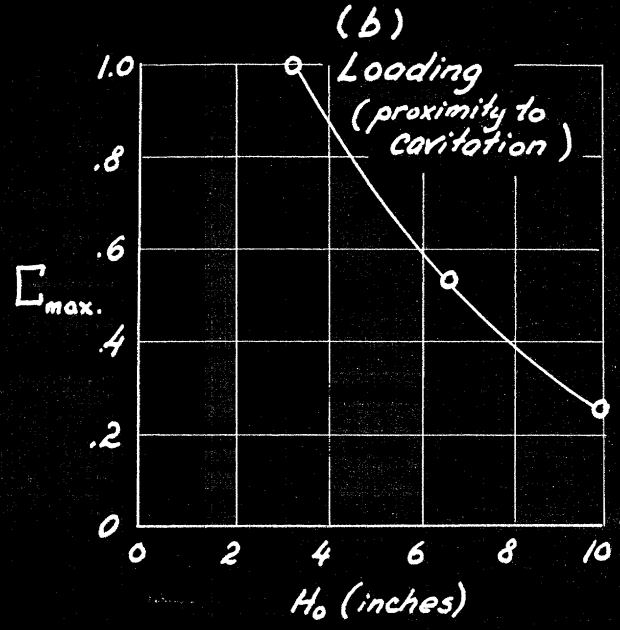

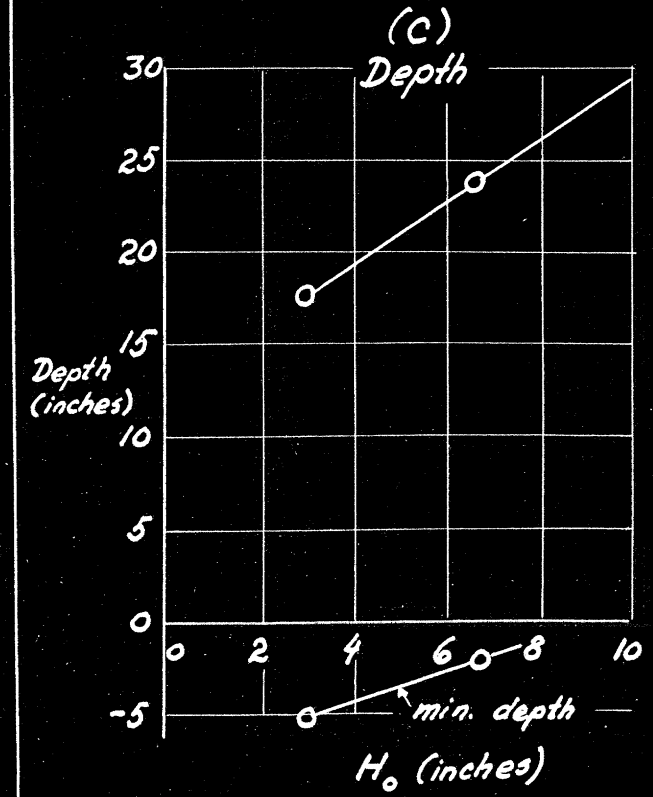

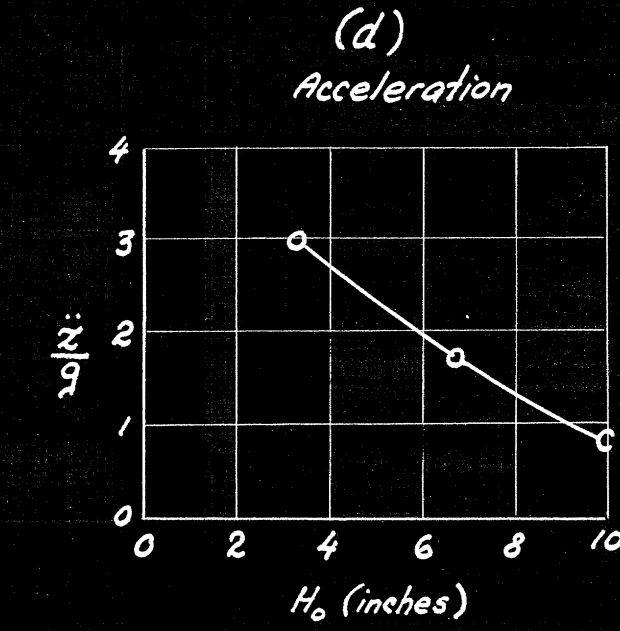

Figure VII-42

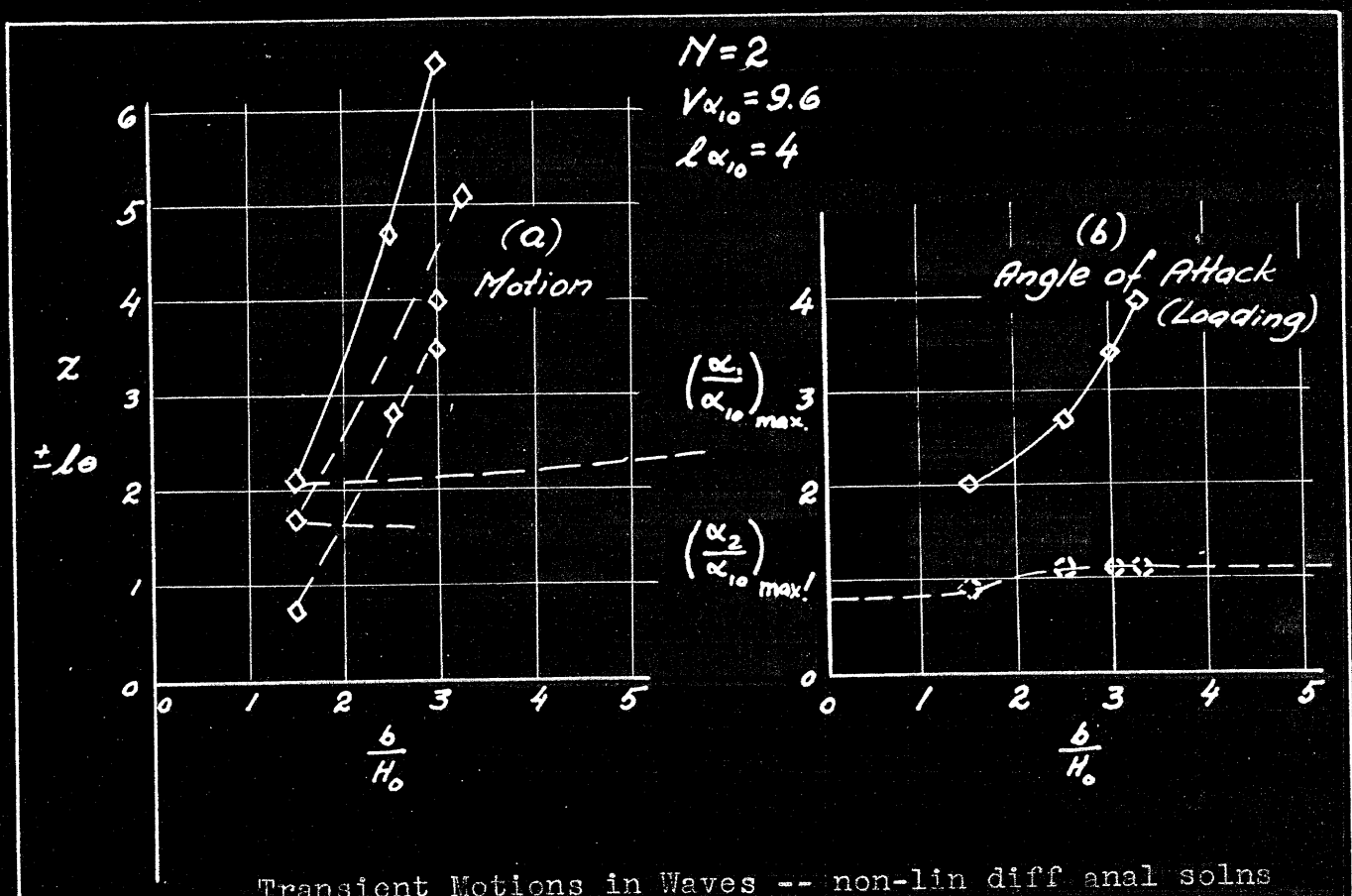

Transient Motions in Waves -- non-lin diff anal solns
PERFORMANCE CHARACTERISTICS OF A
TIETJENS - TYPE HYDROFOIL SYSTEM

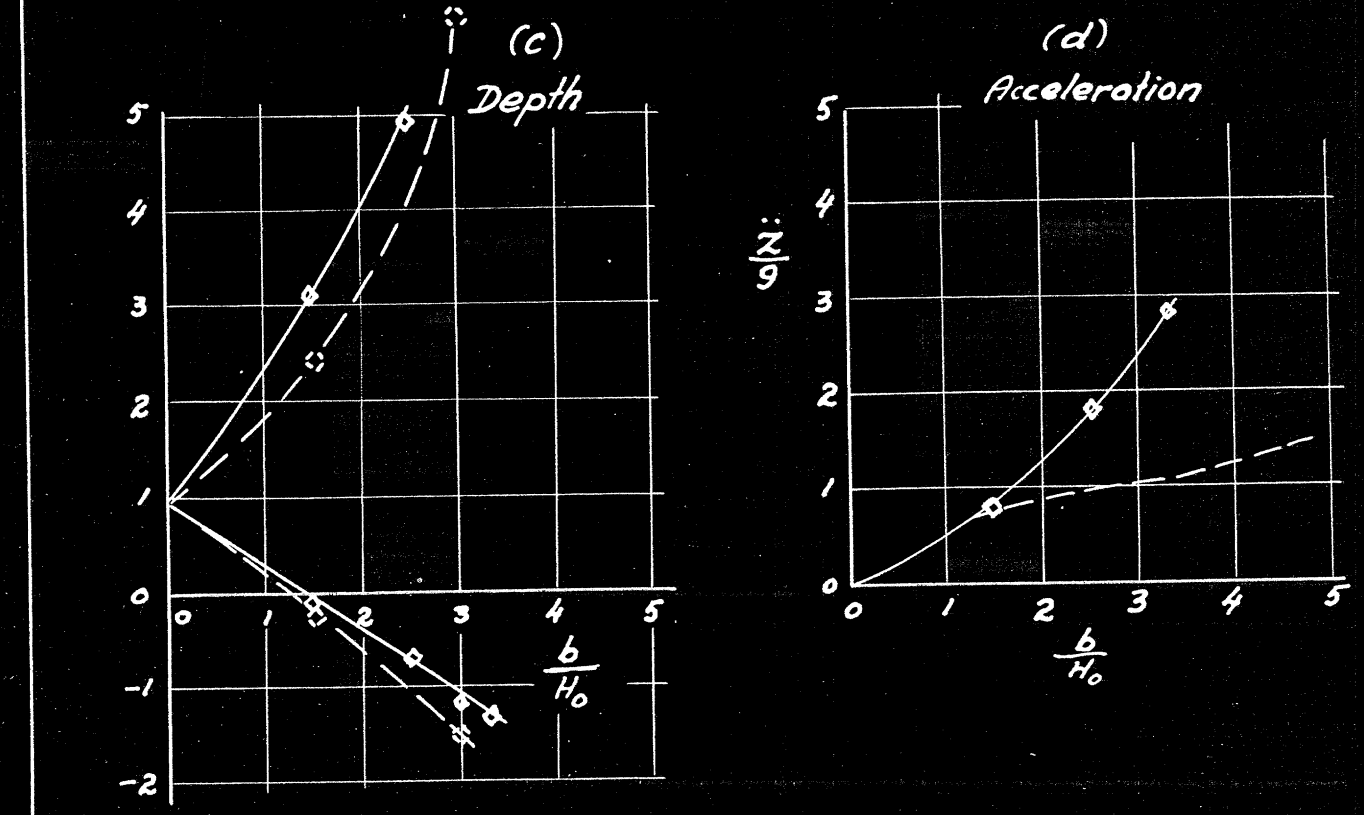

APPENDIX C

EXTRAPOLATION OF DIHEDRAL HYDROFOIL DATA

Appendix C

Extrapolation of Dihedral Hydrofoil Data:

In Chapter II a need was found for extrapolating the data on thirty-degree-dihedral hydrofoils to the case where the tips pierce the surface at all depths down to five chords. The extrapolation is performed as follows:

Given: Data for foil having aspect ratio A = 6, at depths to h = 5. (see Fig. P.)

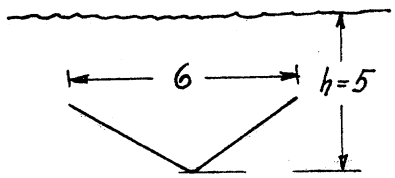

Figure P.

Desired: Data for foil whose tips always pierce the surface. (Fig. Q.)

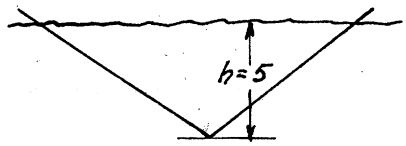

Figure Q.

Data under consideration:

$$\underline{a} = \frac{C_L}{\alpha}, \qquad \sigma = \frac{C_L}{\alpha} S.$$

Procedure: It is noted that the only differences between P and Q are that (1) Q has a greater aspect ratio than P; (2) Q has a lessor average depth than P; and (3) Q pierces the surface while P does not.

Greater aspect ratio will, of course, increase $\underline{a}$, while proximity to the surface and piercing the surface will decrease it. The effect of aspect ratio can be computed from the theoretical relation: $\underline{a} = 2\pi \frac{A}{A+2}$.[1] (This holds exactly for elliptical air foils, approximately for rectangular.)

---

1 Reference 13 , page 145.

The effect of depth on a foil of constant aspect ratio is given in the test data. This curve -- $\underline{a}$ vs. h for A = 6 -- is given in Fig. II - 7 (b).

The correction factor for extrapolating the data (case P) to the continuous foil (case Q) is . $\frac{a_Q}{a_P}$. It is the product of an aspect ratio correction factor and a depth correction factor:

$$\frac{a_Q}{a_P} = \frac{\frac{A}{A+2}_Q}{\frac{A}{A+2}_P} \cdot \frac{(a)_{h\ av\ =\ 2.5}}{(a)_{h\ av\ =\ 4.13}} \cdot$$

For the case h = 5 this factor is $\frac{a_Q}{a_P} = \frac{\frac{17.3}{6}}{\frac{17.3}{6+2}} \cdot \frac{3.50}{3.58} = 1.17$

or $a_Q = 1.17\ (3.58) = \underline{4.18}$.

$$\sigma_Q = \left(\frac{C_L}{\alpha} S\right)_Q = a_Q S_Q = (4.18)\ (17.33) = \underline{72.6}$$

The extrapolation just explained has been used for h > 1.73 in Figure 2.

BIOGRAPHICAL NOTE

The author was born in Cleveland, Ohio, on October 6, 1923. He attended the Toledo, Ohio, public school system, and was graduated from De Vilbiss High School in 1941.

He attended the University of Rochester where he majored in mechanical engineering and was a member of Theta Chi Fraternity. He received the degree Bachelor of Science with Distinction in 1944.

After graduation, he began two years active duty in the U.S. Navy, serving as tactical radar officer on board an assault transport and a destroyer.

The author was married to Dorothea Collins, of Toledo, in January of 1945. They have two sons aged two years,and two weeks.

In 1946 the author entered the M.I.T. Graduate School. During the following two summers he worked on a project to develop a hydrofoil sailboat for the Baker Manufacturing Company, Evansville, Wisconsin. Several towed and motor-powered, passenger-carrying models were built, the successful performance of which persuaded the author to begin this thesis.

During the past year the author has been an instructor in applied mechanics at M.I.T.

REFERENCES

1. Guidoni, A. : Seaplanes - Fifteen Years of National Aviation. Jour. R.A.S., vol XXXII, no. 205, Jan. 1928, pp. 25-64.

2. Nutting, W. W. : The "HD - 4" A 70-Miler with Remarkable Possibilities Developed at Dr. Graham Bell's Laboratories on the Bras D'or Lakes. Publ. 2595, Wash. Govt. Printing Off. 1921.

3. Tietjens, O. : Das Tragflachenboot. Jahrb. 1937 der deutschen Luftfahrtforshung, R. Oldenbourg (Munich), pp. 1361-1370.

4. Hook, C. : German Hydrofoil Boats. Hydrofin Co. Ltd., Cowes, I. W.

5. Grunberg, V. : La Sustentation Hydrodynamique par Ailetts Immergees: Essais d'un Systeme Sustentateur Autostable. L'Aerotechnique, No. 174, 16 anee, supp. to L'Aeronautique, No. 217, June 1937, pp. 61-69.

6. (Article) : Supermarin Forbluffar med sina Sjoegenskaper. Goteborgs Handels - och Sjofarts-tidning, Mar. 1, 1950.

7. Ward, K. E., and Land, N. S. : Preliminary Tests in the NACA Tank to Investigate the Fundamental Characteristics of Hydrofoils. NACA Wartime Report L-766, Sept. 1940.

8. Benson, J. M., and Land, N. S. : An Investigation of Hydrofoils in the NACA Tank, I - Effect of Dihedral and Depth of Submersion. NACA Wartime Report L-758, Sept. 1942.

9. Benson, J. M., and King D. A. : Preliminary Tests to Determine the Dynamic Stability Characteristics of Various Hydrofoil Systems for Seaplanes and Surface Boats. NACA Wartime Report L-756, Nov. 1943.

10. Land, N. S. : Tank Tests of a Grunberg-type high-speed boat, with a Lifting Hydrofoil and Planing Surface Stabilizers. NACA MR, Bu Aer, 22 July 1940.

11. Land, N. S. : Characteristics of an NACA 66, S-209 Section Hydrofoil at Several Depths. NACA Wartime Report L-757, May, 1943.

12. Imlay, F. H. : Theoretical Motions of Hydrofoil Systems. NACA Tech Note 1285, June, 1947.

REFERENCES
(continued)

13. Glauert, H. : The Elements of Airfoil and Airscrew Theory. (2nd ed.) Cambridge Univ. Press, 1948.

14. Stack,J. : Tests of Airfoils Designed to Delay the Compressibility Burble. NACA Report No. 763, 1943.

15. Rayleigh, Lord : Papers. vol. I, Cambridge University Press.

16. Lamb, H. : Hydrodynamics. Dover Pub., 1932.

17. Beach Erosion Board, Corps of Engineers, U.S. Army: A Study of Progressive Oscillatory Waves in Water. Technical Report No. 1. U.S. Govt. Printing Off., 1941.

18. Harney, L. A., and others,: Stastical Study of Wave Conditions at Four Open-Sea Localities in the North Pacific. NACA TN 1493.

19. Cornish, V. : Ocean Waves. Cambridge Univ. Press, 1934.

20. Macnee, A. B. : An Electronic Differential Analyzer. Research Laboratory of Electronics, MIT, Tech Report No. 90, Dec. 16, 1948.